VENTILATORY MECHANICS IN THORACIC SURGERY

Mr.Ghazi Abdelgadir E Elshafie

A thesis submitted to the

University of Birmingham

For the degree of

Doctorate of Medicine

School of Clinical and Experimental Medicine

College of Medical and Dental Sciences

The University of Birmingham

2016

UNIVERSITY OF
BIRMINGHAM

University of Birmingham Research Archive

e-theses repository

This unpublished thesis/dissertation is copyright of the author and/or third parties. The intellectual property rights of the author or third parties in respect of this work are as defined by The Copyright Designs and Patents Act 1988 or as modified by any successor legislation.

Any use made of information contained in this thesis/dissertation must be in accordance with that legislation and must be properly acknowledged. Further distribution or reproduction in any format is prohibited without the permission of the copyright holder.

1 SUMMARY

1.1 Introduction

Measuring chest wall mechanics can be useful in some respiratory conditions (Aliverti A. R., 2005) (Aliverti A. S., 2004). It can be used in assessing the effect of a number of thoracic diseases on chest wall motion as well as the effect of various thoracic surgeries and procedures on chest wall mechanics. The data generated by this assessment were the key to answering a large number of clinical and physiological questions that have challenged researchers in the past. Spirometry and pneumotachography are the current gold standard methods in assessing lung functions (British Thoracic Society and Society of Cardiothoracic Surgeons of Great Britain and Ireland Working Party , 2001). The major limitation of these methods is that both use a mouthpiece, a nose clip, and long connectors (Miller, et al., 2005) (Wanger, et al., 2005). These accessories disrupt normal breathing and increase the dead space, which leads to overestimating tidal volume (Vt). These limitations inspired researchers to investigate lung functions indirectly by measuring the effect of the change in lung volumes in overlying chest wall motion. This enabled them to use the change in chest wall motion to estimate the changes in lung volumes (Aliverti A. R., 2005) (Aliverti A. S., 2004). Here, an analysis of and comparison between various chest wall motion monitoring technologies was made. The aim of this study was to answer a number of clinical and physiological questions about thoracic surgery by using two visual chest wall motion assessment technologies (Optoelectronic Plethysmography [OEP] and

Structured Light Plethysmography [SLP]). These questions and their answers are summarised in the following abstracts.

1.2 *Summary of Chapter 3: The Effect of Diaphragmatic Plication (Fixation)on Chest Wall Mechanics*

Following diaphragmatic plication for unilateral paralysis, its effects on global chest wall function are unknown. The hypothesis here was that chest wall function would improve on both sides of the chest after plication of the paralysed side. In this case report, OEP was used to measure total and regional chest wall volumes in one patient before and after left diaphragmatic plication. Volumes were recorded at quiet breathing. Respiratory capacity showed trends of improvement during quiet breathing when measured before and six months after surgery. These trends of improvement occurred at the ribcage abdominal compartment (the abdominal-ribcage level) in both operated and contra-lateral. Prior to surgery, the ribcage abdominal compartment motion was out of phase with the pulmonary ribcage compartment (the upper ribcage) and abdominal compartment in both sides of the chest. Synchrony of all three compartments showed a trend of improvement after plication. This case report showed trends of improvement in chest wall motion both in the operated and contra-lateral sides following diaphragmatic plication for unilateral paralysis.

1.3 Summary of Chapter 4: The Effect of Chest Wall Reconstruction on Chest Wall Mechanics

Introduction

The effect of chest wall tumours on chest wall mechanics is uncertain, and even less is known about the effects of their resection and reconstruction. The aim in this case report was to describe how chest wall mechanics are altered in chest wall sarcoma and to describe the effect of chest wall resection and reconstruction on chest wall kinetics.

Methods

Optoelectronic Plethysmography was used to assess chest wall motion and volumes in a patient with unilateral extra-thoracic chest wall sarcoma before and five months after resection and reconstruction, during quiet breathing and exercise using cycle ergometry.

Results

During quiet breathing, the unilateral tumour was associated with a trend of a reduction in motion of the abdominal ribcage and abdominal compartments on both sides of the chest, as well as a trend of asynchronous motion of the contra-lateral abdominal ribcage. Surgery corrected these abnormalities in quiet breathing. During exercise, however, there was a trend of reduction in the pulmonary ribcage motion from 0.41(0.14)L pre-operatively to 0.31(0.10)L post-operatively. This impairment was characterised by a trend of an increase in the end expiratory volume (EEV) on the operated side of the chest five months after surgery by 7(1)% and 6(1)% during 50% and 100% exercise, respectively, a finding that was not replicated in the non-operated side.

Conclusion

This case report showed a trend of a negative effect of a chest wall tumour on global chest wall mechanics during quiet breathing and exercise and showed that surgery tended to reverse this abnormality, but only at rest.

1.4 Summary of Chapter 5: The effect of Pectus Carinatum (Pigeon Chest) Repair on Chest Wall Mechanics

Introduction

There is evidence that suggests there is no functional improvement following corrective surgery for pectus carinatum (PC). In this descriptive case series, an observation and description was made of the changes in chest wall function in response to incremental exercise before and after corrective surgery.

Methods

Using OEP, regional chest wall volumes were measured at rest and during exercise, before and after surgery, in conjunction with spirometry in three male patients with PC who underwent a Ravitch procedure for cosmetic reasons.

Results

The EEV showed a trend of an increase of 2(2)% during maximum exercise before surgery. This dynamic hyperinflation or air trapping during exercise was corrected after surgery. Post-operatively, the EEV showed a trend of reduction during maximum exercise by 3(3)% at five months after surgery. The end inspiratory volume did not change. This seemed to be related to the trend of an increase in exercise time to achieve 80% of the predicted maximum heart rate, five months after surgical correction.

Conclusion

This descriptive case series showed a trend of dynamic hyperinflation in PC patients and trends of beneficial effects of corrective surgery. These findings might have an impact on referral patterns for surgery.

1.5 Summary of Chapter 6: The Effect of Lung Volume Reduction Surgery on Chest Wall Mechanics

Introduction

The success of lung volume reduction surgery (LVRS) via endobronchial valves (EBVs) is difficult to assess early post-insertion. This case series described in detail the use of SLP in detecting early the outcome of this procedure.

Methods

SLP measures chest wall motion using a grid of light, which is analysed in terms of regional thoracic movement parameters. Three patients who had EBVs for LVRS were recruited. Measurements were recorded during quiet breathing before surgery and up to two days post-operatively.

Evaluation

In one patient who had successful insertion of EBVs, the chest wall motion on the treated side—compared to overall chest wall motion—showed a trend of reduction from 55(1)% pre-operatively to 48(1)% two days post-surgery. This was matched by radiological evidence of lobar collapse and trend of improvement in his breathlessness score. In the other two patients who failed to exhibit symptomatic benefits after the procedure, the trend of reduction in chest wall motion was much less marked, and this was matched radiologically.

Conclusion

SLP could detect trends of chest wall changes after LVRS via EBVs, which could be useful in detecting failure or success of the procedure.

1.6 Summary of Chapter 7: The Effect of Benign and Malignant Pleural Disease on Chest wall Mechanics

Introduction

Mesothelioma carries a poor prognosis. Differentiating benign from malignant pleural disease can be challenging and may require invasive surgery. The aim

of this case series was to evaluate the effects of benign and malignant pleural disease on chest wall motion using OEP, which may constitute a useful tool in the diagnostic pathway.

Methods

Optoelectronic plethysmography was used to measure the chest wall motion of 16 patients recruited to this study. The measurements were performed before any pathological diagnosis. Pathological diagnosis was obtained via surgical pleural biopsy. After the pathological diagnosis, the patients were divided into three groups retrospectively: a pleural disease-free group (n = 6), an empyema group (n = 6), and a mesothelioma group (n = 4). A radiological assessment was performed in all patients.

Results

The relative contribution of the diseased part of the ribcage pulmonary compartment to the overall ribcage pulmonary compartment motion showed a tendency of being lower in the mesothelioma group, 26(30)%, compared to the control and the empyema groups, 51(5)% and 47(12)%, respectively. The radiological diagnosis matched the pathological diagnosis in only 30% of all patients. When the diseased side of the chest contributed ≤ 32% of the overall chest wall motion, all patients had a pathological diagnosis of mesothelioma.

Conclusion

This case series described the effect of empyema and malignant mesothelioma on chest wall mechanics and showed that the chest wall motion

of the diseased part of the ribcage pulmonary compartment showed a tendency of being lower in the mesothelioma group compared to the control and empyema groups, suggesting that OEP might be useful in future in detecting mesothelioma.

1.7 Summary of Chapter 8: Early Chest Mechanics Changes Post–Lung Resection: The Effect of Thoracic Nerve Blocks

Introduction

It has been reported that video-assisted thoracoscopic surgery (VATS) causes less morbidity than thoracotomy (Maeda, 1988) (Bernard, 2006) (Nomori, Horio, Fuyuno, Kobayashi, & Yashima, 1996). This was thought to be due to the fact that thoracotomy causes more traumatic physiological insults on the chest wall than VATS. Until now, there was no easy way to measure chest wall motion and the relative contribution of each side of the chest immediately after surgery. This case series described the use of a novel technology in the assessment of compartmental chest wall motion and synchrony in a small group of lung resection patients who had undergone different surgical approaches, had different amounts of lung resected and had different analgesia methods.

Methods

SLP was used to measure chest wall mechanics for 15 patients who had thoracic epidural block (TEB) (n = 3), paravertebral block (PVB) (n = 5) or intravenous analgesia (control group) (n = 7) after thoracic surgery via VATS (n = 10) or thoracotomy (n = 5). Chest wall motion measurements were done during quiet breathing before surgery and one day after.

Results

There was a trend of reduction in the motion of the operated side of the chest in all patients who had surgery on the first post-operative day, compared to pre-surgery values of -10(26)%, and a compensatory trend of an increase in chest wall motion on the non-operated side 16 +/- 18% in all patients one day after surgery. When the post-operative changes in chest wall motion were compared between patients who had a lobectomy (n = 7) and a wedge (n = 8), it was found that the reduction in chest wall motion on the operated side showed a trend of being slightly higher in the lobectomy group (n = 7), -11(27)%, compared to the wedge group (n = 8), -8(25)%. When patients who underwent thoracotomy (n = 5) and VATS (n = 10) procedures were compared, it was found that, in the thoracotomy group (n = 5), there was a trend of reduction in the operated side of the chest after surgery compared to the pre-operative value of -10(26)%. In the VATS subgroup, this was -12(25)%. In thoracotomy group there was a trend of an increase in the chest wall motion in the non-operative side after surgery, 7(29)%, compared to preoperative value. In the VATS group, this was 11(29)%. When the TEB, PVB, and control groups were examined, the percentage changes in overall chest wall motion one day after surgery— compared to their pre-operative values—showed a trend of being similar in the three groups. Similarly, the motion of the operated side showed a trend of reduction in all three groups, but this trend of reduction was similar in the three groups.

Conclusion

This study showed that SLP is a useful tool post-operatively, as it is a portable device that can be taken to the bedside of a patient immediately after surgery. The results of this case series showed that epidural analgesia has no tendency of negative effect on the chest wall compared to controls. These results also showed that the trend of reduction on the operated side of the chest was slightly higher in the VATS group compared to the thoracotomy group, which might suggest that both procedures could be as traumatic on chest wall motion.

1.8 Summary of Chapter 9: Early Chest Mechanics Changes Post–Lung Resection: The Effect of Post-Operative Pulmonary Complications on Chest Wall Mechanics

Introduction

Post-operative pulmonary complications (PPCs) are the major causes of death following lung resection and account for up to 84% of all surgical mortality (Stephan, Boucheseiche, & Hollande, 2000). In addition, in the UK, there is a trend of operating on patients who are less fit for surgery in order to improve survival rates, as recommended by the British thoracic guidelines (Brunelli, et al., 2009). This leads to a further increased incidence of PPCs. These complications are responsible for delaying patients' discharge as well as many intensive care admissions (Agostini, et al., 2008). Early detection is fundamental in treating PPCs. Identifying patients with PPCs early has been problematic. This may be in part due to delayed radiological evidence of the condition. In addition, this may be due in part to the difficulties of performing spirometry in the immediate post-operative period and the lack of accuracy of the current scoring systems. PPCs lead to a decrease in lung compliance, which reduces lung expansion. This case study hypothesised that the body tries to compensate by adjusting chest wall motion to overcome reduced lung compliance. The hypothesis was that these changes are detected by chest wall motion technology in the immediate post-operative period. By using chest wall motion technology, this case report aimed to show a relationship between the tendencies of recovery and complications with trends in chest motion. By this method, it was hypothesised that trends of early deterioration could be identified before clinical and radiological manifestations.

Methods

SLP was used to measure the chest wall motion of 11 patients undergoing thoracic surgery. Three out of the 11 patients developed pneumonia post-operatively. The patients were then divided retrospectively based on the clinical diagnosis of post-operative pneumonia into a PPC group (n = 3) and a control group (CG) of patients free of pneumonia (n = 8). The PPC group included all patients who had been diagnosed clinically by the surgeon to have pneumonia. A PPC score was collected for all patients. The SLP measurements were made during quiet breathing while the patients were sitting, before surgery and every day after surgery until the discharge date. Outcomes were given as percentage contributions of the regional compartment of the chest and abdomen. All patients had a chest X-ray (CXR) as inpatients after surgery and thereafter if there was a clinical suspicion of PPCs.

Results

The results showed that none of the patients were clinically - relying on the patients' symptoms and examination of the chest, as made by the surgeon in the ward round- diagnosed with PPCs in the first post-operative day, nor was the PPC score diagnostic. A CXR showed signs of atelectasis in two out of the three patients on Day 1 and three out of three patients by Day 2. The results showed that overall chest wall motion showed a trend of greater reduction in the PPC group compared to the CG group: -9(31)% and 5(14)%, respectively. The results also showed that both groups of patients had trends of reduction in chest wall motion of the operated side on Day 1 after surgery, but this trend reduction was higher in the PPC group than the CG group: -11(30)% and -9(23)%, respectively. There was also a trend of higher degree of dys-synchronisation between the operated side and non-operated side of the chest in the PPC group, compared to the CG group: 240(308)% and 56(483)%, respectively.

Conclusion

This case series demonstrated that a novel technology may have the potential to detect signs of PPCs by analysing trends in chest wall motion before the clinical diagnosis is made. This could have a wide range of clinical applications.

1.9 *Summary of Chapter 10: Late Change in Chest Wall Mechanics Post–Lung Resection: The Effect of Lung Cancer Resection in COPD Patients*

Introduction

The lung volume reduction effect of a lobectomy for lung cancer in chronic obstructive pulmonary disease (COPD) patients is widely recognised (Vaughan, Oey, Nakas, Martin-Ucar, Edwards, & Waller, 2007). The dynamic changes in chest wall mechanics in these patients have not been described.

Methods

Five COPD and six non-COPD patients with suspected lung cancer were recruited for the study. Using OEP, their chest motion was measured before and after lung resection.

Results

Vt at rest in the COPD group showed a trend of improvement six months after surgery by 0.42(66)L, secondary to a trend of increased contributions of the pulmonary ribcage compartment by 104(124)% and the ribcage abdomen compartment by 110(147)%, with a trend of reduction in contribution from the abdomen by -16(48)%. This contrasts with the findings in the non-COPD group, where there was only a 0.08(0.23)L trend of an increase in the tidal volume, due to a trend of an increase in the contribution of the pulmonary ribcage by only 1(46)%. No trend of marked difference in chest wall motion was detected between VATS and thoracotomy approaches six months after surgery.

Conclusion

The lung resection in COPD patients seemed to be related to a trend of improvement in chest wall mechanics. This case series described in detail the possible mechanism of symptomatic benefits of lung resection in this group of patients.

2 DEDICATION

I dedicate this thesis to my mother Dr.Kawther Elshafie and my father Prof. Abdelgadir Elshafie who always believed in me, and for all they done to me and for their unconditional support through out my life, I dedicate this work to my wife, the love of my life Dr. Hadeel Ali who always stood by my side, supporting me unconditionally through the thick and the thin.

3 ACKNOWLEDGMENTS

I would like to acknowledge that I, alone, did the literature review, recruited all the patients, calibrated the machines, collected all the data, cleaned all the data, analysed all the data, generated all the results and wrote this thesis. My MD degree was half self-funded and half funded by Pneumacare Ltd.

I would like to acknowledge the help of Prof. Andrea Aliverti in understanding the experiments results.

Table of Contents

1 SUMMARY 2

1.1 INTRODUCTION 2
1.2 *SUMMARY OF CHAPTER 3: THE EFFECT OF DIAPHRAGMATIC PLICATION (FIXATION)ON CHEST WALL MECHANICS* 3
1.3 SUMMARY OF CHAPTER 4: THE EFFECT OF CHEST WALL RECONSTRUCTION ON CHEST WALL MECHANICS 4
1.4 SUMMARY OF CHAPTER 5: THE EFFECT OF PECTUS CARINATUM (PIGEON CHEST) REPAIR ON CHEST WALL MECHANICS....................5
1.5 SUMMARY OF CHAPTER 6: THE EFFECT OF LUNG VOLUME REDUCTION SURGERY ON CHEST WALL MECHANICS....................6
1.6 SUMMARY OF CHAPTER 7: THE EFFECT OF BENIGN AND MALIGNANT PLEURAL DISEASE ON CHEST WALL MECHANICS 7
1.7 SUMMARY OF CHAPTER 8: EARLY CHEST MECHANICS CHANGES POST–LUNG RESECTION: THE EFFECT OF THORACIC NERVE BLOCKS 9
1.8 SUMMARY OF CHAPTER 9: EARLY CHEST MECHANICS CHANGES POST–LUNG RESECTION: THE EFFECT OF POST-OPERATIVE PULMONARY COMPLICATIONS ON CHEST WALL MECHANICS 11
1.9 *SUMMARY OF CHAPTER 10: LATE CHANGE IN CHEST WALL MECHANICS POST–LUNG RESECTION: THE EFFECT OF LUNG CANCER RESECTION IN COPD PATIENTS* 14

2 DEDICATION....................16

3 ACKNOWLEDGMENTS....................17

4 LIST OF FIGURES 22

5 LIST OF TABLES....................25

6 LIST OF ABBREVIATIONS 27

7 INTRODUCTION 32

8 CHAPTER 1: THE RESPIRATORY SYSTEM 38

8.1 THE ANATOMY OF THE RESPIRATORY SYSTEM 38
8.1.1 THE UPPER RESPIRATORY TRACT....................39
8.1.2 LOWER RESPIRATORY TRACT 40
8.1.3 THE FUNCTIONAL STRUCTURE 43
8.1.4 THE PULMONARY BLOOD SUPPLY AND LYMPH DRAINAGE 44
8.1.5 THE NEURAL SUPPLY FOR THE LUNG 45
8.2 LUNG VOLUMES AND CAPACITIES 45
8.3 ANATOMY AND PHYSIOLOGY OF THE CHEST WALL 48
8.3.1 THE CHEST WALL SKELETON....................48
8.3.2 THE CHEST WALL MUSCULATURE 50
8.3.3 THE DIAPHRAGM 50
8.3.4 THE INTERCOSTAL MUSCLES 52
8.4 **THE PHYSIOLOGY OF THE CHEST 55**

9 CHAPTER 2: MEASUREMENT OF CHEST WALL MOTION 58

9.1 CURRENT PRE-OPERATIVE PHYSIOLOGICAL TESTS IN THORACIC SURGERY: WHAT THEY MEASURE, HOW THEY MEASURE IT, AND WHAT THEIR BENEFITS AND LIMITATIONS ARE 58
9.1.1 *WHOLE BODY PLETHYSMOGRAPHY* 63
9.2 THE NEED FOR CHEST WALL MOTION MEASURING TECHNOLOGY....71
9.3 METHODS OF MEASURING CHEST WALL MOTION 72
9.3.1 *NEGATIVE PRESSURE VENTILATORS* 72
9.3.2 *OESOPHAGEAL AND GASTRIC BALLOONS* 73
9.3.3 *MAGNETOMETER* 74
9.3.4 *MAGNETIC RESONANCE IMAGING (MRI)* 83
9.3.5 *RESPIRATORY INDUCTANCE PLETHYSMOGRAPHY (RIP)* 87
9.3.6 *THE LIFESHIRT* 89
9.3.7 *IMPEDANCE PLETHYSMOGRAPHY* 91
9.3.7.1 TRANSTHORACIC IMPEDANCE (TTI) PLETHYSMOGRAPHY 92
9.3.8 *CAPACITIVE SENSING* 94
9.3.8.1 WEARABLE CAPACITIVE SENSOR....95
9.3.9 *STRAIN GAUGES* 97
9.3.10 *OPTICAL DEVICES* 100
9.3.10.1 OPTIC FIBRES....100
9.3.10.2 VISUAL MOTION ANALYSIS SYSTEMS 103
9.3.10.3 SUMMARY - OPTOELECTRONIC PLETHYSMOGRAPHY 112
9.3.10.4 STRUCTURED LIGHT PLETHYSMOGRAPHY....113
9.3.11 *SUMMARY OF THE ADVANTAGES AND DISADVANTAGES* 118
9.4 THE NEED FOR MEASURING CHEST WALL MECHANICS IN THORACIC SURGERY .122

10 METHODS 124

10.1 ETHICS....124
10.2 RECRUITMENT 124
10.3 TECHNOLOGIES USED IN THE THESIS 125
10.3.1 **OEP: OPTOELECTRONIC PLETHYSMOGRAPHY 125**
10.3.2 **SLP: STRUCTURED LIGHT PLETHYSMOGRAPHY 136**
10.4 STATISTICS 139
10.1 FIGURES: 140

11 CHAPTER 3: THE EFFECT OF DIAPHRAGMATIC PLICATION (FIXATION) ON CHEST WALL MECHANICS 141

11.1 INTRODUCTION 141
11.2 METHODS....141
11.3 RESULTS....143
11.4 DISCUSSION 146
11.5 LIMITATIONS....148

12 CHAPTER 4: THE EFFECT OF CHEST WALL RECONSTRUCTION ON CHEST WALL MECHANICS....150

12.1 INTRODUCTION 150
12.2 METHODS....150
12.3 RESULTS....152
12.4 DISCUSSION 155
12.5 CONCLUSION....156
12.6 LIMITATIONS....156

13 CHAPTER 5: THE EFFECT OF PECTUS CARINATUM (PIGEON CHEST) REPAIR ON CHEST WALL MECHANICS....157

13.1 INTRODUCTION 157
13.2 METHODS 157
13.2.1 PARTICIPANTS 158
13.2.2 STUDY DESIGN 159
13.2.3 STATISTICAL ANALYSIS 161
13.3 RESULTS 162
13.4 DISCUSSION 169
13.5 CONCLUSION 172
13.6 LIMITATIONS 173

14 CHAPTER 6: THE EFFECT OF LUNG VOLUME REDUCTION SURGERY ON CHEST WALL MECHANICS 174

14.1 BACKGROUND 174
14.2 METHODS 176
14.2.1 STUDY DEVICES 176
14.2.2 MEASUREMENT PROTOCOL 177
14.2.3 PATIENTS 178
14.2.4 STUDY DESIGN 179
14.2.5 OUTCOME MEASURES 180
14.2.6 PROCEDURE AND FOLLOW-UP 180
14.2.7 SLP DATA APPRAISAL AND REGIONAL SELECTION 181
14.2.8 STATISTICAL ANALYSIS 181
14.3 RESULTS 182
14.3.1 PATIENT 1 182
14.3.2 PATIENT 2 183
14.3.3 PATIENT 3 185
14.4 DISCUSSION 186
14.5 CONCLUSION 190
14.6 LIMITATIONS 190

15 CHAPTER 7: THE EFFECT OF BENIGN AND MALIGNANT PLEURAL DISEASE ON CHEST WALL MECHANICS 192

15.1 INTRODUCTION 192
15.2 METHODS 195
15.2.1 PARTICIPANTS 195
15.2.2 STUDY DESIGN 196
15.2.3 STATISTICAL ANALYSIS 197
15.3 RESULTS 197
15.4 DISCUSSION 204
15.5 LIMITATIONS 206

16 CHAPTER 8: EARLY CHEST MECHANICS CHANGES POST–LUNG RESECTION: THE EFFECT OF THORACIC NERVE BLOCKS 207

16.1 INTRODUCTION 207
16.2 METHODS 207
16.2.1 PATIENTS 208
16.2.2 STATISTICAL ANALYSIS 210
16.3 RESULTS 210
16.4 DISCUSSSION 216
16.5 LIMITATIONS 219

17 CHAPTER 9: EARLY CHEST MECHANICS CHANGES POST–LUNG RESECTION: THE EFFECT OF POST-OPERATIVE PULMONARY COMPLICATIONS ON CHEST WALL MECHANICS 220

17.1 BACKGROUND 220
17.2 METHODS 221
17.3 RESULTS 226
17.4 DISCUSSION 229
17.5 CONCLUSION 231
17.6 LIMITATIONS 231

18 CHAPTER 10: LATE CHANGES IN CHEST WALL MECHANICS POST–LUNG RESECTION: THE EFFECT OF LUNG CANCER RESECTION IN COPD PATIENTS 233

18.1 INTRODUCTION 233
18.2 METHODS 234
18.2.1 STUDY DESIGN 237
18.2.2 STATISTICAL ANALYSIS 238
18.3 RESULTS 239
18.4 DISCUSSION 243
18.5 CONCLUSION 246
18.6 LIMITATIONS 246

19 CONCLUSIONS. LIMITATIONS AND RECOMMENDATIONS 247

20 APPENDIX 1 269

20.1 PUBLICATIONS 269
20.2 PRESENTATIONS 272

21 REFERENCES 276

4 LIST OF FIGURES

Figure1: The anatomy of the respiratory system 39

Figure 2: The branches of terminal bronchiole ending in the alveolar sacs 43

Figure 3: Schematic representation of the lung volumes and capacities (Spirogram) 46

Figure 4: The thoracic skeleton, anterior view 49

Figure 5: A superior view of the diaphragm and related structures 51

Figure 6: The muscles of respiration 53

Figure 7: The abdominal muscles 55

Figure 8: The changes in the chest wall during inspiration (left) and expiration (right) 57

Figure 9: The measurement cycle of plethysmography 64

Figure 10: The Iron lung 73

Figure 11: Illustration of the method Konno and Mead used to measure chest wall motion 75

Figure 12: Schematic of the magnetometer device depicting coil placement 76

Figure 13: The configuration of the electromagnetic coils 77

Figure 14: Estimation of energy expenditure by electromagnetic coils versus calorimetry 81

Figure 15: Schematic drawing of the portable RIP system in a LifeShirt application 90

Figure 16: Schematic representation of pajamas with sensor units 95

Figure 17: Resistive sensor for respiratory monitoring 98

Figure 18: The optical fibres-textile integration 102

Figure 19: An example of images captured using colour structured light technology 114

Figure 20: Schematic representation of the OEP measuring principle 126

Figure 21: The xyz axis 128

Figure 22: Example of a structured light system and pattern 137

Figure 23: The grid pattern in SLP 138

Figure 24: SLP reconstruction of the chest wall 138

Figure 25: SLP volume 139

Figure 26: Chest radiograph before and after diaphragmatic plication. 144

Figure 27: Synchrony of chest wall before and 6 months after diaphragm plication 146

Figure 28: CT scans before and 5 months post chest wall resection and reconstruction of a right chest wall tumour 151

Figure 29: Synchrony of the chest wall compartments before and after chest wall resection and reconstruction 153

Figure 30: Images of a patient before and pectus carinatum repair 163

Figure 31: Spiromteric measurements before and after pecuts carinatum repair 165

Figure 32: Chest wall tidal volume of PC patients at maximum exercise 166

Figure 33: The EIV and EEV of the chest wall and pulmonary ribcage of PC patients, before and after surgery during quiet berating and exercise 167

Figure 34: The total of exercise to reach 80% of heart rate before and after PC repair 168

Figure 35: The working principle of SLP 177

Figure 36: Patient 1 change in the % contribution of the treated side of the chest to overall chest wall motion before and after EBV insertion 183

Figure 37: Patient 2 change in the % contribution of the treated side of the chest to overall chest wall motion before and after EBV insertion 184

Figure 38: Patient 3 change in the % contribution of the treated side of the chest to overall chest wall motion before and after EBV insertion 185

Figure 39: Overall tidal volume in all groups (the control, empyema and mesothelioma groups) 200

Figure 40: The Pulmonary ribcage tidal volume in the three groups (the control, empyema and mesothelioma groups) 201

Figure 41: The tidal volume of the diseased pulmonary ribcage in mesothelioma and empyema, and the normal side in the control 202

Figure 42: The % contribution of diseased side of the pulmonary rib to overall pulmonary ribcage in the 3 groups (the control, empyema and mesothelioma groups) 202

Figure 43: The 3 and 6 months changes in the volume of the chest wall and its three compartments in the COPD and the Non-COPD groups 239

Figure 44: The 3 and 6 months changes in the volume of RCP and RCA compartments of the chest wall on the operated and non-operated sides of the chest wall in the COPD and the Non-COPD groups 241

5 LIST OF TABLES

Table 1: The advantages and disadvantages of the chest wall motion analysis systems 118

Table 2: Respiratory parameters before and 6 months after diaphragmatic plication: 145

Table 3: Respiratory parameters before and 5 months after chest wall resection 154

Table 4: The change in end expiratory volume (EEV) of the pulmonary ribcage of operated side and non-operated side during exercise 155

Table 5: Demographic data of the three patients with pectus carinatum deformity before surgery 162

Table 6: The respiratory parameters before and after PC repair during quiet breathing and exercise 169

Table 7: Baseline Characteristics of the EBV Patients 179

Table 8: The mesothelioma, empyema and control groups' characteristics 198

Table 9: Respiratory parameters of mesothelioma, empyema and control groups: 199

Table 10: The relative contribution of each chest wall compartment in the mesothelioma, empyema and control groups 199

Table 11: The pathological diagnosis versus the radiological diagnosis versus motion of diseased side of pulmonary ribcage of the empyema and the mesothelioma groups 204

Table 12: The baseline characteristics of the thoracotomy and VATS patients 209

Table 13: The percentage change in chest wall motion characteristics in all patients day 1 after surgery 211

Table 14: The percentage change in chest wall motion characteristics in the lobectomy and wedge patients day 1 after surgery 212

Table 15: The percentage change in chest wall motion characteristics in the thoracotomy and VATS patients day 1 after surgery 213

Table 16: The baseline characteristics of the TEB, PVB and Control groups 214

Table 17: The day 1 Borg score, pain score and spirometery measurements in the TEB, PVB and control groups 215

Table 18: The percentage change in chest wall motion characteristics in in the TEB, PVB and control groups day 1 after surgery 216

Table 19: Hospital stay in TEB, PVB and control groups 216

Table 20: The demographic data of the PPC group and the control group 225

Table 21: The day 1 clinical parameters and the % change in chest wall motion parameters of PPC groups and controls day 1 after surgery compared to per surgery 228

Table 22: The preoperative characteristics of all the patients in the COPD and Non-COPD groups 236

Table 23: The preoperative characteristics of the COPD and Non-COPD patients who had thoracotomy or VATS 242

Table 24: The 3 and 6 months changes in the volume of the chest wall in patients who had thoracotomy lobectomy and VATS lobectomy 243

6 LIST OF ABBREVIATIONS

OEP	Optoelectronic Plethysmography
SLP	Structured Light Plethysmography
EEV	End expiratory volume
LVRS	Lung volume reduction surgery
VATS	Video-assisted thoracoscopic surgery
EBV	Endobronchial valves
TEB	Thoracic epidural block
PVB	Paravertebral block
PPCs	Post-operative pulmonary complications
CG	Control group
CXR	Chest x-ray
COPD	Chronic obstructive pulmonary disease
URT	Upper respiratory tract
LRT	Lower respiratory tract
MRI	Magnetic resonance imaging
RIP	Respiratory Inductance Plethysmography
TTI	Transthoracic Impedance
PC	Pectus carinatum
Vt or TV	Tidal volume
IRV	Inspiratory reserve volume
ERV	Expiratory reserve volume
RV	Residual volume
VC	Vital capacity
FRC	Functional residual capacity

IC	Inspiratory capacity
TLC	Total lung capacity
FEV_1	Forced expiratory volume in one second
PPO	Predicted postoperative values
TLCO	Transfer factor for carbon monoxide of the lung
CO	Carbon monoxide
ATS	The American thoracic society
ERS	The European respiratory society
V	Volume
P	Pressure
ITGV	Intra-thoracic gas volume
RawTOT	Total airway resistance
Gaw	Airway conductance
sGaw	Specific airway conductance (sGaw)
IVC	inspiratory vital capacity
FVC	Forced vital capacity
CDH	Congenital diaphragamatic hernia patients
TI	Inspiratory time
TE	Expiratory time
$V_{E\ Mag}$	Ventilation measured by the electromagnetic coils
$V_{E\ Spiro}$	Ventilation measured by the spirometer
VO_2	Oxygen consumption
EE_{REF}	Energy expenditure measured by indirect calorimetry
EE_{Mag}	Estimate the energy expenditure by the electromagnetic coils
dMRI	Dynamic magnetic resonance imaging

2D	Two-dimension
3D	Three-dimension
NH	Normocapnic hyperpnea
ECG	Electrocardiogram
CPR	Cardiopulmonary resuscitation
FBG	Fibre-optic Bragg grating method
OFSETH	Optical Fibre Sensors Embedded into technical Textile for Healthcare
OR	Optical reflectance motion analysis system
SHFJV	Superimposed high-frequency jet ventilation
HFJV	Single-frequency (high-frequency) jet ventilation
NIV	Non-invasive ventilation (NIV)
NAVA	Neurally adjusted ventialator assist
PSV	Pressure-support ventilation
FIS	Flow incentive spirometry
VIS	Volume incentive spirometry
TDPR	Trans-diaphragmatic pressure reaction
CMAPs	Compound muscle action potentials
W	Whispering
R	Reading
SI	Singing
DMD	Duchenne muscular dystrophy
AB	Abdominal compartment
PND	Neuromuscular diseases
AS	Ankylosing spondylitis

RCP	Upper ribcage or pulmonary ribcage
RCA	Lower ribcage or abdominal ribcage
CW	The chest wall
RR	Respiratory rate
EIV	End inspiratory volume
IQR	Interquartile range
PC	Pectus carinatum
BMI	Body mass index
VENT	Emphysema palliation trial
CT	Computerised tomography
TA	Thoraco-abdominal
HRCT	High-resolution computed tomography
RC	Relative contribution
P	Patient
Min. vent	minute ventilation
MIF	Maximum inspiratory flow
MEF	Maximum expiratory flow
Meso	Mesothelioma
Cont	Control
Empy	Empyema
U	Upper
M	Middle
L	Lower
ITU	Intensive care unit
Pre-Op	Before surgery

SX (op)	Operated side
DX	Non-operated side
ASA	American society of anesthesiologists score
ECOG	Eastern Cooperative Oncology Group Scale of Performance Status
MRC	MRC breathlessness scale
MDT	Multi-Disciplinary Team
IV	Intravenous

7 Introduction

Measuring chest wall mechanics can be useful in some respiratory conditions (Aliverti A. R., 2005) (Aliverti A. S., 2004), but it can be used in assessing the effect of a number of thoracic diseases on chest wall motion as well as the effect of various thoracic surgeries and procedures on chest wall mechanics. The data generated by this assessment were the key to answering a large number of clinical and physiological questions that have challenged researchers in the past. Spirometry and pneumotachography are the current gold standard methods in assessing lung functions (British Thoracic Society and Society of Cardiothoracic Surgeons of Great Britain and Ireland Working Party , 2001) (British Thoracic Society, 2005). The major limitation of these methods is that both use mouthpieces, nose clips, and long connectors (Miller, et al., 2005)(Wanger, et al., 2005). These accessories disrupt normal breathing and increase dead space, which leads to overestimating tidal volume.

These limitations inspired researchers to investigate lung functions indirectly by measuring the effect of the change in lung volumes in overlying chest wall motion. This enabled them to use the change in chest wall motion in estimating changes in lung volumes (Aliverti, Dellaca, Pelosi, Chiumello, Pedotti, & Gattinoni, 2000).

In 1967, Konno and Meads were among the first to measure chest wall motion. They created a system that used threads that are attached to different parts of the chest and the abdomen at one end and to a pulley and a transducer at the other end to measure chest wall motion (Konno K. M., 1967). This opened the way for further development of similar systems that measure chest wall motion.

During the development of chest wall motion analysis technology, the researchers used a number of sensory systems. One example of these was the respiratory inductance plethysmography (Atkins, Mandel, Weinstein, & Mirza, 2010)(section 9.3.5), which used one or two coils to surround the chest and abdomen and attach to a transducer. Other sensory systems, which included magnetometers (Konno K. M., 1967) (section 9.3.3), fibre-optic sensors (Babchenko, 1999)(section 9.3.10), impedance plethysmography (González-Otero , et al., 2015)(section 9.3.7), strain gauges (section 9.3.9), and capacitive devices (Gramse, De Groote, & Paiva, 2003)(section 9.3.8), were utilised to assess zone, boundary, width or curve differences of one or limited specific cross-sections of the trunk used in monitoring breathing and investigation of trunk movement. The universal problem with these systems was that they interfered with natural respiratory mechanics; they could not be used in different postures and could only measure a cross-section of the chest wall rather than provide a global measurement of the whole chest wall. Detailed investigations of each of these limitations were discussed with each method.

These difficulties inspired researchers to develop and focus on optical technology. The major advantage of these optical systems was that they did not interfere with the normal respiratory mechanisms as they used a zero-contact method to measure chest wall motion. The two main examples of such systems were SLP and OEP (section 9.3.10.2). Although these systems had been used to measure chest wall motion in normal individuals and COPD patients (Aliverti, et al., 1997) (Aliverti A. R., 2005), they had never been used before to assess the effect of thoracic surgery and the underlying disease. Through the data generated by SLP and OEP, this paper aimed to answer a number of clinical and physiological questions that could not be answered by using conventional spirometry.

To answer these questions, a basic understanding of the anatomy and physiology of the chest wall is needed. This is covered in the first chapter of this thesis (Chapter 1). The second chapter sheds some details on the basic mechanisms used in chest wall motion analysis technology and how it has progressed through the years (Chapter 2). Then, there is a detailed view of methods used in this thesis, namely SLP and OEP (section 9.3.10.2).

In the remaining chapters, a number of clinical and physiological questions are answered. This first question is related to diaphragm paralysis and its corrective surgery, which is covered in Chapter 3. Unilateral diaphragm paralysis causes breathlessness due its paradoxical motion during respiration (Ko, 2009). Fixing the diaphragm in place through corrective surgery was the treatment for this. It was found that this treatment could lead to significant improvement in symptoms but the mechanism of this improvement is unknown. This chapter aims to examine the effect of unilateral diaphragm paralysis, the effect corrective surgery has on the chest wall motion and how it defines this mechanism of improvement, which cannot be identified using conventional spirometry alone. Chapter 4 examines the effect of chest wall cancer and the effect of chest wall reconstruction using a semi-rigid material

on chest wall mechanics. The type of material used in reconstruction is still a matter of great debate between surgeons; some advocate rigid and some advocate semi-rigid material. How this material copes with the state of quiet breathing and exercise is unknown. In addition, the effect of chest wall cancer on chest wall motion is still yet to be defined. Here, the effect of chest wall cancer on chest wall mechanics before surgery is examined as well as the effect of chest wall reconstruction using a semi-rigid material on chest wall mechanics both during quiet breathing and exercise.
Chapter 5 examines the effect of pigeon chest deformity, or PC, on chest wall mechanics. Patients with PC seek surgical intervention for cosmetic reasons. This corrective surgery is widely perceived to have low clinical value, and the physiological benefits of this surgery are unknown. The effect of PC on chest wall mechanics during quiet breathing and exercise is examined, along with the physiological effect of PC corrective surgery on chest wall mechanics during the same conditions after surgery. If a physiological benefit can be proven, it might change the indication criteria for what is perceived as cosmetic surgery.

Chapter 6 tackles a palliative procedure performed to improve breathlessness symptoms in patients with COPD. In this procedure, the diseased part of the lung is deflated using a one-way valve system (the EBV) to allow the remaining lung to expand. The only way to assess the success of the procedure is via radiological assessment of lung atelectasis. But this method lacks accuracy and cannot detect the success of the procedure in the immediate post-operative period. It is hypothesised that lung atelectasis in one part of the chest would be translated to a reduced chest wall motion on that part. The use of chest wall motion analysis technology is examined in assessing the success or failure of this lung volume reduction surgery by assessing its effect on chest wall motion.

Chapter 7 examines the effect of benign and malignant pleural disease on chest wall mechanics. The diagnosis of pleural disease is challenging due to the lack of specificity of the radiological methods currently used. Currently, a diagnosis can only be achieved through invasive surgery, which is considered to be a high-risk surgery for an elderly cohort of patients. This chapter examines how, via OEP, malignant pleural thickening affects the chest wall motion in a different way than the benign pleural effusion and how this can aid in the diagnosis of the condition.

Chapter 8 explores the early changes in chest wall motion after lung surgery and the effect of two types of analgesia on chest wall motion, namely, TEB and PVB. Theoretically, TEB is thought to result in a reduction in chest wall motion due to its bilateral blockage of the intercostal nerves. On this basis, it has been contraindicated in patients with pre-existing neurological diseases. This study aimed to examine the effect of TEB on the chest wall motor system and compare it to patients who receive no blockage to their nerves. On the other hand, PVB is thought to result in fewer pulmonary complications than TEB. It is thought that this is mainly due to a lesser reduction on chest wall motion after PVB. The effect of PVB on chest wall motion was examined and compared to the effect of TEB.

Chapter 9 explores the use of chest wall motion analysis technology to detect PPCs. The diagnosis of PPCs is problematic for two reasons: the delayed radiological evidence of the condition and the lack of accuracy of current scoring systems. It is hypothesised that, compared to a normal subject, chest wall motion differs in patients with PPCs due to reduced lung compliance. This paper aimed to explore these differences to help diagnose PPCs early after surgery.

Chapter 10 examines the late effect of VATS and open surgery (thoracotomy) on chest wall mechanics, with an emphasis on their effects on COPD patients. It is accepted that VATS is a less invasive surgery compared to open surgery. In addition, VATS results in a lesser degree of respiratory muscle damage and reduction in chest wall motion compared to thoracotomy. Based on the grounds that VATS has been advertised as superior to open surgery in some thoracic conditions, this hypothesis was examined to determine the effect of both procedures on chest wall motion.

Using SLP and OEP, this study aimed to evaluate the effect of different thoracic conditions as well as the effect of surgery on chest wall mechanics.

8 Chapter 1: The Respiratory System

To understand the chest wall mechanics in disease, a basic understanding of the respiratory system in normal individuals is needed. Therefore, this chapter introduces the basics of the respiratory system, focussing mainly on the physiology and the anatomy of the chest wall.

The main function of the respiratory system is gas exchange, which involves providing oxygen to the body and removing carbon dioxide. The respiratory system also acts as barrier to invading organisms and helps in the regulation of pH, blood pressure, and temperature. This system generates sounds through the act of phonation (Kumar & Clark, 2009).

8.1 The Anatomy of the Respiratory System

Anatomically, the respiratory system is divided into the upper respiratory tract (URT) and the lower respiratory tract (LRT) (Figure 1). The main function of the URT is to humidify and clean the air. It also contains the vocal cords, which are responsible for the act of phonation.

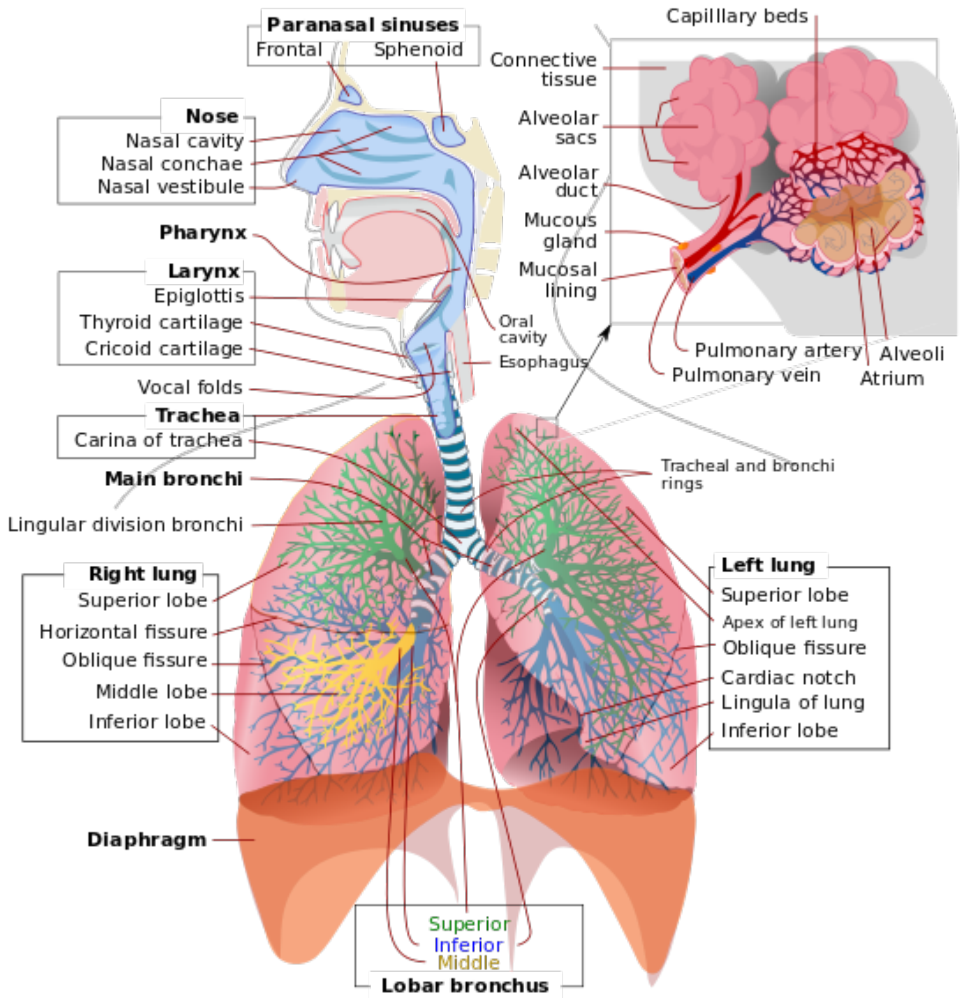

Figure1: Anatomy of the Respiratory System. Adopted from (Villarreal, 2007).

8.1.1 The Upper Respiratory Tract

The URT extends from the nose to the larynx. The nose provides passage for air to be warmed and humidified, and it filters and cleans the air via its hair follicles. It also aids in the act of phonation and has a sensory function, as it has olfactory receptors. The nose has high resistance to air flow; it actually accounts for 50% of respiratory resistance, which is twice as much resistance as provided by the mouth. Therefore, using the mouth for breathing during heavy exercise will reduce the work of the inspiratory muscles by half.

From the nose, the air passes through a nasal cavity that is divided into two halves by a bony septum. Each cavity has drainage openings for the facial sinuses. The cavity wall is rich with capillaries which help to thermo-regulate the air and has mucus-producing ciliated cells that help to stop any foreign particles from passing through. The cavity opens posteriorly into the pharynx.

The pharynx consists of a neso-pharynx, oropharynx, and laryngopharynx. The naso-pharynx represents an anatomical continuation of the nasal cavity and contains the same ciliated mucus-secreting cells that help further protect the respiratory tract from foreign material and pathogens. The oropharynx and laryngopharynx are both pathways for air and food.

Attached to the laryngopharynx is the larynx, which serves as a voice generator and a modulator for the passage of food and air. Moderating the voice is mainly achieved by modifying the tension of the vocal cords via their attached laryngeal muscles. The epiglottis is in opening of the larynx and is a tongue-like structure that closes and protects the larynx during the act of swallowing (Kumar & Clark, 2009).

8.1.2 Lower Respiratory Tract

The LRT extends from the trachea via the bronchi to the lungs. The trachea, commonly known as the windpipe, is a C-shaped hyaline tube that connects the larynx to the bronchi. This has a pseudo-stratified ciliate columnar epithelium. The hyaline cartilage surrounds the trachea from three directions anteriorly and laterally, which ensures the trachea remains open all the time.

Posteriorly, the trachea is made of longitudinal, smooth muscles that separate the trachea from the oesophagus. The trachea also has ciliated epithelium on these cells to repel foreign material towards the larynx, which then can be diverted to the gastrointestinal tract, where it can be digested.

The trachea divides into two bronchi, and each bronchus delivers air to one lung. At this stage, they are called primary bronchi. These branches then further divide into secondary bronchi to supply segments of the lobes of the lungs. These secondary bronchi further divide into smaller bronchioles that supply even smaller segments of the lungs. These smaller bronchioles further divide into terminal bronchioles, which are a millimetre in diameter. Millions of these bronchioles deliver air to the alveoli. The original C-shaped hyaline cartilage of the primary bronchi gradually disappears as it divides into secondary bronchi and tertiary bronchi and is replaced by elastic tissue and smooth muscles. Eventually, all the cartilage disappears as the bronchi further divide into bronchioles. The main function of the smooth muscles in these terminal bronchioles is the regulation of airflow. In the event of increased air flow, these muscles contract to prevent hyperinflation. In the event of reduced air flow, these muscles relax to increase the calibre of the bronchioles to allow more air to enter. Similar to the bronchi, these bronchioles are lined with ciliated epithelium that helps clear the airway from foreign material by trapping it in its mucus secretions and expelling it in the direction of the larynx. Each of these ciliated cells has approximately 200 cilia that beat at 1,000 beats per minute. Thus, the air that reaches the lung has been cleaned, warmed, and humidified.

The chest cavity is almost entirely filled by the lungs. The left lung is smaller than the right lung. The left lung consists of two lobes, and the right lung has three lobes. The smaller size of the left lung is due to the presence of the heart, which occupies the left chest cavity. The chest cavity and lungs are covered with the pleura. The visceral pleura cover the lungs, go into the fissures and cover the hilum and continue as parietal pleura to cover the chest wall. A pleura is made of connective tissue and is covered with simple squamous epithelium. The pleural space is a potential space between these two layers and is negative in pressure to allow passive lung expansion. This pleural space is filled with a thin fluid that provides lubrication for the lungs. The lung parenchyma is made of spongy tissue covering the total surface area of each lung (40-80 m^2) and consists of approximately 300 million alveoli. This provides a massive area for the exchange of oxygen and carbon dioxide. Each alveolus is lined by an epithelial layer made mainly of Type I pneumocytes. These cells are very thin and, as a result, they provide an ideal surface for gas exchange. Type II pneumocytes cover a minority of the alveoli space, but they have the important role of producing the surfactant. The main function of the surfactant is to reduce the surface tension of the alveoli to prevent their collapse. The presence of macrophages in the alveoli adds to the defensive properties of the respiratory system.

Each of the 300 million alveoli has its own pulmonary capillary. The alveoli, together with their capillaries, form the functional unit of the lung. Every 6 to 20 alveoli is supplied by a mixed venous blood through a single pulmonary artery. This is further divided into a network of capillaries that surround each alveolus (Kumar & Clark, 2009).

8.1.3 The Functional Structure

In terms of function, the respiratory system can be divided into a conductive part and a ventilatory part.

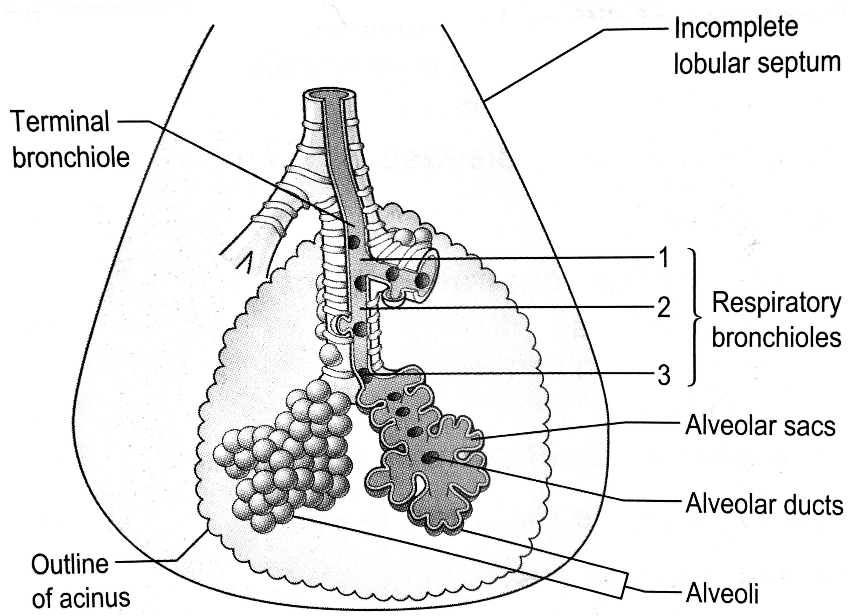

Figure 2 Branches of terminal bronchiole ending in the alveolar sacs (Kumar & Clark, 2009).

The conductive part offers a channel used to deliver air to the areas for gas exchange and consists of all parts of the respiratory tract between the nose and the terminal bronchioles. These channels consist of 16 generations of respiratory bronchi. Although the nose provides 50% of respiratory tract resistance, the rest of the conductive part of the airways provides resistance to the remaining respiratory tract.

The diffusion of oxygen and carbon dioxide occurs in the respiratory part of the airway. It starts at the bronchioles and ends in the alveoli (Figure 2). It consists of a further seven generations of air tracts (ending in the 23rd generation). This area of the respiratory tract is ideal for the exchange of gases between the lung and the blood, as the air in it runs at a very slow speed and provides a minimal resistance to that flow (Davies & Moores, 2010).

8.1.4 The Pulmonary Blood Supply and Lymph Drainage

Very thin branches of the pulmonary artery run along the bronchi. These further divide into very thin arterioles that run with respiratory bronchioles. Pulmonary venules originate in the periphery of the lobules; then, it make it’s way to the septum of lobules and from that segment to form a larger vein, which eventually makes up the pulmonary vein. Each lung has a pair of these veins that drain into the heart. Further arterial supply for the lung originates from the aorta; this supplies the bronchial tree up to the respiratory bronchiole. This blood is oxygenated, supplies the lung tissues, and is an integral part of the physiological shunt of the lung. The lymphatic of the respiratory system runs in a small interstitial space in the connective tissue between the alveolar cells and the alveolar capillaries (Davies & Moores, 2010).

8.1.5 The Neural Supply for the Lung

The lungs obtain a parasympathetic nerve supply from the vagus nerve and a sympathetic supply from the sympathetic chain. These nerves run alongside the pulmonary arteries and the associated air passages. The vagus nerve supplies all the smooth muscles of the airway (Davies & Moores, 2010).

8.2 Lung Volumes and Capacities

Ventilation is the act of air exchange in the lung. This exchange is affected by the metabolic state of the body and the act of coughing and speaking. In the quiet breathing state, this exchange is fractional compared to what occurs during exercise. During rest, the ventilation has an equilibrium state. With the use of the respiratory muscles during inspiration and expiration, the lung can reach a maximum inspiratory and expiratory volume, respectively. At these two points, the lung reaches a new equilibrium between the negative pressure in the intra-pleural generated by the actions of the respiratory muscles and the elastic recoil forces of the lung. The volumes and capacities depend on a number of factors, which include age, gender, sex, and height. Classically, depending on its status during rest and respiratory muscle contraction, the lung’s volume and capacity can be divided as shown in Figure 3.

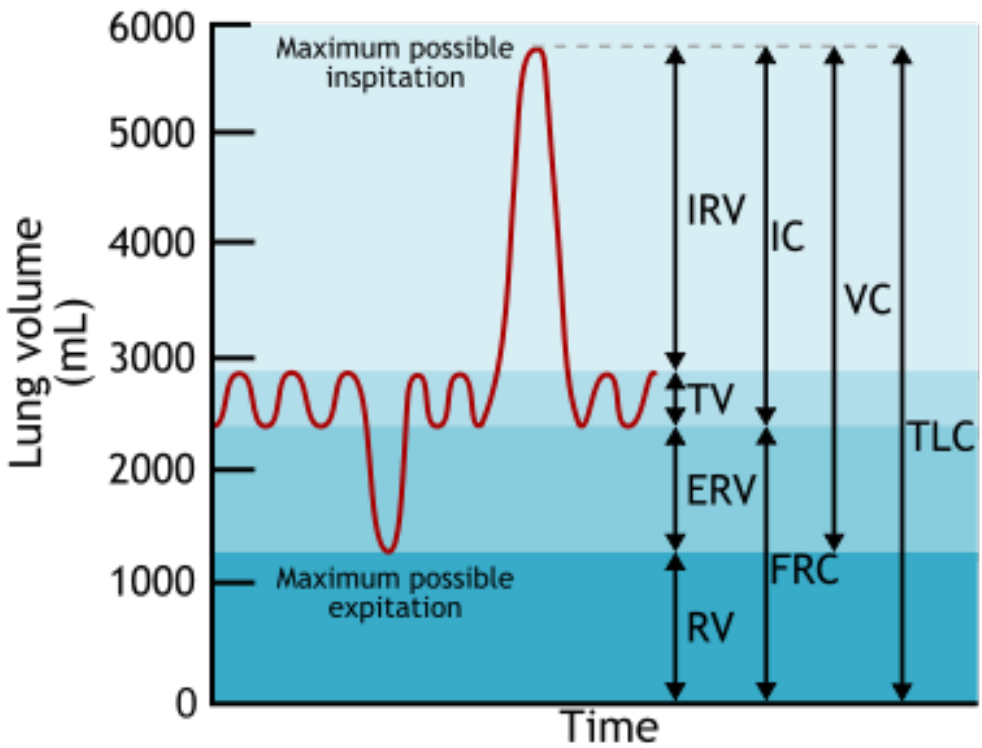

Figure 3: Schematic representation of lung volumes and capacities (Spirogram). Adopted after permission (Komorniczak, 2009).

The Tidal Volume [TV] is the volume of air that moves in and out of the lung during quiet breathing. This is normally around 500 ml.

The Inspiratory Reserve Volume (IRV) is the greatest volume that can be inspired actively from the level of the end inspiratory volume. This is usually around 2,500 ml. This reserve can be utilised during strenuous activity.

The Expiratory Reserve Volume (ERV) is the greatest volume that can be expired actively from the level of the end expiratory volume. This volume is around 2,000 ml. This reserve volume can be utilised in an actively of an increased respiratory demand, e.g. shouting.

Residual Volume (RV) is the volume of air that is left in the lungs after full expiration. This is usually around 1,500 ml. The structure and the rigidity of the chest wall and ribs prevent all the air from being expelled from the lungs.

The Vital Capacity (VC) is the amount of air inspired from the level of full expiration. This is around 5,000 ml. This volume is made up of TV, ERV, and IRV. These values vary between individuals. The variation in VC between individuals depends on the variation of TV, ERV, and IRV.

$$\text{Vital Capacity} = \text{ERV} + \text{IRV} + \text{TV}$$

The Functional Residual Capacity (FRC) is the volume of air that is left in the lungs after passive expiration. This is usually around 3,500 ml, which represents around one third to one half of the VC. The FRC is calculated by adding RV and ERV.

Functional Residual Capacity = RV + ERV

The Inspiratory Capacity (IC) is the amount of air that fills the lungs when a person inspires forcefully from a position of passive expiration. This is around 3,000 ml.

Inspiratory Capacity = IRV + TV

The Total Lung Capacity (TLC) is the total amount of air that both lungs are able to hold. This is about 5,800 ml in men and 4,200 ml in women. This consists of RV plus VC.

$$\text{Total Lung Capacity} = RV + VC$$

The Forced Expiratory Volume in one second (FEV_1) is the volume of air expired from the lung forcefully during one second. This value is an important value to determine a patient's suitability for lung resection. This value is usually low in patients with obstructive lung disease, such as COPD or asthma.

All the above values vary with height, gender, and age. Therefore, the reference range is different for different individuals but is crucial in differentiating healthy and diseased individuals (Stocks & Quanjer, 1995).

8.3 Anatomy and Physiology of the Chest Wall

8.3.1 The Chest Wall Skeleton

The chest wall is composed of 12 pairs of ribs and attached costal cartilages, a vertebral column, intercostal muscles, and a sternum (Figure 4). The first through seventh rib each connects to the sternum by an individual costal cartilage. From the 8^{th} to the 10^{th} rib, every two ribs connect to the sternum with a common costal cartilage. The 11^{th} and 12^{th} ribs are floating ribs, as they have no anterior connections (Standring, 2008). This design of the ribs allows for maximum chest wall expansion. The curving nature of these ribs allows them to have some shock absorbance quality when faced with blunt trauma. The chest wall acts as a shield that protects important internal organs, namely, the lungs, the heart, and the liver. It also acts as an anchor for the upper limbs to allow complex movement. The action of the chest wall provides approximately 20,000 breaths every day. The rib cage and the abdomen are the two main compartments of the chest wall and are separated by the diaphragm. Lung expansion can occur in either component of the chest wall or in both at the same time. Any malfunction of this expansion can lead to severe morbidity.

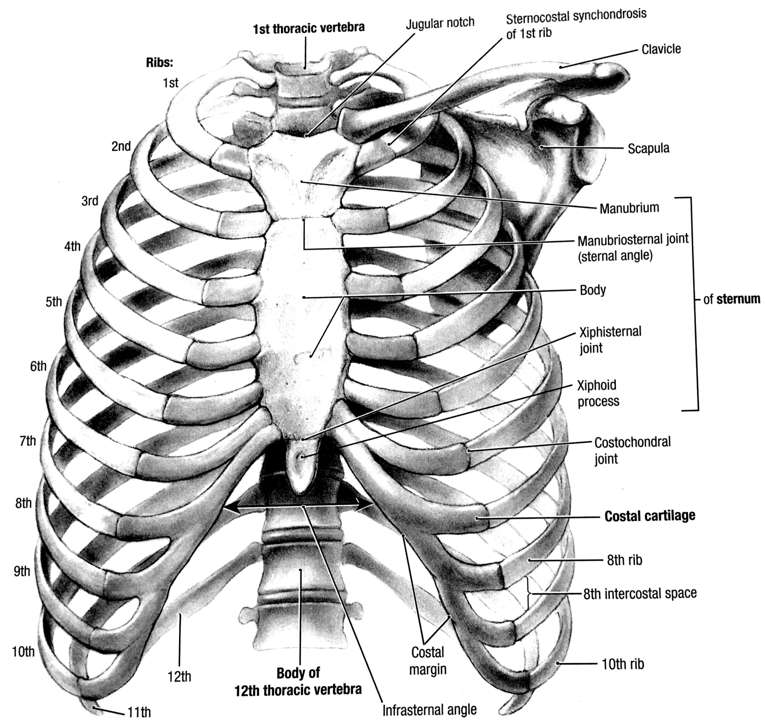

Figure 4: The thoracic skeleton, anterior view (Agur & Dalley, Thorax, 2013)

An important surface anatomy mark of the chest is the sternal angle, which is the joint between the sternum and the manubrium. This angle is approximately 162 degrees but has a large variation. This angle marks the second intercostal space, which is the crossholding area of the tracheal division and the level of the T4 vertebral body.

8.3.2 The Chest Wall Musculature

The muscles involved in respiration change the vertical, horizontal, and deep dimensions of the chest wall during contraction. This action dictates the motion of the air to or from the lung. In addition, the diaphragm acts as a piston in relation to the chest cavity acting like a cylinder (Naidu B., personal communication, 2010). The relaxed diaphragm is dome-shaped and as the diaphragm contracts, it descends like a piston in a cylinder, generating negative intra-thoracic pressure, which allows lung expansion. This descent is accompanied by an upward and forward motion of the lower ribs, which further increases lung expansion. The down motion of the diaphragm increases the intra-abdominal pressure, which helps to support the spine.

From a functional point of view, the muscles of respiration can be divided into inspiratory muscles and expiratory muscles. The expiratory muscles include the internal intercostal muscles and the muscles of the abdomen. The inspiratory muscles are the external intercostal muscles, the diaphragm, and the sternocleidomastoid (Agur & Dalley, 2013)

8.3.3 The Diaphragm

The diaphragm is the primary muscle of ventilation. It is a dome-shaped structure with a surface area of 250 cm^2 and is composed of a peripheral muscular tissue and a central tendon. The diaphragm originates from the crura, arcuate ligaments, the ribs, and the sternum. Due to the presence of the liver, the right hemi-diaphragm is in a higher position than its contra-lateral part. All the muscles of the diaphragm come together in the central tendon.

This tendon is in continuation with the pericardium (Figure 5). The diaphragm is lined with the peritoneum in its inferior surface and the pleurae in its superior surface. The sensory and motor innervation of the diaphragm is energised by the phrenic nerve; each hemi-diaphragm is supplied by one phrenic nerve. Paralysis of the hemi-diaphragm leaves it in a resting position, which is an elevated dome-shaped state. The motion of this paralysed diaphragm is paradoxical to the respiratory cycle, as it descends during expiration and ascends during inspiration. This compromises the inspiratory and expiratory ability of the lungs (Standring, 2008). Normally, the diaphragm descends by 1 to 2 cm during normal breathing inspiration. This leads to a 200-ml increase in the thoracic cavity volume. During forced inspiration, this descent can reach 10 cm. This generates an extra 400 ml of thoracic cavity volume.

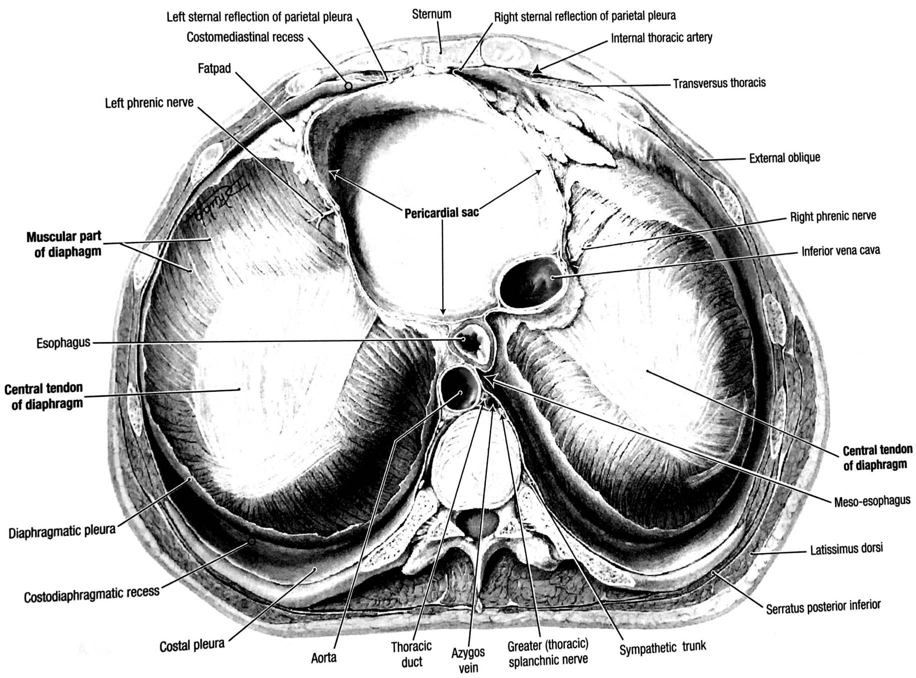

Figure 5: Superior view of the diaphragm and related structures (Agur & Dalley, 2013)

Because of the required expansion, the primary muscle of respiration of the diaphragm is equipped with an extensive blood supply which varies with the respiratory cycle. The blood supply is at maximum during passive expiration when the diaphragm is in the resting position. During inspiration, the diaphragm contracts and applies pressure on its own blood supply, reducing it in the process. The resting position is important for the function of the diaphragm because it allows the blood to return to its maximum (Robertson, Eschenbocher, & Johnson, 1977). As the diaphragm works, the blood supply increases up to 20-fold.

A human breathes around 20,000 breaths per day, which is, to a large degree, credited to the work of the diaphragm. This necessitates an energy system that is efficient and can sustain working for life. This is the reason the majority of the cells that make up the diaphragm (55%) are Type1 slow muscle fibres, which resist fatigue. The Type II muscle fibres are fast muscles fibres and are used mainly when the respiratory demand increases (Rochester, 1985).

8.3.4 The Intercostal Muscles

There are 11 intercostal muscles in 11 corresponding intercostal spaces, as seen in Figure 6.

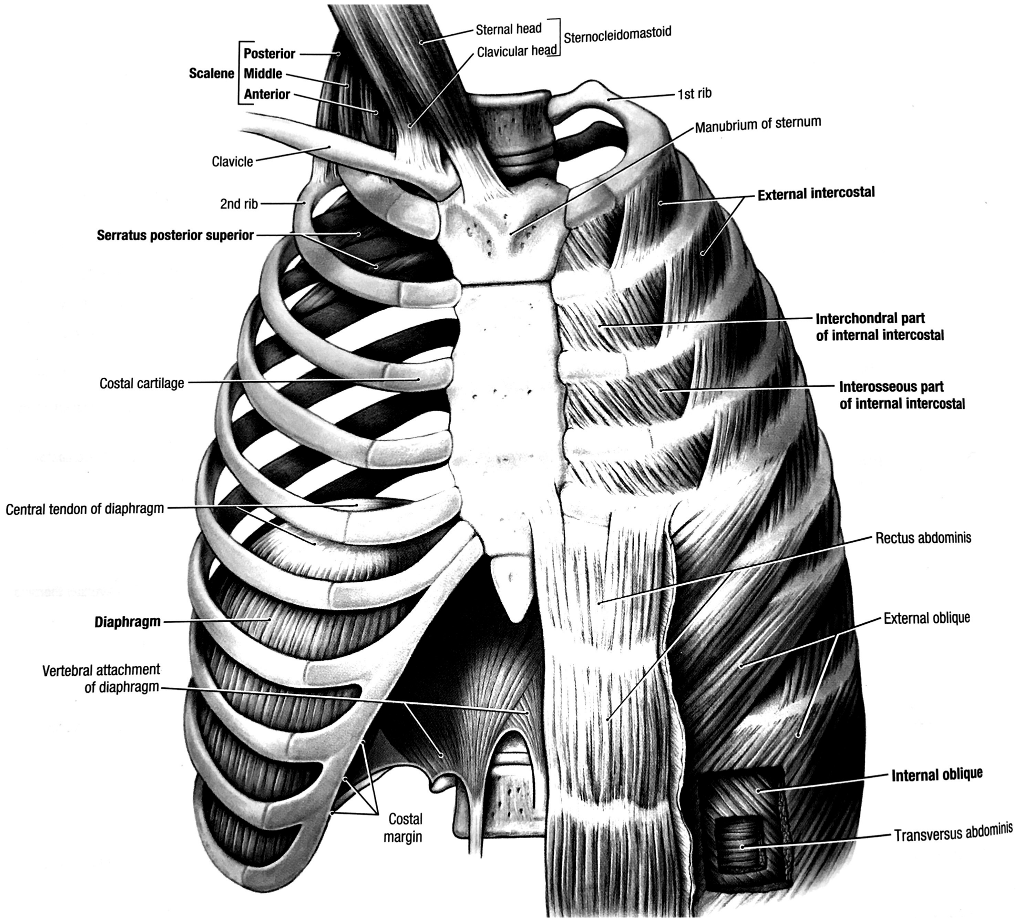

Figure 6: Muscles of respiration (Agur & Dalley, 2013)

<u>The External Intercostal Muscles:</u> These originate in the lower border of the upper rib and insert on the upper border of the lower rib, except for on the 12th rib, where they become a continuation of the external oblique muscle of the abdomen. There are 11 muscles situated between the 1st and 12th rib. The direction of these 11 muscle fibres is forward and downward.

<u>The Internal Intercostal Muscles:</u> As the name suggests, these muscles lie deep to the external intercostal muscles. They originate from the upper border of each rib (except for the first rib) and insert on the lower border of the rib below. They occupy the same intercostal spaces as the external intercostal muscles. These muscle fibres lie in an oblique direction going forward and

upward. The lowest internal oblique muscle is a continuation of the internal oblique of the abdomen.

The Innermost Intercostal Muscle: This is usually an incomplete layer of muscle that lies deep in the neurovascular bundle and internal intercostal muscle but runs in the same direction. Part of this layer is the infra-costal group of muscles. These muscles originate from the lower ribs and insert in the second and third ribs' lower borders.

The intercostal muscles involved in inspiration are the external intercostal muscles. These fibres lie in an oblique direction going forward and downward. The contraction of these muscles causes elevation of the ribs in a bucket-handle-type movement. This movement increases the antero-posterior, vertical, and horizontal diameters of the thoracic cavity. These contractions also make the thoracic wall rigid. This rigidity is important to prevent the chest wall from collapsing due the negative pressure that is generated by the downward movement of the diaphragm during its contraction. Thus, this rigidity helps stabilise the chest wall and maintains the negative pleural pressure needed for lung expansion.

The Abdominal Musculature: The abdomen has four main muscles that are situated in three different layers of the abdominal wall. These muscles are the internal and external oblique muscles, the transverse abdominis, and the rectus abdominis muscle (Figure 7).

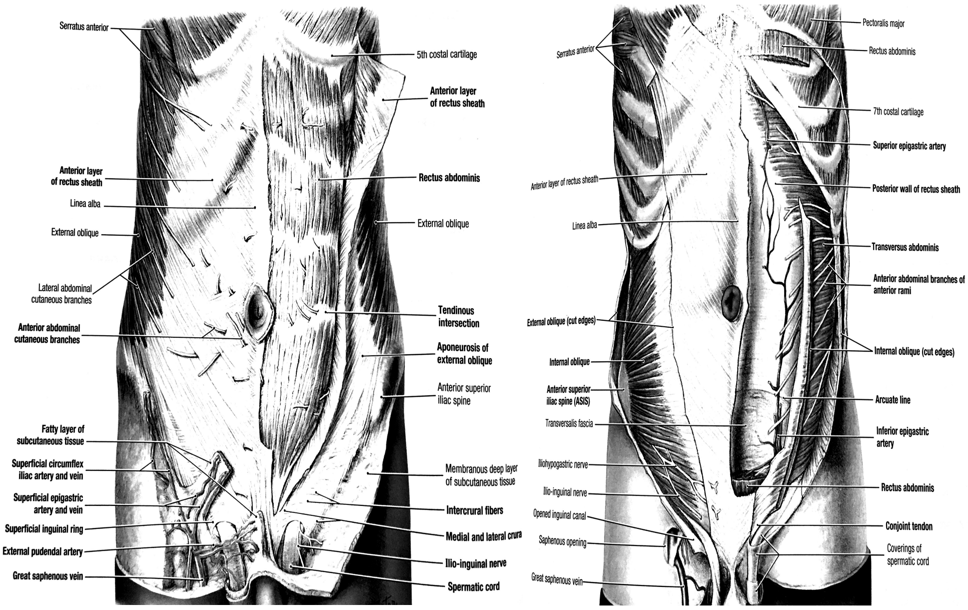

Figure 7: Abdominal muscles (Agur & Dalley, 2013)

The contraction of the abdominal muscles is important in expiration. As these muscles contract, a high pressure in the abdomen is generated that causes elevation of the diaphragm. This elevation increases the intra-thoracic pressure leading to the expiration of air. In addition, these muscles create support for the spine. As these muscles contract and increase the abdominal pressure, this stabilises the spine. During contraction, these muscles aid in placing the diaphragm in the ideal position at the onset of inspiration (Standring, 2008).

8.4 The Physiology of the Chest

The act of breathing requires co-ordination of both the inspiratory and the expiratory muscles; this has to be synchronised to avoid any ventilatory dysfunction. The act of inspiration is an active act. It occurs in a number of steps. Initially, there is the contraction of all inspiratory muscles, which elevates the rib cage and increases all of its three dimensions. This is possible due to the bucket-handle movement of the ribs. Simultaneously, the diaphragm contracts and flattens. The result of all these movements is an increase in the volume of the chest cavity. This results in increasing the size of the lungs. As a result, the pressure inside the lungs drops to -1 mm Hg. This pressure sucks air into the lungs until the pressure normalises with the atmospheric pressure, which is essentially 0 mm Hg.

The act of expiration during quiet breathing is a passive act (Figure 8). It begins with the relaxation of the inspiratory muscles. At the same time, the diaphragm relaxes and assumes its resting dome-shaped position. The recoiling character of the costal cartilage allows it to return to the resting position. This leads to the reduction of the volume of the chest cavity. The lungs decrease in volume under the effect of its elastic recoil force. This increases the pressure in the lungs to 1 mm Hg. The pressure gradient between the lung and the atmosphere (0 mm Hg) causes the air to be expired from the lung. Expiration ends when the lung pressure is equal to the atmospheric pressure.

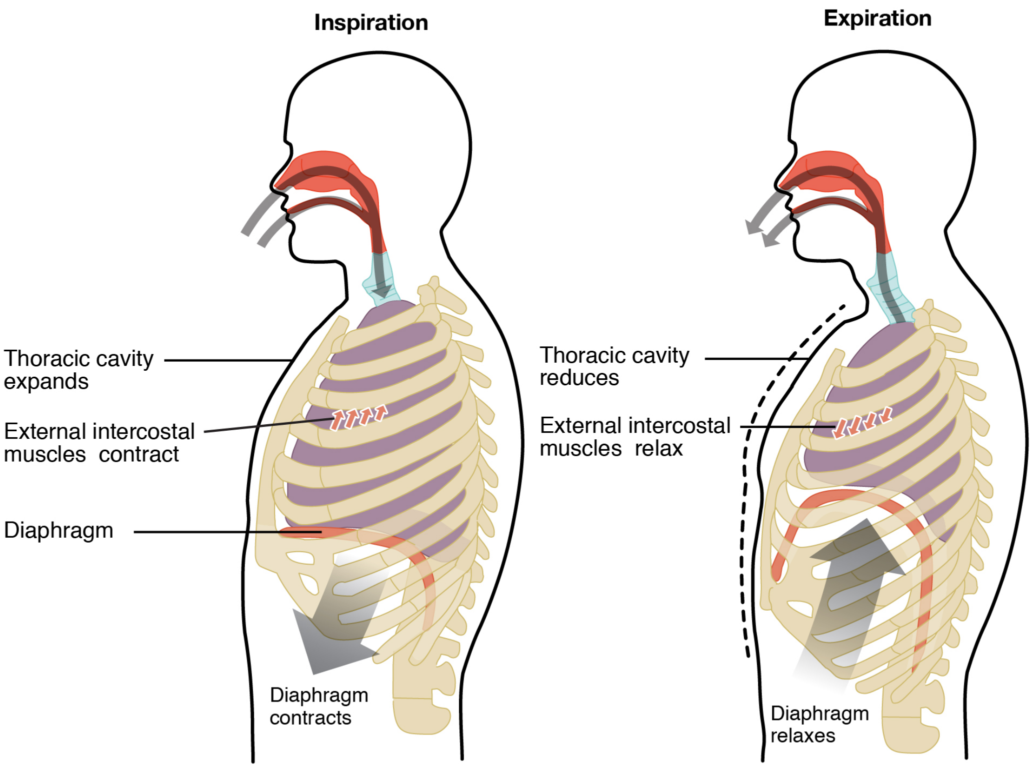

Figure 8: Change in antero-posterior and superior-inferior dimensions (left) and change in lateral dimensions (right) during expiration. Adopted from (OpenStax College, 2013)

9 Chapter 2: Measurement of Chest Wall Motion

9.1 Current pre-operative physiological tests in thoracic surgery: what they measure, how they measure it, and what their benefits and limitations are

In the UK every year, around 500 pneumonectomies and 2,400 lobectomies are performed for lung cancer. These procedures have considerable risk of mortality that ranges between 2% and 8% (Gould & Pearce, 2006). To reduce this risk, the operative option for lung cancer should only be considered if the selection criteria have been met. These include assessment of pre-operative respiratory function, along with functional status and cardiovascular fitness (British Thoracic Society and Society of Cardiothoracic Surgeons of Great Britain and Ireland Working Party , 2001).

Pre-operative respiratory function is measured by basic spirometry. This is the most common and useful lung function test in clinical practice. During forceful exhalation from maximum inhalation, the spirometer measures the amount of air exhaled at different time points.

Spirometers can be divided based on their principle of measurement into pneumotachograph spirometers, turbine spirometers, and ultrasound spirometers. Pneumotachographs use the Venturi effect to measure flow. According to the Venturi effect, if the flow is forced into a narrow area, its pressure drops and its velocity increases. The pneumotachograph measures this pressure drop and uses it to calculate flow. Pneumotachographs can be further divided into Fleisch and Lilly types. The Fleisch type uses capillaries and measures the difference in their pressures. The Lilly type uses a membrane with identified resistance. On the other hand, turbine spirometers use a rotating turbine to quantify forced expiratory flow. Infrared light is used to measure this rotation, which is converted to flow through various calculations. Recently, ultrasound spirometers were introduced, which use ultrasound waves and the Doppler effect to measure flow.

During spirometry measurement, the best value of FEV_1 and forced vital capacity (FVC) is recorded after optimum bronchodilator treatment. This value is normalised to the gender, height, age, and race of the patient. Flow volume loops are obtained as part of the assessment.

Spirometry is exceptionally valuable in clinical practice. It is very reliable in differentiating between restrictive and obstructive lung disorders. It is also the most reliable technique for diagnosing and defining the severity of COPD (British Thoracic Society, 2005). It is also used to diagnose asthma, monitor the disease progression, and respond to treatment for a number of chronic respiratory diseases. In addition, it has been used to measure hyperinflation and dynamic hyperinflation through measuring the IC (Stubbing, Pengelly, Morse, & Jones, 1980) (Marin, Garrizo, Gascon, Sanchez, Gallego, & Celli, 2001). In thoracic surgery, it is used as one of the parameters for the selection of patients with lung cancer for surgery; this was first achieved by assessing the lung function before surgery and by predicting the lung function after surgery (British Thoracic Society and Society of Cardiothoracic Surgeons of Great Britain and Ireland Working Party, 2001). Predication of lung function after surgery can be achieved by calculating the predicted post-operative values (ppo) of FEV_1 and FVC. These calculations take into account the number of segments in each lung (10 on the right and 9 on the left). Depending on how many segments are planned to be resected, the $ppoFEV_1$ and ppoFVC can be calculated by dividing the number of segments to be removed by the total number of segments (19) and multiplying that by the values of pre-operative FEV_1 and FVC, respectively. This calculation assumes that all segments contribute equally to ventilation and overall lung function.

Ventilation of lung is assessed using ventilation perfusion scans, which can give the percentage function of each part of the lung. Patients who undergo these scans inhale radioactive xenon and are given intravenous technetium-labelled macro-aggregates. Then, a gamma camera measures the perfusion of the technetium and the radioactive lung uptake. This radioactive uptake correlates with ventilation and function of the lung. Therefore, $ppoFEV_1$ and FVC can be calculated even more accurately by taking ventilations of segments into account. For example, $ppoFEV_1$ can be calculated using the following equation: $ppoFEV_1$ = pre-operative FEV_1 x % radioactivity of the lung. This value is used in thoracic surgery to evaluate patients with suboptimal spirometry results in order to decide about patient suitability for lung resection (British Thoracic Society and Society of Cardiothoracic Surgeons of Great Britain and Ireland Working Party , 2001). A ventilation perfusion scan is also used in clinical medicine to diagnose a pulmonary embolism.

Another test that is used pre-operatively is the test for the transfer factor for carbon monoxide of the lung (TLCO), which measures the capability of the lung to exchange gas across it alveolar-capillary membranes. This test is done by instructing the patient to inhale a tracer gas from a gas source, to do a breath-holding manoeuvre for 10+/-2 seconds, and then to expire into a gas analyser. The amount of carbon monoxide (CO) in the gas is then measured, from which the TLCO can then be calculated (MacIntre, et al., 2005). In thoracic surgery, this is used to assess patients who are not clearly operable based on their spirometry results alone (i.e. FEV_1 =/< 2.0 L for pneumoectomy and =/< 1.5 L for lobectomy) (British Thoracic Society and Society of Cardiothoracic Surgeons of Great Britain and Ireland Working Party, 2001). In addition, TLCO is used in clinical medicine to help diagnose a number of conditions that can affect the alveolar-capillary surface, which include lung fibrosis, vasculitis, restrictive lung disease, emphysema, pulmonary embolism, and pulmonary hypertension.

In some patients who have suboptimal $ppoFEV_1$, exercise testing in the form of a shuttle walk test is indicated. The test involves walking between cones spaced 10 m apart; this distance is to be walked within a specific time, and the pace is set by a beep. As the test progresses, the pace is increased to test the limits of the patient. This corresponds to a minimum walking speed of 1.9 km/hr and maximum of 8.5 km/hr. Oxygen saturation is monitored during the test. The number of the 10-m shuttles and the oxygen saturation are recorded. If the patient can perform < 25 shuttles or his or her desaturation level is > 4% then he or she is considered to be at a high risk for surgery. If the patient can walk > 25 shuttles and has a desaturation < 4%, then a full cardiopulmonary exercise test is indicated (British Thoracic Society and Society of Cardiothoracic Surgeons of Great Britain and Ireland Working Party, 2001).

One of the limitations of spirometry is that it is an effort-dependent measurement and requires a patient's full co-operation. If the patient effort is suboptimal, there is a high probability for an error in the result (Miller, et al., 2005). Providing the patient with detailed clarifications of the technique before blowing into the spirometer followed by effective encouragement during the procedure results in more accurate and reliable results (Miller, et al., 2005).

Another limitation of spirometry is that it is physically demanding. For this reason, the American Thoracic Society (ATS) and the European Respiratory Society (ERS) recommended that the spirometry test should be avoided in any patient with abdominal or chest pain within one month of a myocardial infarction and, any patient with oral or facial pain (as it will be aggravated by the mouthpiece), any patient with dementia or confusion, and any patient with stress incontinence (Miller, et al., 2005). In addition, spirometry is contraindicated after recent thoracic surgery as it might lead to pain, discomfort, or the rupture of the site of the lung incision (Cooper, 2011).

The limitations of the ventilation profusion scan are that it does not measure the lung volumes or the chest wall motion. In addition, due to the radiation risk, breastfeeding should be interrupted because some types of radioactive materials are used as part of the ventilation perfusion scanning (Parker, et al., 2012).

A limitation of the diffusion capacity testing is that it requires a patient's co-operation to perform the breath holding manoeuvre. In addition, the test does not measure chest wall motion or lung volumes.

9.1.1 *Whole Body Plethysmography*

In 1956, Dubols et al. described whole-body plethysmography based on Boyle's law, according to which the volume (V) of a gas at a constant temperature varies in inverse proportion to the pressure (P) to which it is subjected, with P × V remaining constant (Dubols, 1956) (West, 2004). Spirometry (Miller, et al., 2005) is the most commonly used method to assess lung function in clinical practice and is considered the gold standard in lung function. It cannot, however, provide information on lung RV and TLC, while body plethysmography allows for the evaluation of these and other characteristics such as intra-thoracic gas volume (ITGV) (Criee, et al., 2006) (Coates, 1997) (DuBois, 1956) (Stocks, et al., 1996) (Stocks, et al., 2001) (Goldman, 2001) (Wanger, et al., 2005). Thus, plethysmography remains an essential technique in the assessment of lung function. It measures several gas volumes, such as ITGV, FRC, RV, and TLC (Wanger J. , 2012) (Goldman, 2005). The addition of two or more lung volumes makes up lung capacity. This technique also measures total airway resistance (RawTOT), specific airway resistance (sRaw), airway conductance (Gaw), and specific airway conductance (sGaw). Unlike other techniques such as nitrogen washout or helium dilution that underestimate the FRC because they do not measure poorly ventilated or unventilated spaces (bullae), plethysmography measures the full volume of intra-thoracic gas.

Moreover, whole body plethysmography undertakes some of these measures during breathing at rest and not by forced manoeuvres. Given the differences in measuring conditions and information provided, body plethysmography and spirometry add to each other, and a complete measurement cycle of plethysmography even includes spirometry (Figure 9).

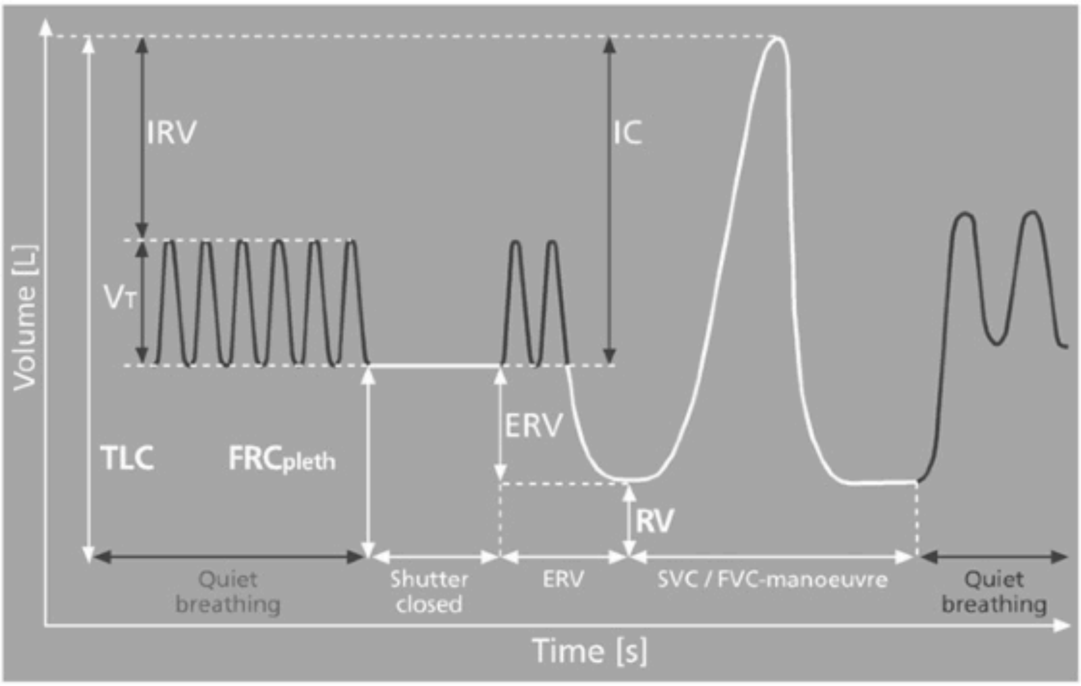

Figure 9: Volume-time display showing the following sequence: quiet breathing for recording specific airway resistance loops, a period when the shutter is closed for the determination of FRC_{pleth}, and subsequently a period during which the patient performs an expiratory reserve volume (ERV) manoeuvre, followed by a slow vital capacity (SVC) manoeuvre in order to determine inspiratory vital capacity (IVC) and derive residual volume (RV) and total lung capacity (TLC). Commonly this is followed by a forced vital capacity (FVC) manoeuvre that also yields the forced expiratory volume in 1 s (FEV_1) and the maximum expiratory flows (MEFs) at different lung volumes. Adopted from (Criee, et al., 2011).

Whole body plethysmography's equipment

It must include:

- Airtight chamber (two models: older children/adults; infants).
- Pneumotachograph. It must meet the standards for spirometric devices (ATS/ERS 2005 [Wanger J., 2005]) and be capable of measuring volumes of 0.5-8.00 L with an accuracy of ±3% as calibrated with a 3.00 L syringe, flows between 0 and 14 L/s, and recording durations of at least 30 s.
- Shutter valve and pressure transducer to measure pressure changes at the mouth. The pressure transducer must have a sensitivity greater than 50 cm H_2O and a flat frequency response in excess of 8 Hz.
- Pressure transducer inside the plethysmograph chamber (constant-volume variable-pressure plethysmographs) to measure the pressure within the chamber. In some systems, another pneumotachograph is placed on the plethysmograph wall to measure volume changes inside the chamber (constant-pressure variable-volume plethysmographs). It must be accurate to ± 0.2 cm H2O.
- Computer, printer, and weather station (depending on the equipment).
- Mouthpieces with disposable in-line filters 99% effective in filtering out viruses, bacteria, and mycobacteria. Dead space of less than 100 mL and a resistance lower than 1.5 cm H2O to a flow of 6 L/s.

Calibration

Flow metres should be calibrated following the protocol established by the manufacturer and adhering to the ATS/ERS 2005 spirometry standards (Miller , et al., 2005). Plethysmographs usually have automatic calibration systems (chamber seal and transducer alignment).

Commonly, the determination of lung function by body plethysmography starts with breathing at rest, followed by the shutter manoeuvre. It is commendable to continue this with spirometric measurements. After opening the shutter, an ERV effort and an IVC effort are performed; this allows the computation of RV and TLC. If possible, this should be followed by a prolonged forced expiration to determine the FEV_1 and the FVC. In this way, information on lung mechanics during normal and forced breathing could be obtained in a single sequence of linked measurements.

The main indication of plethysmography is the diagnosis and characterisation of restrictive ventilatory patterns (assessment of disease severity, course of disease, and response to treatment). It can also be used to assess the severity of restriction in diseases with a mixed ventilatory pattern and airflow limitations. It allows the measurement of unventilated air compartments (subtracting the FRC measured by plethysmography from the FRC measured by helium dilution) and risk assessment for surgery (for instance, for pneumonectomy). It can be performed successfully starting at 6 years of age.

The assessment of TLC is considered indispensable in the diagnosis of restrictive disorders, which are defined as TLC being below the fifth percentile of normal values. A restrictive disorder can be suspected from spirometry when VC is reduced, and the ratio of FEV_1 to VC (FEV_1/VC, Tiffeneau; VC either FVC or IVC) is normal or elevated. It is definitely proven, however, only by a decrease in TLC (American Thoracic Society , 1991). The recommendations for the diagnostic use of these indices have been given in the literature (Criee, et al., 2006) (Goldman, 2005) (Wanger J., 2005) (Quanjer, 1993) (Miller, et al., 2005).

The determination of RV and RV%TLC also allows evaluating for the degree of lung hyperinflation. Values of RV or an RV/TLC ratio above the 95th percentile but below 140% predicted are indicative of mild hyperinflation; values between 140% and 170% predicted indicate moderate hyperinflation; and values above 170% predicted indicate severe hyperinflation. It is important to recognise that lung hyperinflation per se is not identical to the presence of emphysema but can have multiple other causes. Severe hyperinflation, however, is regularly indicative of lung emphysema being involved in the disease. It also should be noted that in the presence of very severe airflow obstruction, plethysmographic volumes tend to be overestimated, probably due to the fact that the pressure variations generated during the shutter manoeuvre are not properly transmitted to the mouth (O'Donnell, 2010).

If FRC is elevated but decreases after bronchodilator administration or in the course of the disease (e.g. after an exacerbation of COPD), this indicates beneficial effects on lung hyperinflation. Body plethysmography is capable of determining both the degree of lung hyperinflation and its changes by direct measurement of FRC, which neither relies on the proper performance of inspiratory manoeuvres nor depends on possible changes of TLC.

Naturally, changes in FRC are inversely related to those of IC, provided that there is no change in TLC. IC has been advocated for particularly in intervention studies in COPD. In the sequence of manoeuvres commonly performed in plethysmography, IC is not directly measured, but derived from IVC and ERV, thereby involving two effort-depending manoeuvres instead of one as in most spirometric IC determinations. Whether the correlation of FRC with indices of clinical state is weaker than that of IC measured at rest is not reliably known. The ratio of IC/TLC is known to be a significant predictor of mortality in patients with COPD (Casanova, 2005).

Whole body plethysmography is a technically demanding, highly informative, non-invasive method to obtain information on airway obstruction and lung volumes that is not available through spirometry (Stocks, et al., 2001) (Brusasco, 2003) (Pride, 1986). It normally takes no more than a few minutes to get reliable values. Importantly, the examination requires only a minimum of co-operation and in most cases is less bothersome for the patient than spirometry; the results obtained for sRaw are virtually independent of the patient's co-operation. Moreover, in contrast to spirometry, it is an examination under physiological conditions, as the measurements are performed during quiet breathing. A closer inspection of the form of the breathing loops can yield valuable information on the type and even site of airway obstruction and the homogeneity of lung ventilation. Therefore, body plethysmography is an important, unique method for assessing the functional state of the airways. The method appears to be of particular value for characterising the multiple, heterogeneous alterations occurring in patients with COPD. It also offers potential for further exploration and development.

Recently, it has been used to differentiate ventilatory responses to ozone in different strains of rats (Dye , 2015). It was also used to evaluate the effect of congenital diaphragmatic hernia (CDH) in children on pulmonary function (Rygl, et al., 2015). In this study, Rygl et al. recruited 30 CDH patients of age 1.32 +/- 0.54 years. A Gore-Tex patch was used in 13% of patients. Pulmonary hypertension was diagnosed in 13% of the patients. These patients were examined using lung function tests and whole body plethysmography. The results showed that in CDH children, there was high incidence of peripheral airway obstruction and increased value of functional residual capacity. Unfavourable prognostic factors (Gore-Tex patch, pulmonary hypertension) correlated with more severe alteration of pulmonary function in infants. Alvarez-Azrgote et al. (Alvarez-Argote, et al., 2016) used whole body plethysmography to examine the effect of mid-cervical contusion injuries and the resulting phrenic nerve injury on ventilator mechanics. Whole body plethysmography was measured before injury and at 3, 7, and 14 days post-injury. Their results showed that there were no significant changes in breathing parameters during eupnoea or exposure to hypoxia (10% O2) or hypercapnia (5% CO2) at any time post-injury. They concluded that unilateral mid-cervical contusions minimally impair ventilatory behaviours despite phrenic motoneuron loss and diaphragm muscle denervation. Another recent application of whole body plethysmography was to diagnose asthma (Schneider, et al., 2015). In a prospective diagnostic study, Schneider et al. used whole-body plethysmography with bronchial challenge testing as well as a bronchodilation test in 400 patients with suspected asthma. The bronchial provocation test was considered positive if the FEV_1 fell by at least 20%

and/or the airway resistance doubled, with an increase of sRaw to at least 2.0 kPA × s. Follow-up evaluation was performed one year later. The prevalence of asthma in the 302 patients who completed the follow-up was 27.5%. The sensitivity of whole body plethysmography with sRaw measurement for asthma was 95.2% (95% confidence interval [CI] 88.3%-98.1%), and its specificity was 81.7% (95% CI 76.1%-86.3%). The sensitivity of FEV_1 was 44.6% (95% CI 34.4%-55.3%), and its specificity was 91.3% (95% CI 86.6%-94.4%). The negative predictive value (NPV) of whole body plethysmography with sRaw measurement was 97.8% (95% CI 94.5%-99.1%), while that of FEV1 was 81.3% (95% CI 76.0%-85.7%). The positive predictive value (PPV) of whole body plethysmography with sRaw measurement was 66.4% (95% CI 57.5%-74.2%), while that of FEV_1 was 66.1% (95% CI 53.0%-77.1%). In this study, Schneider et al. showed that with sRaw measurements, asthma can be ruled out with high certainty.

Despite all of the advantages of whole body plethysmography, it has its limitations. One major limitation is that it does not capture natural breathing patterns during exercise. The reason behind this is that subjects are asked do breathing manoeuvres during exercise to obtain lung volumes, and normal exercise breathing mechanics were never measured. Furthermore, the values generated by machine do not evaluate specific chest wall motion characters, such as, for example, measuring volumes of specific compartments of the chest cavity and the degree synchronisation between part of chest wall compartments in relation to each other and in relation to the abdomen.

9.2 The Need for Chest Wall Motion Measuring Technology

The ability to measure lung volumes and gas flow accurately is essential in the medical field. Classically, this has been measured via a pneumotachograph or spirometry. To perform these measurements, it is required to occlude the nose with a clip and use a mouth tube. This method has a number of limitations, as discussed in section 9.1. In addition, another limitation is that the measurement cannot be performed over a prolonged period of time, as it is uncomfortable for the subject and restricts movement. The mouth tube also creates an extra dead space that leads to overestimation of the tidal volume. Additionally, these mouth and nose devices make the subjects conscious of their breathing; this interferes with the normal and natural breathing pattern and the neurological input from the brain. In fact, Gilbert, Auchinocloss, Brodsky, & Boden concluded that these nose and mouth devices influence the tidal volume, respiratory rate, and the minute ventilation (Gilbert, Auchinocloss, Brodsky, & Boden, 1972). Furthermore, spirometry and pneumotachographs cannot be used without the subject’s effort or co-operation; therefore, they cannot be used with sleeping subjects, patients on a mechanical ventilator, or patients who are uncooperative. All these limitations have inspired researchers to move in the direction of measuring ventilatory parameters indirectly. They measure the thoracic volume changes by measuring its effect on the motion of the overlying chest wall. A number of methods and devices have been used in detecting chest wall motion over the last 70 years.

9.3 Methods of Measuring Chest Wall Motion

9.3.1 *Negative Pressure Ventilators*

The measurement of chest wall motion started just after the Second World War by Fenn, Rahn, and Otis (Otis, Fenn, & Rahn, 1950). In these early beginnings, they used a negative pressure ventilator called a drinker respiratory or an iron lung (Figure 10). In their experiments, relaxed humans were ventilated with this negative pressure ventilator. During the procedure, the researchers recorded the velocity of gas flow in inspired air. They also recorded the difference in pressure inside the negative pressure ventilator and the mouth of the subject. Based on this, they could estimate the elastic resistance and the total resistance of the breathing. Then, they derived formulas from the data generated by the experiments, which were able to provide an estimated description of the mechanics of breathing. Using the formulas, they estimated the work of breathing, the maximal mechanical work output of the respiratory system, and the respiratory muscles' efficiency (Otis, Fenn, & Rahn, 1950). Although most of the results were estimated rather than measured, their work and their formulas were nevertheless the origin for the testing methods used today.

Figure 10: The iron lung. The patient lies within the chamber, which, when closed, effectively produces a changing atmospheric pressure. Adopted from (Hlilpertshauser, 2004).

9.3.2 *Oesophageal and Gastric Balloons*

In the 1960s, oesophageal and gastric balloons were invented. Along with electromyography, these inventions allowed measurement of ventilatory mechanics directly and invasively. These inventions also allowed, for first time, the measurement of intra-thoracic pressures as well as respiratory muscle activity. Agostoni and Rahn used these oesophageal and gastric pressure measurements and simple lung volume measurements during both static and dynamic manoeuvres to measure and calculate the contribution of the thorax and the abdomen to the respiratory cycle (Milic-Emili, Orzalesi, Cook, & Turner , 1964) (Agostoni, Sant'Ambrogio, & Del Portillo , 1960). However, these techniques were not without their downfalls. These forms of testing were, first of all, invasive and inconvenient to patients and not without risks. Second, they could not be used during exercise. Third, they could not be used to calculate the change of volume in the chest cavity (Konno & Mead, 1967). In addition, a high percentage of error was associated with measuring the fatigue state, which was measured by using pressure measurements and nerve stimulation. The cause of the these errors was multifactorial, as described by Romer et al., and included post-activation potential (Romer & Polkey, 2008) (Mador, Magalang, & Kufel, 1994), supramaximal stimulation (Taylor, Allen, & Gandevia, 1996), abdominal compliance (Koulouris, Mulvey, Laroche, Goldstone, Moxham, & Green, 1989), and iso-volumic conditions (Hubmayr, Litchy, Gay, & Nelson, 1989). These downfalls propelled scientists to try to invent new methods of assessing respiratory mechanics.

9.3.3 *Magnetometer*

In 1967, a non-invasive method to measure volume change in the thoracic cavity was introduced by Konno and Mead called the magnetometer (Konno K. M., 1967). They used the costal line to divide the chest wall into two compartments: the abdomen and the ribcage. The correlation between the volume and the linear motion was the basic principle behind their method. Their method involved threads that were connected to different parts of the abdomen and ribcage; each thread was connected to a pulley, which was connected to a linear transducer. The Y-axis was used to record the ribcage's movement displacement, and the X-axis was used to record the abdomen's movement. The lung function was measured simultaneously with a spirometer placed in the subject's mouth (Figure 11). Using this method, Konno and Mead showed that the abdominal contribution to tidal volume was lower in an upright position than a supine position. The thought was that there is some kind of physiological relationship between the different compartments of the body. For example, they discovered that the abdominal contribution to tidal volume was higher when the other compartment was restricted.

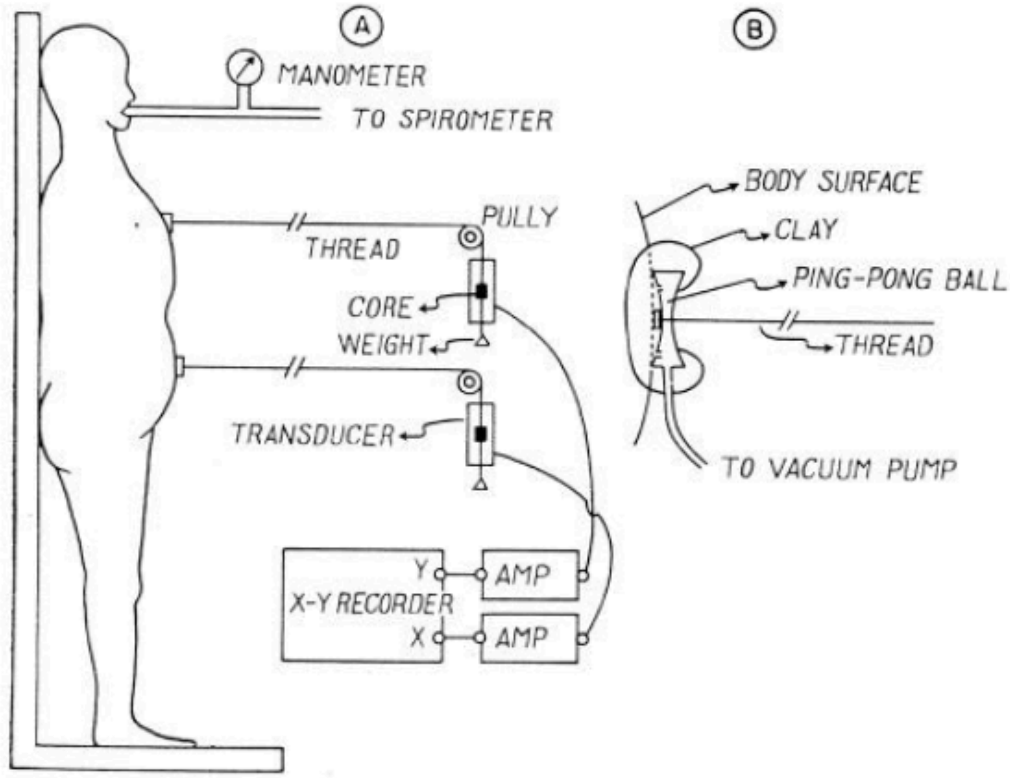

Figure 11: Illustration of the method Konno and Mead used to measure chest wall motion Adopted from (Konno K. M., 1967).

The major limitation of this method was that the contribution of the diaphragm to the tidal volume was neglected, as it was not isolated (Decramer, De Troyer, Kelly, Zocchi, & Macklem, 1984). In addition, the system's accuracy was affected by the change in posture. Furthermore, this method was limited to measuring a range of volumes and could only measure the change in value in two, rather than three, dimensions. Finally, the accuracy of the system was reduced further when used with infants (Carlo, 1982). All these limitations stimulated the development of a new model based on the device created by Konno and Mead. This more advanced model used three dimensions to generate chest volume during all phases of respiration. These dimensions were the antero-posterior dimensions of both the ribcage and the abdomen and the distance from the umbilicus to the sternum (Figure 12).

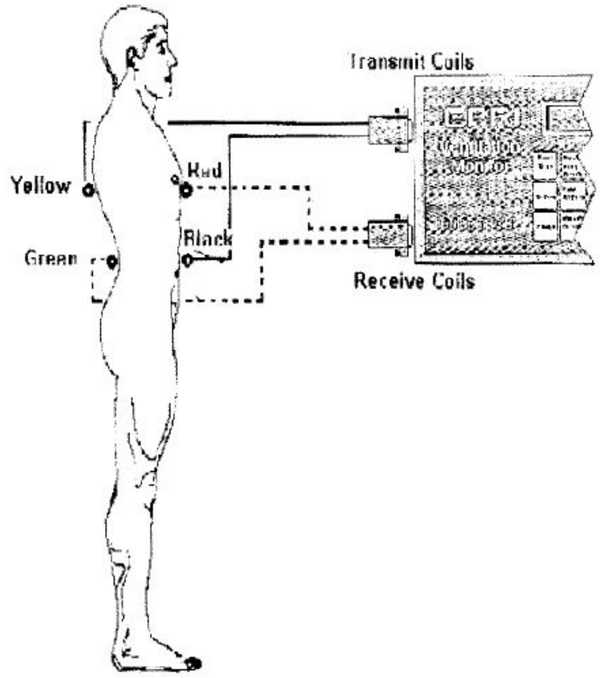

Figure 12: Schematic of the magnetometer device depicting coil placement, from the description of McCool et al. (McCool, et al, 2002). The antero-posterior displacements of the ribcage and abdomen, as well as he axial displacements of the chest wall, were measured using two pairs of electromagnetic coils secured to the ribcage and abdomen.

This new model was developed by McCool et al. (McCool, et al., 2002). Their device was compact and portable and made by pairing four electromagnetic coils that could calculate the variations in distance between the spine and the chest wall and the changes in distance of the ribcage and abdomen. McCool et al. (McCool, et al., 2002) validated their model to quantity tidal volume, inspiratory time (TI), and expiratory time (TE) in subjects in sitting and standing positions and through exercise. The outcomes of their work showed that tidal volume (electromagnetic coils) was highly correlated with tidal volume (spirometer) at quiet breathing (r2 = 0.90) and during workout (r2 =

0.79) for combined data. The average percentage of differences between tidal volume (electromagnetic coils) and tidal volume (spirometer) were 10.1% ± 6.6% at quiet breathing and 13.5% ± 8.6% during workout. Finally, TI (electromagnetic coils) and TI (spirometer) values and TE (electromagnetic coils) and TE (spirometer) values also were highly correlated (r2 = 0.97 and r2 = 0.95, respectively) for pooled data. More recently, another device was developed based on a model with three degrees of freedom. This device had different characteristics from that of McCool et al. (McCool, et al., 2002); it was lighter, smaller, and non-wired and preserves the freedom of movement of the participant. This device was the subject of two publications that demonstrated its ability to estimate ventilation (Gastinger, et al., 2010) and energy expenditure (Gastinger, et al., 2011). This new device (Nomics–WSL2, Liege Science Park, Belgium) was used by Gastinger et al. (Gastinger, et al., 2010) and includes two pairs of electromagnetic coils securely connected to a case (Figure 13).

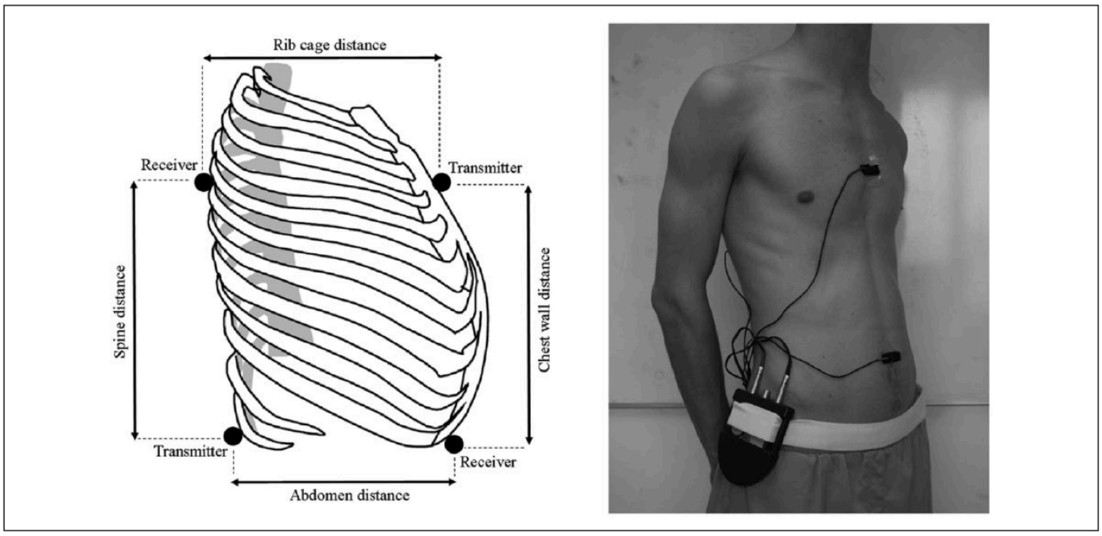

Figure 13. Configuration and placement of the two pairs of electromagnetic coils on the participant. Adopted from (Gastinger, Sefati, Nicolas, Sorel, Gratas-Delamarche, & Prioux, Estimates of ventilation from measurements of rib cage and abdominal distances: a portable device, 2010)

One pair of electromagnetic coils was composed of a transmitter and a receiver (diameter = 0.5 cm, length = 2.5 cm). The case (2 × 10.5 × 12.5 cm, 298 g) was carried on the hip via an elastic strap. The capacity of the device exceeded 20 hours of recording at a frequency of 15.625 Hz. The apparatus communicated with the PC using radio wave frequencies at a range of approximately 30 metres. Twelve healthy males took part in this study, and the antero-posterior displacement of the ribcage and abdomen and the axial displacements of the chest wall and the spine were measured using the electromagnetic coil system. The reference ventilatory measurements were recorded with a spirometer (pneumotachograph) to calibrate and validate this new device. The magnetometers were calibrated on Day 1, which was composed of a sitting, standing, and walking session on a treadmill. From each of these three sessions, three equations per participant were developed, and from these, ventilation was calculated as the sum of changes in the antero-posterior and axial displacement of the trunk as follows:

$$V = \alpha L1 + \beta L2 + \gamma L3 + \xi L4 + \varepsilon$$

where α, β, γ, and ξ are coefficients for the rib cage (L1), the abdomen (L2), the chest wall (L3), and the spine (L4). ε is a constant.

To apply and verify the validity of the calibration manoeuvre of Day 1, each participant carried out three new sessions of sitting, standing, and walking conditions on Day 2. Ventilation measured by the electromagnetic coils ($V_{E\ Mag}$) and ventilation measured by the spirometer ($V_{E\ Spiro}$) were compared in these three different situations. Totals of 707, 732, and 1,138 breaths were analysed in the sitting, standing, and exercise conditions, respectively. For pooled data, $V_{E\ Mag}$ was significantly correlated ($P < .001$) with $V_{E\ Spiro}$ in sitting and standing positions and during the walking exercise. The mean differences between $V_{E\ Mag}$ and $V_{E\ Spiro}$ for the group were 10.44%, 10.74%, and 12.06% in the sitting, standing, and exercise conditions, respectively. This study showed that each individual equation made it possible to determine the ventilation of each participant with satisfactory precision. These results seemed to validate the calibration manoeuvre and demonstrate the capacity of this new device to measure ventilation with reasonable accuracy in sitting, standing, and exercise conditions. Thus, a potential application of this device was estimating energy expenditure from only measuring ventilation. This work was the focus of a further study (Gastinger, et al., 2011).

The theoretical principle of this method was based on the development of individual and group calibration curves. This technique was widely used to estimate energy expenditure from heart rate measurement (Garet, 2005) (Hiilloskorpi, 2003) (Kurpad, 2006) (Livingstone, 2000) (Strath, 2000). The individual curves were determined by the simultaneous recording of oxygen consumption (VO_2) and heart rate during physical activities of different intensities. The calibration curves were then developed and applied to new sessions of activity performed by the participant to estimate VO_2 from heart rate measurements. The VO_2 data were then converted to energy expenditure. The individual relationships of each participant were established between ventilation measured by the electromagnetic coils system ($V_{E\ Mag}$) and energy expenditure measured by indirect calorimetry (EE_{REF}). Individual equations were established for each of the 11 participants, and a group equation was established from the overall data set ($EE_{REF} = a \times V_{E\,Mag} + b$). The application of the different equations extended to resting activities (sitting and standing) and walking on a treadmill. Thus, from the measurement of ventilation by the electromagnetic coil system and the application of individual or group relationships, it was possible to estimate the energy expenditure by the electromagnetic coils (EE_{Mag}) of a participant under resting and walking conditions (Gastinger S. e., 2011).

The multiple electromagnet device designed by Nomics was used in a second study whose aim was to estimate energy expenditure under rest and exercise conditions. The Gastinger et al. study (Gastinger, et al., 2011) showed no significant difference between EE_{REF} and EE_{Mag} for each activity. This result was reported by applying the individual and group equations.

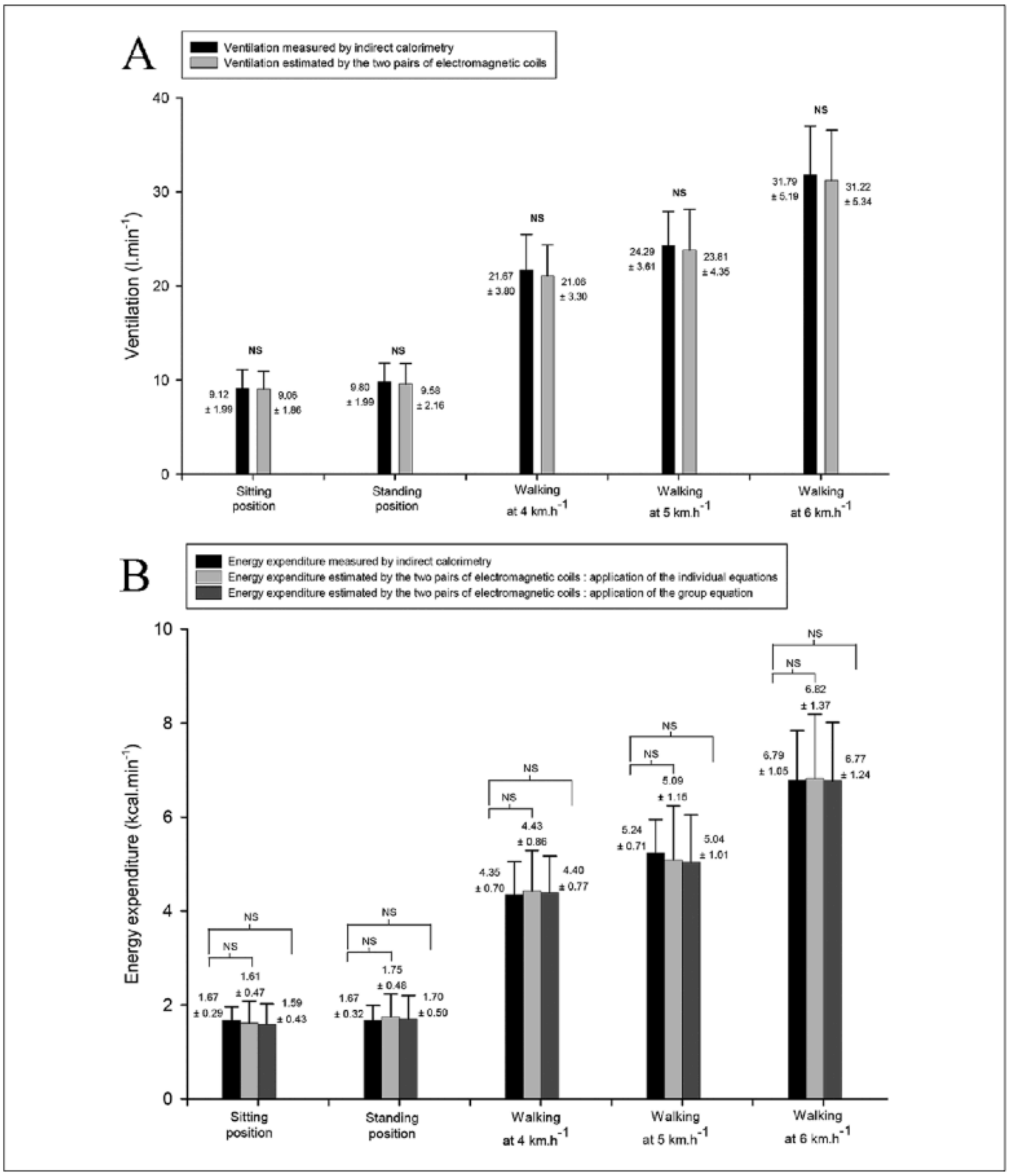

Figure 14. (A) Ventilation measured by indirect calorimetry ($V_{E\ IC\text{-}Val\ mean}$) and estimated by the two pairs of electromagnetic coils ($V_{E\ mag\text{-}Val\ mean}$) during five different activities for the whole group. (B) Energy expenditure measured by indirect calorimetry ($EE_{IC\text{-}Val\text{-}REF\ mean}$) and estimated by the two pairs of electromagnetic coils with the application of the individual ($EE_{mag\text{-}Val\text{-}INDIV\ mean}$) and the group ($EE_{mag\text{-}val\text{-}GROUP\ mean}$) equations during the five different activities. NS, no significant difference. Adopted from (Gastinger, Sefati, Nicolas, Sorel, Gratas-Delamarche, & Prioux, 2011)

These accurate results, found in sitting and standing conditions at rest and during walking exercises at 4, 5, and 6 km/h^{-1}, seemed to validate this method based on this new device, which aimed to estimate energy expenditure under different conditions. This study also showed the advantage of using a group equation to estimate energy expenditure. Nevertheless, this group equation would have to be tested on more participants in future studies to demonstrate its added value. The device presented very few constraints and was very user-friendly due to its small weight and size and its transmission range (30 m). The system transmitted radio signals in the 2.4-GHz wave band. This allowed estimation of daily energy expenditure in a house or an apartment.

To conclude, this system provided an accurate estimation of ventilation and energy expenditure during different body postures (sitting and standing at rest) and ambulatory activities (walking at 4, 5, and 6 km/$^{h-1}$). This new device showed promise in being a valid tool in the estimation of energy expenditure over a wide range of activities of light to moderate intensity. It may be interesting to extend the studied populations, such as to adolescents, athletes, healthy, elderly, overweight, and female participants. The potential of this surrogate measure of total energy expenditure can be enhanced through recent technological innovations allowing measurement of ventilation by miniature sensors placed on the body surface. The emergence, development, and future commercialisation of this technology can be linked to the need to record sedentary behaviour, physical activity level, health status, and socioeconomic environment of the population. The work done based on the electromagnetic coil sensors showed the potential value of the measurement of ventilation to estimate total energy expenditure (Gastinger, et al., 2011). This system, based on the coupling of a magnetometer, must now be integrated into a garment (jacket or T-shirt) associated with other sensors (to measure physiological and mechanical variables) to allow an accurate estimate of total energy expenditure under daily life conditions.

Despite the noticeable progress in the development of the device, the device still cannot provide data about regional chest wall volumes and chest wall synchrony, which is valuable information in evaluating chest wall motion before and after thoracic surgery.

9.3.4 *Magnetic Resonance Imaging (MRI)*

Dynamic magnetic resonance imaging (dMRI) is another technology that was used to evaluate chest wall and lung motion in a number of clinical conditions. In 1999, Suga et al. used two-dimensional (2D) dMRI to evaluate respiratory mechanics in patients with emphysema (Suga, et al., 1999). Their technique consisted of using an echo pulse series at a given thoracic plane during a number of breaths during the respiratory cycles. Then, using a cine-loop view, time-distance curves, and maximum inspiratory and expiratory graphs, they managed to measure the motion of diaphragm and the chest wall. They used this technique in 28 patients with emphysematous lung disease (of which 9 had LVRS) and six healthy subjects. Their results showed that, in contrast to healthy subjects, the patients with emphysema showed reduced or irregular motion of both the chest wall and the diaphragm. In addition, they demonstrated that after LVRS, there was improvement in both chest wall and diaphragmatic motion in all nine patients who had LVRS (Suga, et al., 1999).

Similarly, Plathow et al. used 2D dMRI successfully to evaluate chest wall motion during the breathing cycle of 15 healthy volunteers, whose results showed high correlation with spirometry (Plathow, et al., 2004). Kotani et al. used 2D dMRI to evaluate the effect of idiopathic scoliosis on chest wall and diaphragm motion (Kotani, et al., 2004). In their study, they used 2D MRI to measure the chest wall and diaphragm motion of 18 patients with idiopathic scoliosis and nine healthy controls during deep breathing. They found that the chest wall motion was significantly restricted in the idiopathic scoliosis group, compared to the control group, but there was no static difference between the two groups in the motion of the diaphragm (Kotani, et al., 2004). Furthermore, in 2005, Plathow et al. evaluated the VC of 20 healthy volunteers using three-dimensional (3D) dMRI, and their results showed high correlation with spirometry. In addition, they managed to calculate the split lung volumes and lung surface (Plathow, et al., 2005). In 2006, Plathow et al. used 2D and 3D dMRI to monitor lung motion in 22 patients with mesothelioma before and after chemotherapy. The 2D dMRI was used to measure the craniocaudal thoracic dimension, and the 3D dMRI was used to calculate the lung volumes. Their results showed that lung mobility increased significantly after chemotherapy (Plathow, et al., 2006). In 2014, 2D dMRI was used by Kotani et al. to investigate the effect of training via incentive spirometry on chest wall motion in 10 healthy subjects (Kotani, et al., 2015). In their study, Kotani et al. found that respiratory training resulted in significant improvement in the chest wall motion on both sides of the chest, which correlated with an improvement in spirometry values (Kotani, et al., 2015).

The strengths of dMRI include that it is non-invasive and does not use ionising radiation, making it suitable to be used for children. It also gives a very clear, detailed anatomical and physiological image of the moving chest wall, an image that cannot be achieved with conventional imaging modalities. Furthermore, it can create a large number of images from every angle or orientation.

Over the last 15 years, MRI of the lung has progressed from the confined space of the laboratory to the gateway of clinical practice. This progression was propelled by an improvement in MRI technology. These advances have helped to overcome the main two limitations of the lung MRI, namely the low proton density of the lung and the fast signal decay due to its vulnerability to artefacts on the air-tissue surfaces (Puderbach, et al., 2007). Similarly, recent advances in image processing have made the MRI more sensitive. In 2016, Mogalle et al. used a novel image analysis method successively to detect early diaphragmatic weakness in patients with Pompe disease (Mogalle, et al., 2016).

Magnetic resonance imaging is the imaging of choice in the cohort of patients who should rigorously avoid ionising radiation (Biederer, et al., 2012). This group includes pregnant women, patients who need repeated captures, and patients with neutropenia (Eibel, et al., 2006). Currently the indications of the lung MRI include the assessment of a complicated thoracic mass with chest wall and mediastinum invasion and the assessment of cystic fibrosis (Biederer, et al., 2012).

The lung MRI provides a detailed assessment of the motion of the thoracic organs, which can be repeated multiple times. These features helped in the relative quick establishment of the cardiac MRI (Lotz, Kivelitz, FischbacH r, Beer, & Miller, 2009), but not the lung MRI. This is due to a deficiency in standardised lung MRI protocols for all patient groups (Biederer, Bauman, Hintze, Fabel, & Both, 2011). These protocols are in the process of being discussed and developed (Biederer, et al., 2012).

The limitations of the dMRI include that due to the powerful magnetic field, the scanner can forcedly attract metal objects in the field, limiting the use of equipment such as exercise bikes or electronic chest drains during capture. It is also contraindicated in patients with metal implants, as its radiofrequency energy can cause a number of medical devices, such as defibrillators and heart pacemakers, to malfunction. In addition, the contrast medium used during the MRI capture (gadolinium chelate) can pose its own risk of allergic reaction and kidney damage in subjects with poor kidney function. Furthermore, in children under 6 years old and babies, MRI is usually done after light general anaesthesia to minimise the movement, which improves the quality of MRI images. This subjects children to the risks of general anaesthesia. In addition, MRI can pick up incidental findings on the subjects, which creates unnecessary anxiety and causes people to seek unnecessary treatment, which can have its own risks (e.g. surgery). Finally, the MRI machine is still not portable and currently cannot be used at the bedside or during exercise. Due to all the above limitations, it was not suitable for use in this study.

9.3.5 *Respiratory Inductance Plethysmography (RIP)*

Another modality for measuring chest wall motion is the respiratory inductance plethysmography (RIP) method. The basic principle behind this method is a change in magnetic field, resulting in a change in current. Any current that runs in a loop generates a magnetic field. Any change in the diameter of this loop generates another current, which is proportional to the amount of change in diameter but runs in the opposite direction of the original current. This principle is applied in RIP. A subject wears two belts of coil wires around his chest and abdomen. These wires are running a current. As the chest and abdomen move during breathing, there is a change in the diameter of the loop of the wire belt. This change induces an opposing current by an amount proportional to the change. A number of processors through various formulas can use this change to calculate volume changes in the chest and the abdomen. Respiratory inductance plethysmography technology was developed to non-invasively evaluate lung motion in veterinary asthma research and paediatric research. Its use increased in the last 20 years, as its cost decreased. The technology was in its infancy in the 1990s, and there was a question regarding the accuracy of the device in evaluating the chest wall motion and its volumes. In fact, Russell and Helms suggested that the accuracy of this device in detecting chest wall volume was questionable, as it measures only two components of movement, assuming that chest wall movement is 2D (Russell & Helms, 1994). However in 2015, using the same 2D movement, RIP was validated to measure tidal volume in an animal model. To achieve this, it measured the ribcage and abdominal motion of six intubated pigs that had a fixed tidal volume, and results showed that the tidal volume was linearly correlated with the movement of the ribcage and the abdomen over a large range for tidal volume ranging from 44 to 1,065 ml. A linear regression equation was used to calculate the tidal volume from the RIP data (Su, et al., 2015). Respiratory inductance plethysmography was also successfully used in a pilot study in 25 intubated patients to detect jet ventilation through its effect on chest wall motion (Atkins, Mandel, Weinstein, & Mirza, 2010).

Currently, RIP—like many chest wall motion analysis technologies—is still an experimental technology but has been utilised successfully in a number of sleep studies. It was used successfully to identify rapid eye movement sleep by associating it with an erratic breathing pattern that was detected using the RIP method (Drakatos, et al., 2016). Similarly, it was used successfully in identifying obstructive sleep apnoea (Kogan, Jain, Kimbro, Gutierrez, & Jain, 2016).

The major advantage of the RIP system is that it measures the cross-sectional area instead of the distance. This fact makes the RIP data linearly related to the pulmonary volumes and also makes the system relatively more resistant to changes in posture and motion. Furthermore, RIP has outperformed similar methods (Adams, Zabaleta, Stroh, & Sackner, 1993) (Cohen, Ladd, & Beams, 1997); RIP-measured values in normal subjects remain within +/- 10% for more than 90% of breaths (Chadha, Watson , & Birch, 1982).

Respiratory inductance plethysmography was found accurate in measuring the breathing effort. However, placing the belts very tightly can reduce and restrict the cross-sectional changes of the chest and the abdomen, which affects a patient's true breathing pattern. In contrast, if the belts are loose, they can migrate upward or downward or overlap with each other, affecting the accuracy of measurements. In addition, placing the belts wrong, for example around the hips, does not measure or reflect the diaphragmatic abdominal motion.

All in all, RIP is reliable in measuring tidal volume, and its use is gaining more popularity in clinics and research laboratories. But the device is still not easy to handle, expensive, and occupies a larger body surface area. Due to all of these factors, it was not used in this study.

9.3.6 *The LifeShirt*

A new invention that was based on the RIP principle is the LifeShirt. The system is totally portable. As the name suggests, this system consists of a vest that is attached to a data collector, which is attached to data analysis software. Included in the vest are an electrocardiogram, electromyography, pulse oximetry, temperature probe, and a blood pressure monitor. By using a specialised sensor, the vest can also assess the posture and level of activity.

The vest consists of a sinusoidal coil wire that surrounds the chest and the abdomen with skin contact and tight fitting (Figure 15).

Figure 15: Schematic drawing of the portable RIP system in a LifeShirt application.

LifeShirt has some advantages in that it is mobile and lightweight. In fact, it provides much information about the mechanism of breathing for a number of subjects in their own homes. Clarenback et al. validated the device during activity (Clarenbach, Senn, Brack, Kohler, & Bloch, 2005). Kent et al. showed that the volumes generated via the LifeShirt during mild exercise were comparable to a pneumotachograph's data (Kent, O'Neill, Davison, Nevill, Elborn, & Bradley, 2009). Bradley et al. showed that the device could be used successfully in measuring ventilation in 18 patients with cystic fibrosis during mild exercise (Bradley, Kent, O'Neill, Nevill, Boyle, & Elborn, 2011). LifeShirt – like many chest wall motion analysis technologies—is still in its experimental phase, but it has been currently used in sleep studies, at clinics, or remotely at home. In 2015, the LifeShirt was used to measure the effect of respiratory training via normocapnic hyperpnea (NH) in 26 COPD patients. After four weeks of NH training, the results showed improved thoraco-abdominal co-ordination during endurance testing, compared to the status before NH training (Bernardi, Pomidori, Bassal, Contoli, & Cogo, 2015). In another sleep study, LifeShirt was used on 38 healthy polar workers to evaluate the association between acute motion sickness and disordered breathing during sleep. They showed that acute motion sickness was not associated with apnoea episodes, as detected by LifeShirt (Anderson, Wiste, Ostby, Miller, Ceridon, & Johnson, 2015). The major advantage of LifeShirt is that patients can be monitored remotely at home. Another advantage is that the device is lightweight, which allows freedom of movement and comfort.

The major limitation of the system is that it involves calibration tailored for each individual. In addition, a recent study examining the use of the LifeShirt versus spirometry, in patients with obesity hypoventilation syndrome (OHS) and controls, showed that the LifeShirt-spirometer agreement was not accepted for tidal volume in both groups of patients (Hollier, et al., 2014). Similarly, Kent et al. showed that the volume generated by the LifeShirt during intense exercise was not comparable with a pneumotachograph's data, raising concerns about LifeShirt accuracy during intense exercise (Kent, O'Neill, Davison, Nevill, Elborn, & Bradley, 2009). Due to the above limitations, and the need in this study to measure regional chest wall motion and synchrony between the chest wall compartments—data the LifeShirt cannot provide—this device was not used in this study.

9.3.7 *Impedance Plethysmography*

Another technique to measure chest wall motion is impedance plethysmography. The basic principle of this technology is that the body conducts electricity very weakly. In this method, a weak current runs through the body after being connected to electrical ports. As the chest wall expands, the resistance of the body changes depending on its diameter and volume, and this modifies the electrical current. This modification can be measured and chest expansion can be quantified.

9.3.7.1 Transthoracic Impedance (TTI) Plethysmography

The transthoracic impedance (TTI) plethysmography uses the same impedance principle. This method utilises the change in the small amplitude current caused by the change in body resistance as the chest wall expands and contracts. The system calculates the changes in chest wall expansion.

The advantage of this method is that it is a cheap technology and can be used to obtain electrocardiogram (ECG) tracing. TTI is currently being used extensively in cardiopulmonary resuscitation (CPR), an area that is likely to utilise the technology the most in the future, especially after it has been incorporated into defibrillators. In one study, TTI was used in CPR to provide feedback regarding the rate of chest wall compression. In this study, an algorithm using the TTI signal was created successfully to calculate the chest wall compression rate. The recommendation of the study was that TTI could be incorporated into external defibrillators to improve the quality of CPR (González-Otero , et al., 2015). TTI was also used to identify chest compressions accurately during the CPR cycle in a study that attempted to analyse the effect of pausing chest compression—for ECG analysis during CPR—on reducing the possibility of returning to spontaneous circulation (Steinberg , et al., 2015). In an animal model using TTI, the relationship between optimal chest wall compression, as measured by TTI, and the retention of spontaneous circulation was investigated in 14 pigs who had induced ventricular fibrillation (Zhang, et al., 2012). Similarly, TTI was used in a number of resuscitation studies (Stecher , Olsen, Stickney, & Wik, 2008) (Aramendi, Ayala, Irusta, Alonso, Eftestol, & Kramer-Johansen, 2012). Furthermore, TTI can detect paradoxical breathing, as it does not use the Kanno-Mead principle (section 9.3.3).

However, TTI use in respiratory medicine has been limited for a number of reasons. Brouillette et al. showed that the cardiac movement artefact could cause a serious problem during chest wall measurements (Brouillette, et al., 1987). In addition, the accuracy of the system has been questioned. Corwin et al. used TTI in assessing apnoea duration in 17 infants simultaneously with RIP, and their results showed that RIP was more accurate in detecting the apnoea duration than TTI (Corwin, et al., 1997). Tidal volume is practically not measured by TTI, but the possibility of measuring the tidal volume via TTI is a matter of debate. Some authors find it not possible (Grenvik, Ballou, McGinley, & Millen, 1972) (Kurbicek, Kinnen, & Edin, 1964) while others disagree (Cohen, Ladd, & Beams, 1997) (Ashutosh, Gilbert, & Auchincloss, J H, et al., 1974) (Valentinuzzi, Geddes, & Baker, 1971) (Allison, Holmes, & Nyboer, 1964) (Hamilton, Beard, Carmean, & Kory, 1967). However, TTI can provide a good estimate of tidal volume if it is measured over a long time and captures a large number of breaths, but is not accurate for measuring tidal volume in a small number of breaths (Ashutosh, Gilbert, & Auchincloss, J H, et al., 1974). Another limitation of TTI is that artefacts from heart motion and skin electrodes can influence its outcome. TTI is also influenced by affricates generated by a change of posture or a patient's movement. Improving the position of skin electrodes might reduce but not abolish these errors (Sahakian, Tompkins, & Webster, 1985). Due to the above limitations, this method was not used in this study.

9.3.8 *Capacitive Sensing*

Another method of measuring chest wall motion is capacitive sensing, which is based on detecting permittivity. Permittivity is the ability of an electric field to affect a medium. The human body is mainly made of water, which is a conductive solution; therefore, the permittivity of the body is high: $\varepsilon = 80$. On the other hand, the permittivity of air is very low: $\varepsilon = 1$. As air enters the lungs, two things happen. First, as the diaphragm descends, the dimension of the chest cavity and the abdomen changes. Second, the permittivity of a water-filled body changes as more air enters the body. This new permittivity value is between the permittivity values of the air and the water. Two electrodes are attached to the body at different points anteriorly and posteriorly. By sensing the changes in permittivity as the chest wall expands, the system can calculate the changes in chest cavity volume. The basic principle of this method is to measure the change of permittivity of the body.

9.3.8.1 Wearable Capacitive Sensor

The capacitive sensing principle can be used in portable devices. An example of this device was presented by Gramse in 2002 (Gramse, De Groote, & Paiva, 2003), which was essentially a monitor embedded in a child's clothing (Figure16).

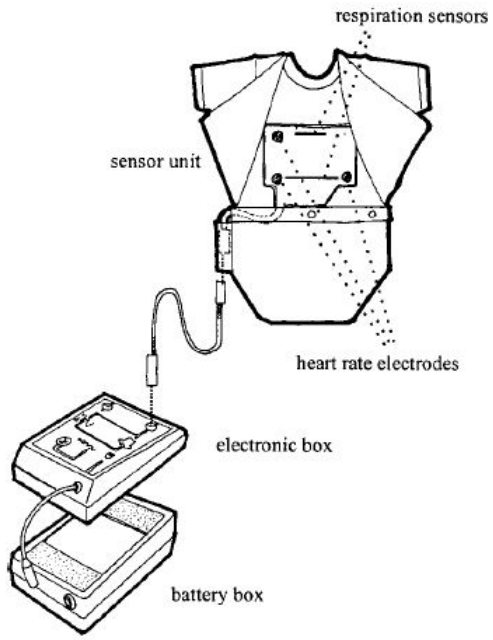

Figure 16: Schematic representation of pyjamas with sensor units (two respiratory sensors and three heart rate electrodes). Adopted from (Gramse, De Groote, & Paiva, 2003),

Capacitive sensing technology is still in its experimental stage, and it has been used mainly to measure diaphragm motion (Estrada, et al., 2014) (Torres, Fiz, Galdiz, Gea, Morera, & Jane, 2006) and has been incorporated into sensing mattresses to assess respiratory and body motion (Chang, Huang, Chen, Chang, & Yang, 2014) (Wartzek, Wever, & Leonhardt, 2011). Diaphragm sensing and the capacitive sensing mattress used in the sleeping studies seem to be the most promising fields for future development of capacitive sensing.

Torres, Fiz, Galdiz, Gea, Morera, & Jane used a capacitive accelerometer in an animal model to assess the motion of the diaphragm during an incremental respiratory protocol (Torres, Fiz, Galdiz, Gea, Morera, & Jane, 2006). Estrada et al. used capacitive sensing technology to assess the asynchronous diaphragm movement in COPD patients during an incremental inspiratory protocol (Estrada, et al., 2014). Watzek et al. developed a contactless capacitive sensor that was positioned under a mattress to monitor respiratory rate (Wartzek, Wever, & Leonhardt, 2011). Chang et al. used a capacitive sensing mattress as a ventilatory monitor to assess subjects during sleeping (Chang, Huang, Chen, Chang, & Yang, 2014).

Unlike LifeShirt, this device has the advantage of being able to automatically calibrate and use the best calibration each time. The system also has a handling feedback mechanism. Using the capacitive sensing principle of using the capacitance of electrodes positioned on both sides of the chest and abdomen, Kundu et al. developed a device to quantify the respiratory frequency (Kundu, et al., 2013). Hoffmann et al. developed another respiratory monitoring device using the capacitive principle (Hoffmann, et al., 2011) and used a fabric incorporated with pressure sensors that surrounded the body like a belt and moved with chest expansion. Hoffmann equipped the fabric with wireless transmission, which allowed subjects additional mobility. The system was portable and could be used in a number of environments.

This capacitive system unfortunately has a number of limitations that prevent it from been used to measure chest wall motion. One limitation of the system is that it underestimates the volume when the abdominal motion increases, i.e. when the measurement is taken in the following positions: sitting, lying down, and sleeping. Another limitation of the capacitive sensing belt system is that it can only be used in some positions. For example, saturation of the signals can be caused by a prone position. Furthermore, the capacitive sensing belt system requires constant, firm contact with the skin to produce good readings. In addition, body motion changes the parameters readily, leading to some errors. Thus, this method does not give accurate measurements in all positions. In addition, the system can be affected by an environmental electromagnetic interference, as the sensor itself produces an electric field; therefore, it can be affected by other devices that generate a similar field, e.g. pacemakers. Furthermore, the system is dependent on and sensitive to a patient's characteristics (height and weight) and clothing. Due to the above limitations, it was not possible to use this technology to measure chest wall motion in this study.

9.3.9 *Strain Gauges*

Another method for measuring chest wall motion is the use of strain gauges. Their basic principle is measuring the circumference of the thorax. The lung volume is nonlinearly related to the thorax circumference, when the abdomen is static. This relationship is influenced by the body position. An early version of this device was the mercury strain gauge. The basic principle of the device was to calculate the resistance of mercury within an elastic tube that surrounded the chest. When the tube stretched, the mercury resistance increased. Another version of the device replaced the mercury with sensitive coils (Brimacombe, Macfie, & McCrirrick, 1991). These gauges were voltage generating devices that fired on expansion (Figure 17).

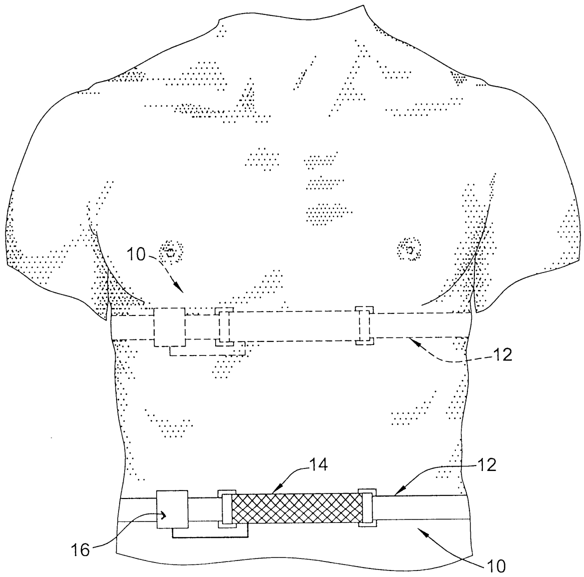

Figure 17: Resistive sensor for respiratory monitoring, from the description by Opher Pail (Pail, 2003). The indicating apparatus (10) includes two straps (12), the sensor (14), and a control unit (16).

The device can measure the change in the circumference of the chest wall. It consists of a control unit that is attached to an elastic belt and a sensor that is attached to the same belt, but with some distance between the sensor and the control unit. As the chest contracts, the sensor moves closer to the control unit. This movement generates an electrical current that can be used to measure the change in diameter of the chest.

These devices are utilised generally for measuring respiratory rate, but have also been used for measuring the tidal volume and have given tidal volume values from -16.9% to +15.2% of the values generated by spirometry (Brimacombe J. , 1993).

Strain gauges of the thoracic and abdominal compartments and the electromyography measurements were used to investigate the effect of an arithmetic task on breathing patterns of eight asthmatic and seven healthy children. The study showed that in contrast to healthy children, the activity of the intercostal muscle of asthmatic children started to diminish 10 +/- 30% before their maximal chest expansion when not subjected to the arithmetic task. During arithmetic task, however, there were no differences between the two groups (Fokkema, Maarsingh, van Eykem, & van Aalderen, 2006). In addition, the thorax motion was measured using strain gauges in a study that investigated the association between thorax movement and trapezius activity during singing in four student singers and four opera singers. The study found that the upper trapezius acted as an accessory expiratory muscle by causing the compression of the upper thorax during the act of phonation (Pettersen & Westgaard, 2004). In another vocal study, strain gauges were used to evaluate the effect of emotional stimulus during singing on the thorax and the abdominal motion and showed that emotional stimulus gave the lateral abdomen a prominent role for the positioning of the thorax and abdominal wall during singing (Pattersen & Bjorkov, 2009).

Strain gauge devices are still experimental devices, which have been used in some asthma studies and vocal studies. One advantage of the strain gauges over RIP is that they do not have a heart artefact and can be used in testing children (Russell & Helms, 1994). Unfortunately, however, the fact that the device is influenced by body position (Agostoni, Mognoni, Torri, & Saracino, 1965) and the difficulty in accurately positioning the gauges has restricted their clinical use. The major disadvantage of the gauge devices is that they rely on the circumference measurement, which has a nonlinear relationship with the tidal volume. Baird et al. used these strain gauges and pneumotachographs to measure tidal volume in 24 full-term infants and found there was a poor correlation between the two (Baird & Neuman, 1991). Due to the above limitations, this method was not used in this study.

Despite these limitations and the device's limited clinical use, vocal studies is the field that seems to have benefited from this technology and is likely to utilise it in the future (Pettersen & Westgaard, 2004) (Pattersen & Bjorkov, 2009) (Pettersen, 2005).

9.3.10 *Optical devices*

9.3.10.1 Optic Fibres

An optical device is another method to measure chest wall motion. Babchenko et al. developed a fibre-optic sensor that measured chest circumference changes (Babchenko, 1999). This method used a fibre-optic wire that transmitted a beam of light. The wire was firmly adhered to the chest and enclosed it, following all the curvatures. As the chest expanded, it induced a change in the chest curvature, which was transmitted to the fibre-optic wire. This change in curvatures of the wire induced an electrical change that could be translated into the change of circumference. This method was followed by the fibre-optic Bragg grating (FBG) method that was developed by Wehrle et al. (Wehrle et al. , 2001). In this method, Wehrle et al. incorporated the FBG fibres into a moulding strap that could follow the exact curvature of the chest wall. By doing so, he could not only measure the changes in chest wall movement but also the muscular activity of the chest. Optical Fibre Sensors Embedded into Technical Textile for Healthcare (OFSETH) is a project that uses the fibre-optic principle to fill the need for a mobile monitoring device that can measure several physiological parameters. De Jonckheere et al. demonstrated that these pure optical sensing technologies have advantages over non-optical monitoring, in that they can be used in monitoring an anaesthetised patient under MRI (De Jonckheere, et al., 2007).

De Jonckheere et al. then reported on a macro-bending sensor and a Bragg grating sensor, which are two textile-incorporated devices that use the pure optical sensing technique. They demonstrated that these devices could measure stretching and elongation of a textile worn by a patient with not much discomfort to the patient (Figure 18) (De Jonckheere, et al., 2009). De Jonckheere worked out the ideal position for placement of the two devices to minimise the optical losses and maximise the translation of textile elongation into an electrical current that can be detected by the sensors. The action of the two devices together permitted accurate measurement of the motion of the chest wall and the abdomen.

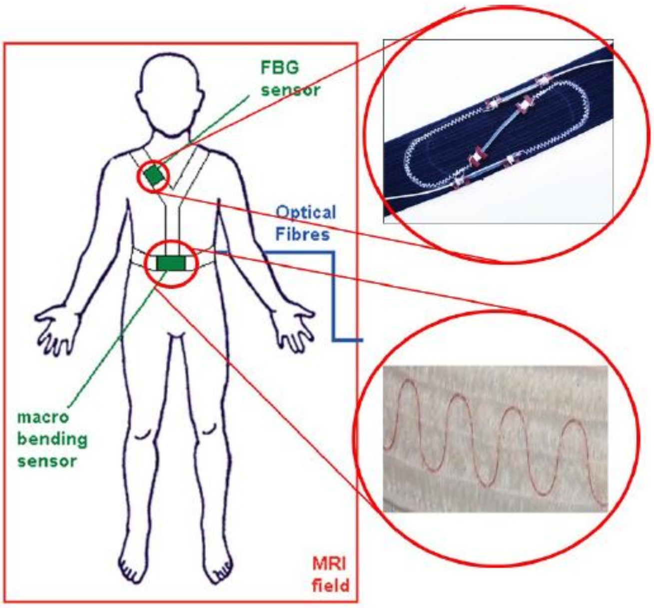

Figure 18: The optical fibre–textile integration, illustrating the optimal position of macro-bending and FBG sensors. Adopted from (De Jonckheere, et al., 2009).

The wireless technique of monitoring has been used extensively in the medical field, such as for breath movement, for example. D' Angelo et al. used a mobile kit with optic fibres to measure ventilatory movement (D'angelo, et al., 2008). D'Angelo's kit was made of a simple top that had fibre-optic wires connected wirelessly to a computer system. These wires could detect changes in curvature as the chest wall expanded and contracted. These data were converted by the computer system into breathing patterns.

A great interest in fibre-optic sensors has arisen recently due to one of their major advantages, which is that they can be used in electromagnetically charged environments. Therefore, they can be used during an MRI capture, as the system depends only on the change in the laser light intensity, which depends on the change of the body curvature during chest expansion. Ciocchetti et al. used a fibre-optic system successfully to measure the inspiratory and expiratory phases in four healthy volunteers during MRI examination. Their findings correlated well with OEP in terms of inspiratory and expiratory times but did not correlate well with lung volumes (Ciocchetti , et al., 2015). Lau et al. use a novel fibre-optic system successfully to measure the breathing rates of 20 healthy volunteers during MRI capturing, with an accuracy of +/- 2 breaths per minute, compared to a standard hospital system (Lau, et al., 2013). Another advantage of fibre-optics is that they are flexible, cheap, robust, and lightweight (Massaroni, Saccomandi, & Schena, 2015).

There is an increasing number of requests for MRI-based procedures worldwide, with an associated increasing demand for MRI-compatible systems to measure and monitor physiological parameters to evaluate a patient's status in real time (Massaroni, Saccomandi, & Schena, 2015). This will motivate future research on this field in the future.

The major drawback of this technology, which prevented it from being used in this study, is that, like the strain gauges, optic fibres only measure the thoracic circumference, which has a nonlinear association with tidal volume. Furthermore, the relationship between the chest wall circumference and lung volume is affected by the body position (Agostoni, Mognoni, Torri, & Saracino, 1965). Added to that is the fact that the device is difficult to position accurately.

9.3.10.2 Visual Motion Analysis Systems

The major breakthrough in chest wall motion monitoring occurred when motion analysis was invented. Until then, natural exercise respiratory mechanics could not be measured. The marriage of the OR (an optical reflectance motion analysis system) and the ELITE system (a television processor system) resulted in the birth of the first motion analysis system to measure respiratory mechanics (Ferrigno & Pedotti, 1985). This new system was used initially to analyse limb motion only, but in 1994, Ferrigno et al. used the ELITE and OR systems to generate a formula to measure 3D chest wall volume changes during quiet breathing and exercise (Ferrigno, Carnevali, Aliverti, Molteni, Beulcke, & Pedotti, 1994). They used 32 markers and four cameras in that system to measure change in volume. This system had a high degree of correlation with spirometry but, unfortunately, it also had a high percentage of error (21.3% BTPS) (Cala, et al., 1996). To correct this, in 1996, Cala et al., using the same technology as Ferrigno et al., extended the borders of the chest wall to better outline the costal margin and improve the system accuracy. They did this by increasing the number of chest wall markers from 32 to 86 (Cala, et al., 1996). Cala at al.'s changes and modification reduced the error to approximately 2% for tidal volume and less than 3.5% for the change in tidal volume. Through an error prediction equation, the percentage error was calculated in any cross-sectional area in the whole chest and was found to be 7-8% (Cala, et al., 1996). In 1997, Kenyon et al. used the motion analysis software for the first time to measure chest wall mechanics during exercise (Kenyon, et al., 1997). They measured chest wall mechanics of five men (age 13-38) while undergoing an incremental exercise test to the point of exhaustion (Kenyon, et al., 1997).

The work of Aliverti et al. added to this by describing the relationship between the abdomen compartment and the abdominal ribcage compartment (the diaphragm area) (Aliverti, et al., 1997). In 2000, the ELITE system transformed what is now known as OEP (Aliverti, Dellaca, Pelosi, Chiumello, Pedotti, & Gattinoni, 2000) and which has been used in many clinical studies since then.

Aliverti et al. used OEP to assess chest wall motion in COPD patients before and after salbutamol use. They showed that the increase in functional residual capacity after the administration of salbutamol in COPD patients is due to an increase in the volume of the abdominal compartment. They also showed that some COPD patients increased their end expiratory abdominal wall volume during exercise, developing dynamic hyperinflation, which is an air-trapping phenomenon. They also discovered that some patients with dynamic hyperinflation reduced their EEV during exercise after salbutamol administration, which resulted in a reduction in the ability to exercise (Aliverti A. R., 2005). Using OEP, they also showed that a person with COPD could develop dynamic hyperinflation during exercise and increase their tidal volume by increasing the end inspiratory volume of the abdomen and the ribcage. In contrast, COPD patients who decreased their EEV during exercise (euvolumics) still had an increase in their tidal volume. They found the improvement in the tidal volume in these euvolumics was due to the reduction of the EEV of the abdomen (Aliverti A. S., 2004). Sutterlin et al. used OEP with an animal to measure the effect of high superimposed high-frequency jet ventilation (SHFJV) and single-frequency (high-frequency) jet ventilation

(HFJV) in chest volumes. In a porcine model, they showed that SHFJV was more effective than HFJV in increasing lung volumes (Sutterlin, 2015). Lima et al. used OEP to measure the effect of non-invasive ventilation (NIV) on the chest wall motion of 13 cystic fibrosis patients. They found that there was an increase in the exercise capacity of these children post-NIV, and this increase was mainly due to an increase in pulmonary ribcage volume and a decrease in abdominal volume (Lima C. A., 2014). Lima et al. also examined the effect of incentive spirometry in chest wall volume of stroke patients. Using OEP, they found that there was an increase in chest wall volume of all three compartments of the chest wall during and shortly after incentive spirometry. They also found that the stroke patients had a greater degree of asynchrony in expansion between the two sides of the chest thorax, but this asynchrony decreased during and after incentive spirometry. These results were evidence of the beneficial effects of incentive spirometry as a rehabilitation tool for patients with stroke (Lima, et al., 2014). Silva et al. assessed the effect of posture on chest wall mechanics in obese children and children of normal weight during quiet breathing using OEP. They found that in a supine position, abdominal volume and its contribution to chest wall motion was significantly greater in obese children but not in controls. These results suggested that obese children could develop area postural hypoventilation (Silva, et al., 2015). In contrast, using OEP, Nozoe et al. examined the effect of posture on chest wall mechanics of healthy adults. They examined the effect of supine and left and right lateral positions on the chest wall mechanics of 18 healthy subjects. There was no difference in chest wall volume between the right and left thorax in the supine position. However, in lateral positions, the dependent part of the chest showed reduced motion mainly due to a reduction of motion of the abdominal ribcage and the abdominal compartments on that side (Nozoe, et al., 2014). This signified the accuracy of OEP in measuring chest volume in a variety of thoracic surgery operating positions. OEP was utilised by Kartianou et al. to measure the effect of physical activity on chest expansion of COPD patients. They discovered that COPD patients who had a greater ability to increase their tidal volume expansion and to maintain adequate IRV had superior levels of physical activity (Kartianou, et al., 2015). Lunardi et al. used OEP to assess the effect of lung expansion techniques (flow incentive spirometry [FIS], deep breathing, and volume incentive spirometry [VIS]) on chest wall mechanics in patients who had abdominal surgery. They found that there was no significant difference in chest wall volumes between the three groups and the control, suggesting that incentive spirometry was not superior to deep breathing alone in terms of chest wall expansion (Lunardi, Paisani, Marques de Silva, Cano, Tanaka, & Carvalho, 2015). OEP was also used in assessing the effect of changing the level of ventilatory support on chest wall mechanics. Meric et al. examined the effect of two ventilator settings—neurally adjusted ventilator assist (NAVA) and pressure-support ventilation (PSV)—on chest wall mechanics. They found that NAVA, unlike PSV, did not affect tidal volume. During the PSV mode, the increasing pressure was associated with an initial increase and then a decrease in tidal volume. Both NAVA and PSV decreased the abdominal contribution to chest wall motion. This study suggested that the NAVA mode should not be adjusted according to the tidal volume only (Meric, Calabrese, Pardon, Lejaille, Lofaso, & Terzi, 2014). Da Gama et al. examined the effect incremental inspiratory exercise loading had on chest wall mechanics for both genders. Using OEP and surface electromyography, they found total and compartmental chest wall volumes increased during incremental loading. This increase occurred earlier in women than in men. During the incremental loading, the decrease of activity of the sternocleidomastoid muscle happened before affecting the diaphragm. This was an important physiological finding that addressed gender differences in chest wall mechanics and the activity of the accessory respiratory muscles during exercise, which could be important in planning clinical interventions (Da Gama, et al., 2013). Another application of OEP was its use to examine the effect of FIS and VIS on chest wall mechanics of elderly subjects. Lunardi et al. recruited 16 subjects for this study. They found that both FIS and VIS similarly increased chest wall volumes in elderly subjects. However, in controls (young adults), the increase of chest volume was higher during VIS than during FIS. Both FIS and VIS caused a similar degree of chest wall asynchrony. On the other hand, in the control group, the level of chest wall asynchrony was lower during FIS than during VIS. Their work concluded that such differences should be considered when performing incentive spirometry in clinical settings (Lunardi, et al., 2014). Furthermore, OEP was used as a diagnostic tool for unilateral diaphragmatic weakness by Boudarham et al. They examined the chest wall motion and the diaphragm response of subjects suspected to have unilateral diaphragm paralysis and subjects with bilateral diaphragm paralysis by using trans-diaphragmatic pressure reaction (TDPR) and the diaphragmatic compound muscle action potentials (CMAPs) attained by transcutaneous electrical stimulation. OEP was found to be as accurate as the TDPR and

CMAPs methods in diagnosing unilateral paralysis of the diaphragm, as it could detect asymmetric chest wall motion in all patients with this unilateral condition. Furthermore, OEP did not detect any asymmetric chest wall motion in subjects with bilateral paralysis, making OEP a valid, alternative, non-invasive tool in the diagnosis of unilateral diaphragmatic paralysis (Boudarham , et al., 2013). Moreover, OEP was used by Binazzi et al. to examine the effect of phonation in COPD patients and also to explore gender differences during the process. They found that male subjects had a decreased expiratory flow during whispering (W), reading aloud (R), and singing (SI). During W, their abdominal volume decreased, and during R, SI, and W, their pulmonary ribcage volume decreased. In female patients, their end expiratory flow decreased by decreasing their abdomen volume during R and W. The authors found that gender influenced the breathing patterns to a greater degree than the physical characters of the subjects. This study highlighted the importance of gender-related breathing patterns, which could be significant in clinical practice (Binazzi, Lanini, Gigliotti, & Scano, 2013). OEP was also utilised by Brandao et al. to measure chest wall motion in heart failure patients and controls during inspiratory-loaded exercise. He found that, compared to controls, patients with heart failure had reduced ribcage volume variation. The left ventricular ejection fraction correlated well with the percentage contribution of left chest wall motion during inspiratory loading. He also found that reduced motion of the ribcage abdomen of the left side of the chest correlated with the degree of the heart enlargement (Brandao, et al., 2012). OEP was employed by La Mauro et al. to examine chest wall mechanics in patients with the congenital muscular disorder Duchenne muscular dystrophy (DMD). The condition is caused by progressive degeneration of the respiratory muscles. Using OEP, they examined chest wall mechanics of 66 patients, divided into four age groups, with different grades of DMD, during quiet breathing in supine and sitting positions. In the sitting position, there was no significant difference in chest wall volume among the different age groups. However, in supine position, the percentage contribution of the abdominal compartment to chest wall volume (Delta [AB]) decreased gradually with advancing age. In addition, patients who had nocturnal hypoxia showed a lower degree Delta (AB) than controls. This suggested that Delta (AB) was an early warning sign of nocturnal hypoxia and a good indicator of the disease progression (La Mauro, et al., 2010). OEP was also used to assess the chest wall motion of other types of neurological diseases, namely neuromuscular diseases. Lanini et al. examined the effectiveness of the coughing process in patients with neuromuscular diseases (PNDs) by examining their chest wall mechanics via OEP. They found that PNDs could not decrease their end expiratory chest wall volume and had a greater degree of chest wall distortion during coughing, compared to controls. Their work suggested that this was the cause of the defective coughing process in PNDs (Lanini, et al., 2008). Romagnoli et al. utilised OEP in examining the chest wall mechanics of patients with ankylosing spondylitis (AS). They assessed the adaptive mechanics of the chest walls of AS patients in a hypercapnic rebreathing test. During the test, the increase of the abdominal compartment volume of AS patients was greater than the increase in ribcage volume; this response was not found in healthy controls. The diaphragm and abdominal muscles contributed to expanding the chest wall volume irrespective of the degree of AS. Their study showed that AS patients co-ordinated their abdominal muscles to adapt to their restricted pulmonary ribcage (Romagnoli, et al., 2004). For instance, this was used to describe the increase in EEV and to measure the synchronisation between different chest wall compartments in 16 chronic obstructive pulmonary disease COPD patients. The comparison of respiratory mechanics in both genders, 5 women and 10 men, during exercise was conducted by Vogitatis et al.

OEP Validation

Validation of OEP was done by Cala et al. in 1996 (Cala, et al., 1996). Using spirometry and OEP, chest wall volumes were recorded in two healthy individuals during normal breathing and vital capacity manoeuvres. Their results showed that there was a good correlation between the two systems in the measurement. The regression equations for the OEP volume, V(OEP)(y), versus for the spirometry volume, V(SP)(x), for the two subjects were $y = 1.01x - 0.01$ ($r = 0.996$) and $y = 0.96x + 0.03$ ($r = 0.997$) for normal breathing and $y = 1.04x + 0.25$ ($r = 0.97$) and $y = 0.98x + 0.14$ ($r = 0.95$) for the vital capacity manoeuvre, respectively (Cala, et al., 1996). This shows that OEP can accurately estimate the spirometric volumes. Similarly, Kenyon et al. showed a high level of correlation between spirometric values and OEP values during intense exercise for five normal subjects ($r^2 = 0.994$) (Kenyon, et al., 1997). Subsequently, OEP generated a large number of publications as seen above.

9.3.10.3 Summary - Optoelectronic Plethysmography

Unlike the abovementioned systems, OEP can measure variations in the complex structure of the chest wall and abdomen during all phases of respiration. It does this by reconstructing a 3D image of reflective chest wall markers placed in the ribcage and the abdomen. The markers are monitored by eight infrared cameras. Section 10.3.1 showed how the OEP system operates. One of the major advantages OEP has over the previously mentioned methods is that it does not need individually tailored calibration, as a single calibration can be used with a large number of patients, making it a time-efficient process. An additional advantage of OEP is that it provides a direct method for quantifying the volume of a 3D image of a subject, using the data of 89 chest markers. In addition, the patient’s performance and co-operation does not influence the accuracy of the results as in the case of conventional spirometry. Another major advantage over all previously mentioned methods is that OEP can measure compartmental volumes of different parts of the chest and abdomen. A unique feature of OEP is that it can also specifically measure the right and left side of each compartment separately and can measure synchrony between the different compartments. Furthermore, OEP measurements can be done in all positions during rest and exercise. The OEP was chosen to assess chest wall motion mechanics in this thesis because of all the advantages it has over other previously mentioned methods. The major limitation of OEP is that it is an immobile device and cannot be used bedside in a hospital environment. This necessitated the need for development of another portable motion analysis technology, namely SLP.

9.3.10.4 Structured Light Plethysmography

The history of light plethysmography started with the work of A.J Peacock et al., who developed an optical system that could map the size and dimension of the chest wall and record these changes during breathing when in an erect position (AJ Peacock, 1984). They projected strips of light on the subject's trunk and followed the shape of the chest when these strips of light became distorted. The shapes of the strips were then photographed, generating one image from one side the trunk. These analogue data were then digitalised and could be used, by operating a spline-fitting process, to calculate the chest wall volumes, the cross-sectional contour at all levels, and the position of any point. They used this technique with great success and recommended the use of this technique in clinical scenarios. Morgan et al. reported similar optical mapping on recumbent patients (Morgan, et al., 1984). They used a single camera to measure the three dimensions of the visual part of the chest wall of six subjects in the recumbent position. They captured the image of the visual side only when the subject was lying down, as the other side was not visible but at the same time immobile. Using steps similar to the Peacock method, they measured chest wall volumes in a recumbent position. They reported a high degree of accuracy when compared to spirometry. Both these systems laid the foundation for the development of structured light plethysmography technology (Richard Iles, 2010). They were the first systems to use direct light successfully to measure chest wall motion in different subjects in different positions. Tracking of motion recently became possible due to novel computer graphics and image processing technology, which led to the development of structured light technology. This technology has been used in a number of methods. The simplest method was developed by Zhang et al. (Zhang, Curelss, & Seitz, 2002), who used a colour-structured light technique to reconstruct images and used alternating colour strips of light on the subjects. The researchers then matched the coloured transitions with the edges of the images using a dynamic programming algorithm. The result was a 3D construction of the body structure (Figure 19).

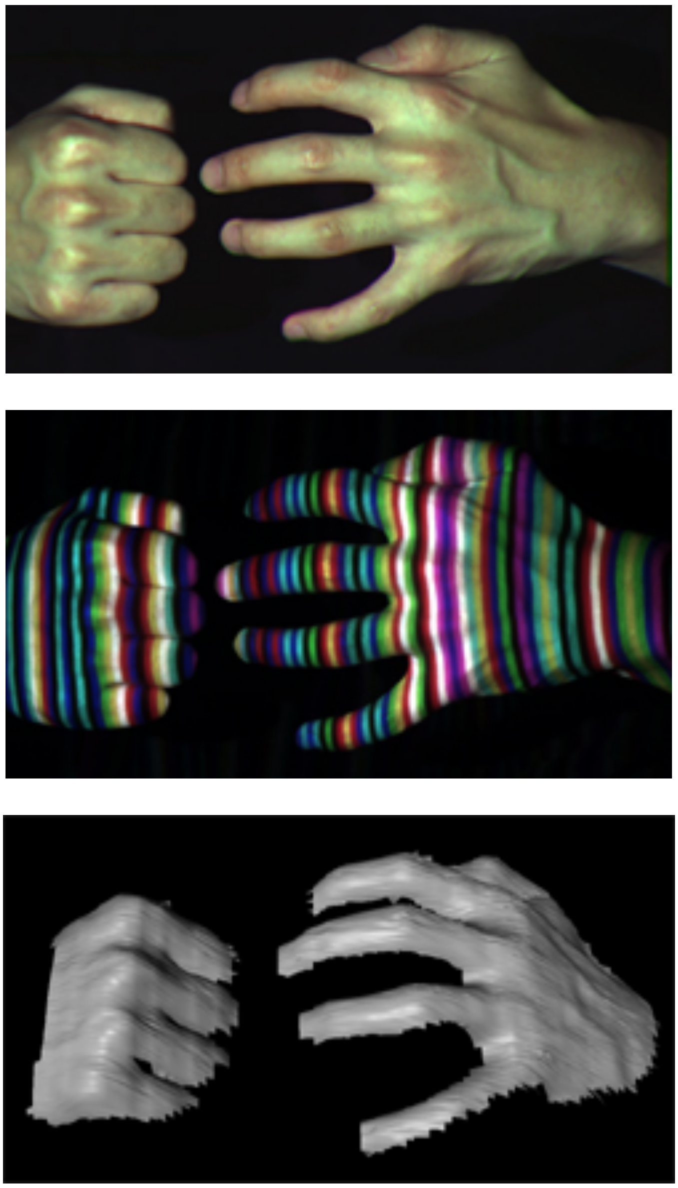

Figure 19: An example of images captured using colour-structured light technology (Zhang, Curelss, & Seitz, 2002) from top to bottom. Top figure: hand model; Middle figure: projected coloured light pattern; Lower figure: resulting 3D reconstruction.

Thereafter, multiple technologies used more complex light patterns and complex algorithms to improve the accuracy of end results. An example of these methods was used by S. Rusinkiewicz et al. In their method, they used a 3D acquisition system based on a 60 Hz structured light rangefinder that used a binary strip pattern to improve reconstruction accuracy (Rusinkiewicz, Hall-Holt, & Levoy, 2002). To improve this accuracy further, Scharstein and Zhang used a phase-shifted wave method in 2003 and 2006 (Scharstein & Szeliski, 2003) (Zhang & Huang, 2006), respectively.

Structured light plethysmography is a novel and portable device that measures dynamic regional chest wall motion. It measures both ribcage and abdominal motion using a light grid, which is simultaneously 'seen' by a digital vision system. Grid movement during breathing is analysed and outcomes are displayed in terms of regional thoraco-abdominal movement parameters as well as a 3D reconstruction. The method is non-contact, easy to operate, and requires minimal patient co-operation. Section 10.3.2 describes the working principle of SLP.

Like OEP, SLP estimates chest wall motion using a sophisticated computer program and image processing technology. The advantage of SLP over OEP is that no chest wall marker placed on the subject is required for making a capture. SLP is currently being used on normal, fit subjects and on animals to measure ventilatory parameters. It is now also being used to test infants.

SLP was validated against spirometry (by using the two methods in 40 healthy subjects) and had a good correlation (Richard Iles, 2010). In the study, SLP capture was done on 40 healthy individuals with an age of 27 +/- 12 years, weight of 74 +/-14 kg, and height of 176 +- 5.6 cm. Each patient used a nose clip, held a spirometer in their hand, breathed normally, and performed around two forced expirations. SLP measurements were made during these procedures. When the SLP data and the spirometry data were compared, the correlation was $R^2 = 0.91$ when quiet breathing data were considered, and was $R^2 = 0.97$ when forced expiration data were considered. SLP was used in this study because it filled the gap that OEP had in its lack of ability to capture in a bedside situation.

Only part of the history of chest wall motion monitoring technology was reviewed here, as it is the part that is relevant to this thesis.

In this study, OEP and SLP were chosen to measure chest wall motion in patients undergoing thoracic surgery for a number of reasons: both systems can measure regional chest wall motion; both can measure synchrony between regional chest wall compartments; the captures are done in natural breathing conditions with no restraints; they do not require patients' co-operation; they are both non-invasive; they do not need individual tailored calibration; unlike RIP, magnetometers, strain gauges, and optical fibres, they can measure change in three dimensions; they have no radiation hazards; and they are not affected by heart motion artefacts. The combination of the two technologies was selected to be used in this study because OEP, unlike

SLP, can be used during exercise and can capture chest wall motion during changes in posture and during motion. However, unlike OEP, SLP is portable, can be used at the bedside, and has an automatic calibration property, but it needs a dark room for its capture, as it uses direct projected light on the subject's chest. The summary of advantages and disadvantages of the various chest motion systems presented in this chapter is illustrated in Table 1.

9.3.11 *Summary of the Advantages and Disadvantages*

Table 1: Advantages and disadvantages of the described systems

Technology	***Advantages***	***Disadvantages***
Negative Pressure Ventilators	1. Can measure total resistance to breathing.	1. Unnatural conditions. 2. Needs patient co-operation.
Oesophageal and gastric balloons	1. Can measure abdominal contribution to the respiratory cycle.	1. Invasive. 2. Does not measure chest wall motion directly.
Magnetometer	1. Neat, sold, and mobile (can be used in the community). 2. Can be used to estimate energy expenditure.	1. Needs individually tailored calibration. 2. Can only measure change in two dimensions. 3. Requires contact between the machine and the body. 4. Does not measure regional chest wall volumes and chest wall synchrony.
Magnetic Resonance Imaging (MRI)	1. Can measure both chest wall and diaphragm motion. 2. Can measure regional chest volumes.	1. Sensitive to metals (i.e. cannot be used for a patient on an exercise bike). 2. Cannot be used during exercise. 3. Cannot be used bedside.
Respiratory Inductance Plethysmography	1. Resistant to change in postures and motion (measures cross-section rather than distance). 2. Reliable in measuring tidal volume.	1. Difficult to handle. 2. Expensive. 3. Can only measure change in two dimensions. 4. Needs contact with the body. 5. Belt tension can restrict chest wall motion. 6. Belts can migrate and overlap and affect the capture accuracy. 7. Does not measure regional chest wall

		volumes. 8. Cannot detect or measure synchrony.
The LifeShirt	1. Can be used remotely. 2. Can measure thoraco-abdominal co-ordination during exercise. 3. Lightweight. 4. Allows freedom of movement.	1. Requires individually tailored calibration. 2. Cannot measure tidal volume. 3. Does not measure regional chest wall volumes.
Transthoracic Impedance (TTI) Plethysmography	1. Cheap. 2. Simple transducer, can be used in combination to obtain ECG tracing. 3. Can be incorporated in defibrillators.	1. Affected by cardiac shadow artefacts. 2. Can be affected by artefacts during change in posture of patient movement. 3. Its ability to measure the tidal volume is debatable. 4. Does not measure regional chest wall volumes. 5. Cannot detect or measure synchrony. 6. Needs contact with the body.
Capacitive devices	1. Have wireless transmission. 2. Can measure asynchrony. 3. Can be incorporated into mattresses and used in sleeping studies. 4. Use automatic calibration.	1. Change of position and motion can cause reading errors. 2. Requires constant contact with the body. 3. Sensitive to height and weight of patient. 4. Does not measure regional chest wall volumes.
Strain Gauges	1. Can measure the tidal volume. 2. Unlike RIP, they are not affected by heart artefacts.	1. They measure circumference (have nonlinear relationship with tidal volume). 2. Need contact with the body. 3. Do not measure regional chest volumes or synchrony. 4. Restrict chest wall motion, preventing natural breathing.

Optical fibres	1. Can be used to measure chest wall motion as well as in combination to measure muscular activity of the chest. 2. Very mobile. 3. Can be used in an electromagnetically charged environment (MRI setting). 4. Can measure breath rate and inspiratory and expiratory times. 5. Cheap. 6. Lightweight.	1. Measure the circumference, which has a nonlinear association with the tidal volume (a relation that is affected by changes in the body). 2. Cannot measure chest wall synchrony. 3. Need contact with the body. 4. Difficult to position accurately.
OEP	1. Can measure regional chest volumes. 2. Can measure synchrony between regional chest compartments. 3. The capture is done in natural breathing conditions (no chest restraints). 4. Does not need patient's co-operation. 5. Non-invasive. 6. Measures chest wall motion directly. 7. Does not need individually tailored calibration. 8. Easy to calibrate. 9. Can measure change in three dimensions rather than two dimensions (as opposed to the RIP and Magnetometer) or circumference (strain gauges and optical fibres). 10. Has no radiation hazards. 11. Is not affected by artificial heart defects. 12. Can be used during exercise. 13. Resistant to change in postures and motion.	1. Needs manual calibration. 2. Immobile (cannot be used bedside or in an MRI environment). 3. Expensive. 4. Cannot measure muscular activity.

SLP	1. Portable. 2. Can measure regional chest volumes. 3. Can measure synchrony between regional chest compartments. 4. The capture is done in natural conditions. 5. Does not need patient's co-operation. 6. Non-invasive (uses harmless direct light). 7. Measures chest wall motion directly. 8. Does not need individually tailored calibration. 9. Can measure change in three dimensions rather than two dimensions (RIP and Magnetometer) or circumference (strain gauges and optical fibres). 10. Easy to calibrate, 11. Has no radiation hazards. 12. Is not affected with artificial heart defects, 13. Has automatic calibration property.	1. Needs a dark room. 2. Cannot measure muscular activity. 3. Cannot be used bedside or in an MRI environment. 4. Cannot be used during exercise (affected by change in postures and motion).

Table 1 summarises the characteristics of an ideal measurement system for chest wall motion and volume.

In this day and age, OEP is an experimental technique used to measure chest wall mechanics in a number of populations across the medical field. This includes neuromuscular disease patients (D'Angelo, et al., 2011) (Lo Mauro, et al., 2010), lung transplant patients (Wilkens, et al., 2010) (De Groote, et al., 2004), patients with pectus excavatum (Acosta, 2014), healthy athletes (Layton, et al., 2011), and heart failure patients (Brandao, et al., 2012).

9.4 The Need for Measuring Chest Wall Mechanics in Thoracic Surgery

Over 23,000 thoracic operations are conducted in the UK every year. Although many of these thoracic procedures have been carried out over the last 20 years, controversies concerning their safety, associated morbidity, and mortality remain. Outcomes of these operations are classically measured radio-graphically or functionally via lung function and exercise tolerance tests. A large number of authors have demonstrated a significant impairment in lung function and exercise tolerance in some types of thoracic procedures compared to others. Other studies have disagreed and indicated no difference between them. Little is known about how these operations alter dynamic chest wall function. The limitations of current methodological measurements are the probable cause for this controversy and deficiency of knowledge, as respiratory mechanics have typically been measured either invasively or by breathing manoeuvres. Performing these measurements in the immediate post-operative period in a large number of patients or during exercise is difficult and neither practical nor accurate. Nevertheless, novel advances in motion analysis technology have allowed accurate measuring of respiratory dynamics in intense exercise, potentially permitting further understanding of ventilatory mechanics. Using the chest wall motion analysis systems of OEP and SLP, the effect of eight thoracic surgery procedures and conditions on chest wall motion was studied in this thesis, namely diaphragm fixation (Chapter 3), chest wall resection and reconstruction (Chapter 4), PC surgical repair (Pigeon Chest) (Chapter 5), endobronchial valve use for lung volume reduction (Chapter 6), benign and malignant pleural effusion (Chapter 7), epidural vs. paravertebral nerve blocks (Chapter 8), post-operative pulmonary complications (Chapter 9), late changes following VATS, and Thoracotomy (Chapter 10).

10 Methods

10.1 Ethics

The studies in this thesis were undertaken in a regional thoracic centre. The National Research Ethic Service Committee of the West Midlands-The Black Country approved these studies on the 5th of February 2013 with REC reference: 10/h1202/58, Protocol number: Version2, 24.01.2013, and IRAS project ID: 59742. Informed consent was obtained from the participants. These studies were carried out in accordance with the Code of Ethics of the World Medical Association (Declaration of Helsinki) for experiments involving humans.

10.2 Recruitment

10.2.1 Inclusion criteria

1- All male or female thoracic surgery patients aged 16 or older who were willing to participate.

10.2.2 Exclusion criteria

1- Any unstable patient who cannot perform OEP or SLP.

2- Anyone below 16 years of age.

10.2.3 Collection of Sample

1- Recruitment was done through the preadmission clinic for all the thoracic patients who had been listed for elective thoracic surgery.

2-All clinically stable patients who had been referred from other specialties in the regional thoracic centre, who were going to have thoracic surgery.

3- All clinically stable patients who had been transferred from other hospitals to our regional thoracic centre, and are going to have thoracic surgery.

10.3 Technologies used in the thesis

10.3.1 OEP: Optoelectronic Plethysmography

Optoelectronic plethysmography was done by the SMART-D Motion Analysis System, BTS SpA, viale Forlanini, 40 – 20024 Garbagnate Milanese, Milan, Italy. OEP measures the complex structure of the chest wall and abdomen during all phases of respiration. It reconstructs a 3D image of the 89 reflective chest wall markers placed in anatomical reference points on the ribcage and the abdomen. The sensing of the markers is monitored by eight infrared cameras. Figure 20 shows how the OEP system operates.

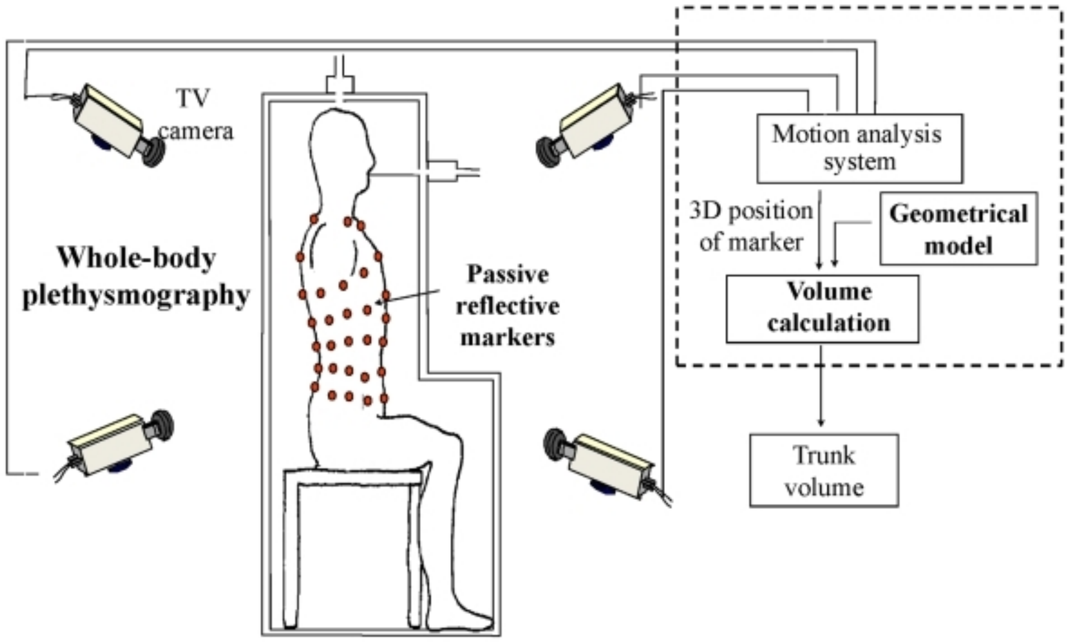

Figure 20: Schematic representation of the OEP measuring principle. Adopted from (Aliverti, et al., 2009)

These specialised cameras (solid-stat CCDs) have a frequency of 120 frames per second. Around each of the eight cameras is ring of flashing infra light LED projectors. The firing of these projectors is in sync with the cameras. This allows an ideal capture with no comet-tail noise. Further reduction of the noise and sharpening of the signal is achieved via an electronic shutter system. The detection of the 2D position of each marker in each camera is monitored by a devoted parallel processor that uses real-time pattern recognition algorithms. The system has a specialised devoted parallel processor to sense the 2Dl position of each marker in each camera. This processer uses shape recognition systems to detect real-time changes. During this process, the system recognises and categorises the 2D positions of every marker. During the process, each marker is recognised by two or more cameras. Using all of this information and a stereo-photogrammetry process, the system reconstructs a 3D image of all markers with a great degree of accuracy.

Tracking of each marker is done manually to exclude any additional noise. Noise is usually proportional to the degree of marker movement and the intensity of the activity. The noise is greatest during exercise captures. After cleaning the data from noise through manual tracking, the analysis of motion follows. This analysis is done by an automatic analyser that can trace the motion and the 3D co-ordinates of each marker. By knowing the positions of all markers during their motion, the system creates a large number of triangles joining these marker co-ordinates. Using a computational method, the chest wall volumes are obtained by calculating the volumes between all the triangles that have been created (Aliverti, Dellaca, Pelosi, Chiumello, Gatihnoni, & Pedoti, 2001). In the typical OEP measurement, the chest wall (CW) is divided into the upper ribcage or pulmonary ribcage (RCP), lower ribcage or abdominal ribcage (RCA), and adnominal compartment (AB). These measurements are either absolute volumes or changes in volumes (motion). Another unique feature of OEP is that it also specifically measures the right and left side of each compartment separately. In addition, OEP measures synchrony between the different compartments and also measures inspiratory flow, expiratory flow, respiratory rate, and minute ventilation. Furthermore, OEP measurements are taken in all positions during rest and exercise.

The processes of OEP capture:

The following softwares were used:

1. BTS SMARTCapture, Version 1.10.458.0, Copyright 2010 BTS Spa, BTS S.p.A., viale Forlanini, 40 – 20024 Garbagnate Milanese, Milan, Italy.
2. Diamov, Copyright 2001, TBM lab Politecnico di Milano, Milan, Italy.

The step-by-step OEP capture occurred as follows:

1. The Static Calibration
    a. The SMART-D Motion Analysis System was switched on.
    b. The SMART Capture icon was clicked on the desktop.
    c. The three-dimension xyz axis was assembled and positioned on the bicycle seat (Figure 21).

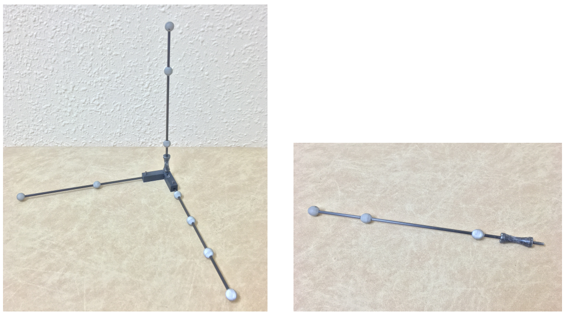

Figure 21: The three-dimension xyz axis (Left), wand (Right).

    d. Clicking on the ‘Monitor’ icon turned the cameras on.
    e. All the three-dimension xyz axis markers were checked for visibility in all cameras.
    f. New calibration was initiated by clicking on ‘New calibration’.

g. The ‘capture’ icon was clicked on. The ‘frames’ section showed the reading in seconds. This was recorded for about 50 seconds.
h. The ‘capture’ icon was clicked again to stop recording.

2. The Dynamic Calibration
    a. The three-dimension xyz axis was disassembled into a wand (Figure 21).
    b. The ‘wand sequence’ was selected from the left hand side of the screen.
    c. The ‘Monitor’ icon was clicked.
    d. Visibility of all the markers was checked on all cameras.
    e. The ‘capture’ icon was clicked.
    f. The wand was positioned horizontally and moved to cover the entire space the patient’s chest was supposed to occupy. The wand was positioned vertically and moved to cover the same space. This was recorded for about two minutes. The ‘capture’ icon is clicked to stop recording.
    g. A system calibration window appeared and the ‘start’ icon was clicked to start the system calibration.
    h. The ‘convergence’ icon had to show at least three bars for the calibration to be successful. Then, the ‘OK’ icon was clicked.

3. The Test Capture

    a. The three-dimension xyz axis was assembled and positioned on the bicycle seat.
    b. The ‘New’ icon was clicked. The ‘calibrations folder’ was selected. The file was then given a name. The ‘OK’ icon was clicked.
    c. The ‘Monitor’ and ‘capture’ icons were clicked in a sequence to start the test capture.
    d. The axis was then moved within the calibrated space for about one minute.
    e. The ‘capture’ icon was clicked to stop recording. The ‘save’ icon was clicked to save the test capture.
    f. The “go 3D” icon was clicked to reconstruct a 3D image of the xyz axis on the monitor.
    g. The image was made smaller by using the shift key and the mouse.
    h. The ‘Play’ icon was clicked, which showed the axis moving within the calibrated space. All markers were checked for being visible and within the calibrated space.
    i. The ‘Save’, ‘Select all tracks’, and ‘OK’ icons were clicked in a sequence to save the test captures.
    j. The SMART tracker was then closed by clicking the cross at the top right corner of the screen.

4. The Capture

    a. The ‘New’ icon was clicked. A file name was then selected.
    b. The patient was asked to sit on the bicycle.
    c. The 89 chest wall markers were placed on the patient's chest, according to the protocol (Cala, et al., 1996) (Aliverti A. S., 2004).
    d. Two tripods were placed on the patient’s sides for the patient to hold.
    e. The patient was instructed to avoid bending and covering the dots.
    f. The heart rate was monitored using a standard NHS pulse oximeter.
    g. The patient was asked to breathe normally.
    h. The ‘capture’ icon was clicked.
    i. The camera screens were checked to prevent reflections from some objects in the room.
    j. The patient was asked to perform a vital capacity manoeuvre.
    k. Then the patient performed one of the following:
        i. If a quiet breathing capture was desired, the patient was asked to breathe normally for three minutes.
        ii. If an exercise capture was desired, the patient commenced an incremental exercise protocol, which consisted of pedalling unloaded for one minute and then with an incremental load of 5 Watts/minute. The patient

was required to maintain 60 revolutions per minute until he or she reached 80% of the maximum predicted heart rate ([220-Age] x 80%).

l. The ‘capture’ icon was clicked to stop recording, and the capture was then saved by clicking the ‘Save’ icon.
m. The ‘go 3D’ icon was then clicked to produce the 3D reconstruction image of the chest wall markers.
n. This was saved by clicking on the ‘Save’, ‘Select all tracks’, and ‘OK’ icons in sequence.
o. The SMART tracker was then closed by clicking the cross icon at the top right corner of the screen.

5. The Tracking

a. SMART tracker software was opened and the desired file was selected for tracking by clicking on ‘Open’ and ‘Open File’ icons in a sequence.
b. The ‘Hide/Show calibrated volume’ icon and the ‘Hide/Show floor’ icon were clicked on the ‘appearance tool bar’ on the right side of the screen.
c. The ‘Hide/show reconstructed data’ icon was right-clicked to increase the dot size from 3 to 5.
d. The ‘Open model’ icon was clicked and the ‘Jolly89.xmf’ file was selected.

e. The ‘Fast labeling mode’ icon was clicked on the left-hand side tool bar.
f. Each dot was clicked to label it according to the ‘Jolly89.xmf’ model.
g. After finishing labelling the anterior chest and abdomen, the image was rotated clockwise to start labelling the back.
h. After all the labelling was completed, a check was done for the missing dots by going to the end of the recording. Those dots were marked as red in the model editor window. A note was made about the dots in red (missing dots).
i. The ‘Hide/show graph viewer’ icon was clicked on the right side of the screen.
j. The ‘Tracks’ icon on the right-hand side was clicked. A window appeared. A reference dot was selected. The missing dot to be re-tracked was selected.
k. The graph on the right side was checked for the time when the dot first disappeared. The slide control was used to place the recording before the time when the dot was missed.
l. The right and left arrows on the keyboard and the mouse were used to go forward and backward, to detect the missing dot, label it, and re-track it.
m. This procedure continued until the graph was completed for the re-tracked dot.
n. This was repeated to re-track all missing dots.

o. This was saved by clicking on the ‘Save’, ‘select 89 markers’, and ‘OK’ icons in sequence.

p. The SMART tracker was then closed by clicking the cross on the top right corner of the screen.

q. The ‘Calcolo Volumi’ folder was clicked and all its files were copied. This was then moved into the same folder as the tracked file.

r. The disk operating system in windows was opened.

s. ‘CD..’ was typed, followed by clicking the ‘Enter’ button on the keyboard. This was repeated twice.

t. ‘CD’ was typed before the path of the tracked file, and the ‘Enter’ button was clicked.

u. The “vemgbis seduto.sup” command was typed, followed by the tracked file name, and then the ‘Enter’ button was clicked.

v. A message was shown stating the number of frames.

w. The window was closed.

x. This created a file ending with a ‘.dat’ extension.

y. The Diamov program was opened by clicking on ‘Diamov.exe’.

z. The ‘Open’ icon was clicked, and the file ending in ‘.dat’ generated in the above steps was selected.

aa. A window showing the breath waves appeared.

bb. The ‘Ctrl’ key and the mouse were used to select the number of breath waves to be analysed.

cc. The ‘Find Maxima and Minima’ icon was clicked in the toolbar.

dd. The ‘Save’ icon was clicked. The file name was selected and saved.

ee. The ‘signals’ and ‘ventilatory parameters’ icons were clicked in a sequence. A window appeared. In the ‘normalize from a MXN file’ field, the ‘max min’ file generated in the previous step was selected.

ff. In the ‘BBB and MED file names’ field, the output file name was written.

gg. The ‘OK’ icon was clicked. A new file appeared in the window containing the chest volume data. This was the final result of the OEP capture.

Synchronisation in OEP

The level of synchronisation/dys-synchronisation was assessed by comparing the wavelengths of two sets of breath (before and after surgery). The time in seconds between the two end inspiration peaks (before and after surgery) was measured. In case of complete synchronisation, this time equals zero. This time was then divided by the time needed to complete a full breath cycle, and the results were multiplied by 360 degrees. This provided the level of dys-synchronisation in degrees. The percentage change of dys-synchronisation could therefore be calculated by subtracting the degree of synchronisation after surgery (in degrees), minus the degree of synchronisation before surgery (in degrees), divided by the degree of synchronisation before surgery (in degrees), which is then multiplied by 100.

10.3.2 **SLP: Structured Light Plethysmography**

The SLP capture was done via Thora-3D, PneumaCare Limited, Cambridge, UK. In a typical SLP capture, the subject is placed in a sitting or lying position against a hard surface like a chair or bed and asked to breathe quietly and normally for five minutes. Male subjects are usually topless and females wear a tight T-shirt with as few creases as possible.

The PneumaView-3D software (version 1.1, Copyright @2011-2013 PneumaCare Limited, Cambridge, UK) was initiated by clicking on its icon on the SLP machine disk top. A new capture was added by clicking on ‘add new patient’, and the patient details were then added. The ‘Save Changes’ icon was clicked. Then, the ‘Capture’ icon was selected from the right side of the screen. The light grid size was then selected from three options, ‘small’, ‘medium’, or ‘large’, based on the individual chest size of each subject. Then, the ‘Start tidal manoeuvre’ icon was clicked. This initiated the light grid. The rig was moved within 4 feet to allow the light grid to cover the whole of the chest wall (Figure 22). The ideal position of the grid on the patient chest was from just below the umbilicus to the sternal notch and between the two anterior axillary lines.

Figure 22: Example of a structured light system and pattern. Adopted from (Mair, 2012).

Then, the ‘OK’ icon was clicked, and the capture was initiated. Each capture was done during five minutes of quiet breathing. On the screen, a graph appeared with the captured breath waves. After five minutes, the machine automatically ended the capture. This was saved on individual subjects’ files.

The tracking stage was automatically conducted by the SLP machine and involved the detection of grid intersection points. The corners of the squares were ‘grid intersection points’, and there were (23 × 28) of these (see Figure 23). The system then identified these grid intersection points using complex algorithms via two cameras, each positioned at different angles and different locations.

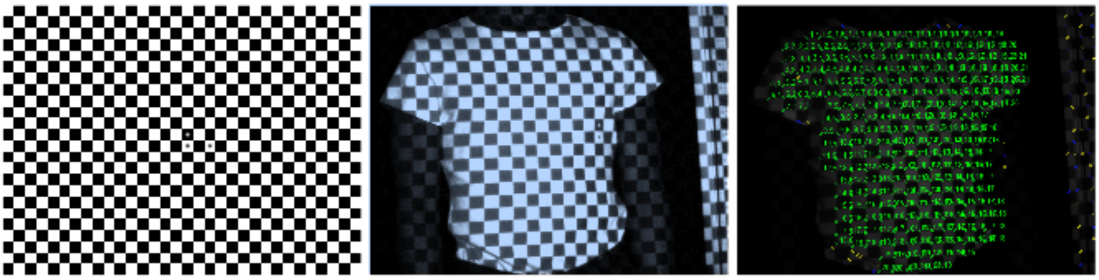

Figure 23: The grid pattern (left), the grid pattern on a subject (centre), and the grid pattern intersection points (right). Adopted from (De Boer, 2010).

In the calibration stage, definition of the internal and external margins of the two cameras and the light source was made. This was followed by reconstruction of the image, isolating the chest area and filling in the defects through a complex algorithm (see Figure 24).

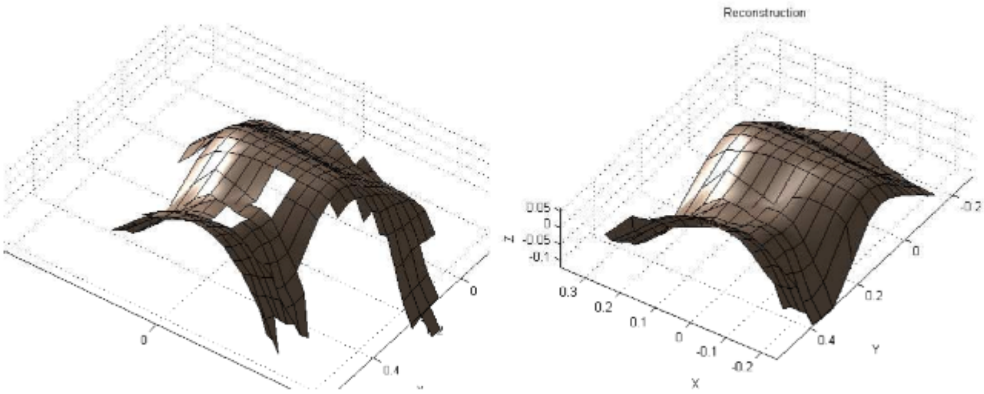

Figure 24: A reconstruction before (left) and after (right) isolating the chest area and filling in missing points. Adopted from (De Boer, 2010).

This was followed by chest wall volume calculations; these involved calculating the volume between the reconstructed image and the back support of the subject. This step is illustrated in Figure 25.

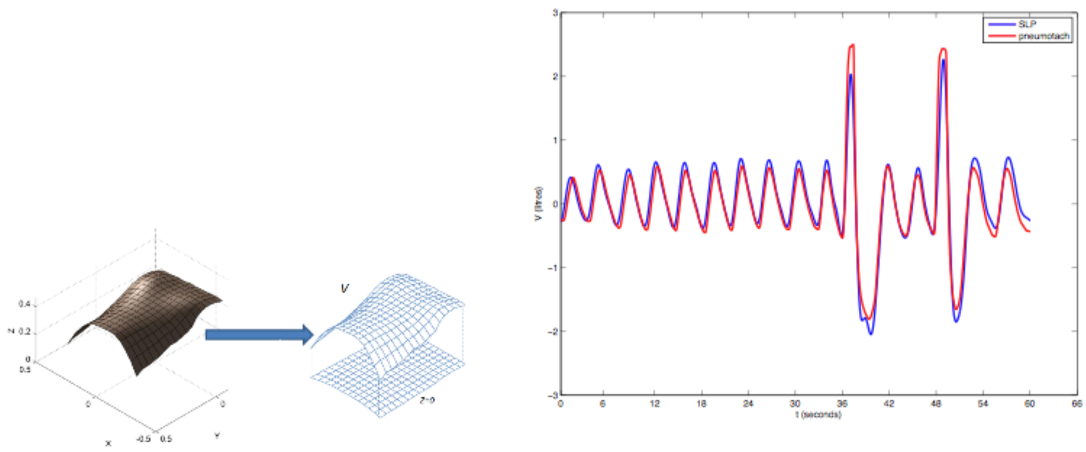

Figure 25: The ‘chest wall volume’ V was calculated by SLP (left) and a typical example of SLP volume data superimposed on pneumotach volume data of the same measurement. Adopted from (De Boer, 2010).

SLP measured synchronisation using the Konno-Meed X-Y plot (Stocks J. , 1996).

10.4 Statistics

The statistical analysis was executed by IBM© SPSS© Statistics Version 22.0.0.0. In this pilot study, the normality of the OEP and SLP data was assessed using the Kolmogorov-Smirnov test. The results showed that the data were not normally distributed. Accordingly, the continuous data were presented as the median or median and interquartile range (IQR). Categorical data were presented as a number and percentage. The OEP and SLP data is given in terms of chest wall motion in each single breath (each capture measured a number of breaths). Therefore, the median and IQR of the chest wall motion during a number of breaths were taken for one patient or a group of patients. In chapters 3 and 4 this was done for one patient (n=1). In the chapters 5 to 10 this was calculated for a group of patients (n=number of patients in each group). These measurements were done in different time points, and each patient had only one measurement.

Due the small number of patients in this study, no attempt was made to calculate the P value, as complex statistical tests could not be used in one patient or in a small number of patients, as is the case in this thesis.

To compare the demographic data between two groups, the Mann-Whitney U test was used to assess the continuous data, and the Chi-Square test was used to assess the categorical data. To compare the demographic data between more than two groups, the Kruskal-Willis test was used for the continuous data and the Chi-Square test for the categorical data. A statistical significance of P value less than 0.05 was used for the analyses. Any P value <0.05 was deemed significant. As this is a pilot study, power calculation was not done.

10.1 Figures

All figures used in this thesis are either original creations or figures with permission to use.

11 Chapter 3: The Effect of Diaphragmatic Plication (Fixation) on Chest Wall Mechanics

11.1 Introduction

Diaphragmatic paralysis has a significant symptom burden on patients' quality of life. This is largely because of its paradoxical movement during respiration (Ko, 2009). We know that by plicating (double-breasting and making taut) the floppy paralysed diaphragm, there is improvement in pulmonary function and patients' symptoms of breathlessness (Freeman, Wozniak, & Fitzgerald, 2006) (Celik, Celik, Aydemir, Tunckaya, Okay, & Doqusoy, 2010). However, little is known about how this improvement alters dynamic chest wall function. In this thesis, the hypothesis is that, due to the paradoxical movement of a unilateral, paralysed diaphragm, the ribcage abdominal compartment chest wall motion on both sides of the chest is impaired and plication reverses this impairment by preventing that paradoxical movement.

11.2 Methods

This case report was undertaken in a regional thoracic centre. The National Research Ethic Service Committee of West Midlands-The Black Country approved the study on the 5th of February 2013, with the REC reference: 10/h1202/58, Protocol number: Version2, 24.01.2013, and IRAS project ID: 59742. Informed consent was obtained from the participants. This study was carried out in accordance with the Code of Ethics of the World Medical Association (Declaration of Helsinki) for experiments involving humans. Using OEP (Cala, et al., 1996) (Aliverti A. S., 2004), total and regional chest wall volumes were measured in one male patient with left-sided idiopathic diaphragmatic paralysis (Figure 26). He was diagnosed with 'asthma' and had a long history of postural shortness of breath and recurrent respiratory tract infections. He was scheduled for diaphragmatic plication. Surgery was performed under general anaesthesia and through an open incision in the chest or posterolateral thoracotomy. Plication was performed by a double-breasted technique, first using interrupted mattress sutures and then a continuous stitch (Freeman, Wozniak, & Fitzgerald, 2006). The patient returned to a dedicated thoracic surgery ward post-operatively. According to the unit protocol, he was managed with a daily physiotherapy programme, which included deep breathing exercises, supported coughing, and mobilisation. The patient's data were collected and included the participant's age, height, weight, smoking status, and relevant past medical history. Spirometry was performed (Carefusion Microlab) prior to every chest wall motion capture. Chest wall motion was measured during quiet breathing pre-operatively and post-operatively at six months. The six-month period was chosen as the second time point for logistical reasons, as it was the most convenient time for the patient to have his capture and coincided with his clinic appointment. The patient did not wish to do the capture before then. Acquisition of data was performed using the SMART suite software (Cala, et al., 1996) (Aliverti A. S., 2004). OEP cameras were calibrated each day prior to the tests. The acquisition/procedure required 79 hemispherical and 10 spherical reflective markers to be placed on the participant's chest wall and back using bioadhesive hypoallergenic tape (Cala, et al., 1996) (Aliverti A. S., 2004). The standard placement of markers was done according to Cala et al.

(Takeda, et al., 1991). OEP acquisition protocol included observations of heart rate, oxygen saturations, and blood pressure, and the pre-procedure was recorded from one minute before quiet breathing to five minutes after the acquisition. All acquisition was done while the patient was in an erect position. During the OEP acquisition, ribcage and abdominal volumes were recorded by eight infrared cameras operating at 60Hz and tracking the displacement of the markers during vital capacity and during quiet breathing for three minutes. From the overall and regional chest wall volumes measured by OEP, the subsequent parameters were acquired: tidal volume (VT) as the overall and compartmental chest wall volume changed, respiratory rate (RR), and minute ventilation (VT x RR) (Cala, et al., 1996) (Aliverti A. S., 2004). Each OEP capture gave us a median or Median + IQR of a total and regional chest wall motion of the number of breaths during three minutes of quiet breathing.

The statistical analysis was executed by IBM© SPSS© Statistics Version 22.0.0.0. The normality of the data was assessed using the Kolmogorov-Smirnov test, which was used to assess the normality of the data. The results showed that the data were not normally distributed. Accordingly, the data were presented as median or median + IQR. No attempt was made to calculate the P value, as complex statistical tests could not be used for just one patient.

11.3 Results

Our results showed that our patient's pre-operative spirometry was impaired. His FEV_1 was 1.8 L (55% predicted; patient's height was 179 cm) and FVC was 2.6 L (62% predicted). There was an improvement in FEV_1 six months after the operation: 2.1 L (63% predicted). Similarly, there was an improvement in FVC: 3.1 L (73% predicted) in the same time frame.

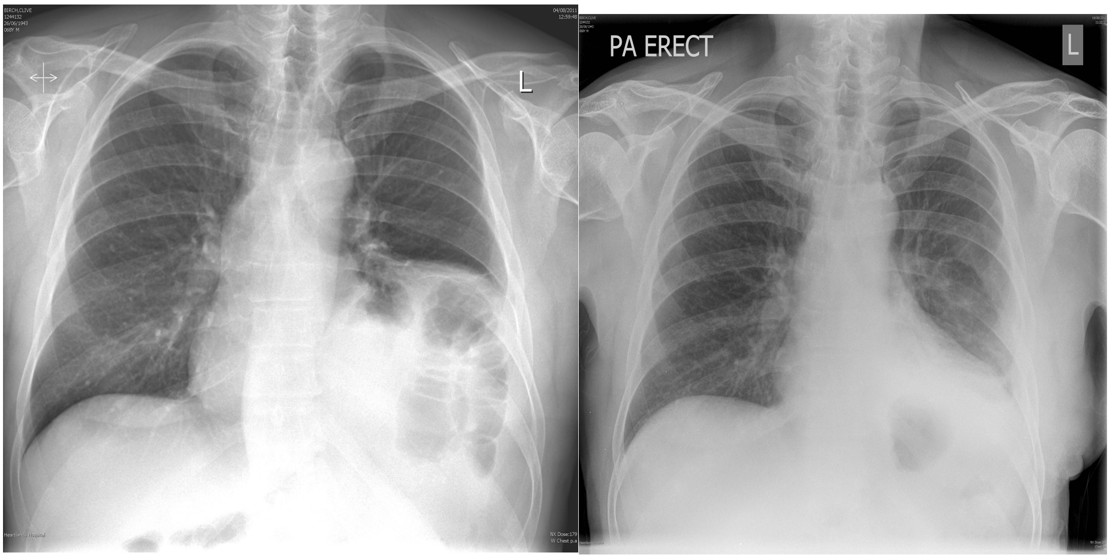

Figure 26. Chest radiograph before and after diaphragmatic plication: These two PA erect chest radiographs illustrate the thin over-stretched paralysed diaphragm pre-operatively on the left, which assumes a 'normal' position one week following left diaphragmatic plication (right).

In quiet breathing, the tidal volume improved from 0.71 (0.23) L pre-operatively to 0.88 (0.11) L six months after the surgery. Sub-compartment analysis reflected an increase in the contribution of the ribcage abdominal compartment from 0.01 (0.05) L pre-operatively to 0.17 (0.05) L at six months at rest. However, the pulmonary ribcage contribution to total tidal volume did not improve (Table 2). There was an improvement in the tidal volume in both the operated paralysed side (left) and the contra-lateral 'normal' side. On the operated side, the overall tidal volume increased from 0.36 (0.11) L pre-operatively to 0.44 (0.08) L six months after surgery during quiet breathing.

On the contra-lateral 'normal' side, there was also a marked improvement in overall tidal volume from 0.36 (0.11) L pre-operatively to 0.44 (0.05) L six months after surgery during quiet breathing. These increases on both sides are due mainly to improvements in the expansion of the ribcage abdominal compartments (Table 2).

Table 2: Respiratory parameters before and six months after diaphragmatic plication.

	Before Operation		6 months	
	MEDIAN	IQR	MEDIAN	IQR
Overall Tidal Volume (L)	0.71	0.23	0.88	0.11
Tidal Volume on the Operated Side (L)	0.36	0.11	0.44	0.08
Tidal Volume on the Non Operated Side (L)	0.36	0.11	0.44	0.05
Minute Ventilation (L)	10.53	2.72	14.25	1.55
Mean Inspiratory Flow (L/Sec)	0.51	0.10	0.65	0.05
Mean Expiratory Flow (L/Sec)	0.28	0.14	0.37	0.06
Overall Ribcage Pulmonary Tidal Volume (L)	0.13	0.09	0.08	0.04
Overall Ribcage Abdomen Tidal Volume (L)	0.01	0.05	0.17	0.05
Overall Abdominal Tidal Volume (L)	0.60	0.10	0.62	0.09
Ribcage Pulmonary Tidal Volume – Non-Operated Side (L)	0.07	0.04	0.06	0.02
Ribcage Pulmonary Tidal Volume – Operated Side (L)	0.06	0.05	0.03	0.02
Ribcage Abdomen Tidal Volume – Non-Operated Side (L)	0.01	0.03	0.05	0.02
Ribcage Abdomen Tidal Volume – Operated Side (L)	0.01	0.02	0.11	0.04
Abdominal Tidal Volume – Non-Operated Side (L)	0.29	0.06	0.32	0.04
Abdominal Tidal Volume – Operated Side (L)	0.29	0.05	0.30	0.04

Respiratory parameters measured using OEP during quiet breathing before and six months after unilateral diaphragmatic plication (n = 1), data are in Median + IQR.

It was found that during quiet breathing before the operation, the expansion of the ribcage abdominal compartment was lagging behind the abdominal expansion during inspiration on both sides of the chest. After the operation, this lag disappeared on both sides and resulted in complete synchronisation of both sides following unilateral diaphragmatic plication (Figure 27).

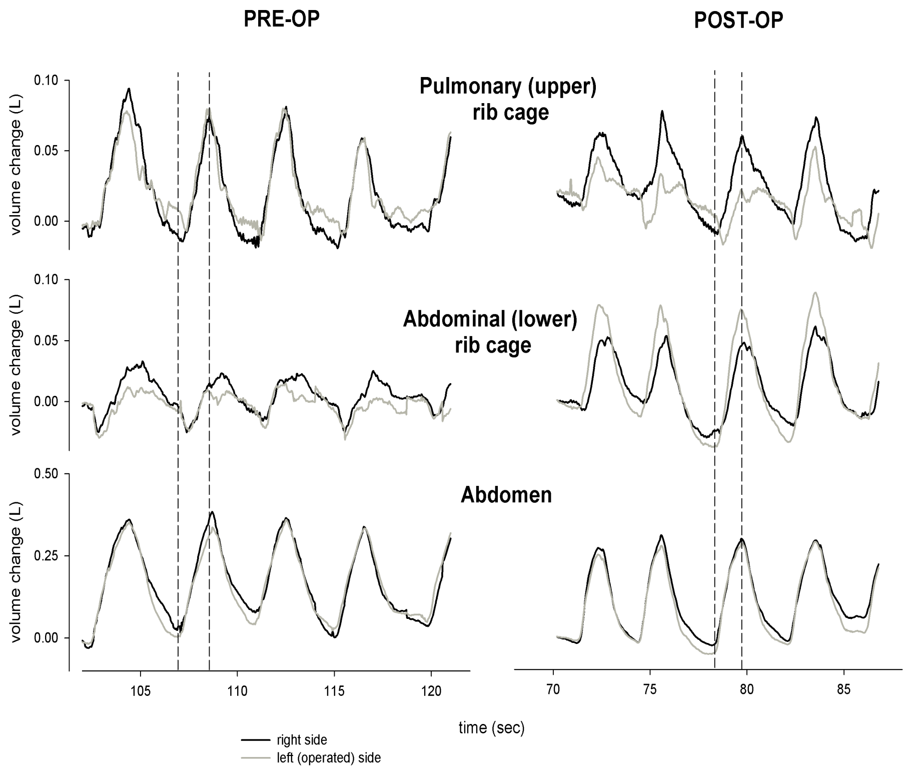

Figure 27: Synchrony of chest wall before and six months after diaphragm plication. The figure shows the phases of breathing on both sides of the chest wall, in the three compartments (pulmonary rib cage, abdominal ribcage, and abdomen), during quiet breathing before the operation and six months after unilateral diaphragmatic plication. It was found that before the operation, the expansion of the abdominal ribcage was lagging behind the abdominal expansion, showing complete inward paradoxical movement during inspiration on both sides of the chest. After the operation, that inward paradoxical movement disappeared on both sides and resulted in complete synchronisation of both sides following unilateral diaphragmatic placation (n = 1). The data are shown in volume (litres) and time (seconds).

11.4 Discussion

This case report illustrated that lung function assessed by spirometry showed a trend of improvement at six months post-operatively compared to pre-operative values in one patient who had undergone surgical plication for unilateral diaphragmatic paralysis. This is in keeping with other large published results. Feeman et al. also reported improved spirometry, dyspnoea score, and functional status in 41 patients, six months after having had diaphragmatic plication (Freeman, Wozniak, & Fitzgerald, 2006). They reported improvement in FEV1 and FVC of 21% and 17%, respectively, which are comparable to the observed results in this study of improvements in FEV1 and FVC of 18% and 24%, respectively, during the same time period. These improvements seemed to be sustained long-term, as reported by Celik et al., who observed, in 13 patients who had undergone diaphragmatic plication with a mean follow-up of 5.4 years, an improvement in FVC and FEV1 of 43.6 ± 30.6% ($p < 0.05$) and 27.3 ± 10.9% ($p < 0.05$), respectively (Celik, Celik, Aydemir, Tunckaya, Okay, & Doqusoy, 2010). Paralysis of the diaphragm resulted in a paradoxical motion of both sides of the lower ribcage with inspiration, which resulted in more severe respiratory impairment than if the diaphragm had been fixed in position (Ko, 2009). It was hypothesised that abolishing the superior paradoxical movement of diaphragm by plication would improve the efficacy of the respiratory muscles, which would result in improved lung volumes. The results supported the hypothesis. In the patient in this study, there was a trend of improvement during quiet breathing in the overall tidal volume of the chest cavity six months after the surgery. This was a direct result of preventing the paradoxical movement of the paralysed diaphragm. It was also found that during quiet breathing, the increase of tidal volume six months after surgery was mainly due to a trend of an increase in the contribution of the ribcage abdominal compartment of the chest wall. Surprisingly, the magnitude of improvement seemed to be similar in both the operated and contra-lateral sides. In an animal model with eight dogs, Takeda et al. (1991) reported improvement in the contra-lateral hemi-diaphragm contractility and diaphragmatic contribution to breathing after diaphragmatic plication following unilateral diaphragmatic paralysis (Takeda, et al., 1991). Takeda’s results have not been replicated in humans. Celik et al. reported using fluoroscopy while the plicated diaphragm was immobile, remained elevated, and had no paradoxical motion, but they did not comment on the function of the diaphragm on the non-operated side (Celik, Celik, Aydemir, Tunckaya, Okay, & Doqusoy, 2010). The descriptive case report in the present thesis showed a trend of improvement of both sides of the chest wall and the diaphragm (abdominal ribcage compartment) after a unilateral plication of a paralysed diaphragm. From a physiological and anatomical viewpoint, both sides of the diaphragm are interconnected. The central tendon acts as a rigid mechanical linkage between the two sides. Simplistically, one can envisage when the over-stretched paralysed side loses tension and the interconnected 'normal side' has nothing against which to contract. In this study, it was thought that plication restores this tension and thus restores function of the contra-lateral diaphragm. By this mechanism, it was thought that it eliminates the paradoxical motion of the diaphragm and restores synchrony in the interconnected chest compartments on both sides of the chest. In summary, this descriptive case report was the first report to describe in humans the almost equal trend of improvement in dynamic chest wall motion/volumes both on the operated side and the contra-lateral side following plication for idiopathic unilateral diaphragmatic paralysis.

This descriptive case report showed some trends of improvement on bilateral chest wall motion in one patient who had unilateral plication of a paralysed diaphragm.

11.5 Limitations

The major limitation of this descriptive case report was that it involved only one patient having one type of diaphragm plication; therefore, the generalisability of results was not possible. The procedures were not commonly performed and the OEP tests required additional hospital visits that many patients were not prepared to commit to.

Interpretations of the results should be taken with caution. This single case report did not take into account the variation of larger population demographics such as body mass index, which might affect regional chest wall motion, as reported by Barcelar Jde et al. (Barcelar Jde, et al., 2013). It is unclear whether the results from the present study could be replicated in all patients with unilateral diaphragm plication, as the muscular build-up of the diaphragm and the chest wall varies from patient to patient and between genders and can influence the chest wall motion. As this is only a case report, analysis of the effect of such variation on the outcome of unilateral plication is not possible. The findings are in the process of being validated.

12 Chapter 4: The Effect of Chest Wall Reconstruction on Chest Wall Mechanics

12.1 Introduction

Sarcomas are rare tumours for which dyspnoea can be a presenting symptom (Gross, Younes, & Haddad, 2005). Whether this is a result of dysfunctional chest wall motion in these patients is yet to be discovered. Ideal reconstructive prosthesis is still a matter of debate and largely depends on a surgeon's preference. The effect of the type of prosthesis on chest wall dynamics has not been reported before. This descriptive case study describes in detail how chest wall mechanics can be altered in a patient with isolated extra-thoracic chest wall sarcoma who undergoes a chest wall resection and reconstruction using non-rigid prosthesis both during quiet breathing and exercise.

12.2 Methods

This case report was undertaken in a regional thoracic centre. The study was approved on the 5th of February 2013 by the National Research Ethic Service Committee of West Midlands-The Black Country, with REC reference: 10/h1202/58, Protocol number: Version2, 24.01.2013, IRAS project ID: 59742. Informed consent was obtained from the participant. This study was carried out in accordance with the Code of Ethics of the World Medical Association (Declaration of Helsinki) for experiments involving humans.

Using OEP, total and regional chest wall volumes were measured using eight infrared cameras, tracking the displacement of 89 chest wall markers on the patient's chest, and calculating compartmental motion and volumes (Acosta, 2014). Our subject was a 76-year-old male patient diagnosed with spindle cell sarcoma of the right postero-lateral extrathoracic aspect of the chest wall. The tumour was 12 cm x 8 cm in size, lying deep and inferior to the right scapula extending down to the 10th rib and involving the fourth rib (Figure 28). Surgery was performed by mobilising the latissimus dorsi muscle of the tumour. The fourth rib, and the serratus anterior muscle attached to the tumour were excised en bloc. The resulting defect was covered with a tightly secured Prolene mesh and a rotated latissimus dorsi flap. Spirometry was performed prior to every chest wall motion capture. Chest wall motion was measured in an erect position during quiet breathing and exercise using cycle ergometry pre-operatively and post-operatively at five months, as previously described (Acosta, 2014). Each OEP capture provided median or median + IQR of a total and regional chest wall motion of a number of breaths during quiet breathing and exercise.

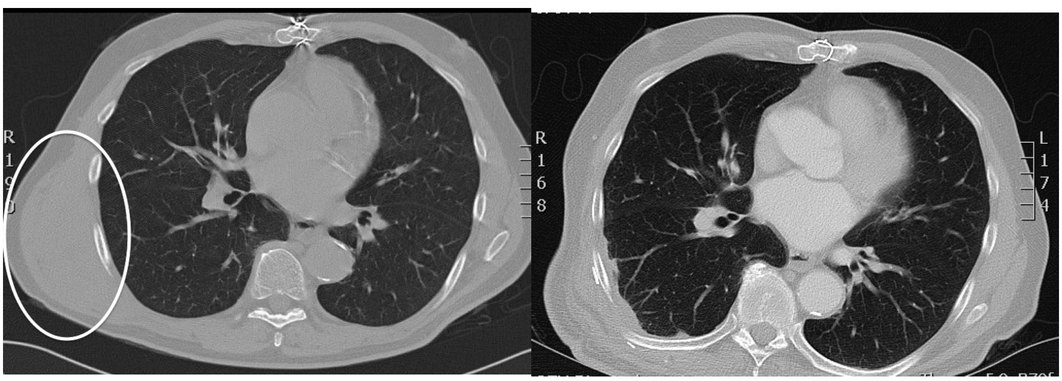

Figure 28: CT scans before and five months after chest wall resection and reconstruction of a right chest wall tumour. These two CT scans of the chest illustrate the pre-operative chest wall sarcoma (circle, left) and five months post-operatively and the Prolene mesh reconstruction (right) (n = 1).

The statistical analysis was executed by IBM© SPSS© Statistics Version 22.0.0.0. The normality of the data was assessed using the Kolmogorov-Smirnov test. The results showed that the data were not normally distributed. Accordingly, the data were presented as median + IQR. No attempt was made to calculate the P value, as complex statistical tests could not be used for one patient.

12.3 Results

During quiet breathing, there was asynchronous abdominal ribcage compartment motion on the opposite side of the tumour, compared to all other compartments. This asynchrony was corrected when measured five months after surgery (Figure 29).

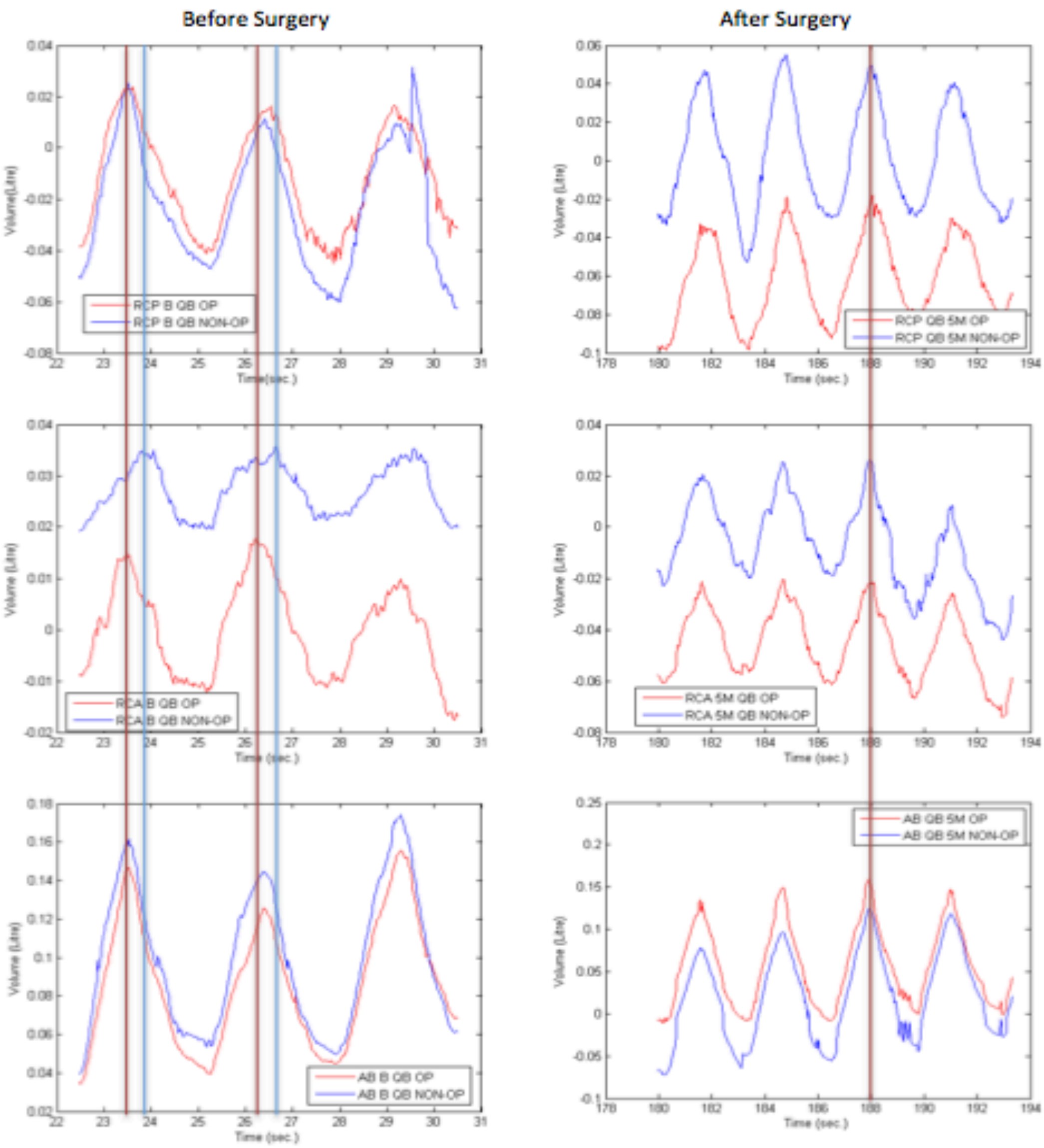

Figure 29: Synchrony of the chest wall compartments before and after chest wall resection and reconstruction. This graph demonstrates a breath-by-breath analysis examining the synchrony between chest compartments. The left panel shows pre-operative chest wall motion during quiet breathing, from top to bottom of the pulmonary ribcage (RCP), abdominal ribcage (RCA), and the abdomen (AB), respectively. The red line represents the operated side and the blue line the non-operated side. The right panel shows motion in each compartment five months after surgery. The lower ribcage on the opposite side to the tumour side lagged by 58(22) degrees out of phase, when compared to the side with the tumour. After surgery, this asynchrony improved to 14(17) degrees (n = 1). Data are shown as volume (litres) and time (seconds).

Five months after surgery during quiet breathing, the overall tidal volume showed a trend of improvement by 19(31)% compared to the pre-operative value. This was due to a trend of increased contribution of the abdominal ribcage and abdominal compartments by 102(80)% and 17(35)% respectively, equally on both sides of the chest.

During exercise, there was a 19(51)% trend of reduction of pulmonary ribcage motion on the operated side five months after surgery, and this was not replicated on the non-operated side.

Table 3: Respiratory parameters before and five months after chest wall resection.

	Preoperatively	5 months post op
	Value (L)	Value (L)
Overall Tidal volume	0.45 (0.12)	0.53 (0.05)
Tidal Volume of pulmonary rib cage	0.14 (0.04)	0.15 (0.02)
Tidal volume of abdominal rib cage	0.04 (0.02)	0.08 (0.01)
Tidal volume of abdomen	0.25 (0.08)	0.30 (0.03)
Tidal volume of right abdominal rib cage (operated side)	0.02 (0.01)	0.04 (0.01)
Tidal volume of left abdominal rib cage (non-operated side)	0.01(0.01)	0.04 (0.01)
Tidal volume of right chest (operated side)	0.22 (0.07)	0.25 (0.03)
Tidal volume of left chest (non-operated side)	0.24 (0.04)	0.27 (0.03)

Respiratory parameters measured using OEP during quiet breathing before right chest wall resection and five months after (n = 1). Data are shown in Median + IQR.

Sub-analysis of the EEV and end inspiratory volume during exercise showed that the reduction of motion in the pulmonary ribcage on the operated side was due to an increase in the EEV on that side (Table 4). There was also a 56% trend of reduction of the ERV on that side of the upper ribcage during the same time frame.

Table 4: The change in EEV of the pulmonary ribcage of operated side and non-operated side during exercise.

		Change at 5 Months
△ EEV on RCP operated side	50% Exercise	7(1) %
	100% Exercise	6(1) %
△ EEV on RCP non-operated side	50% Exercise	- 2(2) %
	100% Exercise	- 1(1) %

The table shows the percentage change in EEV volume of the RCP on both sides of chest during 50% and 100% exercise before and five months after surgery. It is clear that the EEV of RCP on the operated side increased after surgery during 50% and 100% exercise, suggesting a defective expiratory mechanism on the that side (n = 1). The data are shown as median (IQR).

The FEV1 was 2.70 L pre-operatively (99% predicted), and the FVC was 3.67 L (108% predicted). Five months after surgery, there was a reduction in FEV1 to 2.38 L, but the FVC remained unchanged at 3.69 L.

12.4 Discussion

This descriptive case report showed that an extra-thoracic chest wall sarcoma exerts a restrictive mass effect on regional chest wall motion resulting in asynchrony and reduced volumes in the abdominal ribcage and abdomen compartments due to the position of the tumour. Similar findings were described in individuals with restrictive pulmonary disease (Romagnoli, et al., 2004). This defect improved following resection and reconstruction with a semi-rigid, taut Prolene mesh. Because the chest wall works as a unit, the impairment was apparent on both sides of the chest, though the tumour was unilateral. It was uncertain why it was the contra-lateral abdominal ribcage side that lagged behind all other compartments, but it may have been due to a mechanical displacement of that part of the chest due to the presence of such a large tumour.

Removing the extra thoracic chest wall tumour and covering the defect with a Prolene mesh seemed to reverse the restriction and restored synchrony during quiet breathing. After surgery, however, the results showed a trend of reduction in the motion of the pulmonary ribcage compartment during exercise compared to pre-operative values, due to defective expiratory mechanics on the operated side following reconstruction. This was further supported by a persistently reduced FEV_1 after surgery.

12.5 Conclusion

This descriptive case report described in detail the trend of the negative effect of the chest wall tumour on global chest wall mechanics during quiet breathing and exercise and described how surgery may partially reverse this trend. Further studies with larger numbers are required to validate the results, to look at the effects of rigid- and physiological-type repairs, and to correlate findings with the patient’s function and disability.

12.6 Limitations

The limitation of this study was that it involved only one patient who underwent one type of chest wall reconstruction using a non-rigid prosthesis. This was due to recruitment limitation, as chest wall cancer is a rare disease (David & Marshall, 2011). Detailed discussion of the limitations of recruitment is addressed in the conclusion section of this thesis.

13 Chapter 5: The Effect of Pectus Carinatum (Pigeon Chest) Repair on Chest Wall Mechanics

13.1 INTRODUCTION

Pectus carinatum is a deformity that is characterised by the protrusion of the anterior chest wall caused by overgrowth of the costal cartilage. Males are four times more susceptible to the deformity than females, and it is linked to connective tissue diseases, such as Marfan syndrome and scoliosis (Martinez-Ferro, Fraire, & Bernard, 2008). Patients with PC present themselves for a surgical option for a number of reasons, including reduced exercise tolerance. Principally, however, they aim to reverse a poor or negative body image and its resulting psychosocial effects. A recent study concluded that surgical correction of PC might improve dyspnoea and exercise capacity (Oncel, Tuscan, Akyol, Dereli, & Sunam, 2013). It was hypothesised in the present study that this improvement could be related to a change in chest wall function. However, the effects of PC correction on dynamic chest wall motion during exercise are unknown. This is of particular relevance as these procedures are perceived as having low clinical value and are now being rationed, both in the UK and globally, because of the financial climate. This proves that physiological benefits and mechanisms may be important in deciding who receives treatment.

13.2 METHODS

This descriptive case series was undertaken in a regional thoracic centre. The study was approved on the 5th of February 2013 by the National Research Ethic Service Committee of West Midlands-The Black Country, with REC reference: 10/h1202/58, Protocol number: Version2, 24.01.2013, and IRAS project ID: 59742. Informed consent was obtained from the participants. This study was carried out in accordance with the Code of Ethics of the World Medical Association (Declaration of Helsinki) for experiments involving humans.

13.2.1 Participants

Optoelectronic plethysmography (BTS, Milan, Italy) has been validated for quantifying overall and compartmental chest wall volumes (Acosta, 2014) (Cala, et al., 1996) (Aliverti, Dellaca, Pelosi, Chiumello, Gatihnoni, & Pedoti, 2001) (Dellaca, Ventura, Zannin, Natile, Pedotti, & Tagliabue, 2010) (Vogiatzis, Aliverti , Golemati, Georgiadou, Lo Mauro, & Kosmas, 2005) and was used in three male patients with PC, who were aged 18(2) years and were scheduled for a surgical correction by a modified Ravitch procedure.

‘This involves a 6–10-cm transverse skin incision that was centred over the mid-portion of the defect. Subcutaneous, and then pectoralis and rectus muscle flaps were elevated to the extent of the deformity. The muscle flaps were elevated until they could oppose to the midline. Bilateral subperichondrial resection of deformed cartilage and transverse sternal osteotomy and xiphisternum excisions were performed as required to allow the sternum to return to a neutral or desired position. The osteotomy of the anterior table of the sternum was performed just above the deformity, allowing the sternum distally to pivot and thus attain the desired position with minimal sub-sternal dissection. Wedging open the osteotomy with bone fragments harvested from rib ends allowed depression of the sternum to the desired 'neutral' position. The osteotomy is fixed in place using a metal stabilizer. The perichondrium was re-approximated, and the pectoralis and rectus muscles were re-apposed in a midline raphe. At this stage, the body of the sternum was fixed to this raphe using sutures. Submuscular and subcutaneous drains were placed to allow adequate drainage of blood. After surgery, patients were managed on the ward with opiate-based, patient-controlled intravenous analgesia initially, followed by regular oral analgesia, usually commenced within 48 h. Drains were removed sequentially once the total daily drainage was minimal (less than 50 ml). Patients were encouraged to begin mobilizing within 24 h and were often fully mobile by the second post-operative day under the guidance of physiotherapists. A key element in maintaining a good result was a posture-maintaining exercise regimen, which patients were encouraged to continue for at least 6 months.' (Makarawo, Steyn, & Naidu, 2011).

13.2.2 Study Design

This study was a case series descriptive study, which was done at a large thoracic surgery unit. Ethical approval was obtained from a supervising research ethical board. All participants in the study provided informed consent. Chest wall motion was assessed in all participants before surgery, post-operatively at one month, two months, and five months. Data collected pre- and post-operatively included each participant's age, height, weight, pain score, and any relevant past medical history. Spirometry was performed (Carefusion Microlab) prior to the capture of chest wall motion measurements, according to ATS/ERS guidelines (Miller, Hankinson, Brusasco, Burgos, Casaburi, & Coates, 2005). The measurement of chest wall motion and volumes was made with SMART suite software (BTS, Milan, Italy). Daily calibrations of the OEP cameras were done before each test. Then, a total of 89 reflective adhesive markers (79 hemispherical and 10 spherical) were positioned on the subjects' chest walls (Cala, et al., 1996) (Aliverti A. S., 2004). Standard placement of markers was done according to Cala et al. (Cala, et al., 1996).

OEP acquisition protocol included observations of heart rate, oxygen saturations, and blood pressure, which were recorded after one minute of quiet breathing and after the patient reached 80% maximum heart rate (220 – Age x 80/100). During the OEP acquisition, chest wall volumes were recorded by eight infrared cameras operating at 60Hz. The OEP system tracked the displacement of the markers during vital capacity, quiet breathing, and a standardised exercise protocol.

This protocol consisted of 15 minutes of rest, during which the OEP markers were placed. The patient was seated on a cycle ergometer, and chest wall motion was measured during three minutes of quiet breathing to establish baseline values for the chest wall volumes. Then, the patient commenced an incremental exercise protocol which consisted of pedalling unloaded for one minute and then with an incremental load of 5 Watts/minute. The patient was required to maintain 60 revolutions per minute until he reached 80% of the maximum predicted heart rate ([220-Age] x 80%). An identical exercise protocol was used before and after surgery for all patients.

The chest wall volume is divided into three compartments: ribcage pulmonary or RCP, ribcage abdomen or RCA, and the AB. From total chest wall and compartmental (RCP, RCA, and AB) chest wall volumes acquired by OEP, the following parameters were obtained: tidal volume (VT), as the total chest wall volume variation; total and compartmental volumes at EEV and end of inspiration (EIV); RR; and VT x RR. These were evaluated during rest, 100% maximum exercise (time when 80% maximum heart rate is achieved, which is known as exercising time), and 50% maximum exercise ([exercise starting time - exercising time] divided by two).
Informed consent for clinical photography for open publication was obtained from each patient.

13.2.3 Statistical Analysis

The statistical analysis was executed by IBM© SPSS© Statistics Version 22.0.0.0. The normality of the data was assessed using the Kolmogorov-Smirnov test. The results showed that the data were not normally distributed. Accordingly, the data were presented as median + IQR. No attempt was made to calculate the P value, as complex statistical tests could not be used for only three patients.

13.3 RESULTS

Table 5: Demographic data of the three patients with the PC deformity before surgery.

	Median	IQR
Age	**18**	**2**
Weight (kg)	**63**	**23**
Height (cm)	**185**	**11**
BMI	**18.4**	**4.3**
FEV1 (L)	**4.7**	**0.9**
%FEV1 Predicted	**99.0**	**8.0**
FVC (L)	**5.2**	**1.54**
%FVC Predicted	**92.0**	**47.0**
FEV1/FVC (%)	**89.5**	**9.20**

The demographic data of the PC patients (n = 3) before surgery. The data are presented in median and IQR. Kg: kilogram, Cm: centimetre, BMI: body mass index, FEV1: forced expiratory volume in 1 second, FVC: forced vital capacity.

The group consisted of young males (n = 3) with PC deformities who underwent surgical correction for cosmetic reasons (Figure 30).

Figure 30: Image of a patient before and after PC repair: These are the pre-operative (left) and post-operative (right) photos of one of the patients in the study. Informed consent for clinical photography for open publication was obtained from the patient.

During OEP measurements, all patients achieved the target of 80% predicted maximum heart rate during cycle ergometry. A trend of reduction in respiratory function post-operatively was evidenced by changes in spirometry, as shown in Figure 27. Although there was a considerable trend of recovery in FEV_1 and FVC after surgery, these measurements were still lower than baseline at five months post-operation (Figure 31).

According to data obtained from OEP, chest wall tidal volume during maximum exercise decreased immediately post-operation and partially recovered after five months (Figure 32). The results showed that these patients' chest wall EEV showed a trend of an increase by 2(2)% during 100% exercise before surgery. This could represent a trend of air trapping or dynamic hyperinflation. Interestingly, this trend seemed to be reversed after surgery. Post-operatively, chest wall EEV showed a trend of reduction during 100% exercise by -1(3)%, -1(1)%, and -3(3)% at one month, two months, and five months, respectively (Figure 33).

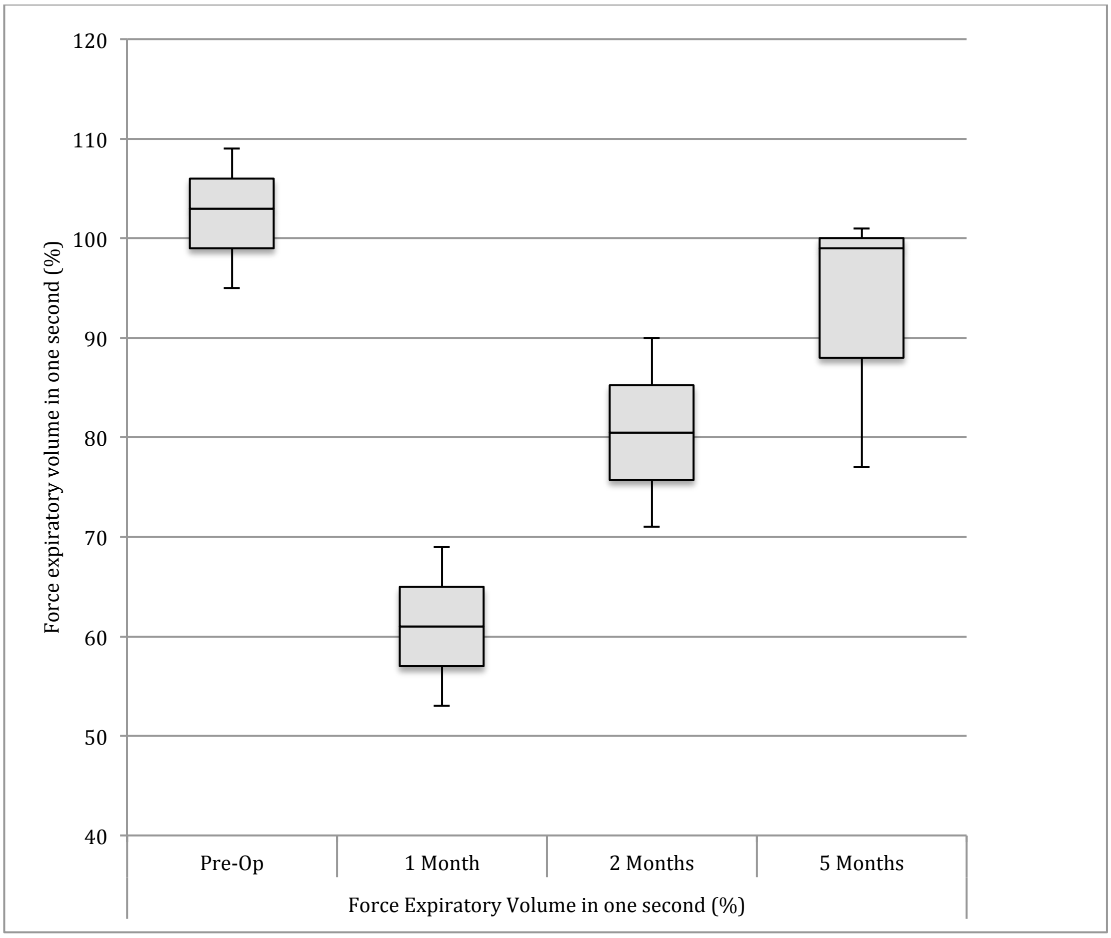

120
110
100
90
80
70
60
50
40
Force expiratory volume in one second (%)
Pre-Op
1 Month
2 Months
5 Months
Force Expiratory Volume in one second (%)

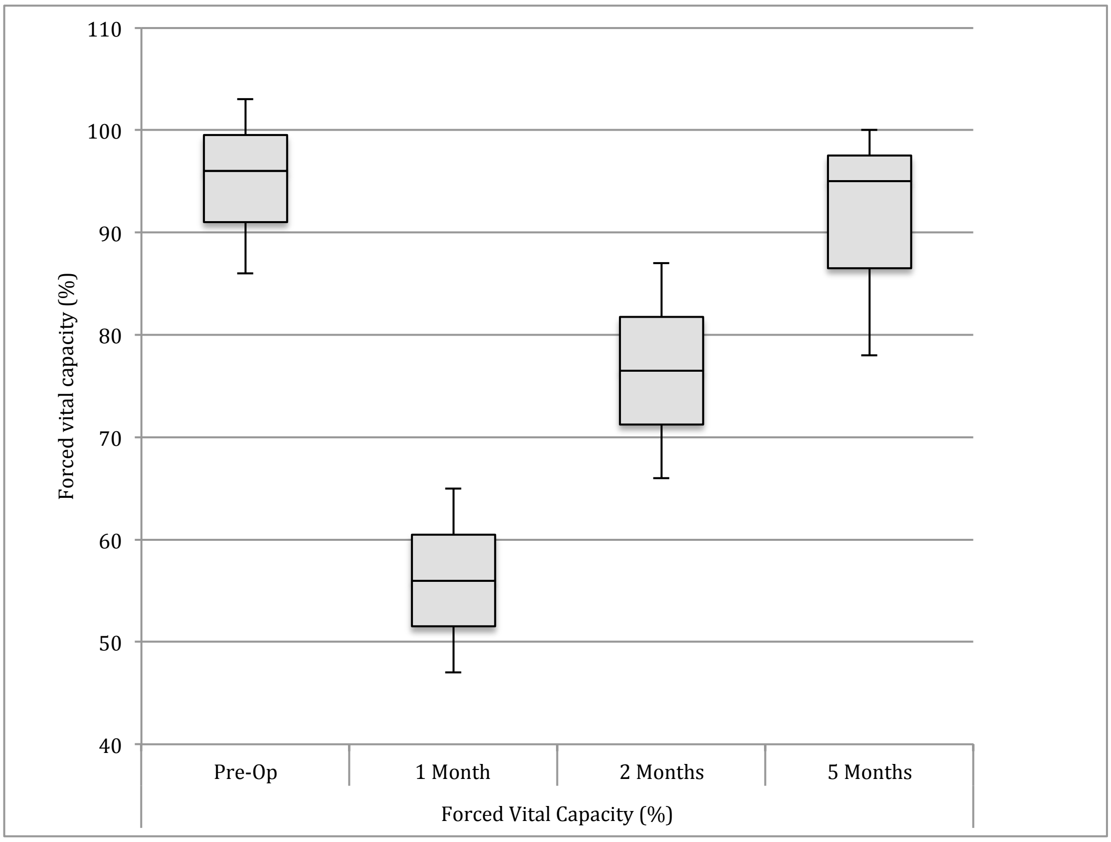

110
100
90
80
70
60
50
40
Forced vital capacity (%)
Pre-Op
1 Month
2 Months
5 Months
Forced Vital Capacity (%)

Figure 31: Spirometric measurements before and after PC repair. Pre- and post-operative (one month, two months, and five months) spirometric measurements (FEV1 and FVC as a percentage of the predicated value of a healthy person with the same height, age, and gender) of the three patients with PC (n = 3). The data are shown as boxplots (median, IQR, and quartiles).

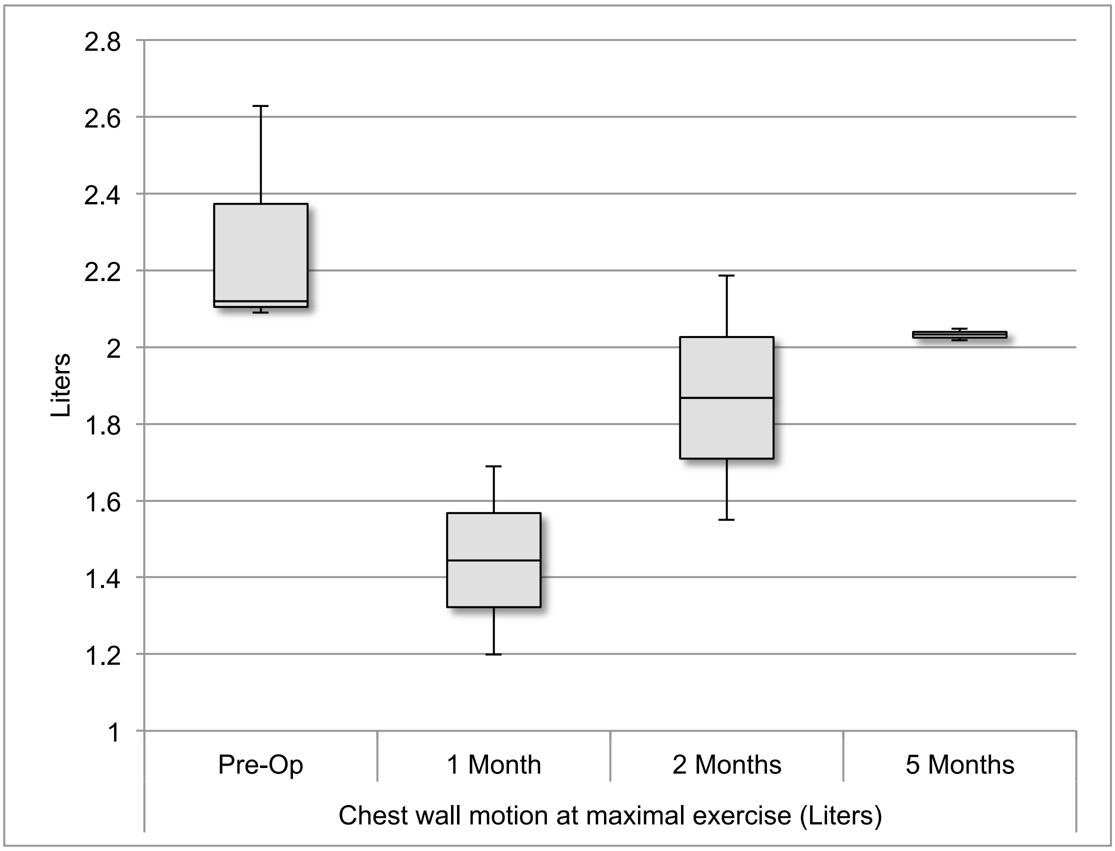

Figure 32: Chest wall tidal volume at maximum exercise: The chest wall tidal volume at maximum exercise before and (one month, two months, and five months) after PC repair (n = 3). The data are shown as boxplots (median, IQR and quartiles).

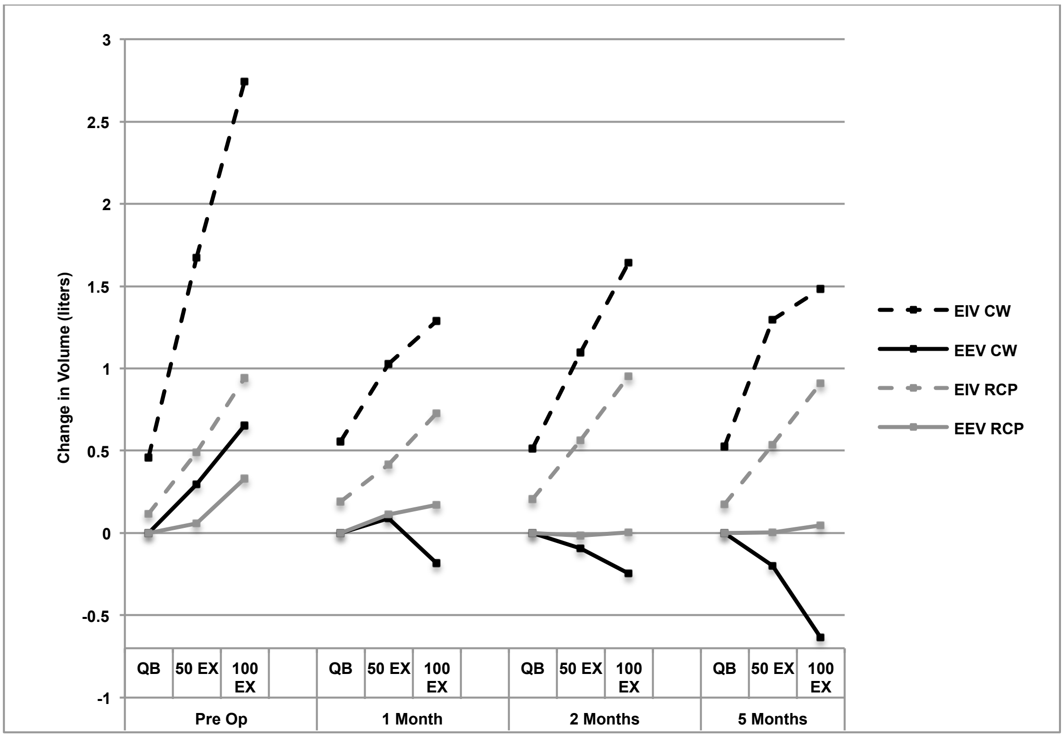

Figure 33: The EIV and EEV of the chest wall and pulmonary ribcage before and after surgery during quiet berating and exercise. The changes in total chest wall EIV (dashed black line); and total chest wall EEV (solid black line); and at quiet breathing (QB), 50% and 100% exercise (50 EX) (100 EX), pre- and post- operatively. The changes in RCP EIV (dashed grey line); and EEV RCP (solid grey line); at quiet breathing (QB), 50% and 100% exercise (50 EX) (100 EX), pre- and post-operatively (n = 3). The data are plotted as medians.

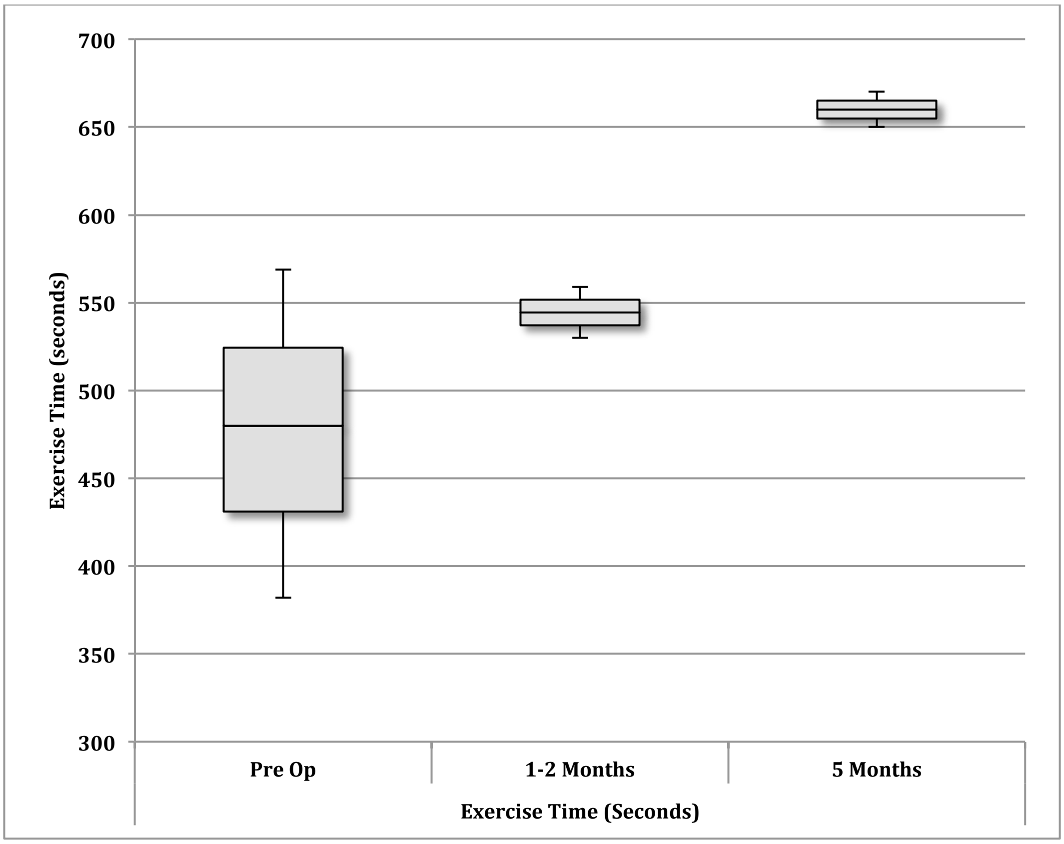

Figure 34: The total of exercise to reach 80% of heart rate before and after PC repair. The total time of exercising until reaching 80% of maximum heart rate, before and (one to two months and five months) after PC repair (n = 3). The data are shown as boxplots (median, IQR, and quartiles).

The trend dynamic hyperinflation in the RCP compartment seemed to be normalised five months after surgery. The RCP EEV showed a trend of an increase by 4(3)% during 100% exercise before surgery. At two and five months post-operation, there were no noticeable changes in RCP EEV from quiet breathing to 100% exercise at 0(1)% and 0(3)%, respectively (Figure 33). The five-month end results seemed to mimic findings in normal subjects. A trend of what looked like dynamic hyperinflation was observed pre-operatively and seemed to be reversed after surgery, not only collectively but also in each individual patient. This trend of reversal of dynamic hyperinflation seemed to be related to a trend of an increase in exercise time to reach the maximum (80% predicted) heart rate five months after surgical correction for all three patients. The exercise time Increased from 480 (93) seconds pre-operatively to 660 (10) seconds five months after surgery (Figure 34). The changes in respiratory rate and minute ventilation at quiet breathing and during exercise are shown in Table 6.

Table 6: The respiratory parameters before and after PC repair during quiet breathing and exercise.

		Before	1 Month	2 Months	5 Months
Quiet Breathing	Tidal Volume	0.44(0.18)	0.57(0.19)	0.47(0.09)	0.52(0.12)
	Respiratory rate	18(6)	18(5)	18(4)	22(6)
	Minute Ventilation	8.57(2.68)	10.80(4.88)	8.52(2.33)	10.37(3.16)
50% Exercise	Tidal Volume	1.19(0.75)	0.81(0.32)	1.01(0.58)	1.78(1.10)
	Respiratory rate	19(9)	26(6)	20(8)	21(5)
	Minute Ventilation	21.98(4.25)	22.40(5.13)	19.77(4.19)	34.13(15.83)
100% Exercise	Tidal Volume	2.30(0.52)	1.47(0.54)	1.91(0.65)	2.03(0.38)
	Respiratory rate	24(5)	31(12)	24(8)	26(8)
	Minute Ventilation	58.16(15.81)	47.03(31.40)	43.96(10.73)	54.55(13.24)

The respiratory rate (breaths/minute), minute ventilation (litres), and tidal volume (itres) during exercise and quiet breathing (QB), before and (one month, two months, and five months) after surgery (n = 3). The data are shown as median and IQR.

13.4 DISCUSSION

Pectus carinatum correction is classified as a cosmetic operation. The impact of PC correction surgery on exercise and chest wall motion is poorly understood. Our data shows our patients with PC showed a trend of developing what seemed to be an air-trapping or dynamic hyperinflation phenomenon during exercise. Corrective surgery seemed to reverse this phenomenon. Illi S. et al. showed that, by using OEP in healthy subjects, the EEV of the pulmonary ribcage compartment decreased significantly during exercise compared to during quiet breathing. This finding mimicked the results found here after surgery, suggesting that, after surgery, PC chest wall physiology tended to revert back to normal physiology (Illi, Hostettler, Aliverti, & Spengler, 2013).

It was also observed in this study that patients had a trend of improvement in exercise capacity (exercise time), which could be related to a trend of reversal of this dynamic hyperinflation. Although the results were based on a descriptive case series that only involved three patients, the unique findings of this study warranted further validation. Parallels could be drawn from the change in belief over the last 10 years from the idea that pectus excavatum surgery was purely a cosmetic operation to now being acknowledged to have important physiological benefits and, in many cases, being the primary indication for surgery.

Exercise time was used to reach an 80% maximum heart rate as an indicator of exercise capacity, as opposed to the more cumbersome formal cardio pulmonary exercise testing. There is, however, a good correlation between the two, as has been reported before (Kline , 1989) (Dolgener, 1994). All patients were subjected to the same exercise protocol with identical increase in the resistance while pedalling on a bicycle, and the experiment ended if the patient reached 80% of his maximum predicted heart rate. To exclude motivation bias, heart rate was used as a marker at the end of exercise, as patients had no control of their heart rate when they exercised. The training bias was excluded, because the patients were asked not to perform any exercise for six months after surgery; this was to minimise any trauma to their chest wall.

Oncel et al. reported improvement in exercise capacity after PC repair, but this improvement was self-reported and lacked any objective data on the extent of the improvement (Oncel, Tuscan, Akyol, Dereli, & Sunam, 2013).
Dynamic hyperinflation is the accumulation of new breath on top of a previous breath 'before the lung reach it static equilibrium volume' (Blanch, Bernabe, & Lucangelo , 2005). It is a maladaptive phenomenon, occurring at the expense of an increased mechanical load and elastic work of breathing (Warner, 2001). The concept of reversal of a dynamic hyperinflation, which has been observed after surgery and may result in a better exercise capacity, has been reported in a sub-type of a COPD patient after bronchodilator therapy (Aliverti, et al., 2005). This phenomenon is thought to be a physiological response to airflow obstruction. However, this is not the likely mechanism in PC patients. In PC patients, mal-position of the sternum places the respiratory muscles into mechanical disadvantage, preventing them from achieving their maximal contractility as previously reported (Koumbourlis, 2015). This is supported by the fact that a patient with PC has significantly decreased maximum expiratory pressures compared to controls, often less than half of the predicted normal maximal expiratory pressures (Koumbourlis, 2015) (Kubiak, Habelt, Hammer, Hacker, Mayr J , & Bielek, 2007) (La Mauro, et al., 2012). This impairment is not usually associated with symptoms in a young patient during quiet breathing (Kubiak, Habelt, Hammer, Hacker, Mayr J , & Bielek,

2007) (La Mauro, et al., 2012). During exercise, however, the decreased maximum expiratory pressures are not enough to achieve adequate expiration of air, leading to what seems to be dynamic hyperinflation, as has been observed and described. Corrective surgery might put the respiratory muscles in an optimal mechanical position to achieve effective expiratory contractility to abolish dynamic hyperinflation. Patients' breathlessness may be worse because of dynamic hyperinflation, thus hindering exercise (Aliverti et. al., 2005).

The present study showed trends of chest wall benefits in this small number of patients. However, there was not enough evidence to suggest that the potential benefits of surgery outweigh any potential risk of surgery. To rectify this, a larger multicentre study is needed. In addition, these future studies should incorporate the use of full cardiopulmonary testing, as it can assess cardiopulmonary function and fitness in more depth.

It is unclear whether dynamic hyperinflation occurs in all PC patients. In the future, evaluating this can help identify patients who might benefit from surgery.

13.5 CONCLUSION

This was the first descriptive case series to describe trends of dynamic hyperinflation in three PC patients and the trends of the beneficial effects of corrective surgery. This might be related to trends of improvement in exercise capacity after surgery. A larger sample is needed to validate the results. The long term consequences on chest wall motion and exercise tolerance are yet to be explored.

13.6 Limitations

Recruitment limitation limited the sample size. This was because PC is a rare disease with a prevalence of 0.06% (Mielke & Winter, 1993), and the procedure is rarely done in the regional thoracic centre (four to eight operations annually) where this study was conducted. Gender variation could not be assessed in the study as all the recruits were male, and no female patient had undergone this surgery in the regional thoracic unit in the last two years. This was because more males than females usually seek medical advice, as the deformity is more visible in males due their smaller breast size.

14 Chapter 6: The Effect of Lung Volume Reduction Surgery on Chest Wall Mechanics

14.1 BACKGROUND

Lung volume reduction surgery using EBVs improves clinical outcomes and quality of life in selected patients with emphysema (Sciurba, 2010) (Herth, 2012). EBVs are designed to exclude the most affected emphysematous regions from ventilation by inducing lobar absorption atelectasis. However, the response to this intervention is inconsistent, as existing collateral ventilation can provide cross-ventilation and prevent lobar atelectasis. The use of EBVs in the Emphysema Palliation Trial (EURO-VENT and US-VENT) showed that the benefits of EBVs are most pronounced in patients where lobar atelectasis is achieved. These benefits include improvements in lung function, a six-minute walk test, and quality-of-life score (Sciurba, 2010) (Herth, 2012). The measured outcomes for EBV procedures are currently radiological via CXR and CT scans, but these methods poorly identify non-responders immediately after the procedure. This is because radiological features of atelectasis may take weeks to develop even though the valves may have started working immediately (Hopkinson, 2011). This may cause a delay in identifying non-responders after EBV insertion. Thus, it would be clinically relevant to be able to detect changes in ventilation immediately after surgery in these patients. Furthermore, the VENT trial identified a sub-group of EBV patients with sub-radiological atelectasis who demonstrated symptomatic improvement. Therefore, a method that could accurately identify this sub-group of responders early after the procedure would also be useful and potentially disrupt the existing patient care pathway.

Several devices, such as RIP bands and piezoelectric belts, have been in use for many years to measure breathing through motion of the thorax and abdomen. Structured light plethysmography is a more recent technology (De Boer, 2010) that allows quantification of the relative motion of selected regions of the thoraco-abdominal wall (TA). Thus, it can allow comparison of movement of, for example, the left to right hemi-thorax. Movement of a projected grid of light on the anterior thoraco-abdominal wall is recorded by two digital video cameras. Distortion of the grid through motion is then translated, using previously reported algorithms (De Boer, 2010), to estimate the anterior displacement of the TA regions and to generate a TA wall movement-over-time trace, which is derived from the average axial displacement of the whole TA wall. The graphical output of the device includes a 3D reconstruction that allows sub-regions of the TA wall to be selected to produce a movement-over-time trace for each of these sub-regions. Calculation of the percentage contribution of each sub-region to the resultant total movement allows comparison between sub-regions.

This descriptive case series examined and described in detail the contribution of the operated side of the chest to the total chest wall movement before and after surgery. It was hypothesised that chest wall motion analysis using SLP can measure changes in ventilation via a corresponding reduction in chest wall motion on the operated side of the chest immediately after EBV insertion and may therefore assist in the early detection of success or failure of LVRS with EBVs.

14.2 METHODS

This descriptive case series was undertaken in a regional thoracic centre. The study was approved on the 5th of February 2013 by the National Research Ethic Service Committee of West Midlands-The Black Country with REC reference: 10/h1202/58, Protocol number: Version2, 24.01.2013, and IRAS project ID: 59742. Informed consent was obtained from the participants. This study was carried out in accordance with the Code of Ethics of the World Medical Association (Declaration of Helsinki) for experiments involving humans.

14.2.1 Study Devices

An SLP device (Thora-3Di™, PneumaCare Ltd) was used to measure chest wall motion during tidal breathing. The SLP device used had a sampling rate of 30 frames per second, which was sufficient to capture the dynamics of TA wall displacement. The grid pattern projected by the SLP device could be adjusted to accommodate the size of each participant's TA region. However, for this study, a grid size of 14×10 was used. Figure 35 illustrates the working principle of SLP.

Structured light plethysmography projected a grid of light onto the TA wall of a participant. Changes in the grid pattern were recorded using two cameras (located in the scanning head) and then translated into a virtual surface corresponding to the shape of the TA wall of the subject. Data were viewed in the integrated Pneumaview 3D software package. Average axial displacement of the virtual grid provided a one-dimensional movement-over-time trace. On the selection of a frame of the trace, numerical parameters for the selected frame were calculated.

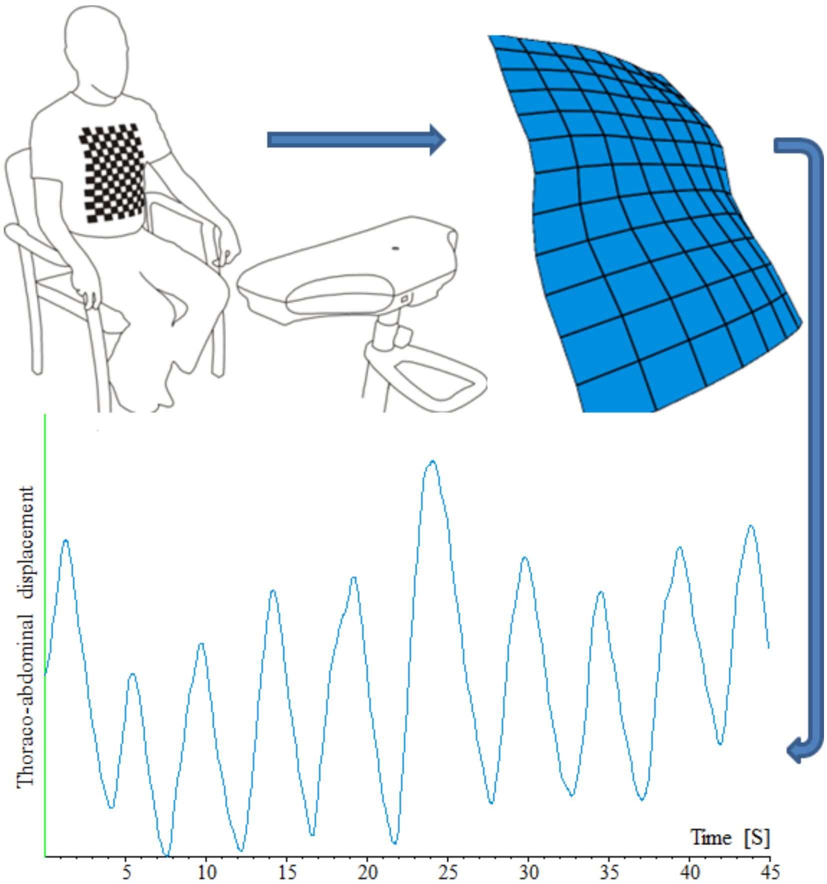

Figure 35: Working principle of SLP. Please note that the patients in this study were positioned at a 45-degree angle.

14.2.2 Measurement Protocol

The participants were asked to remove their clothing from the chest and abdomen. The participants were asked to lie down at a 45-degree angle on the bed with their neck in a neutral position and their back as straight as possible. The device head, in which the projector and cameras were housed, was positioned perpendicularly to the patient's chest wall at approximately 1 meter's distance, and the torso (chest and abdomen) was illuminated with a visible light-grid pattern from the projection source. The centre cross-point of the grid was aligned with the patient's xyphisternum so that the vertical grid centre line sectioned the chest equally into right and left regions. The device head positioning was adjusted until a sharp image of the grid of light over the chest and upper abdomen was achieved. Once the participant was positioned comfortably and had settled, the participant was asked to breathe 'normally' and remain still for the duration of the measurement. Data collection was started and data collected during five minutes of tidal breathing. Measurements were made pre-surgery and post-surgery in the recovery room and on subsequent days up to three days post-operatively.

14.2.3 Patients

From May 2014 through August 2014, three male patients with heterogeneous emphysema (n = 2) and giant bulla (n = 1) at a regional thoracic unit were recruited. All patients received therapy with a Zephyr EBV. (Table 7 shows the baseline characteristics of the patients.) Eligibility criteria and exclusion criteria followed the VENT study protocol (Sciurba, 2010) (Herth, 2012), except on Patient 3, as it was a joint decision between the patient and the surgeon. All patients were discussed in a multi-disciplinary meeting before being offered the intervention.

Table 7: Baseline characteristics of the three EBV patients.

	Patient 1	Patient 2	Patient 3
Variable			
INDICATION	Giant Bulla	Emphysema	Emphysema
Demographic characteristic			
Age – years	76	75	61
Gender	Male	Male	Male
Height (metres)	1.57	1.67	1.65
Weight (kilograms)	59.2	54.8	62.4
Body-mass index	24.0	19.6	22.9
Lung function			
Forced expiratory volume in one second			
Value – litres	0.72	0.72	0.55
Percentage of predicted value	34	27	19
Forced vital capacity			
Value – litres	3.26	2.19	2.26
Percentage of predicted value	118	63	63
Diffusing capacity of lung for carbon monoxide			
Value - ml carbon monoxide/min/mm Hg	4.66	2.51	1.45
Percentage of predicted value	72	32	17
Residual volume			
Value – litres	4.76	6.11	5.57
Percentage of predicted value	192	234	247
Total lung capacity			
Value – litres	7.93	8.77	8.11
Percentage of predicted value	145	137	133
Exercise Performance			
Distance on 6-minute walk test - m	380	265	300

The lung function data are presented as the median of the number of breaths.

14.2.4 Study Design

Visual indexes of the severity of lobar emphysema and fissure integrity using high-resolution computed tomography (HRCT) were made by an experienced thoracic radiologist in the lung volume reduction multi-disciplinary meeting to determine eligibility and optimal selection criteria. Three patients deemed suitable for EBVs were recruited into the study. The research study was approved by the Local Research Ethics Committee. Informed consent was obtained from all participants involved.

14.2.5 Outcome Measures

The primary effectiveness end points were change in chest wall motion on the side of the valve insertion as a percentage of the total chest movement (expressed as % Relative Contribution, %RC); change in percentage of predicted FEV1 in litres; change in percentage of predicted FVC in litres; and distance on the six-minute walk test. The secondary efficacy end point was the change in the patient's dyspnoea score using a Borg Scale (which ranged from 0-10, with a higher score indicating a worse dyspnoea). Only three patients were recruited in this pilot study, as they were the only three patients available to be recruited during a six-month period, as EBV for LVRS was a novel procedure that was rarely done in this hospital. The aim of this study was to show a trend of change that might be related to the success or the failure of the procedure.

14.2.6 Procedure and Follow-up

A flexible bronchoscope down an endotracheal tube was used for valve implantation in patients under general anaesthesia. Antibiotics were given for seven days after the surgery. The Chartis system was used to assess the presence of collateral ventilation, and only if the results confirmed that there was no collateral ventilation was the patient accepted for valve placement. Valves were placed unilaterally in lobar, segmental, or sub-segmental bronchi on the basis of individual anatomy to completely isolate the targeted lobe. Follow-up data (including vital signs, a review of adverse events, and radiographic evidence of atelectasis on plain chest X-ray) were collected pre-operatively (baseline), in the recovery room, and on Day 1 and Day 2 post-surgery. Standardised HRCT was performed at baseline and at three months.

14.2.7 SLP Data Appraisal and Regional Selection

No drift or excessive interference on any of the traces was visible. All data were assessed to be of sufficient quality for inclusion in the analysis. The upper-left and upper-right regions were selected from the 3D reconstruction, corresponding to the regions above the xiphisternum and segmented vertically through the centreline. Each region contained an equal number of grid points. The abdominal (lower) section of the grid was excluded from the analysis. Percentage RC, expressed as a percentage of the total chest (upper-right plus upper-left) movement, was calculated for the operative side of the chest.

14.2.8 Statistical analysis

The statistical analysis was executed by IBM© SPSS© Statistics Version 22.0.0.0. The normality of the data was assessed using the Kolmogorov-Smirnov test. The results showed that the data were not normally distributed. Accordingly, the data were presented as median and IQR. Each data point represented the median or median + IQR for each patient (n = 1). As the data represented only three patients, no attempt was made to calculate the P value, as complex statistical tests could not be used for only three patients. The SLP data were given in terms of chest wall motion in each breath. Therefore, the median + IQR of the chest wall motion during a number of breaths were taken for each patient.

14.3 RESULTS

14.3.1 Patient 1

Patient 1 (P1) had an insertion of one Zepher EBV (5.5 mm) to the right middle lobe with no significant post-operative complications. His Borg breathlessness score showed a trend of improvement, going from 7 pre-operatively to 3 in the recovery room to 0 two days after surgery. Similarly, his six-minute walk test showed trends of improvement from 380 m before surgery to 386 m three months after surgery. In P1, chest wall motion on the operative side showed a trend of reduction immediately after the operation in the recovery room, and this trend of reduction progressed during the inpatient period (Figure 36). The contribution of the chest wall motion on the operative side, compared to overall chest wall motion, showed a trend of reduction from 55(1)% pre-operatively to 48(1)% two days after surgery (Figure 36).

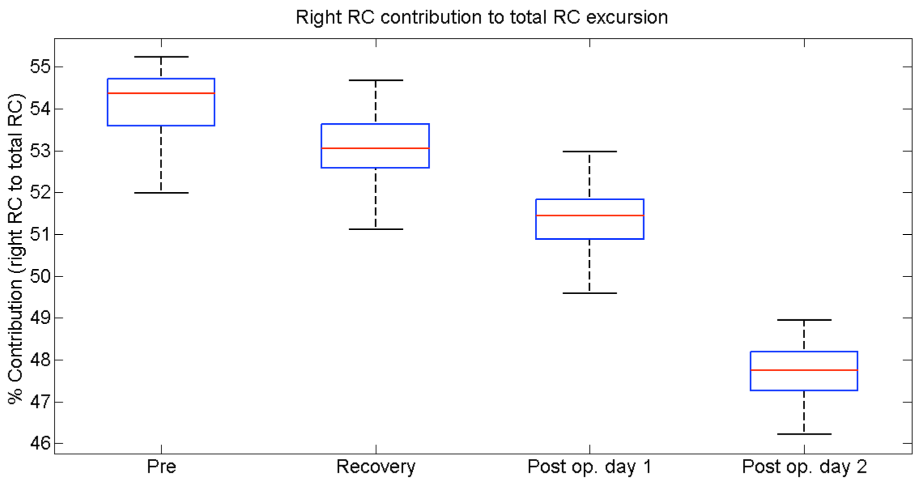

Figure 36: Patient 1's change in the percentage contribution of the treated side of the chest to overall chest wall motion before and after EBV insertion. The change in P1's %RC on the operated (right) side as a percentage of total chest wall motion before surgery (pre), in the recovery room, Day 1 post-operative, and Day 2 post-operative. The data are presented as boxplots (median, IQR, and quartiles) of the chest wall motion during five minutes of tidal breathing (n = 1).

P1 spirometry results showed a trend of improvement in the percentage of predicted FEV1, from 34% pre-operatively to 42% three months after surgery. His percentage of predicted FVC similarly showed a trend of improvement from 118% to 140% during the same time frame. His chest X-rays in the recovery room and on the two post-op days did not show evidence of atelectasis. However, his CT chest done three months after surgery showed clear evidence of atelectasis.

14.3.2 Patient 2

Patient 2 (P2) had an insertion of five Zepher EBVs (ranging in size from 4.0 to 7.0 mm) to the five segments of the right lower lobe. His chest wall motion on the operative side showed a trend of reduction immediately after the operation in the recovery room, and this trend of reduction progressed during Day 1, but the trend of reduction was surprisingly lost on Day 2 (Figure 37). The contribution of the chest wall motion on the operative side compared to the overall chest wall motion showed a trend of reduction from 53(1)% pre-operatively to 45(1)% on Day 1 post-surgery. However, this benefit was lost on Day 2, as the chest wall motion on the operated side was now 50(1)%, a value that was close to the pre-operative value (Figure 37).

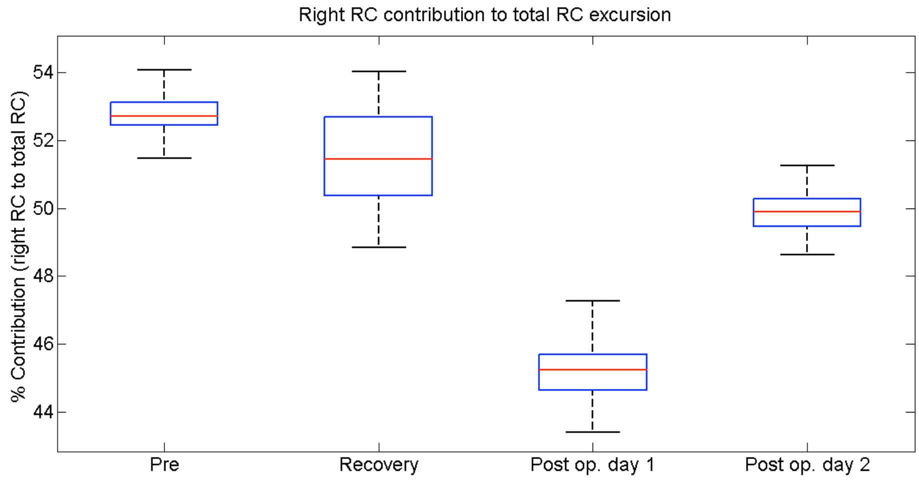

Figure 37: Patient 2's change in the percentage contribution of the treated side of the chest to overall chest wall motion before and after EBV insertion. Change in P2's %RC on the operated (right) side as a percentage of total chest wall motion before surgery (pre), in the recovery room, Day 1 post-operative, and Day 2 post-operative. The data were presented as boxplots (median, IQR, and quartiles) of the chest wall motion during five minutes of tidal breathing (n = 1).

P2 spirometry results showed no noticeable change in the percentage of predicted FEV1, which went from 27% pre-operatively to 29% three months after surgery. His percentage of predicted FVC showed a trend of improvement, from 63% to 86% during the same time frame. His chest X-ray, taken in the recovery room and on the first two post-op days, did not show evidence of atelectasis. Three months after surgery, his CT chest showed no atelectasis, but evidence of a paravalvular leak, suggesting that the valve had moved after insertion. It was suggested that this happened on Day 2. As a result of this, he had a second operation to reposition his EBVs.

14.3.3 Patient 3

Patient 3 (P3) had an insertion of three Zepher EBVs to the left upper lobe (apico-posterior segment size 5.0 mm valve, and anterior segmental and lingual orifice bronchiole sized for size 4.0 mm valve each). His Borg breathlessness score pre-surgery did not show a trend of marked change after surgery. His chest wall motion on the operative side did not show a trend of marked change after the operation (Figure 38). There was no marked trend reduction of chest wall motion on the operative side compared to the overall chest wall motion on Day 1 after surgery, and this only changed minimally, from 48(2)% pre-operatively to 50(1)% on Day 1 after surgery (Figure 38).

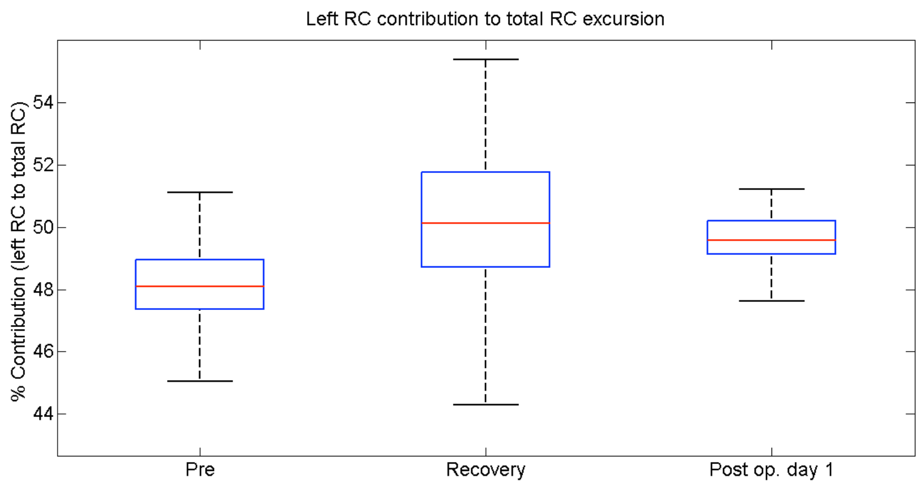

Figure 38: Patient 2's change in the percentage contribution of the treated side of the chest to overall chest wall motion before and after EBV insertion. Change in P1's %RC on the operated (left) side as a percentage of total chest wall motion before surgery (pre), in the recovery room, and on Day 1 post-operative. The data are presented as boxplots (median, IQR, and quartiles) of the chest wall motion during five minutes of tidal breathing for this patient (n = 1).

P3 spirometry results showed a trend of reduction of the percentage of predicted FEV1, which went from 19% pre-operatively to 16% three months after surgery. His percentage of predicted FVC showed a trend of reduction, from 63% to 54% during the same time frame. His chest X-ray in the recovery room and on post-operative Days 1 and 2 did not show evidence of atelectasis. His CT chest three months after surgery showed no evidence of atelectasis. This patient had no symptomatic improvement so he underwent a second operation four months after the first operation, and all three Zepher EBVs were removed.

14.4 DISCUSSION

EBV LVRS is a palliative surgery in very high-risk patients with associated significant post-operative morbidity and mortality (Sciurba, 2010). Identifying those patients who have an unsuccessful procedure is of paramount importance early after surgery, as this allows for timely intervention to remove the EBVs; EBVs are foreign bodies that are associated with a risk of lung infection in this high-risk group of patients with very poor pulmonary reserve (Sciurba, 2010). In addition, the EBVs are prone to migration (Jenkins, Vaughan, Place, & Kornaszewska, 2011), and removing un-working EBVs in a timely manner might prevent this complication. To date there has been no sensitive clinical or radiological measure that can assess the success or failure of this procedure in the recovery room. These case series examined the use of SLP in detecting chest wall changes after EBV LVRS in the recovery room and on subsequent inpatient days. P1 had a successful insertion of EBVs for LVRS, and that was evident from CT findings three months after surgery. The results in this patient also showed a trend of improvement in the Borg score and spirometry during the same time frame.

He also showed some trend of improvement in the six-minute walk test, but that was below the minimally clinically important difference for the six-minute walk test (estimated to be 54-80 metres) (Wise & Brown, 2005). These trends of improvement in the Borg score and the spirometry were accompanied by a trend of reduction in chest wall motion on the operative side immediately in the recovery room, which was followed in subsequent days by a trend of further reduction in chest wall motion on the operative side. P2 had an unsuccessful procedure due to a paravalvular leak, as evident in the patient's CT findings three months after surgery. This patient, however, did report some trend of initial improvement in breathlessness in the recovery room and on post-operative Day 1. But this trend of improvement was lost on post-operative Day 2 and thereafter. This was accompanied by a trend of progressive reduction in chest wall motion on the operative side in the recovery room and on Day 1, but this trend of reduction was lost on Day 2. These trends suggested that after the initial success of valve insertion as per the operation notes, the valves had moved from their places on Day 2, which might have resulted in the above findings, leading to the need for a re-operation to reposition the valve. P3 had an unsuccessful procedure, as evident from CT findings three months after surgery. This was supported by his Borg score and spirometry, which did not show a trend of marked change after surgery, necessitating the later need for surgery to remove all three valves. This was matched by unchanged chest wall motion after surgery.

As it was only one patient, a concrete conclusion could not be made, but it is possible that this trend in the reduction in chest wall motion in P1 could indicate a degree of sub-radiological atelectasis that is not appreciated on a routine chest X-ray. A subgroup of EBVs with sub-radiological atelectasis that still demonstrated clinical improvement was previously identified in the VENT trial (Sciurba, 2010) (Herth, 2012). Similarly, concrete conclusions were not possible here based on a single patient. However, it was thought that P2's initial trend of reduction in chest wall motion could be due to this sub-radiological atelectasis on the first day, which seemed to be lost on Day 2—as evident by the loss of the trend of marked reduction in his chest wall motion on the operated side—once the valve migrated, as evidenced by his second operation. P3, on the other hand, had an unsuccessful procedure with no atelectasis, which was reflected in the trend of a lack of change in chest wall motion.

The SLP device is non-contact, minimising cross-infection, and it uses only visible light so it presents no radiation risk to the patient. All measurements were made during tidal breathing. Hence, all patients were able to comply with the protocol.

In these data, the BORG breathlessness score showed a trend of improvement in the patient who had a successful procedure and did not change in the patients who had had a failed procedure. Although this seemed to be a good measure to assess the procedure outcome, its major limitation was that the BORG score is a subjective measurement, influenced by a person's feelings and relying on a subject's sense of breathlessness. Unlike measurements of chest wall motion, this score did not measure targeted areas of chest to give an objective measurement.

Generalisation of the results was not possible, because there were not enough successful procedures to assess the impact of this investigation. The results only showed a trend of change in chest wall motion in a small number of patients who had successful (n = 1) or failed procedures (n = 2).

One possible alternative explanation of the results is that the chest wall changes in P1—who had a successful procedure—could be affected by the fact that he had a giant bulla with severe underlying COPD and minor emphysema, compared to P2 and P3 who had a very severe underlying COPD and emphysema. Although the EBVs had a similar mode of action in both groups, it could be that the lung's response to the bronchial blockage differed in P1 vs P2 and P3 due to the difference in underlying lung pathology. A larger study examining a homogenous sample is needed to verify the results.

Although this series involved only three patients who had different diseases, this descriptive case series described how EBV LVRS might cause trends of change on chest wall motion. These changes might be associated with procedure outcome and might have a potential in the future to be used as an indicator that may detect success or failure of this high-risk surgery. These interesting initial results from this novel application of an emerging technology led to this paper and its potential publication. An early indicator of procedure failure has the potential to allow re-examination, implement necessary treatments, re-design the existing care pathway, and increase clinical efficiency.

14.5 CONCLUSION

These descriptive case series described in detail how SLP may have the potential to detect trend changes in chest wall motion after EBV for LVRS. This trend of change might be related to the outcome of the procedure and could be used in the future to detect the success or failure of EBV therapy. It may also provide a useful tool for monitoring and understanding the physiological processes and clinical benefits of LVRS using EBVs. A larger study with a homogenous sample is needed to verify these results.

14.6 Limitations

Another limitation of the study was that P1 did not fit the criteria for LVRS, but did fit the criteria for bullectomy. This was the only patient of the three whose chest wall motion progressively showed a trend of reduction after surgery; this could be due to the fact that he had better lung reserve (severe COPD and minor emphysema) than the other two patients with very severe COPD and severe emphysema.

Recruitment limitation

EBV for LVRS is a rare procedure in the regional thoracic centre at which this study was conducted; it sees approximately eight cases annually. Furthermore, the procedure is not without complications; in this study, three other recruits were withdrawn, as they developed pneumothorax after surgery. Measurements could not be done during exercise, as the SLP machine required the patients to fix their backs against a hard surface (a chair or bed).

In addition, the SLP capture could only be done in a relatively dark room, as light interferes with the quality of the capture. Furthermore, abdominal and chest tubes and stomas, as well as skin folds, interfere with the quality of capture.

15 Chapter 7: The Effect of Benign and Malignant Pleural Disease on Chest Wall Mechanics

15.1 Introduction

Malignant pleural disease is a problem of global significance (Tassavainen, 2004). Mesothelioma is a lethal disease. The median survival is from 14 to 4 months, depending on the disease subtype (Meyerhoff, et al., 2015) (Welch, Dement, & West, 2015). It is estimated that mesothelioma and asbestos-related disease result in 1,523,000 disability-adjusted life-years in a single year (World Heatlh Organion , 2006). The incidence is increasing globally every year (Bianchi & Bianchi, 2007). The peak of asbestos use was in the 1970s, and it takes around 40 years to develop asbestos-related disease; as such, the current global epidemic is only in its infancy (Gaafar & Eldin, 2005) (Takahashi & Karjalainen, 2003). The incidence of disease is going to increase in the coming years (Luo, Liu, & Mu, 2003) (Joshi, Sahin, & Ozesmi, 2006) (Virta, 2013). The 40-year latency period between exposure and development of disease adds to the complexity of early diagnosis. The diagnosis is usually suspected in a patient with history of asbestos exposure who presents with a range of symptoms. Dyspnoea and non-pleuritic chest pain are the two most common presentations, with at least one of these reported in up to 90% of patients. Other symptoms include pleuritic pain, fever, and weight loss. Other patients might be free of symptoms but found to have a pleural effusion incidentally on physical examination or via chest radiography (Winston , 2014). Clinical symptoms and signs are non-specific, and thus the diagnosis of mesothelioma is challenging. If the patient has a pleural effusion, the first step in diagnosing the disease is sampling the pleural fluid in a patient who has typical exposure and presenting symptoms. This involves aspiration of the pleural fluid and cytological examination. Unfortunately, the cytological examination is positive for malignant cells in only 33% of cases (Jett & Aubry, 2008). To add to the complexity of diagnosis, even in the 33% of cases with positive cytology, a definitive diagnosis of mesothelioma cannot be made. A definitive diagnosis of mesothelioma is only accepted if the positive cytology matches the clinical and radiological features of mesothelioma (Moore, Parker, & Wiggins, 2008). In the case of negative cytology and/or lack of a clinical suspicion of the diagnosis, tissue diagnosis is mandated. This can be done via a contrast computed tomogram (CT)–guided percutaneous needle biopsy of the pleura. However, the sensitivity of this approach is only 76%, and the needle biopsy procedure is associated with around a 5% risk of pneumothorax (Benamore, Scott, Richards, & Entwisle, 2006). In addition, CT exposes patients to radiation (Brenner & Hall, 2007), and differentiating between mesothelioma and benign pleural disease is challenging. The most common features suggesting malignant mesothelioma on a CT scan are 1) a circumferential pleural rind, 2) nodular pleural thickening, 3) pleural thickening of > 1 cm, and 4) mediastinal pleural involvement, with sensitivities of 41%, 51%, 36%, and 56%, respectively (Leung, Muller, & Miller, 1990). In a series of CT scans of 66 patients with mesothelioma, researchers found that 37.9% of the patients had volume contraction, 77.2% had pleural thickening, and 31.8% had involvement of the mediastinal pleura (Okten, Koksal, Onal, Ozcan, Simsek, & Erturk, 2006). Despite the positive predictive value of all of the above features, their absence does not confidently rule out the diagnosis of mesothelioma. Furthermore, spirometry is not useful in the diagnosis or monitoring of mesothelioma (Plathow, et al., 2006). A definite diagnosis of pleural disease in many cases requires an invasive biopsy, which is done either via medical thoracoscopy or VATS. The medical thoracoscopy biopsy procedure has a sensitivity of around 90% to diagnose malignant pleural disease and is associated with complications such as pneumothorax (Loddenkemper & Schonfeld, 1998). If medical thoracoscopy fails to obtain a diagnosis, the patients are referred for surgical biopsy, which is the definitive procedure, but this is also associated with false negative results (Boutin & Rey, 1993). Furthermore, the VATS procedure is invasive and cannot be conducted in patients who are not medically fit enough for general anaesthesia or single-lung ventilation. In addition, VATS is associated with a number of complications including chest infection, bleeding, prolonged air leak, myocardial infarction, stroke, and death (Imperatori, et al., 2008). Such complications can be avoided if a reliable non-invasive test can be used to diagnose malignant pleural disease. Diagnosing malignant pleural effusion is of paramount importance. In addition to providing a prognosis for patients, it guides treatment such as radiotherapy and palliative talc pleurodesis, which can be performed under a local anaesthetic without the need for more invasive surgery.

The effects of benign and malignant pleural disease on chest wall dynamics have not been examined before, but have been useful in subgrouping other lung diseases (La Mauro, et al., 2012) (Acosta, 2014) (Aliverti, et al., 2005). It was hypothesised that measuring chest wall dynamics via a non-invasive technology could help us differentiate between the two conditions.

15.2 Methods

This descriptive case series was undertaken in a regional thoracic centre. The study was approved on the 5th of February 2013 by the National Research Ethic Service Committee of West Midlands-The Black Country with REC reference: 10/h1202/58, Protocol number: Version2, 24.01.2013, and IRAS project ID: 59742. Informed consent was obtained from the participants. This study was carried out in accordance with the Code of Ethics of the World Medical Association (Declaration of Helsinki) for experiments involving humans.

15.2.1 Participants

Optoelectronic plethysmography (BTS, Milan, Italy), a validated method of measuring total and regional chest wall volumes and motion, was used in 16 patients recruited for this study. All patients had a CT scan of their chest as part of their clinical workup before OEP measurements. The measurements were made between 1 and 10 days before the diagnostic VATS pleural biopsy and, therefore, before any pathological diagnosis. The research team and patients were thus blind to the diagnosis during the capture. After the pathological diagnosis, they were divided into three groups: a control group, an empyema group, and a mesothelioma group. The control group had six patients free of pleural disease. They were six consecutive patients free of pleural, and restrictive or obstructive, lung disease who were waiting for lung nodule resection. The empyema group consisted of six patients with unilateral empyema. The mesothelioma group consisted of four patients with unilateral epithelioid mesothelioma. A radiology consultant independently interpreted all CT scans without the knowledge of the pathology results, OEP findings, or clinical history. Based on the radiological features of 1) a circumferential pleural rind, 2) nodular pleural thickening, 3) pleural thickening of > 1 cm, and 4) mediastinal pleural involvement, he decided on a radiological diagnosis of malignant or benign pleural thickening. The operative findings were collected for all patients. A summary of the patients' characteristics is found in Table 1.

15.2.2 Study design

This descriptive case series was undertaken in 16 patients in a regional thoracic centre. The study was approved by the Local Research Ethics Committee. Informed written consent was obtained from all the participants involved. Acquisition of chest wall motion was performed using the SMART suite software (BTS). OEP cameras were calibrated each day prior to the tests. The acquisition procedure required 79 hemispherical and 10 spherical reflective markers to be placed onto a participant's chest wall and back using a bioadhesive hypoallergenic tape. Standard placement of markers was done according to Cala et al. The OEP acquisition protocol included the measurement of observations (heart rate, oxygen saturations, and blood pressure) after five minutes of quiet breathing. During the OEP acquisition, ribcage and abdominal volumes were recorded by eight infrared cameras operating at 60 Hz. The OEP system tracked the displacement of the markers during vital capacity and quiet breathing. From total and compartmental (ribcage and abdominal) chest wall volumes acquired by OEP, the following parameters were obtained: tidal volume, as the total chest wall volume variation; total and compartmental volumes at end of expiration and end of inspiration; respiratory rate; and minute ventilation.

15.2.3 Statistical analysis

The statistical analysis was executed by IBM© SPSS© Statistics Version 22.0.0.0. The normality of the data was assessed using the Kolmogorov-Smirnov test. Our results showed that the data were not normally distributed. Accordingly, the data were presented as median or median + IQR. Each group data set point consisted of the median + IQR of the chest wall motion during a number of breaths in each group. As the data represented only 16 patients, no attempt was made to calculate the P value, as complex statistical tests could not be used for only 16 patients. The Chi-Square test was used to assess the categorical demographic data, and the Kruskal-Willis test was used for the continuous demographic data (in addition the Mann-Whitney U test, which was used to compare between the duration of symptoms in the empyema and mesothelioma groups). Any P value < 0.05 was deemed significant.

15.3 Results

A summary of demographic data of all patients is shown in Table 8.

Table 8: The mesothelioma, empyema, and control groups' characteristics.

	Control	Empyema	Mesothelioma	P value
Number of Patients	6	6	4	
Age	65 (10)	59 (28)	75 (2)	0.046
Female gender	3	2	1	0.701
COPD	0	0	0	
ASA	1 (1)	2 (2)	2 (2)	0.464
BMI	29 (6)	29 (5)	25 (7)	0.060
Duration of Symptoms (Weeks)	-	25 (36)	26 (27)	0.826

The data represent the total number or median and IQR of the age, gender, COPD status, ASA status, BMI, and the duration of symptoms of the patients in the mesothelioma (4), empyema (6), and control (6) groups. The Chi-Square test was used to assess the categorical data, and the Kruskal-Willis test was used for the continuous data. (In addition, the Mann-Whitney U test was used to compare between the duration of symptoms in the empyema and mesothelioma groups.) Any P value < 0.05 was deemed significant.

The operative findings confirmed no pleural abnormality in the control group. In the mesothelioma and empyema groups, the operative findings confirmed thickened parietal and visceral pleural surfaces in both groups of patients. One patient in both the mesothelioma group and the empyema group had an effusion.

None of the patients had a chest drain in situ during the captures. The overall tidal volume, respiratory rate, and minute ventilation are shown in Table 9.

Table 9: Respiratory parameters of mesothelioma, empyema, and control groups.

	Control		Empyema		Mesothelioma	
	Median	IQR	Median	IQR	Median	IQR
Overall VT (L)	0.49	0.19	0.61	0.35	0.58	0.18
RR	17	7	22	9	24	8.86
Min. vent. (L)	9.40	3.90	11.39	6.13	13.53	2.22
MIF (L/sec)	0.35	0.18	0.46	0.15	0.53	0.11
MEF (L/sec)	0.29	0.10	0.33	0.21	0.39	0.07

The overall tidal volume (VT) (litres), respiratory rate (RR), minute ventilation (min. vent.), maximum inspiratory flow (MIF), and maximum expiratory flow (MEF) in the three groups. (Cont.: controls group [n = 6], Empy: Empyema group [n = 6], Meso: Mesothelioma group [n = 4]). The data are presented as median and IQR.

The relative contribution of RCP, RCA, and the abdomen to overall chest wall tidal volume is shown in Table 10.

Table 10: The relative contribution of each chest wall compartment in the mesothelioma, empyema, and control groups.

	Control		Empyema		Mesothelioma	
	Median	IQR	Median	IQR	Median	IQR
% RCP	32	27	26	18	34	23
% RCA	14	10	12	12	13	8
% AB	46	30	62	31	56	25

The relative contribution of pulmonary rib cage (%RCP), abdominal rib cage (%RCA), and abdomen (%AB) to overall chest wall tidal volume in the three groups (Cont. = controls [n = 6]) (Empy. = Empyema [n = 6])(Meso.= Mesothelioma [n = 4]). The data are presented as median and IQR.

The overall tidal volume seemed to be similar in the three groups: controls 0.49 (0.19) L, empyema 0.61 (0.35) L, and mesothelioma 0.58 (0.10) L (Figure 39).

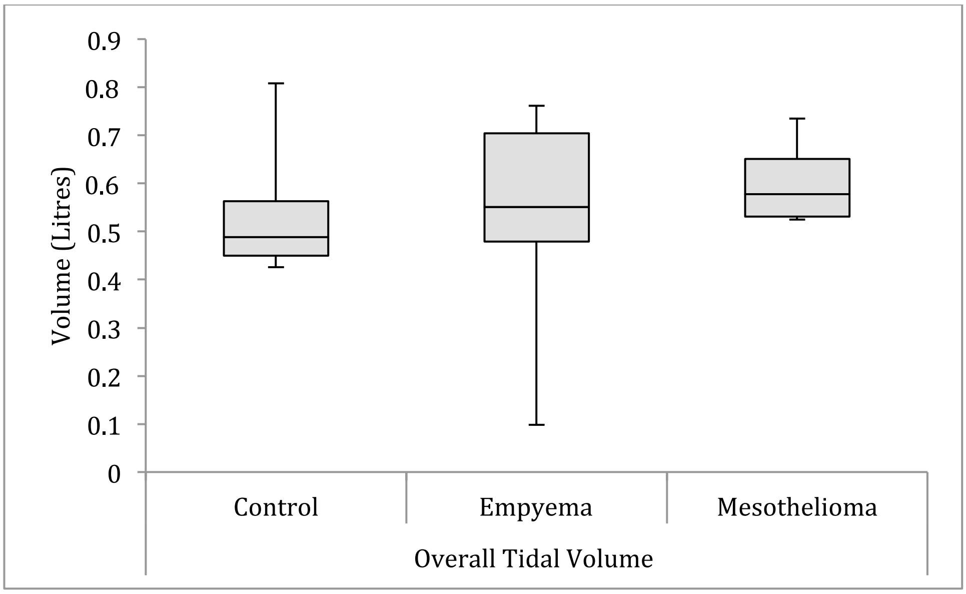

Figure 39: Overall tidal volume in all groups: the overall tidal volume (Tidal volume CW) in the three groups (controls [n = 6], empyema [n = 6], mesothelioma [n = 4]). The data are shown as boxplots (median, IQR, and quartiles).

Similarly, it seemed that there was no marked difference in upper ribcage tidal volume in the three groups (Figure 40).

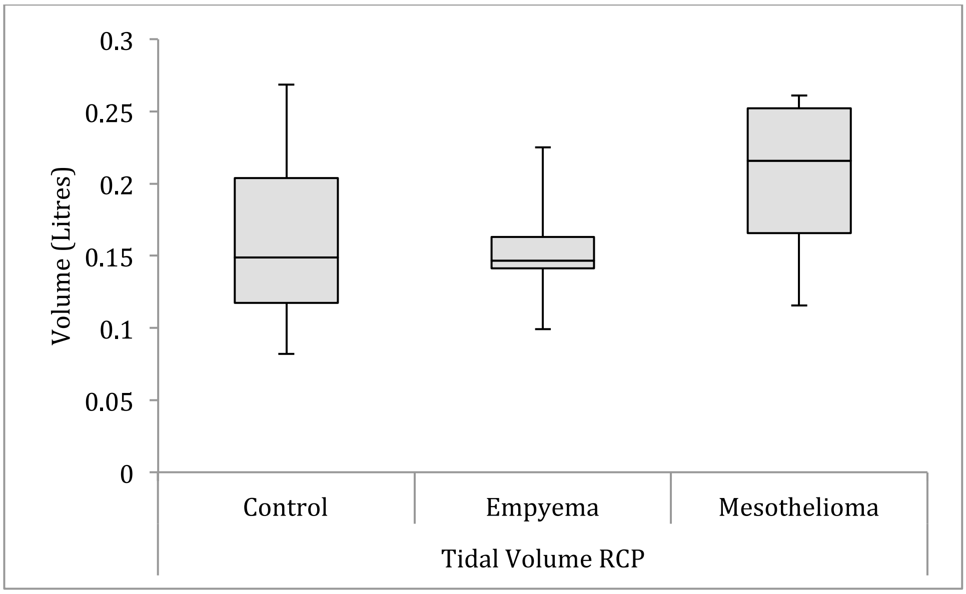

Figure 40: The pulmonary ribcage tidal volume in the three groups: The upper rib cage tidal volume in three groups (controls [n = 6], empyema [n = 6], mesothelioma [n = 4]). The data are shown as boxplots (median, IQR, and quartiles).

The absolute tidal volume of RCP on the diseased side did not differ among the three groups (Figure 41). However, the relative contribution of the diseased part of the RCP to the overall RCP was lower in the mesothelioma group: 26(30)%, compared to 52(5)% and 47(12)% in the control and empyema groups, respectively. There was no difference between the empyema group and control group. The results showed that all patients who were diagnosed with mesothelioma had a relative contribution of the diseased part of the RCP ≤ 32% to overall RCP motion, and all patients with benign pleural disease had a relative contribution of the diseased part of the RCP to the overall RCP of > 32% (Figure 42).

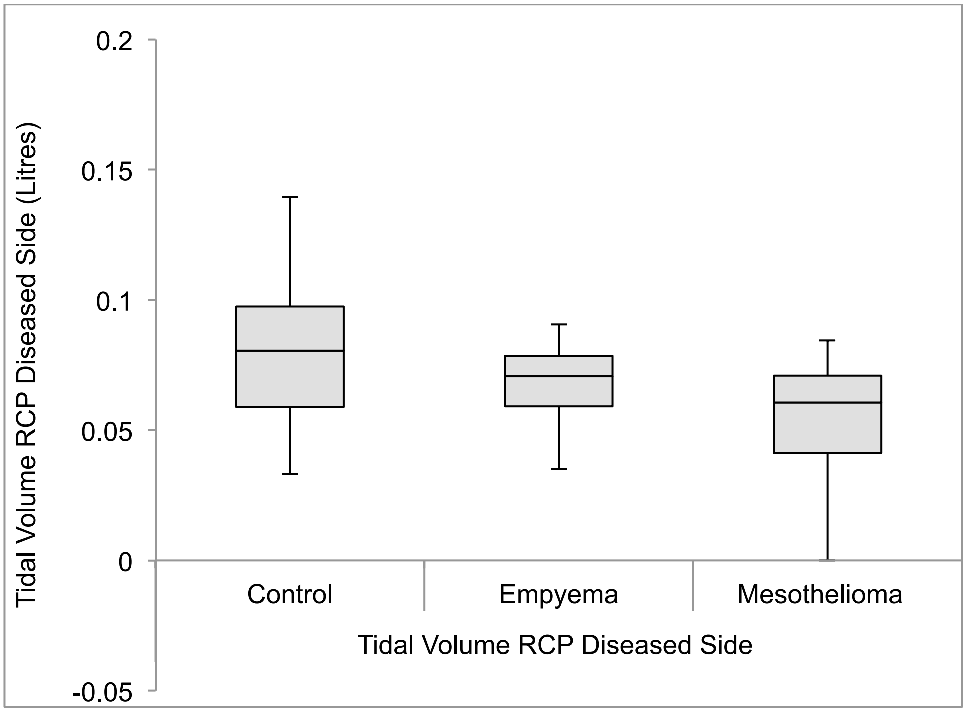

Figure 41: The tidal volume of the diseased pulmonary ribcage in mesothelioma and empyema, and the normal side in the control: The absolute tidal volume of diseased side of pulmonary ribcage in the two groups (empyema [n = 6], mesothelioma [n = 4]), and the normal side in the control group (n = 6). The data are shown as boxplots (median, IQR, and quartiles).

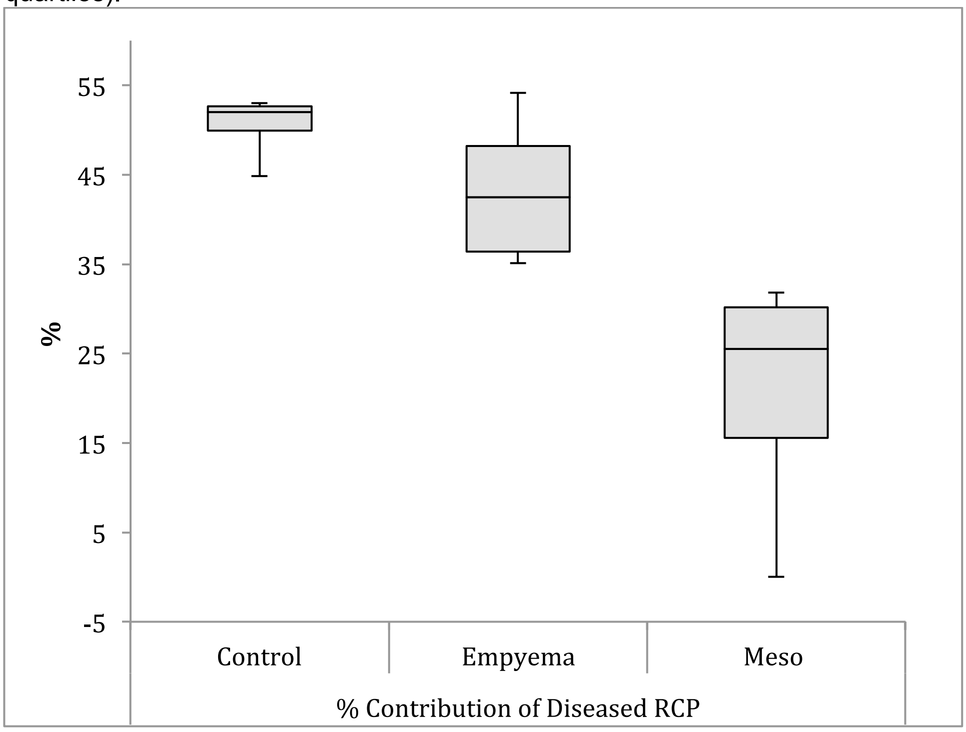

Figure 42: The percentage contribution of the diseased side of the pulmonary rib to overall pulmonary ribcage in the three groups: The percentage contribution of the diseased side of the pulmonary rib to overall pulmonary ribcage, in the mesothelioma and empyema groups, and the normal side in the control group. (Empyema [n = 6], mesothelioma [n = 4], and control group [n = 6]). The data are shown as boxplots (median, IQR, and quartiles).

The relative contribution of the normal side of the RCP to the overall RCP was higher in the mesothelioma group: 74(30)%, compared to 48(5)% and 53(12)% in the control and empyema groups, respectively. However, there was no difference between the empyema group and control group. The radiological diagnosis matched the pathological diagnosis in only 30% of all patients. The accuracy of the radiological diagnosis in all groups, which was done by a radiologist who was blind to the pathological results, is shown in Table 11.

Based on the radiological features, the distribution of disease was similar in both the mesothelioma and the empyema groups; there was a widespread distribution of the disease in two out the four patients in the mesothelioma group and two of six patients in the empyema group. One of the four patients in the mesothelioma group had pleural effusion, and one of the six patients in the empyema group had a pleural effusion. None of the patients in the control group had any feature of pleural abnormality on their CT scans. After evaluating all radiological features, the final radiological diagnosis was done by an experienced thoracic radiologist who was blind to the pathological diagnosis.

Table 11: The pathological diagnosis versus the radiological diagnosis versus motion of diseased side of pulmonary ribcage of the empyema and the mesothelioma groups.

Patient Number	Pathological Diagnosis	Radiological Diagnosis	Motion of Diseased Side of Pulmonary Ribcage
1	Mesothelioma	Mesothelioma	≤ 32%
2	Mesothelioma	Uncertain	≤ 32%
3	Mesothelioma	Mesothelioma	≤ 32%
4	Mesothelioma	Malignant effusion	≤ 32%
5	Empyema	Uncertain	> 32%
6	Empyema	Simple effusion	> 32%
7	Empyema	Uncertain	> 32%
8	Empyema	Uncertain	> 32%
9	Empyema	Empyema	> 32%
10	Empyema	Uncertain	> 32%

This table compares the pathological diagnosis, radiological diagnosis, and the contribution of the chest wall motion of the diseased part of the pulmonary ribcage, in the mesothelioma (n = 4) and the empyema (n = 6) groups.

15.4 Discussion

To date, there have been no sensitive radiological methods that can diagnose mesothelioma. Diagnosis of malignant or benign pleural disease from CT interpretation was incorrect in 70% of cases in the present study. In addition, medical thoracoscopy and VATS surgery is associated with significant post-operative morbidity and mortality. Indeed, in patients who have a pathological sample, there is an incidence of false negative results (Boutin & Rey, 1993). A sensitive non-invasive technology is needed to identify these patients. In this case series, the use of OEP in assessing chest wall mechanics was blindly examined in three groups of patients (a unilateral empyema group, a unilateral mesothelioma group, and a control group) during quiet breathing. Although all the patients in the mesothelioma and empyema groups had similar operative anatomical features, it was found that their physiological characteristics were strikingly different. Although tidal volume showed a tendency of being similar among the three groups, the relative contribution of the diseased part of the RCP in the mesothelioma group showed a trend of being lower than that of the empyema and control groups. In the mesothelioma group, this trend of reduction in motion on the affected side seemed to be compensated by the non-diseased part of the RCP, a phenomenon that did not occur in the remaining groups. The results showed that all patients with mesothelioma and none of the benign groups had a relative contribution of the diseased side of the pulmonary ribcage of ≤ 32%. To the knowledge of this study's authors, there are no studies of chest wall motion and pleural disease in the literature. Chest wall motion analysis has been used in the past to assess a number of clinical conditions (9.2.10.2), and it is thought that the same technology may be useful in detecting trends in chest wall motion that might be related to mesothelioma. A larger study is needed to validate these promising findings.

The physiological explanation for this finding may lie in the differences in the pathological process. Malignant mesothelioma is characterised by papillary mesothelial proliferation sheets of atypical mesothelial cells, and an abnormal fibroblastic proliferation (Herbert & Gallagher, 1982) (Kouki, 2008). In contrast, in inflammatory conditions, the mesothelial lining is usually replaced by granulation tissue (Herbert & Gallagher, 1982) which may be more pliable. In this study, it is believed that these pathological differences between the two conditions could explain the physiological outcomes. The more aggressive and proliferative nature of the malignant mesothelioma seems to have a higher degree of restrictive effect on the lung and chest wall, compared to the granulation tissue of empyema.

This case series described in detail the effect of empyema and malignant mesothelioma on chest wall mechanics. The results showed a general trend of reduction in chest wall motion of the diseased part of the chest in the mesothelioma group. These trends of chest wall changes might have the potential to help detect mesothelioma in the future. Further larger studies are needed to validate the results.

15.5 Limitations

These results only covered quiet breathing changes, and further work is needed to evaluate the chest wall mechanics during exercise. Future work could also focus on examining the effects of other malignant pleural disease on chest wall motion. In addition, the effect of de-bulking surgery on chest wall motion as well as the reduction of symptoms and quality of life could be examined in further studies. The relationship between the extent of the disease and the degree of chest wall impairment could also be assessed in a future larger study.

Another limitation of the study was that the trend of the radiological distribution of the disease was different between the groups (widespread radiological distribution of the disease in two patients [50%] in the mesothelioma group and two patients [33%] in the empyema group). This might influence the chest wall motion and explain the difference in the results.

16 Chapter 8: Early Chest Mechanics Changes Post–Lung Resection: The Effect of Thoracic Nerve Blocks

16.1 INTRODUCTION

There is evidence that keyhole surgery/VATS is associated with less morbidity than thoracotomy (Maeda, 1988) (Bernard, 2006) (Nomori, Horio, Fuyuno, Kobayashi, & Yashima, 1996). One of the reasons put forward for this is that the physiological insult to the chest wall is less traumatic with VATS than thoracotomy. Thoracotomy involves cutting a significant amount of muscle and retracting ribs, which is avoided in VATS cases. Until now, there was no way to easily measure relative continuation/motion in both sides of the chest immediately after surgery. This case series described in detail the use of novel technology in the assessment of compartmental chest wall motion and synchrony in a small group of lung resection patients who had undergone different surgical approaches, had different amounts of lung resected, and used different analgesia methods.

16.2 METHODS

This descriptive case series was undertaken in a regional thoracic centre. The study was approved on the 5th of February 2013 by the National Research Ethic Service Committee of West Midlands-The Black Country with REC reference: 10/h1202/58, Protocol number: Version2, 24.01.2013, and IRAS project ID: 59742. Informed consent was obtained from the participants. This study was carried out in accordance with the Code of Ethics of the World Medical Association (Declaration of Helsinki) for experiments involving humans.

This case series used a novel portable device to measure dynamic regional chest wall function immediately after VATS and thoracotomy lung resection in patients. SLP measured both ribcage and abdominal motion using a light grid, which was simultaneously seen by a digital vision system. Grid movement during breathing was analysed and outcomes were displayed in terms of regional thoraco-abdominal movement parameters and a 3D reconstruction. Measurements were made during quiet breathing while the patient was sitting, before the operation and on Day 1 post-operatively. The patient's height, weight, heart rate, oxygen saturation, Borg score of breathlessness, pain score, lung function via conventional spirometry, and type of analgesia used were also measured.

16.2.1 Patients

From May 2014 through January 2015, 15 patients who had lung resections at a regional thoracic unit were recruited. The analgesia technique varied based on patient and doctor preference and the surgery carried out. The techniques included TEB, continuous PVB, and intravenous morphine infusion. Table 12 shows the baseline characteristics of the patients.

Table 12: The baseline characteristics of the thoracotomy and VATS patients.

Number of patients	15
Female gender	5
Age (years)	69 (21)
Weight (kg)	75 (27)
Height (cm)	172 (13)
BMI	27 (7)
Thoracotomy : VATS	5 T : 10 V
Side (Right : Left)	11 R: 4 L
Type (Lobectomy: Wedge)	8 L : 7 W
(Upper: Middle: Lower) lobes	10 U: 2 M : 2 L
Borg score before surgery	0 (0)
Pain score before surgery	0 (0)
FEV1 Litre	2.8 (1.2)
FEV1 %	98 (19)
FVC Litre	3.5 (1.7)
FVC %	109 (24)

	Thoracotomy	VATS	P value
Number of patients	5	10	
Female gender	2	3	0.803
Age (years)	62	71 (13)	0.841
Weight (kg)	82	75 (21)	0.894
Height (cm)	169	173 (20)	0.689
BMI	1.69	1.73 (0.20)	0.315
Side (Right: Left)	1 Left: 4 Right	3 Left: 7 Right	
Type (Lobectomy: Wedge)	4 Lobectomy: 1 Wedge	3 Lobectomy : 7 Wedges	
(Upper: Middle: Lower) lobes	3 U: 1 M: 1 L	7 U: 2 M : 5 L	
Borg score before surgery	0	0 (0)	
Pain score before surgery	0	0	
FEV1 Litre	2.44	2.62 (1.17)	
FEV1 %	101	84 (21)	0.108
FVC Litre	3.415	3.16(1.78)	
FVC %	114	97 (37)	0.296

The baseline characteristics of the patients (BMI: Body mass index, FEV^1: forced expiratory volume in one second, FEV^1%: forced predicted expiratory volume in one second, FVC: forced vital capacity, FVC%: forced predicted vital capacity), thoracotomy n = 5, VATS n = 10. The data were presented as total number, median, or median and IQR (IQR was not calculated in some variables due to the small number of available values). The Mann-Whitney U test was used to assess the continuous data, and the Chi-Square test was used to assess the categorical data. Any P value < 0.05 was deemed significant.

16.2.2 Statistical Analysis

The statistical analysis was executed by IBM© SPSS© Statistics Version 22.0.0.0. The normality of the data was assessed using the Kolmogorov-Smirnov test. The results showed that the data were not normally distributed. Accordingly, the data were presented as median or median and IQR. Each group data set point consisted of the median and IQR of the chest wall motion during a number of breaths for each group. SLP data were given as the chest wall motion for each breath. As the data represented only 15 patients, no attempt was made to calculate the P value in chest wall motion, as complex statistical tests could not be used for only 15 patients. In assessing the demographic data of two groups, the Mann-Whitney U test was used to assess the continuous data, and the Chi-Square test was used to assess the categorical data. In assessing the demographic data of more than two groups, the Kurskal-Wallis test was used to assess the continuous data, and the Chi-Square test was used to assess the categorical data. Any P value < 0.05 was deemed significant.

16.3 RESULTS

When using SLP before and after lung resection surgery, consistent changes in chest wall motion are detectable. There is a trend of reduction in the motion of the operated side of the chest in all patients who had surgery on the first post-operative day compared to pre-surgery values, -10(26)%, and a compensatory trend of an increase in chest wall motion on the non-operated side, 8(30)%, in all patients on Day 1 after surgery. There was also a trend of an increase in the degree of dys-synchronisation by 38 (78)% between the chest wall and the abdomen on Day 1 after surgery, compared to the pre-operative value (Table 13).

Table 13: The percentage change in chest wall motion characteristics in all patients on Day 1 after surgery.

All Patients Percentage change in chest wall motion day 1 after surgery compared to preoperative value		
	Median	IQR
Overall Chest wall	3	27
Operated side of the chest	-10	26
Non-Operated Side of the chest	8	30
Synchronisation between the Op and Non-Op side	42	496
Synchronisation between the Chest and Abdomen	38	78

The percentage changes in chest wall motion and respiratory phases one day after surgery, compared to the pre-operative value in the all patients. The values given are the percentage changes from the pre-operative value (n = 15). The data are shown as median and IQR.

When the post-operative changes in chest wall motion were compared between patients who had a lobectomy (n = 7) and wedge (n = 8), it was found that the reduction in chest wall motion on the operated side showed a trend of being higher in the lobectomy group (n = 7), -11(27)%, as compared to the wedge group (n = 8), -8(25)%. On the non-operated side, the lobectomy subgroup had a trend of an increase in chest wall motion after surgery, 12(30)%, compared to the preoperative value. This was not replicated in the wedge group, which had an trend of an increase of 8(29)%. The degree of dys-synchronisation between the operated and non-operated side and between the chest wall and abdomen after surgery compared to the pre-operative values showed a trend of being higher in the lobectomy group, 290(475)%, as compared to the wedge group, -33(299)% (Table 14).

Table 14: The percentage change in chest wall motion characteristics in the lobectomy and wedge patients on Day 1 after surgery.

Percentage Change in Chest Wall motion after surgery compared to Preoperative value				
	Lobectomy (n=7)		Wedge (n=8)	
	Median	IQR	Median	IQR
Respiratory Rate	13	59	-5	42
Inspiratory time	-8	35	3	24
Expiratory time	-15	40	5	55
Overall Chest wall	12	33	0	23
The Operated side of the chest	-11	27	-8	25
The Non-Operated Side of the chest	12	30	8	29
Synchronisation between the Op and Non-Op side	290	475	-33	299
Synchronisation between the Chest and Abdomen	58	37	4	55

Changes in chest wall motion and respiratory phases one day after surgery, as compared to the pre-operative value in the lobectomy group (n = 7) and wedge group (n = 8). The values given are the percentage change from the pre-operative value. The data are shown as median and IQR.

When patients who underwent thoracotomy (n = 5) and VATS (n = 10) procedures were compared, it was found that, in the thoracotomy group (n = 5), there was a trend of reduction in the operated side of chest after surgery, -10(26)%, as compared to the pre-operative value, and in the VATS subgroup this was -12(25)%. In the thoracotomy group, there was a trend of an increase in the chest wall motion in the non-operative side after surgery, 7(29)%, as compared to the pre-operative value. In the VATS group, there was a trend of an increase in the chest wall motion in the non-operative side after surgery, 11(29)% (Table 15).

Table 15: The percentage change in chest wall motion characteristics in the thoracotomy and VATS patients on Day 1 after surgery.

	Thoracotomy (n=5)		VATS (n=10)	
	Median	IQR	Median	IQR
Respiratory Rate	12	86	4	46
Inspiratory time	-7	38	-1	25
Expiratory time	-15	68	1	57
Overall Chest wall	3	41	6	25
The Operated side of the chest	-10	26	-12	25
The Non-Operated Side of the chest	7	29	11	29
Synchronisation between the Op and Non-Op side	9	690	60	499
Synchronisation between the Chest and Abdomen	42	61	23	87

Changes in chest wall motion and respiratory phases one day after surgery, compared to the pre-operative values, in the thoracotomy (n = 5) and VATS groups (n = 10). The values given are the percentage changes from the pre-operative value. The data are shown as median and IQR.

Next, the chest wall motion was analysed on the first post-operative day in patients who had had three types of analgesic techniques on the first post-operative day. These patients were divided into three groups: the TEB group, which included patients who had epidural analgesia (Fentanyl 4mg/ml + Bupivacaine 0.125% at a rate up to 15 ml/hr); the PVB group, which had continuous PVB (Bupivacaine 0.125% at a rate up to 15 ml/hr); and a control group, which had intravenous analgesia (morphine infusion). Table 16 shows the baseline characteristics of the patients.

Table 16: The baseline characteristics of the TEB, PVB, and control groups.

	TEB	PVB	Control	P value
Number of Patients	3	5	7	
Number of Females	2	0	3	0.081
Age (years)	79 (12)	75 (21)	64 (18)	0.632
Weight (kg)	63 (29)	74 (21)	88 (22)	0.150
Height (cm)	152 (35)	174 (9)	170 (16)	0.379
BMI	29 (12)	26 (5)	29 (11)	0.238
Borg score before surgery	0 (2)	0 (0)	0 (3)	
Pain score before surgery	0 (0)	0 (0)	0 (0)	
FEV^1 Litre	1.74 (0.61)	2.79 (1.95)	2.77 (1.33)	
FEV^1 %	101 (7)	100 (18)	84 (35)	0.845
FVC Litre	2.95	3.44	3.63	
FVC %	121	98	98	0.782
Thoracotomy : VATS	02:01	02:03	01:06	
Side (Right : Left)	03:00	03:02	05:02	
Type (Lobectomy: Wedge)	02:01	04:01	01:05	
(Upper: Middle: Lower) lobes	03:00	02:00:03	05:03:04	

Baseline characteristics of the patients (TEB group [n = 3], PVB group [n = 5], control/intravenous morphine group [n = 7], BMI: Body mass index, FEV^1: forced expiratory volume in one second, FEV^1%: forced predicted expiratory volume in one second, FVC: forced vital capacity, FVC%: forced predicted vital capacity). Data are presented as total number, median, or median and IQR (IQR was not calculated in some variables due to the small number of available values). The Kurskal-Wallis test was used to assess the continuous data, and the Chi-Square test was used to assess the categorical data. Any P value < 0.05 was deemed significant.

On the first post-operative day, the pain score showed a trend of being similar among the three groups. The pain score was 2(1), 1(2), and 1(1) in the TEB group, PVB group, and control group, respectively. Similarly, there were no noticeable differences in the Borg breathlessness score or FEV^1 percentage among the three groups (Table 17).

Table 17: The Day 1 Borg score, pain score, and spirometry measurements in the TEB, PVB, and control groups.

	Day one post operatively		
	TEB	PVB	Control
Post-op Borg score	2 (1)	1 (2)	1 (4)
Post-op Pain score	2 (1)	1 (2)	1 (1)
FEV^1 litre	0.65 (0.69)	1.35 (0.20)	1.17 (1.05)
FEV^1 %	50 (13)	45 (15)	46 (24)
FVC Litre	1.17 (1.2)	1.94 (0.70)	1.42 (1.48)
FVC %	65 (8)	53 (18)	50 (26)

The first post-operative day's measurements, which include the Borg score of breathlessness, pain score, FEV^1, FEV^1 %, FVC, and FVC%. (TEB group [n = 3], PVB group [n = 5], and control/intravenous morphine group [n = 7]). Data are presented as median and IQR.

When all patients (VATS and thoracotomy) were assessed, the percentage changes (percent change from the pre-operative value) in overall chest wall motion one day after surgery seemed to show a similar trend among the three groups: 3(12)%, 18(52)%, and 0(23)% in the TEB group, PVB group, and control group, respectively. Similarly, the motion of the operated side showed a trend of reduction in all three groups, but this trend of reduction seemed to be similar in the three groups: -10(29)%, -16(23)%, and -6(28)% in the TEB group, PVB group, and control group, respectively. There was also a noticeable difference among the three groups on the non-operative side after surgery (Table 18). There was no noticeable difference among the three groups in respiratory rate, inspiratory time, and expiratory time (Table 18). There was also no marked difference between the three groups in synchronisation of motion between the chest and abdomen (Table 18).

Table 18: The percentage change in chest wall motion characteristics in the TEB, PVB, and control groups on day 1 after surgery.

Day 1 post-operative changes compared to pre-operative values			
	TEB	PVB	Control
% Change in motion of Overall Chest wall	3 (12)	18 (52)	0 (23)
% Change in motion of the Non Operated Side of the Chest	7 (31)	15 (25)	6 (32)
% Change in motion of the Operated side of the chest	-10 (29)	- 16 (23)	-6 (28)
% Change in Respiratory Rate	-16 (50)	25 (72)	-6 (32)
% Change Inspiratory time	2 (14)	-15 (36)	6 (13)
% Change in Expiratory time	30 (76)	-24 (32)	5 (34)
% Change of synchronisation between the Op and Non-Op side	9 (552)	290 (705)	-18 (299)
% Change of synchronisation between the Chest and Abdomen	58 (34)	61 (31)	-17 (47)

Changes in chest wall motion and respiratory phases one day after surgery, as compared to the pre-operative value in the three groups. The values given are the percent changes from the pre-operative value. TEB group (n = 3), PVB group (n = 5), control/ intravenous morphine group (n = 7). Data are presented as median and IQR.

None of the 15 patients had any complications after the procedure. The average hospital stay showed a tendency of being lower in the TEB group, 1(1) day, than in the PVB group, 3(1) days, and the control group, 2(1) days (Table 19).

Table 19: Hospital stay in TEB, PVB, and control groups: Hospital stay in days in three groups.

	TEB	PVB	Control
Hospital Stay (Days)	1 (1)	3 (1)	2 (1)

TEB group (n = 3), PVB group (n = 5), and control/intravenous morphine group (n = 7). Data are presented as median and IQR.

16.4 DISCUSSSION

This case series of acutely unwell post-operative lung resection patients showed that the use of a novel chest wall motion analysis device known as SLP can be useful. The technique consistently detected a trend of reduction on the operated side and a compensatory increase in chest wall motion on the non-operated side. The results showed that the trend of reduction on the operated side of the chest was slightly higher in the VATS group than the thoracotomy group. This could be related to the number of intercostal nerves compressed during VATS versus thoracotomy. During the thoracotomy procedure, a large cut was made on the chest wall through one intercostal space, and thus instrumentation during the procedure resulted in the compression of one intercostal nerve. In addition, during thoracotomy, one or two chest drains were inserted through a separate intercostal space, which led to the compression of a second intercostal nerve. Thus, thoracotomy caused the compression of a total of about two intercostal nerves. On the other hand, VATS surgery involved instrumentation through three to four port sites created though incisions made through three or four different intercostal spaces, compressing three or four different intercostal nerves. Usually, one of these ports was utilised for a chest drain, and if another drain was needed, a separated incision on another intercostal space could have been utilised. Thus, VATS caused a compression of around four to five intercostal nerves, which was twice as much as the number of intercostal nerves compressed by thoracotomy. It was believed that the higher number of nerves compressed through VATS might have resulted in the higher tendency of reduction of chest wall motion on the operated side in VATS, as compared to thoracotomy, as shown in these results.

In addition, this early study suggested that there is a trend of no marked difference in other parameters of chest wall changes after surgery, between lobectomy versus wedge, or the type of analgesia utilised. It is known that there is a reluctance among anaesthetists to give epidural blockage to patients with rib fractures, fearing that it might cause a negative effect on chest wall motion, leading to respiratory compromise. The results of this case series showed that epidural analgesia has no tendency of negative effect on the chest wall compared to controls. This suggests that epidural analgesia—at the strength used in this study—might not have a negative effect on chest wall motion. Therefore, it might be potentially safe for use in patients with rib fracture, but a larger study is needed to validate the result and confirm its safety.

It is also noted that there is a trend of an increase in chest wall motion on the non-operated side after surgery. This could be due to a compensatory mechanism by the body to adjust to a loss of chest wall motion on the operated side. In addition, the loss of volume in one lung allows the other lung to compensate for the loss by expanding to a greater degree than before surgery.

This study showed that SLP is a useful post-operative tool because it is a portable device that can be taken to the bedside of the patient immediately after surgery, and it does not interfere with post-operative patient care in the recovery room or high-independence wards. In addition, SLP is useful post-operatively because it does not require patient effort, as all that is required from the patient is lying on the bed. SLP has the potential to provide valuable information on the progress of patients immediately after surgery, as it can be used non-invasively for chest wall motion analysis, which might reflect changes in ventilation. As seen throughout this thesis, this can have wide clinical implications in the future.

A larger multi-centre study is needed to validate the results.

16.5 Limitations

One of the limitations of this study was that only a small sample was able to be recruited for a number of reasons that will be discussed in detail in the conclusion chapter. This led to the number of patients being compared in the subgroups to be even smaller. From these small numbers (and even smaller numbers in the subgroup) no concrete conclusion about the absence of difference in the chest wall motion between the subgroups could be made. All that could be seen was a trend of change, but a larger study is needed with a larger number of patients with similar demographics in each group to confirm or deny the results.

The results were based on the local current regime and the strength of TEB and PVB anaesthetics; further work is needed to evaluate the effects of different regimes and strengths of TEB and PVB. Measurement could not be done during exercise, as the SLP machine required the patients to fix their backs against a hard surface (a chair or bed) and the captures were done on these patients on their first post-operative day when they were not in physical condition to do any exercise. In addition, the SLP capture could only be done in a relatively dark room as light interferes with the quality of the capture. Furthermore, abdominal and chest tubes and stomas, as well as skin folds, interfered with the quality of capture.

17 Chapter 9: Early Chest Mechanics Changes Post–Lung Resection: The Effect of Post-operative Pulmonary Complications on Chest Wall Mechanics

17.1 BACKGROUND

Post-operative pulmonary complications (PPCs are responsible for approximately 84% of post–thoracic surgery deaths (Stephan, Boucheseiche, & Hollande, 2000). PPCs are responsible for delaying patients' discharge as well as many intensive care admissions (Agostini, et al., 2008). More than 30,000 patients die from lung cancer in the UK annually; this represents 5.6% of the mortalities in the UK (Office for National Statistics, 2001). Lung cancer in the UK presents later than in the rest of Europe and lung cancer patients in the UK have a higher rate of co-morbidities than patients in the rest of Europe (Impertori, Harrison, & Leitch, 2006) (Brunelli, 2009). This is reflected in a decreased number of lung resections for cancer in the UK as compared to the US and the rest of Europe, with 11%, 21%, and 17%, respectively (Jack , Gulliford, & Ferguson, 2003). This has led to a low survival rate in the UK (Sant, Aareleid, & Berrino, 2003). To improve the resection rate in the UK, patients need to be operated on who are less fit for surgery than as recommended by the British thoracic guidelines (Brunelli, et al., 2009). This approach would lead to an even further rise in the incidence of PPCs. Early detection is fundamental in treating PPCs, but identifying patients with PPCs early has been problematic. This may be due in part to delayed radiological evidence of the condition. In one study, 55% of patients with initially negative chest X-rays developed infiltrates in their latter X-rays in 48 hours (Hagaman, Rouan, Shipley, & Panos, 2009). Furthermore, radiation is associated with its own side effects. This may be due in part to the difficulties of performing spirometry in the immediate post-operative period and to how well it reflects regional lung function and symptoms in these groups of patients. Furthermore, the current scoring systems, although they have been validated to detect PPCs, still lack accuracy (Agostini P. B., 2011). PPCs lead to a decrease in lung compliance, which reduces lung expansion. In this paper, it is hypothesised that these changes in patients who develop PPCs could be detected by chest wall motion technology in the immediate post-operative period prior to clinical signs developing. By using chest wall motion technology, the aim is to show a relation in tendency between recovery and complications with trends in chest motion. It is hypothesised that using this method can lead to identifying trends of early deterioration before clinical and radiological manifestations, which might lead to faster recognition and treatment of PPCs.

17.2 Methods

This descriptive case series was undertaken in a regional thoracic centre. The study was approved on the 5th of February 2013 by the National Research Ethic Service Committee of West Midlands-The Black Country with REC reference: 10/h1202/58, Protocol number: Version2, 24.01.2013, and IRAS project ID: 59742. Informed consent was obtained from the participants. This study was carried out in accordance with the Code of Ethics of the World Medical Association (Declaration of Helsinki) for experiments involving humans.

SLP was used to measure regional thoraco-abdominal motion of 11 consecutive patients undergoing thoracic surgery in a regional thoracic unit. Inclusion criteria included all patients who were having a thoracic procedure during a one-month period and who were willing to participate in the study. Out of 25 patients asked to participate in the study 11 agreed to do so. SLP measured both ribcage and abdominal motion using a light grid, which was simultaneously seen by a digital vision system. Grid movement during breathing was analysed, and the outcomes were displayed in terms of regional thoraco-abdominal movement parameters and as a 3D reconstruction. Three of the 11 patients developed PPCs post-operatively; all had pneumonia on the operated lung.

The patients were divided based on the clinical diagnosis of PPCs post-operatively into a PPC group and a control group (CG). This division was made retrospectively, as data collection was made and PPC status was assigned retrospectively. The PPC group included all patients who had been diagnosed clinically by the physician to have PPCs. All PPC group patient developed PPCs on the same side of the operation. The PPC score was collected before surgery and every day after surgery until the discharge date for all patients. The PPC score included eight parameters, each with a score of 1 for positive results or 0 for negative results: chest X-ray atelectasis, white blood cells > 11.2 or respiratory antibiotics, temperature of more than 38°C, positive sputum microbiology, Sats of < 90% on room air, a diagnosis of pneumonia, readmission to the intensive care unit, and a productive cough. A total score of 4 or more is diagnostic for PPCs. The control group included all patients who were not clinically diagnosed to have PPCs during the ward round. Clinical diagnosis as used here is a diagnosis that relies purely on patient history and examination without radiological input; it is a diagnosis based on a patient's symptoms and signs elicited during a medical examination, before the results of CXR become available for review. Routine Day 1 post-operative CXR was done the morning after each procedure. Table 20 shows the demographic data of the two groups. The SLP measurements were made during quiet breathing while the patient was sitting, before surgery, and every day after surgery until the discharge date. Outcomes were given as the percentage contribution of the regional compartment of the chest and abdomen. Data collected included the PPC score, conventional spirometry, oxygen saturation, the need for antibiotics, the need for bronchoscopy, the Borg score for breathlessness, and a validated pain score (a horizontal Visual Analogue Scale [VAS]). VAS has been used extensively in evaluating post-thoracic surgery pain (Helms, et al., 2011) (Concha, Dagnino, Cariaga, Auilera, Aparicio, & Guerrero, 2004) (Ohlmer , Leger, Scheiderer, Elfeldt, & Wulf, 1997) (Valairucha, Maboonvanon, Napachoti, Sirivanasandha, & Suraseranuvongse, 2005). The system has been used in clinical practice for a long time and has been validated against a number of established pain scoring systems. Downie et al. showed that the VAS pain score had a high correlation with a five-point verbal descriptive and numeric rating scale (Downie, Leatham, Rhind, Wright, Branco, & Anderson, 1978). Scott et al. also showed high correlations between the horizontal and vertical orientations of the VAS (Scott & Huskisson, 1979).

The need for bronchoscopy was decided based on a clinical suspension made by the surgeon to remove a mucus plug that caused the lung to collapse. Bronchoscopy is indicated in this situation to re-inflate the lung. The decision of starting antibiotics is made by the surgeon based on the clinical suspension of pneumonia.

A PPC score is a valid score to diagnosis PPCs, as it has shown correlation with clinically diagnosed PPCs requiring antibiotic therapy or bronchoscopy (Agostini, et al., 2011). It has also been used in a randomised controlled trial to assess PPCs following thoracic surgery (Reeve, Nicol, Stiller, McPherson, Birch, & Gordon et al. , 2010). All patients had a CXR as inpatients after surgery and thereafter if there was a clinical suspicion of PPCs. The study end points were the patient being discharged from the hospital, refusing to continue in the study, or becoming clinically unwell.

These case series aimed to describe a relationship of tendency between PPCs and trends in chest motion.

Table 20: The demographic data of the PPC group and the control group.

	PPC group	Control	P value
Number of Patients	3	8	
Female gender	1	4	0.621
Age	54 (27)	72 (13)	0.031
BMI	29 (9)	26 (11)	0.473
VATS/Thoracotomy	1 VATS: 2 Thoracotomy	7 VATS: 1Thoracotomy	
Side (right/left)	2 Right: 1Left	6 Right: 2Left	
Type	1 Wedge: 2Lobe	4 Wedge: 4 Lobe	
Subtype	1 Upper: 1Middle:1Lower	6 Upper: 1Middle:1Lower	
pre op Borg score	0 (2)	0 (0)	0.087
pre op pain score	0 (0)	0 (0)	0.521
FEV1 L (max)	2.97 (0.48)	1.74 (0.47)	
FEV1 % max	101 (35)	84 (20)	0.819
FVC L max	3.39 (3.63)	2.69 (1.92)	
FVC % (max)	73 (115)	98 (36)	0.456
COPD	0	0	
Smoking			
Current	0	0	
Ex-smokers	2	3	
Non-smokers	1	5	

Demographic data of the PPC group (n = 3) and the control group (n = 8). FEV1 : forced expiratory volume in one second, and FVC: forced vital capacity. The data were collected directly pre-operatively and presented as a total number or median and IQR. The Mann-Whitney U test was used to assess the continuous data, and the Chi-Square test was used to assess the categorical data. Any P value < 0.05 was deemed significant.

Statistics

The statistical analysis was executed by IBM© SPSS© Statistics Version 22.0.0.0. The normality of the data was assessed using the Kolmogorov-Smirnov test. The results showed that the data were not normally distributed. Accordingly, the data were presented as median or median and IQR. Each group of data set points consisted of the median and IQR of the chest wall motion during a number of breaths for the whole group, as SLP measured the chest wall motion per breath. Multiple measurements were not taken for each patient, and each patient had only one measurement. As the data represented only 11 patients, no attempt was made to calculate the P value, as complex statistical tests could not be used for only 11 patients. Because this was a pilot study, a power calculation was not done.

To compare the demographic data between the groups, the Mann-Whitney U test was used to assess the continuous data, and the Chi-Square test was used to assess the categorical data. A statistical significance of P value less than 0.05 was used for the analyses. Any P value < 0.05 was deemed significant.

17.3 RESULTS

The results showed that, based on the patients' symptoms and chest examinations, none of the patients were clinically diagnosed with PPCs on the first post-operative day, nor was the PPC score diagnostic. (The PPC scores on the first post-operative day in the three patients in the PPC group were 1, 3, and 3.) To diagnosis PPCs using the PPC score, a minimum score of 4 was required. PPCs were diagnosed clinically by surgeons in all three patients on Day 2 after surgery, based on the patients' symptoms and chest examinations. The PPC score was diagnostic of PPCs on Day 2 for one patient (with a score of 5), and on Day 3 for the second patient (with a score of 6), but the score was not diagnostic for the third patient at any given time point. The spirometry results showed a greater trend of reduction in both FEV^{1}% and FVC% in the PPC group than the CG on Day 1 after surgery (Table 23). Chest X-rays showed signs of atelectasis in two of three patients on Day 1 and three of three patients by Day 2. The length of the hospital stay was 8(3) days in the PPC group and 3(3) days in the control group. Only one patient in the PPC group had readmission to ITU. All patients who had a thoracotomy procedure had chest physiotherapy, as did all patients who developed PPCs. Patients who had an uncomplicated VATS procedure did not have any chest physiotherapy.

The results showed that on Day 1 after surgery, compared to the pre-operative value, the percentage change of the time to reach the maximum expiratory flow, showed a trend of being higher in the PPC group compared to the CG group, with 5(15)% and -3(58)%, respectively (Table 21). Similarly, the percentage change to reach maximum inspiratory flow showed a trend of being higher in the PPC group than the CG group, with 2(4)% and -1(6)%, respectively (Table 21).

Table 21: The Day 1 clinical parameters and the percentage change in chest wall motion parameters of PPC groups and controls on Day 1 after surgery compared to before surgery.

	PPC group	Control Group (CG)
Number of Patients	3	8
Day 1 Parameters in Each Group		
Borg score	1 (3)	1 (2)
Pain score	1 (2)	2 (1)
Number of drains	1 (1)	1 (1)
CXR Atelectasis/consolidation	1 (1)	0 (0)
White Blood Count > 11.2 or Antibiotics	1 (1)	0 (1)
Temperature >38	0 (0)	0 (0)
Positive sputum in microbiology	0 (0)	0 (0)
O2 saturation of <90% Room air	0 (1)	0 (0)
Clinical Diagnosis of pneumonia	0 (0)	0 (0)
Readmission to ITU	0 (1)	0 (0)
Productive caught	0 (1)	0 (0)
PPC score	3 (2)	0 (1)
Day 1 percentage Change from Pre-Surgery: Spirometry and Chest Wall Motion		
FEV1 %	-57 (8)	-40 (36)
FVC %	-60 (8)	-41 (32)
Respiratory Rate	-6 (60)	0 (53)
Inspiratory time	8 (51)	-1 (12)
Expiratory time	4 (134)	1 (58)
Total time of respiratory cycle	7 (103)	0 (44)
Overall Chest Wall Motion	-9 (31)	5 (14)
Motion of operated side	-11 (30)	-9 (23)
Synchronisation between the operated and non-operated side of the chest wall	240 (308)	56 (483)
Synchronisation between the rib cage and abdomen	4 (78)	35 (84)
Time to reach maximum expiratory flow	5 (12)	-3 (58)
Time to reach maximum inspiratory flow	2 (4)	-1 (6)

The table shows the Day 1 clinical parameters in the control group (n = 8) and the PPC group (n = 3) and the Day 1 percentage change from pre-surgery in spirometry and chest wall motion in each group. The data are presented as total number or median and IQR. The Mann-Whitney U test was used to assess the continuous data, and the Chi-Square test was used to assess the categorical data. Any P value < 0.05 was deemed significant.

The results showed that overall chest wall motion showed a trend of greater reduction in the PPC group than the CG group, -9(31)% and 5(14)%, respectively. The results also showed that both groups of patients had trends of reduction in chest wall motion on the operated side on Day 1 after surgery, but this trend of reduction was higher in the PPC than CG group, with -11(30)% and -9(23)%, respectively. There was a trend of higher degree of dys-synchronisation between the operated side and non-operated side of the chest in the PPC group, as compared to the CG group, with 240(308)% and 56(483)%, respectively (Table 23).

17.4 DISCUSSION

Our data showed that by measuring trends in chest wall motion, SLP might be able to detect which patients developed PPCs prior to the development of clinical signs. The clinical diagnosis of PPCs by the doctor in charge was only made on Day 2 after surgery in all three patients who developed a PPC. The PPC score was diagnostic (based on a PPC score of >/= 4) only in one patient on Day 2 and one patient on Day 3 and was not diagnostic for the third patient in the PPC group; changes in SLP parameters were apparent in all three patients on Day 1. There was a trend of a higher degree of reduction in the overall chest wall motion in the PPC group compared to the CG one day after surgery. There was also a trend of greater reduction in the motion of the operated side in the PPC group compared to the CG on Day 1 after surgery. These seem to be related to a trend of a higher degree of dys-synchronisation between the sides of the chest in the PPC group compared to CG on Day 1 after surgery. These findings seem to be related to the CXR findings of PPCs. In one patient, chest wall motion changes were apparent before CXR manifestation of PPCs. This is of particular importance in light of high false negative results of the initial radiology to diagnose PPCs; Hagaman et al.

reported that 55% of those who develop PPCs have a negative initial radiology (Hagaman, Rouan, Shipley, & Panos, 2009). Thus, the results of the present study showed that SLP technology may have potential in detecting early signs of PPCs before the conventional X-ray. In addition, unlike the X-ray, SLP is a radiation-free technology, which utilises harmless direct light to measure chest wall motion. This trend of loss in synchrony between both sides of the chest may represent an early sign of respiratory distress prior to changes in respiratory rate. Loss in synchrony of breathing patterns has also been described in patients with COPD (Zaid, 2015).

On the other hand, a possible alternative explanation of the results is that the difference between the PPC group and control group in terms of chest wall motion could be due to the fact that 66% of patients in the PPC group had thoracotomy, compared to 13% in the control group. Similarly, 66% of the PPC group were ex-smokers, compared to only 37% in the control group. This might affect the quality of lung parenchyma in both groups and might affect compliance and the ability for the lungs to expand, which might affect the chest wall motion. A larger homogenous sample with equal number of thoracotomies and ex-smokers in each group is needed to exclude the effects of these variables.

Although CXR could diagnose PPCs in two of three patients, its downfall was that, unlike SLP, it still missed the third patient with PPCs. In addition, CXR exposes patients to ionising radiation; in contrast, SLP is a non-invasive technology that only uses only direct light, which is totally safe on patients.

Diagnosing PPCs is of paramount importance, as it is a major cause of mortality and morbidity, especially in the growing elderly co-morbid cohort of patients. The results of this pilot study suggested that patients with an increasing trend in the degree of change of dys-synchronisation on both sides of the ribcage, and patients with a trend of a high degree of reduction in the motion of both the overall chest wall motion and the operated side of the chest, might be starting to develop PPCs. Recognising PPCs early and non-invasively facilitates targeting treatment to patients who are at risk. Targeted treatment includes interventions such as mini tracheostomy, incentive spirometry, and increased physiotherapy, which have all been shown to reduce PPCs in at-risk groups. Targeting treatment has potential significant economic benefits because it channels precious resources, but if intervention is effective, it thereby reduces the financial impact of PPCs. Further adequately powered studies are required to validate this novel technology.

17.5 CONCLUSION

This case series demonstrated that a novel technology may have the potential to detect signs of PPCs by analysing trends in chest wall motion before a clinical diagnosis is made. This could have a wide range of clinical applications.

17.6 Limitations

The limitation of the study was that it only involved three patients with PPCs. The reason for this is that during recruitment for the study, it was impossible to predict who would have a chest infection before surgery. A further, larger study will help better define these changes. Another limitation was that the measurement could not be done during exercise, as the SLP machine required the patients to fix their backs against a hard surface (a chair or bed). In addition, the SLP capture could only be done in a relatively dark room, as light interfered with the quality of the capture. Furthermore, abdominal and chest tubes and stomas, as well as skin folds, interfered with the quality of capture.

18 Chapter 10: Late Changes in Chest Wall Mechanics Post–Lung Resection: The Effect of Lung Cancer Resection in COPD Patients

18.1 INTRODUCTION

Chronic obstructive pulmonary disease is an obstructive airway disease that results in a state of hyperinflation and a reduction in lung and chest wall recoil. This in turn can result in a dysfunction of the respiratory muscles (Fressler, Scharf, Ingenito, McKenna, & Sharafkhaneh, 2008). There is evidence that in some of these patients, the diaphragm is flattened and has reduced contractility (Braun, Arora, & Rochester , 1982), especially at a later stage of the disease. Lung volume reduction surgery has been used in selected COPD patients to improve exercise capacity, lung function, quality of life, and survival (NETT group , 2003). It does this by reversing dynamic hyper-inflation, thereby improving the overall mechanics of breathing (Geddes, Davies, & Koyama, 2000) (Fishman, Martinez, & Naunheim, 2003) (Clark, Zoumot, & Bamsey, 2014) by restoring lung recoil and respiratory muscle function after surgery (Fressler, Scharf, Ingenito, McKenna, & Sharafkhaneh, 2008). Similarly, following lung resection of emphysematous lung in COPD patients for lung cancer, studies have reported improved respiratory function (Cassart & et, 2001) (Vaughan, Oey, Nakas, Martin-Ucar, Edwards, & Waller, 2007). Optoelectronic plethysmography is a system that measures regional chest wall motion and has been used extensively in understanding the respiratory mechanics of COPD patients (Aliverti, et al., 2005). To the knowledge of this paper's authors, in COPD patients suspected to have lung cancer, the effect of lung resection on chest wall mechanics has never been described before. By using OEP these case series aim to describe trends of change in chest wall mechanics following lung resection in patients with COPD, as compared to patients without COPD.

18.2 METHODS

This descriptive case series was undertaken in a regional thoracic centre. The study was approved on the 5th of February 2013 by the National Research Ethic Service Committee of West Midlands-The Black Country with REC reference: 10/h1202/58, Protocol number: Version2, 24.01.2013, and IRAS project ID: 59742. Informed consent was obtained from the participants. This study was carried out in accordance with the Code of Ethics of the World Medical Association (Declaration of Helsinki) for experiments involving humans.

Optoelectronic plethysmography (BTS, Milan, Italy), a validated method of measuring total and regional chest wall volumes (Acosta, 2014) (Cala, et al., 1996) (Aliverti, Dellaca, Pelosi, Chiumello, Gatihnoni, & Pedoti, 2001) (Dellaca, Ventura, Zannin, Natile, Pedotti, & Tagliabue, 2010) (Vogiatzis, Aliverti , Golemati, Georgiadou, Lo Mauro, & Kosmas, 2005), was used in 11 patients who were scheduled for lung resection on suspension of lung cancer. Five were COPD patients (COPD group) and six were non-COPD patients (non-COPD group). The demographics of the COPD and non-COPD groups are in Table 24. There was a trend of difference in the FEV_1/FVC ratio, as was to be expected based on the definition of COPD. There was a trend of no difference in the amount of the lung resected between the COPD group and the non-COPD group: 0.28(1.72) L and 0.54(0.33) L, respectively. The duration of the surgery was 3(1) hours and 3(1) hours in the VATS and the thoracotomy groups, respectively. A definitive pathological diagnosis was obtained for all patients, and 9 of 11 had lung cancer (Table 22).

Table 22: The pre-operative characteristics of all the patients in the COPD and non-COPD groups.

	COPD Group (n-5)	Non-COPD (n=6)	P value
Number of Females	1	2	0.621
Age	61 (9)	66 (13)	0.359
Height	174 (24)	173 (10)	0.784
Weight	71 (42)	83 (20)	0.521
BMI	25 (14)	27 (10)	0.58
ECOG	1 (1)	1 (1)	0.885
ASA	3 (1)	3 (0)	0.887
MRC	3 (2)	1 (1)	0.405
Smoking:			
Ex-smokers	3	3	
Current smokers	2	1	
Non-smokers	0	2	
FEV1%	68 (18)	82 (20)	0.109
FVC%	111 (18)	97 (25)	0.201
FEV1/FVC	0.65 (0.17)	0.80 (0.10)	0.01
Procedure:			
VATS	3	2	
Thoracotomy	2	4	
Resection extent:			
Wedge	2	0	
Lobectomy	3	6	
Anatomical location:			
Upper Lobe	4	5	
Lower Lobe	1	1	
Side:			
Right	3	3	
Left	2	3	
Lung volume resected (Litre)	0.28 (1.72)	0.54 (0.33)	0.715
Emphysema Distribution:			
Heterogeneous	5	-	
Pathology			
Squamous cell carcinoma	2	3	
Adenocarcinoma	0	3	
Small cell carcinoma	1	0	
Inflammatory	2	0	
Duration of surgery (hours)	3 (1)	3 (1)	0.558
Hospital stay (days)	7 (9)	5 (6)	1.000

The table shows the characteristics of pre-operative patients in the COPD group (n = 5) and the non-COPD group (n = 6). BMI: body mass index, ECOG: Eastern Cooperative Oncology Group Scale of Performance Status, ASA: American Society of Anaesthesiologists score, MRC: MRC breathlessness scale, FEV1%: Predicted forced expiratory volume in 1 second, FVC%: Predicted forced vital capacity. VATS: Video-assisted thoracoscopic surgery. The data are presented as total number or median and IQR. The Mann-Whitney U test was used to assess the continuous data, and the Chi-Square test was used to assess the categorical data. Any P value < 0.05 was deemed significant.

18.2.1 Study Design

These case series were undertaken in a regional thoracic centre. The research study was approved by the Local Research Ethics Committee. Informed consent was obtained from all involved participants. Chest wall motion was measured in participants pre-operatively, post-operatively once up to three months after surgery, and once more than six months after surgery. Data collected included the participant's age, height, weight, pain score, spirometry, and any relevant past medical history. Surgery was performed either via VATS/keyhole surgery or a postero-lateral thoracotomy. The participants were assigned to either operation by the operating surgeon, depending on the experience of the surgeon (two out of five surgeons were not performing VATS lobectomy at the time of this study) and by the appropriateness of the approach determined by the extent and nature of the disease.

Acquisition of chest wall motion was performed using SMART suite software (BTS, Milan, Italy). OEP cameras were calibrated each day prior to the tests. The acquisition/procedure required 79 hemispherical and 10 spherical reflective markers to be placed onto the participant's chest wall and back using bio-adhesive hypoallergenic tape. The standard placement of markers was done according to Cala et al. (Cala, et al., 1996). OEP acquisition protocol included observations of heart rate; oxygen saturations and blood pressure were recorded after three minutes of quiet breathing. During the

OEP acquisition, chest wall volumes were recorded by eight infrared cameras operating at 60 Hz. The OEP system tracked the displacement of the markers during quiet breathing. The chest wall volume was divided into three compartments: RCP, RCA, and AB. From the total chest wall (CW) and compartmental (RCP, RCA and AB) chest wall volumes acquired by OEP, the following parameters were obtained: tidal volume (VT), as the total chest wall volume variation; total and compartmental volumes at EEV and EIV; RR; and minute ventilation (VT x RR). These parameters were analysed during quiet breathing.

18.2.2 Statistical analysis

The statistical analysis was executed by IBM© SPSS© Statistics Version 22.0.0.0. The normality of the data was assessed using the Kolmogorov-Smirnov test. The results showed that the data were not normally distributed. Accordingly, the data were presented as median or median and IQR. Each group data set point consisted of the median and the IQR of the chest wall motion during a number of breaths for the whole group, as SLP gives the data on chest wall motion per each breath. Multiple measurements were not taken for each patient; each patient had only one measurement. As the data represented only a small number of patients, no attempt was made to calculate the P value, as complex statistical tests could not be used for a small number of patients.

To compare the demographic data between the groups, the Mann-Whitney U test was used to assess the continuous data, and the Chi-Square test was used to assess the categorical data. A statistical significance of a P value less than 0.05 was used for the analyses. Any P value < 0.05 was deemed significant.

18.3 RESULTS

In the non-COPD group, there was a trend of minimal change in the overall chest wall motion six months after surgery, as compared to the pre-operative value (Figure 40). In contrast, in the COPD group, the total chest wall motion showed a trend of an increase by 0.42(0.66) L at six months after surgery, as compared to the pre-operative value. The RCP and the RCA compartments seemed to have contributed to this improvement (Figure 43).

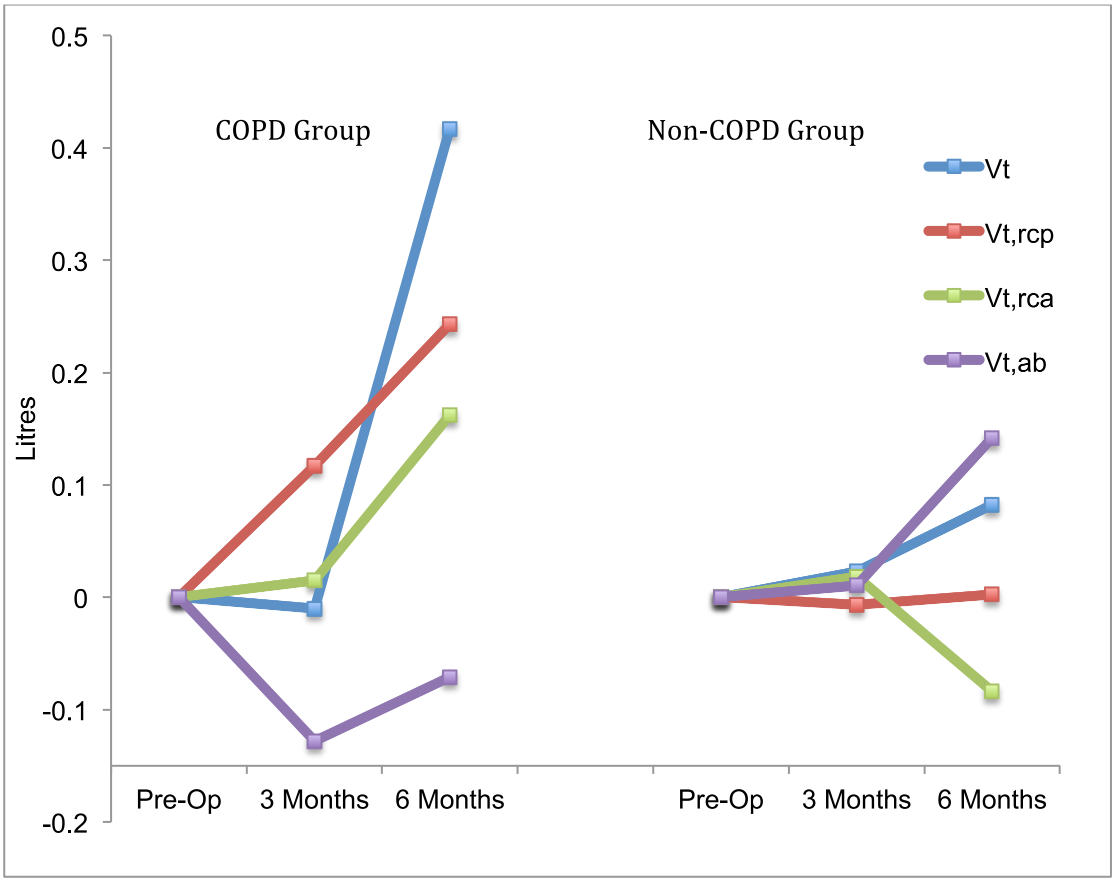

Figure 43: The three- and six-month changes in the volume of the chest wall (Vt) and its three compartments (RCP, RCA, and AB) in the COPD and the non-COPD groups: The changes in the volume (litres) of the chest wall overall and in its three compartments, in the COPD group (n = 5) (left) and the non-COPD group (n = 6) (right), during quiet breathing three and six months after surgery, as compared to pre-operative values. Vt: total chest wall change in volume, Vt,RCP: pulmonary ribcage compartment, Vt,RCA: ribcage abdomen compartment, Vt,AB: abdominal compartment. Pre-op: before surgery. The data are presented as medians.

The overall change in chest volume six months after surgery compared to the pre-operative volume showed a trend of being higher in the COPD group than the non-COPD group, with 0.42(0.66) L and 0.08(0.23) L, respectively.
In the COPD group, there was a trend of an increase in volume change in the RCP of the non-operated side six months after surgery: 0.06(06) L. Similarly, there was a trend of an increase in the volume change of the RCP on the operated side six months after surgery, with 0.07(0.13)L. In contrast, in the non-COPD group, there was a trend of minimal change in the RCP motion on both the operated and the non-operated side three and six months after surgery. In addition, the COPD group had a trend of an improvement in the chest wall motion on both sides of the chest in the RCA compartment six months after surgery. This contrasts with the findings in the non-COPD group during the same time frame (Figure 44).

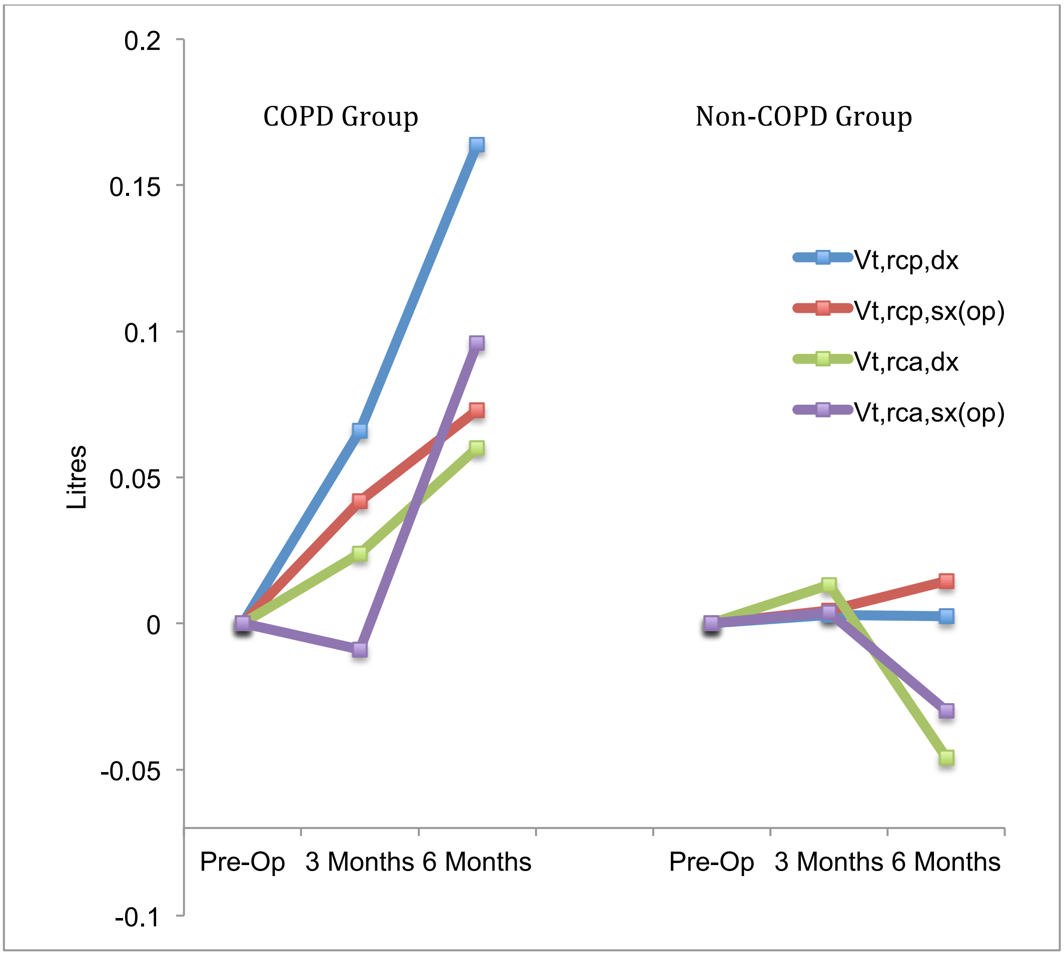

Figure 44: The three- and six-month changes in the volume of the RCP and RCA compartments of the chest wall on the operated and non-operated sides of the chest wall in the COPD and non-COPD groups. The changes in volume on the operated and non-operated sides of Vt,RCP and Vt,RCA of the COPD group and non-COPD group during quiet breathing, three months and six months after surgery, as compared to pre-operative values. Vt,RCP, dx: the non-operated side of the RCP compartment, Vt,RCP, sx (op): operated side of the RCP compartment, Vt,RCA, dx: non-operated side of the RCA compartment, Vt,RCA, sx (op): operated side of the RCA compartment. Pre-op: before surgery. The data are presented as medians.

When considering the difference between surgical approaches, namely thoracotomy (n = 6) or VATS (n = 3), in all lobectomy patients, Table 23 shows their pre-operative characteristics.

Table 23: The pre-operative characteristics of the COPD and non-COPD patients who had a thoracotomy or VATS.

	Thoracotomy Group	VATS Group	P value
Number of Patients	6	3	
Female Gender	0	3	0.003
BMI	27 (8)	25 (19)	0.431
ECOG	1 (1)	1 (1)	0.741
COPD	2	1	0.001
ASA	3 (1)	3 (0)	0.257
NEW MRC	1 (2)	2 (2)	0.587
FEV1%	81 (32)	76 (20)	0.368
FVC%	96 (26)	106 (17)	0.101
FEV1/FVC	0.80 (0.22)	0.75 (0.10)	0.368
AGE	63 (13)	68 (7)	0.517
Lung volume resected (Litres)	0.54 (0.94)	0.63 (0.80)	0.796
Resection extent:			
Lobectomy	6	3	
Anatomical location:			
Upper Lobe	6	3	
Lower Lobe	0	0	
Side:			
Right	2	3	
Left	4	0	
Pathology:			
Squamous cell carcinoma	4	0	
Adenocarcarcinoma	1	2	
Small cell carcinoma	0	1	
Inflammatory	0	0	
Duration of surgery (hours)	3 (1)	3 (2)	0.823
Hospital stay (days)	8 (10)	3 (4)	0.091

The characteristics of pre-operative patients. BMI: body mass index, ECOG: Eastern Cooperative Oncology Group Scale of Performance Status, ASA: American Society of Anaesthesiologists score, MRC: MRC breathlessness scale, FEV1%: Predicted forced expiratory volume in 1 second, FVC%: Predicted forced vital capacity, VATS: Video-assisted thoracoscopic surgery. The data are presented as total numbers or medians and IQR. The Mann-Whitney U test was used to assess the continuous data, and the Chi-Square test was used to assess the categorical data. Any P value < 0.05 was deemed significant.

The results showed there was no trend of marked difference between a thoracotomy and VATS on chest wall motion six months after surgery following a lobectomy (Table 24).

Table 24: The three- and six-month changes in the volume of the chest wall in patients who had a thoracotomy lobectomy and a VATS lobectomy.

	Three Months After Surgery		Six Months After Surgery	
	Thoracotomy Lobectomy	VATS Lobectomy	Thoracotomy Lobectomy	VATS Lobectomy
	(n=6)	(n=3)	(n=6)	(n=3)
Vt,rcp	-0.01(0.16)	0.04(0.21)	0.05(0.23)	-0.02(0.13)
Vt,rca	0.01 (0.14)	-0.03(0.16)	0.02 (0.25)	-0.01(0.15)
Vt,ab	-0.19 (0.62)	0.01(0.05)	0.14(0.23)	0.10(0.27)
Min. vent.	-1.40 (3.15)	-0.11(4.96)	0.85 (4.36)	-0.45(4.10)
Vt,rcp,dx	0.01(0.12)	-0.01(0.07)	0.02(0.17)	-0.01(0.03)
Vt,rcp,sx (op)	-0.01 (0.05)	0.05(0.13)	0.02(0.06)	0.01(0.12)

The change in chest wall motion (in litres) in the thoracotomy lobectomy (n = 6) and VATS lobectomy (n = 3) groups after lung resection, as compared to the pre-operative value. Vt: tidal volume, RCP: the pulmonary ribcage compartment, RCA: the ribcage abdomen compartment, AB: the abdomen compartment, dx: non-operated side, sx: operated side, cw: total chest wall, Min Vent: minute ventilation. The data are presented as median and IQR.

18.4 DISCUSSION

In COPD patients, a lobectomy for early lung cancer improves lung function (Vaughan, Oey, Nakas, Martin-Ucar, Edwards, & Waller, 2007). Yet, the mechanism of this improvement is unclear. In this paper, it was hypothesised that lung resection improves the motion of the RCP compartment and the RCA compartment. These results showed that there was a trend of a higher degree of increase in overall chest wall motion in the COPD group after surgery, as compared to the non-COPD group. This trend of improvement was in the RCP and RCA compartments on both sides of the chest. Interestingly, COPD patients who had a unilateral lung volume reduction either by open surgery or bronchoscopic lobectomy with EBVs had trends of improvement in the synchrony of the three compartments on the treated side. Changes in volumes in a procedure primarily designed to reduce hyperinflation were not described. Thus, the present findings of the trend of changes on the contralateral side of treatment are novel, but fit in with other studies. These results might suggest that lung resection for cancer in COPD patients might have a similar effect as LVRS in improving the contractility of the respiratory muscles (Teschler, et al., 1996) (Martinez, et al., 1997). Improvements in tidal volume secondary to chest wall recoil, has been put forward as a mechanism of functional improvements after LVRS by Fessler et al. (Fressler, Scharf, Ingenito, McKenna, & Sharafkhaneh, 2008). The results in this thesis also showed that, after surgery, the RCA compartment (which reflects the function of the diaphragm) had a trend of an improvement in its motion after surgery. These results were supported by the work of Cassart et al. In 2001, through a CT scan reconstruction of the diaphragm, they showed that in some patients, LVRS improves the zone of opposition of the diaphragm against the chest wall, which may indicate an improvement in the mechanics of the diaphragm movement (Cassart, et al., 2001). This increase in the area of opposition after surgery resulted in a lower frequency of motor unit firing of the diaphragm (Gorman, McKenzie, Butler, Tolman, & Gandevia, 2005), indicating a state of relaxation and dooming of the diaphragm. These are ideal starting points for the diaphragm’s contraction and descent, resulting in more efficient movement.

Interestingly, despite lung resections in the non-COPD group, there was no trend of marked differences in RCP compartment motion six months after surgery. While the numbers were small, this result is valid because trends of difference in COPD patients were able to be detected. The implication is that if there were any immediate trends of changes in chest wall volumes, these were reversed within three months after surgery. This ties in well with studies that showed that improvement in lung function after surgery happens mainly in the first six months (Chapter 3). Much of the loss in early lung function occurs due to pain and mechanical disruption of the chest.

An alternative explanation of the differences between the non-COPD and COPD groups in terms of chest wall motion is that there were more thoracotomies in the non-COPD group compared to the COPD group (66% versus 40%, respectively). A larger study with an equal number of thoracotomies in each group is needed to verify this.

In addition, it was thought that VATS is a minimally invasive procedure and has a beneficial, less traumatic effect on the mechanics of breathing than a thoracotomy (Bernard, 2006). In this study, muscle dysfunction, as assessed by intra-abdominal pressure, was worse after a thoracotomy than VATS days after surgery. However, this study did not measure the chest wall mechanics directly. In fact, the study relied on global pressure generated by the diaphragm and both sides of the chest. In addition, it did not assess breathing in the most common breathing pattern, which is quiet breathing, but rather relied on forced expiratory and inspiratory manoeuvres that are influenced by motivation and the patient's co-operation.

There may have been early differences in chest wall motion that this study was not able to measure. This is because there are no robust comparisons of OEP measures in acutely unwell patients who are immobile with drains as compared to those in an outpatient setting. Three and six months after surgery, there were no trends of differences between VATS and thoracotomy, suggesting that both procedures might affect the chest wall motion equally.

The numbers in this case series were small and require validation in a larger study.

18.5 Conclusion

This case series contained the first published data to describe the effects of lung cancer resection on patients with COPD and showed that it has a trend of LVRS like physiological benefits, which tend to arise in the RCP and RCA compartments, on both the operative and the non-operated sides. This finding was not apparent in patients who did not have COPD. It was also suggested that there were minimal differences between VATS and thoracotomy approaches after surgery in terms of chest wall motion six months after surgery.

18.6 Limitations

The results were gathered only during quiet breathing. Further study is needed to evaluate the effect of the procedures during exercise.

19 Conclusions. limitations and recommendations

This thesis described how chest wall motion analysis technology could be useful in thoracic surgery to answer a number of clinical and physiological questions. This thesis attempted to use chest wall motion analysis technology either as a diagnostic tool or for the evaluation of an intervention outcome. Its use as a diagnostic tool was divided into two categories: 1) diagnosis before surgery and 2) diagnosis after surgery. In evaluating an intervention outcome, its use was divided after a number of interventions:

1. Cosmetic Surgery:

   Chapter 5: The Effect of Pectus Carinatum (Pigeon Chest) Repair on Chest Wall Mechanics

2. Prognostic Surgery:

   a) Chapter 4: The Effect of Chest Wall Reconstruction on Chest Wall Mechanics

   b) Chapter 10: Late Changes in Chest Wall Mechanics Post Lung Resection: The Effect of Lung Cancer Resection In COPD patients

3. Palliative Surgery:

   a) Chapter 6: The Effect of Lung Volume Reduction Surgery on Chest Wall Mechanics

   b) Chapter 3: The Effect of Diaphragmatic Plication (Fixation) on Chest Wall Mechanics

4. Post-operative Intervention:

   Chapter 8: The Effect of Thoracic Nerve Blocks on Chest Wall Mechanics

Before surgery, chest wall motion analysis technology was attempted to be used as a diagnostic tool to diagnose the nature of pleural effusion based on its effect on chest wall mechanics. Diagnosis of mesothelioma is challenging as patients present with non-specific symptoms. A cytological examination is positive for malignant cells in only one third of patients with mesothelioma (Jett & Aubry, 2008), and even after this, a definitive diagnosis cannot be made. Diagnosing mesothelioma using a CT scan is challenging. The sensitivity of the CT scan for radiological features of mesothelioma ranges from 36% to 56% (Leung, Muller, & Miller, 1990). Despite the positive predictive values of all of the above features, their absence does not confidently rule out the diagnosis of mesothelioma. In addition, a CT-guided needle biopsy for mesothelioma diagnosis has a sensitivity of only 76% and is associated with 5% risk of pneumothorax (Benamore, Scott, Richards, & Entwisle, 2006). In addition, spirometry is not useful in diagnosing the disease (Plathow, et al., 2006). Diagnosing mesothelioma requires an invasive procedure via medical thoracoscopy or VATS, each with their associated morbidity. Even then, in patients who have a pathological sample, the results can be false negatives (Boutin & Rey, 1993). This case series examined the use of a non-invasive technology to identify patients with mesothelioma by detecting changes in chest wall motion that might be unique to the disease. The use of OEP was blindly investigated in assessing chest wall motion in three groups of patients (a unilateral empyema group, unilateral mesothelioma group, and a control group with no pleural pathology). The pathological diagnosis was not known at the time of the captures. The results showed that the chest wall motion on the diseased side of the mesothelioma group showed a trend of marked reduction in chest wall motion (≤ 32%), compared to the trend in the empyema and the control groups (> 32%). The non-diseased side of the chest in the mesothelioma group had a trend of increased motion, which seemed to be a compensatory mechanism for the reduction of motion on the operated side. This phenomenon was observed in different diseases studied in this thesis. The compensation is likely related to the fact that a contralateral normal lung finds more space to expand as the diseased/operated lung sinks or become restricted and as both lungs share the same intra-thoracic cavity. This phenomenon did not occur in the other two groups. In this study, the radiological diagnosis—done by a specialised thoracic radiologist—was accurate in 30% of the patients. The reason for this difference in trends in the reduction of chest wall motion in the mesothelioma group and empyema group is likely due to the fact that mesothelioma is an aggressive disease that leads to a papillary sheet proliferation and aggressive fibroblastic proliferation. This can explain the trend of the higher degree of the resection of chest wall motion in the mesothelioma group, a feature that is not found in inflammatory conditions such as empyema. These trends of chest wall motion changes, which are exclusive to mesothelioma, might have the potential to help detect this aggressive disease in the future.

One limitation of the study was that the trend in radiological distribution of the disease was different between the groups (widespread radiological distribution of the disease in two patients [50%] in the mesothelioma group and in two patients [33%] in the empyema group). Thus, the difference in chest wall motion between the groups could be explained by the difference in the degree of the radiological distribution. Another limitation of this study was the small sample size.

Therefore, future work should focus on evaluating a large number of patients with mesothelioma who had similar radiological distribution to the empyema group. In addition, these results only covered quiet breathing changes, and further work is needed to evaluate chest wall mechanics during exercise. Future work could also focus on examining the effects of other malignant pleural disease on chest wall motion. In addition, the effects of de-bulking surgery on chest wall motion as well as the reduction of symptoms and quality of life could be examined in further studies. The relationship between the extent of the disease and the degree of chest wall impairment could also be assessed in a future larger study.

This thesis attempted to use this technology as a diagnostic tool after surgery for the diagnosis and detection of PPCs. PPCs are responsible for 85% of post-thoracic surgery mortality (Stephan, Boucheseiche, & Hollande, 2000). Identifying patients with PPCs early is challenging, and this is partly due to the delayed radiological evidence of the condition (Hagaman, Rouan, Shipley, & Panos, 2009). In addition, CXR and CT scans expose patients to ionising radiation. Furthermore, spirometrical measurement is difficult to perform immediately after a traumatic thoracic surgery, and the current scoring system still lacks accuracy (Agostini P. B., 2011). This thesis aimed to use chest wall motion analysis technology immediately after surgery on patients with thoracic surgery in order to detect trends in chest wall motion that might be related to PPCs. Chest wall motion analysis was done blindly in all patients who underwent thoracic surgery. The diagnosis of PPCs was done clinically by the supervising surgeon. According to this, 3 of 11 patients studied developed PPCs during their post-operative hospital stay, but none of them were clinically diagnosed with PPCs on Day 1. The patients were then divided retrospectively into a PPC group (n = 3) and control group (n = 8). A PPC score was obtained as well and was not diagnostic of PPCs in all patients on Day 1. However, the chest wall motion results showed a higher degree of reduction in overall chest wall motion in the PPC group than in controls on Day 1 after surgery. There was also a trend of a higher degree of dys-synchronisation between the sides of the chest in the PPC group than in the control group on Day 1 after surgery. CXR showed evidence of PPCs in two of three patients on Day 1. This showed that trends in chest wall motion can be related to the development of PPCs, which were detected before the clinical diagnosis in all three patients and before radiological diagnosis in one of three patients. This reduction in chest wall motion could be an early sign of reduced lung compliance that occurs with chest infection, and the loss of synchrony could be an early sign of respiratory distress. This loss of synchrony has been observed before in some patients with COPD (Zaid, 2015).

However, another possible alternative explanation of the study could be related to the disproportionate number of thoracotomies and the number of smokers in each group. Thirteen percent of patients in the control group had a thoracotomy, compared to 66% of patients in the PPC group. In addition, 37%

of patients in the control group were ex-smokers, compared to 66% in the PPC group. The higher number of thoracotomies in the PPC group could have led to these differences in chest wall motion. Similarly, the higher percentage of ex-smokers in the PPC group could have affected the quality of the lung parenchyma, which might have affected lung compliance and, therefore, chest wall motion. This might explain the difference between the two groups. Although CXR could detect PPCs in two of three patients, SLP was able to detect all three. In addition, CXR exposes patients to ionising radiation that SLP does not because SLP uses direct light.

Another limitation of the study was that it only involved three patients because it was impossible to predict who would have PPCs after surgery. Therefore, 11 patients had to get captured in order to have three with PPCs.

Future studies should focus on increasing the number of patients to validate these results, making sure these groups are homogenous for patients' characteristics. Future studies should also examine these patients during exercise using OEP, which might result in more profound chest wall changes that can help further define these PPC-related changes in chest wall motion.

In the evaluation of the procedure outcome in the cosmetic surgery category, this study evaluated the pigeon chest/PC deformity. Patients with PC present themselves for surgery for mainly cosmetic reasons. Although there has been evidence of improvement in exercise capacity after surgical correction (Oncel, Tuscan, Akyol, Dereli, & Sunam, 2013), the mechanism of this improvement is still unknown. In this thesis, this technology was used to assess chest wall mechanics in pigeon deformity before and after surgical correction. The results demonstrated the presence of a trend of an increase in EEV during exercise as compared to quiet breathing. This phenomenon occurred in the overall chest wall motion but, more specifically, in the RCP compartment, demonstrating a trend of dynamic hyperinflation or air-trapping in three patients with this deformity. Furthermore, these data were the first data to show that the corrective cosmetic repair for this deformity resulted in a trend of reversal of this increase in the EEV, or a trend of reversal in dynamic hyperinflation, which seemed to mimic what is observed in normal individuals (Illi, Hostettler, Aliverti, & Spengler, 2013). This seemed to be related to a trend of improvement in the exercise time to reach 80% of maximum heart rate and a trend of improvement in the spirometry measurement.

The mal-position of the sternum in a PC patient can prevent maximum contractility of the respiratory muscles (Koumbourlis, 2015). This is supported by the fact that PC patients have decreased expiratory pressure when compared to controls (Koumbourlis, 2015) (Kubiak, Habelt, Hammer, Hacker, Mayr J , & Bielek, 2007) (La Mauro, et al., 2012). The results in this thesis showed that correcting the position of the sternum resulted in a trend of improved chest wall motion (reversal of dynamic hyperinflation). This could likely be a result of improved respiratory muscle contractility, as muscles are restored to a better anatomical position. This study excluded training bias by asking the patients not to perform any exercise for six months after surgery.

However, these results were only based on three patients with PC. Therefore, generalisation was not possible. Another limitation of the study was that exercise time was measured using heart rate. It is correlated with cardio pulmonary exercise testing (Kline , 1989) (Dolgener, 1994) but is not as robust, as it can be influenced by a patient's anxiety while performing the test. Anxiety is an emotional status that could not be excluded in this study while the tests were being performed in this young cohort of patients. Furthermore, although these results showed some benefits of surgery in the patients, there was not enough evidence in the results—based on a small number of patients—for the benefits to outweigh the potential risk of surgery. In addition, it is still unclear whether dynamic hyperinflation occurs in all PC patients.

This paper recommends that future studies of PC include a large number of patients with diverse demographic characteristics in order to evaluate whether dynamic hyperinflation occurs in all PC patients and whether all patient with PC benefit physiologically from this repair. This paper also recommends conventional cardiopulmonary testing in combination with chest wall motion technology to be used to investigate PC patients; this is required to better quantify exercise capacity benefits.

In the evaluation of the procedure outcome in the prognostic surgery category, it was known that chest wall tumours can cause a range of symptoms such as breathlessness (Gross, Younes, & Haddad, 2005). However, little is known about whether this is the result of chest wall dysfunction. Furthermore, little is known about the effect of chest wall reconstruction on chest wall mechanics. This case report attempted to assess chest wall mechanics before and after the chest wall resection of an extra thoracic chest wall tumour and reconstruction of the chest wall. This case report showed a trend of a negative effect of the chest wall tumour on global chest wall mechanics during quiet breathing and exercise; it showed that the tumour resulted in a trend of reduction in the volume of the abdominal ribcage and abdomen compartments on both sides of the chest and that surgery resulted in a trend of reversal of this abnormality in this patient, but only at rest. This showed that although a tumour is unilateral, its effect on the chest wall motion is bilateral. This is likely because the chest works as a unit and is interconnected by the sternum, and any reduction of motion on one side can be transmitted through the sternum to other side. These results showed a trend of asynchrony between the RCA compartments on both sides of the chest before surgery. After surgery, there was a trend of re-synchronisation of these compartments. The mechanism of this was unclear, but it could be due to the mechanical displacement of the tumour in that part of chest, leading to one side of the chest lagging behind the opposite part in the respiratory cycle. This reversed after the removal of the tumour. During exercise, the results showed a trend of reduction in the RCP motion on the operated side. This mainly resulted from a trend of an increase in the EEV and a trend of a reduction in the ERV on the operated side, a finding that was not replicated on the non-operated side. This might suggest an expiratory dysfunction during exercise after surgery. This was also supported by a reduction in FEV1. This paper speculated that this could have occurred as a result of the placement of a prosthesis that might have restricted the expiratory motion of the chest wall on the operated side.

However, a concrete conclusion of the effects of a chest wall tumour and its reconstruction on chest wall mechanics could not be made based on one patient. All that could be reported from these results were trends of change in chest wall motion in one patient with a specific type of tumour, who underwent a specific type of chest wall reconstruction. As a patient's demographic does affect chest wall motion—as previously reported (Barcelar Jde, et al., 2013)—generalisation of the results was not possible. Similarly, the chest tumour that was examined was of a specific size in a specific location of the chest with a specific pathology. Therefore, different tumours with different characteristics might affect the chest wall motion differently. To conclude, these results were based on a specific condition, patient, and tumour characteristics, so generalisation was not possible.

Future studies should involve patients with a variety of tumour pathologies and characteristics and undergoing reconstruction using a variety of prosthetic materials.

Second, in the same category, the study was used to assess the effect of lung cancer resection on COPD patients. The state of hyperinflation in COPD patient can result in respiratory muscle dysfunction (Fressler, Scharf, Ingenito, McKenna, & Sharafkhaneh, 2008). There is also evidence that some patients with severe and late-stage COPD have a flattened diaphragm with reduced contractility (Braun, Arora, & Rochester , 1982). LVRS has improved survival and life quality in selected patients with COPD (NETT group , 2003). This has been done by improving the mechanics of breathing in these cohorts of patients, namely by the reversal of dynamic hyperinflation (Geddes, Davies, & Koyama, 2000) (Fishman, Martinez, & Naunheim, 2003) (Clark, Zoumot, &

Bamsey, 2014), which restores respiratory muscle and lung recoil (Fressler, Scharf, Ingenito, McKenna, & Sharafkhaneh, 2008). Likewise, there is evidence of improved lung function after lung resection for cancer in COPD patients (Cassart & et, 2001) (Vaughan, Oey, Nakas, Martin-Ucar, Edwards, & Waller, 2007). OEP has been used extensively to understand the ventilatory mechanics of COPD patients (Aliverti e. a., 2005). The effect of lung resection for lung cancer in COPD patients on chest wall mechanics had never been explored before. This study aimed to describe the trends of changes in ventilatory mechanics after lung cancer resection in COPD patients compared to a control group of non-COPD patients. These results showed that there was a higher trend of increase in overall chest wall motion in the COPD group after surgery than in the non-COPD group. This trend of increased overall motion was mainly due to a trend of an increase in motion in the RCP and RCA compartments on both sides of the chest. It has been reported that after LVRS, there is trend of improvement in synchrony in all three compartments on both sides of the chest (Zoumot, et al., 2015). In these reports, the changes in volume are not described. The present study's results showing a trend of improvement on the contralateral side fit well with this report. The present data might suggest that lung cancer resection for COPD patients might improve contractility of the respiratory muscles, similar to what has been observed after LVRS (Teschler & et, 1996) (Martinez & et, 1997). It has been reported that the reason for the improvement in tidal volume following LVRS is due to improvement in chest wall recoil (Fressler, Scharf, Ingenito, McKenna, & Sharafkhaneh, 2008). In addition, the present results showed that the department that reflected the function of the diaphragm (the RCA) had a trend of improvement post-operatively. This fits with previous reports. Cassart et al. reported that, via a CT-constructed image of the diaphragm, LVRS improved the zone of opposition of the diaphragm against the chest wall, which suggested improved function of the diaphragm (Cassart & et, 2001). Likewise, Gormen et al. reported that this increase in the area of opposition resulted in the motor unit of the diaphragm firing less frequently, indicating a state of relaxation and dooming of the diaphragm (Gorman, McKenzie, Butler, Tolman, & Gandevia, 2005). This position is ideal as a starting point of diaphragm motion and contraction, resulting in more efficient motion. In the non-COPD group, there were no marked trends of difference in the RCP compartment six months post-operatively. The fact that the immediate changes in chest wall motion are reserved six months after surgery, fits well with other studies that showed improvement in chest wall motion after surgery happen in the first six months (Chapter 3). The early loss of chest wall function is mainly due to pain and the mechanical disruption to the chest wall.

However, the unequal number of thoracotomies in the COPD and non-COPD groups—40% and 66%, respectively—can explain this difference in chest wall mechanics. A future larger study with more homogenous groups is needed to verify the results.

It has been reported that VATS is less traumatic on the chest wall compared to thoracotomy (Bernard, 2006). However, this report was based on differences in intra-abdominal pressure and did not directly measure chest wall motion, nor did it measure the most common state of breathing, which is quiet breathing. Instead, it relied on forced expiratory and inspiratory manoeuvres that could be influenced by the patient's cooperation and motivation. The results in this thesis showed that six months after surgery there was no trend of difference in chest wall motion between VATS and thoracotomy, suggesting that the recovery from both procedures was the same as had been previously reported (Kuritzky, Ryder, & Ng, 2013).

Future studies should focus on studying these trends across a large number of patients to validate these results and to evaluate whether this changes during exercise.

In the evaluation of the procedure outcome in the palliative surgery category, this study used SLP to evaluate the outcomes of EBV for LVRS. It was known that LVRS using EBV can improve clinic outcomes in selected patients (Sciurba, 2010) (Herth, 2012). However, the response to this intervention is inconsistent, and the VENT trial (EURO-VENT and US-VENT) showed that the benefits are more pronounced in patients who achieve lung lobe atelectasis. Currently atelectasis is evaluated by CXR and CT scans, but radiological features of atelectasis may take weeks to develop, although the valves start to work immediately (Hopkinson, 2011). Furthermore, the VENT trial identified a cohort of responders with sub-radiological atelectasis. Identifying non-responders early is of profound benefit as it allows for the removal or repositioning of valves in a timely manner. Leaving un-working EBVs is associated with a risk of lung infection in patients who have poor pulmonary reserves (Sciurba, 2010). In addition, EBVs are prone to migration (Jenkins, Vaughan, Place, & Kornaszewska, 2011), but removing un-working EBVs early might prevent this complication. This is why a method to identify non-responders in a timely manner is needed. In this study, this chest wall technology was used to assess chest wall motion before and after EBV insertion of LVRS. This study aimed to identify trends in chest wall motion that could be related to the success or failure of EBV insertion. The results in one patient with a giant bulla—who had a successful insertion of EBVs for LVRS, as evident on a CT scan three months after surgery—showed a trend of improvement in his breathlessness score and spirometry. He also showed minor improvement in the six-minute walk test, but that was not clinically significant (Wise & Brown, 2005). This trend of improvement in the breathlessness score and spirometry seemed to be related to a trend in reduction of chest wall motion on the operated side immediately after surgery, which has progressed in the following days. The second patient had an unsuccessful procedure due to a paravalvular leak proved by his CT scan three months after surgery. His breathlessness score showed a trend of improvement immediately after surgery, but was lost on Day 2 after surgery. This seemed to be related to an initial trend of reduction in chest wall motion on the operated side immediately after surgery, which was similarly lost on Day 2 after surgery. In the third patient, who had an unsuccessful procedure as evidenced by his CT scan findings three months after surgery, the results showed no trend of improvement in either his breathlessness score nor spirometry after surgery. This seemed be related to a trend of no reduction on the operated side of the chest after surgery.

A concrete conclusion could not be drawn based on one patient, but this trend of reduction of chest wall motion in the first patient could indicate a degree of sub-radiological atelectasis not detected on routine CXR. These responders with sub-radiological atelectasis were identified before in the VENT trial (Sciurba, 2010) (Herth, 2012). In the second patient, the initial trend of reduction in chest wall motion could have been due to sub-radiological atelectasis on the first day. This seemed to have been lost on Day 2, as evident in the loss of the trend of marked reduction in the chest wall on the side of surgery once the valve migrated, as evident from the second operation. In patient three, who had an unsuccessful procedure and no atelectasis, this was reflected in no trend of change in chest wall motion. These findings might indicate that the trends of changes in chest wall motion might be related to the success or failure of the procedure.

The Borg breathlessness score could show a trend of improvement in the patient who had a successful procedure and vice versa. Although this seemed to be a good measure to assess the procedure outcome, its major limitation was that breathlessness is subjective and relies on the sense of breathlessness, which differs between individuals. Similarly, it can be affected by a patient's feelings (such as anxiety, for example). On the other hand, chest wall motion is an objective measurement.

One limitation of the study was that Patient 1 did not fit the criteria for LVRS, but did fit the criteria for bullectomy, and the procedure was done after the patient approved it and after the procedure was discussed in the regional MDT. This was the only patient of the three whose lung chest motion progressively showed a trend of reduction after surgery. This could be due to the fact that he had a better lung reserve (severe COPD and minor emphysema) than the other two patients with very severe COPD and severe emphysema.

A limitation for recruitment in this study was the number procedures performed each year. EBV for LVRS is a rare procedure in the regional thoracic centre this study was conducted in and sees approximately eight cases annually. Furthermore, the procedure is not without complication; in this study, three other recruits for the study were withdrawn as they developed pneumothorax after surgery. Measurements could not be done during exercise, as the SLP machine requires the patients to fix their backs against a hard surface (a chair or bed). In addition, the SLP capture could only be done in a relatively dark room as light interferes with the quality of the capture. Furthermore, abdominal and chest tubes and stomas, as well as skin folds, interfere with the quality of capture.

Future studies should involve a large number of patients with varying degrees of severity of COPD, divided into homogenous groups. Future studies should also be conducted on patients undergoing exercise (using OEP), as chest wall changes could be more pronounced.

This study also used the OEP technology to assess the physiological impact of diaphragmatic plication of unilateral diaphragm paralysis on chest wall mechanics. This case report contains the first published human data showing trends of improvement in chest wall motion, both on operated and contra-lateral sides following diaphragmatic plication for unilateral paralysis. Currently, it is only known that plication for unilateral paralysis improves spirometry and dyspnoea scores (Freeman, Wozniak, & Fitzgerald, 2006) (Celik, Celik, Aydemir, Tunckaya, Okay, & Doqusoy, 2010). In an animal model—using invasive measures—plication of unilateral diaphragm paralysis improved contractility on both sides of the diaphragm (Takeda, et al., 1991), but the mechanism of this improvement in humans was uncertain. Using non-invasive technology, the results of the present study are the first results in humans to shed light on the possible mechanism of this improvement; this case report showed a trend of improvement on both sides of the chest mainly in the RCA compartment, which reflects the diaphragm function. This study also reported a trend of improvement in the synchronisation of different compartments after plication on both sides of chest. This result could be as a result of the motion of the non-paralysed diaphragm acting more efficiently by contracting against a fixed point: the fixed hemi-diaphragm. The limitations of these results were that they only involved one patient with a specific type of diaphragm plication. Therefore, it is still uncertain that this is mechanism of improvement can apply to all types of plication or to all patients with a specific type of plication, as this single case report does not take into consideration the effects of variation in patient demographics on chest wall motion as demonstrated in the literature (Barcelar Jde, et al., 2013).

This paper recommends that a future study investigating diaphragm plication using this technology should involve a large number of patients and reflect a wide range of demographics. This future study should also evaluate the effects of different types of diaphragm plication methods with longer follow-up times.

In the evaluation of the procedure outcome of the post-operative intervention category, chest wall motion technology was used to assess the effect of VATS and thoracotomy on chest wall motion. It was known that VATS has less morbidity than thoracotomy (Maeda, 1988) (Bernard, 2006) (Nomori, Horio, Fuyuno, Kobayashi, & Yashima, 1996). It was speculated that this is due to the fact that VATS causes less damage to the chest wall. Until the era of chest wall motion technology, there was not an easy way to measure this damage. Here, chest wall motion technology was used to assess the effect of VATS and thoracotomy and different types of resections on chest wall motion, as well as the effect of different types of regional analgesia and the amount of lung resected on chest wall motion. These results showed that SLP was useful in detecting a trend of reduction on the operated side and a compensatory trend of increase in motion on the non-operated side. It also showed that the trend of reduction in chest wall motion was higher in the VATS patients compared to the thoracotomy patients. This is likely due to the fact that thoracotomy disturbs two intercostal nerves, and VATS disturbs four. In thoracotomy, the intercostal nerves that are disturbed are the one that runs in the area of the large intercostal incision and the one that is disturbed at the site of chest drain insertion. In VATS, three intercostal nerves are disrupted at the three areas where the VATS ports are inserted; another intercostal nerve is disrupted at the area of chest wall insertion. It is likely that the number of compressed intercostal nerves could be related to a greater reduction in chest wall motion in VATS than in thoracotomy. These results showed there was no trend of marked difference in chest wall motion when the amount of lung resected and the type of analgesia used were considered. The knowledge is useful, as there is reluctance among anaesthetists to give epidural anaesthesia to patients with traumatic broken ribs, as they fear that this will suppress their respiratory muscles and chest wall motion. These results showed that there is no trend of difference in chest wall motion between patients who had epidural blockage, PVB, or intravenous analgesia (controls), suggesting that it might be potentially safe for epidural analgesia to be used in patients with traumatic broken ribs.

One limitation of this study was that due to the small number patients able to be recruited, dividing these patients into further subgroups made this number even smaller. Concrete conclusions could not be drawn from these small numbers, but rather they described a trend of change that needs to be clarified and validated in a larger study in the future, with groups that have similar homogeneity.

These results were based on the specific doses of TEB, PVB, and IV analgesia that are used in the local hospital, so these results are dose-specific and cannot be generalised. Future work should evaluate different strengths of TEB, PVB, or IV analgesia. Furthermore, all the captures were done during quiet breathing, and this paper recommends that a future attempt should be made to measure these changes in chest wall motion during exercise using OEP.

Overall, one of the main limitations of these studies was the small sample sizes, which were due to recruitment difficulties. This was due to the fact that some procedures are rarely performed in the centre in which this study was conducted. For example, the centre conducts one or two diaphragmatic plications each year, around six chest wall reconstructions a year, around eight EDVs for LVRS each year, and fewer than four PC repairs each year. Although the centre does around 10 VATS lobectomies and 10 thoracotomies each month, the recruitment drop rate is high: around three of four patients are recruited. This is mainly due to the high-risk procedure that is performed in this mostly elderly cohort of patients that can lead to serious complications. This drop rate is also due to the long-term follow-up that can last six months. In addition the clinical information provided in this study is insufficient to draw any firm conclusions. To tackle these difficulties in future studies, this paper recommends multi-centre collaboration to increase the sample sizes, to reduce the heterogeneity between the groups and to increase the clinical data base.

OEP: There are advantages and limitations to using OEP. One advantage of OEP is that it can be performed on unconscious patients and patients who are not able to tightly seal their mouths on a mouthpiece. Furthermore, OEP can measure respiratory mechanics and provide information on these mechanics in patients with obesity, diaphragm paralysis, chest wall deformities, and paralysis and during exercise.

OEP has a number of limitations. First, the marker displacement is time-consuming and requires training to correctly identify the anatomical landmarks. Marker placement errors are common, as misplacing the marker even by a few millimetres makes it unreadable by the operating system. Operating the system itself needs extensive training to master the capturing process. A number of artefacts can be produced during a capture, which have to be identified and removed, but this is a time-consuming and tedious process. In addition, the OEP purchase and set-up cost is high. The test requires the patient to be bare-chested, which necessitates a female technician to perform or be present at the time of capture. This increases the number of staff that are needed to carry out the captures.

Future designs of the OEP machine should focus on improving the tedious process of OEP capture by creating an auto-tracking software that automatically detects the dots, removes the artefacts, and creates a 3D image. Similarly, a future design should aim to create an infrared reflective T-shirt to replace the current infrared reflective dots; this would significantly decrease the capture time. (It takes around 30 minutes to prepare, apply, and remove the dots, but this can be reduced to two minutes if the reflective T-shirt is created, as it could be worn and taken off by a patient without help.) The current manual calibration of OEP is time-consuming; an upgrade to an automatic calibration module is needed, similar to the design adopted for SLP.

Finally, an attempt should be made to create a portable OEP that can be taken to the bedside.

SLP: The advantages of SLP are that it is a portable device that can brought to a recovery room or high-dependency ward and can be used on unconscious patients. Another advantage of SLP is that it requires minimal training for use. The major limitation of SLP is that the machine is very light-sensitive and needs a dark room for its capture. In addition, the current SLP design has a short rigid handle that makes manoeuvrability around the bedside tedious. It is also supplied by electricity via an electric cable, which reduces its manoeuvrability. This paper recommends a future design that has a longer flexible handle with a built-in battery to improve manoeuvrability.

20 APPENDIX 1

Papers and Abstracts published related to this thesis

20.1 Publications

2015:	Elshafie, G., et al., The use of structured light plethysmography in assessing the outcome of Lung reduction, J Cardiothoracic S, Sep 2015 (accepted for publication)
2015:	Elshafie, G., et al., Cardiopulmonary benefits of a cosmetic chest wall surgery?, J Cardiothoracic S, Sep 2015 (accepted for publication)
2015:	Elshafie, G., et , al. Chest wall mechanics before and after diaphragm plication. J Cardiothoracic S. Sep 2015. DOI: 10.1186/s13019-015-0317-7
2015	Elshafie, G., Kumar, P., Naidu, B., Surgical correction of pectus carinatum reverses dynamic hyperinflation and improves exercise capacity? Am J Respir Crit Care Med 2015, May 191:A4253
2015	Elshafie, G., Motamedi, S., Wilson, R., Naidu, B., Novel Chest Wall Motion Analysis Technology Can Detect The Success/Failure Of Lung Volume Reduction Surgery Via Endobronchial Valves

(EBV) Insertion In The Recovery Room. Am J Respir Crit Care Med 2015, May191: A1153

2015 Elshafie, G., Aliverti, A., Pippa, L., Kumar, P., Kalkat, M., Naidu, B., Surgery corrects asynchrony of ribcage secondary to extra-thoracic tumor but leads to expiratory dysfunction during exercise. Am J Respir Crit Care Med 2015, May 191:A5017

2015 Elshafie, G., et al. The improvement of exercise capacity after surgical correction of pectus carinatum is associated with reversal of dynamic hyperinflation. Interact CardioVas Thorac Surg, 2015, 21(suppl 1):S9

2014: Elshafie, G., et al. The effect of diaphragmatic plication on chest wall dynamics
Interact CardioVasc Thorac Surg 2014,19 (suppl 1): S47

2014: Elshafie, G., De Boer, W., Steyn, R., Bishay, E., et al. Novel thoraco-abdominal motion analysis technology can measure early respiratory changes following lung resection. ERJ 2012 Sept 2014, 44(Suppl 58):4260

2016	Chapter 6: The Effect of Lung Volume Reduction Surgery on Chest Wall Mechanics (submitted)
2016	Chapter 7: The Effect of Benign and Malignant Pleural Disease on Chest wall Mechanics (submitted)
2016	Chapter 8: Early Chest Mechanics Changes Post Lung Resection: The Effect of Thoracic Nerve Blocks (submitted)
2016	Chapter 9: Early Chest Mechanics Changes Post Lung Resection: The Effect of Post-operative Pulmonary Complications on Chest Wall Mechanics (submitted)
2016	Chapter 10: Late Changes in Chest Wall Mechanics Post Lung Resection: The Effect of Lung Cancer Resection In COPD patients (submitted)

20.2 Presentations

2015	The Effect of Benign and Malignant Pleural Disease on Chest wall Mechanics **Mesothelioma interest group meeting, Birmingham, UK**
2015	The use of structured light plethysmography in assessing the outcome of Lung reduction. **The 25th Annual Congress of the World Society of Cardiothoracic Surgeons, Edinburgh, UK.**
2015	Cardiopulmonary benefits of a cosmetic chest wall surgery?. **The 25th Annual Congress of the World Society of Cardiothoracic Surgeons, Edinburgh, UK.**
2015	Surgical correction of pectus carinatum reverses dynamic hyperinflation and improves exercise capacity?. **The American Thoracic Society International Conference 2015, Denver, Colorado, USA.**

2015	Early detection of success of endobronchial valve (EBV) lung volume reduction (LVR) using Chest wall motion analysis. **The American Thoracic Society International Conference 2015, Denver, Colorado, USA.**
2015	Surgery corrects asynchrony of ribcage secondary to extra-thoracic tumor but leads to expiratory dysfunction during exercise. **The American Thoracic Society International Conference 2015, Denver, Colorado, USA.**
2015	The improvement of exercise capacity after surgical correction of pectus carinatum is associated with reversal of dynamic hyperinflation. **The 23rd European Conference on General Thoracic Surgery, Lisbon, Portugal.**
2015	Surgical correction of pectus carinatum reverses dynamic hyperinflation and improves exercise capacity?. **The Society of Cardiothoracic Surgeons of Great Britain and Ireland annual meeting 2015, Manchester, UK**

2015	Early detection of success of endobronchial valve (EBV) lung volume reduction (LVR) using Chest wall motion analysis. **The Society of Cardiothoracic Surgeons of Great Britain and Ireland annual meeting 2015, Manchester, UK**
2015	Surgery corrects asynchrony of ribcage secondary to extra-thoracic tumor but leads to expiratory dysfunction during exercise. **The Society of Cardiothoracic Surgeons of Great Britain and Ireland annual meeting 2015, Manchester, UK**
2015	Novel thoraco-abdominal analysis technology can measure early respiratory changes following lung cancer resection. **The British Thoracic Oncology Group Annual Meeting, Dublin, Ireland**
2014	The Effect Of Diaphragmatic Plication On Chest Wall Dynamics. **The European association of Cardiothoracic surgery. 28th Annual Meeting, Milan, Italy**

2014	Novel thoraco-abdominal motion analysis technology can measure early respiratory changes following lung resection. **The European Respiratory Society 2014 Annual Congress in Munich, Germany**
2013	Improvement in lung function following diaphragmatic plication for unilateral paralysis is due to improved abdominal chest wall motion on the operated and contralateral side during quiet breathing and exercise. **The Society of Cardiothoracic Surgeons of Great Britain and Ireland Annual meeting 2013, Brighton, UK**

21 References

Acosta, J. B. (2014). Exercise improvement after pectus excavatum repair is not related to chest wall function. *Eur J Cardiothoracic Surg , 45* (3), 544-548.

Adams, J. A., Zabaleta, I. A., Stroh, D., & Sackner, M. A. (1993). Measurement of breath amplitudes: Comparison of three noninvasive respiratory monitors to integrated pneumotachograph. *Ped. Pulmonol. , 16*, 254-258.

Agostini, P., Cieslik, H., Bishay, E., Kalkat, M., Rajesh, P. B., Steyn, R. S., et al. (2008). The impact and risk factors for post operative pulmonary complications following lung resection in current UK practice - Are there modifiable factors? *Thorax , 63*, A10-A12.

Agostini, P., Naidu, B., Cleslik, H., Rathinam, S., Bishay , E., Kalkat, M. S., et al. (2011). Comparison of recongnition tools for postoperative plmonary complications following thoracotomy. *Physiotherapy , 97* (4), 278-283.

Agostoni, E., Mognoni, P., Torri, G., & Saracino, F. (1965). Relation between changes of rib cage circumference and lung volume. *J. Appl. Physiol. , 20*, 1179-1186.

Agostoni, E., Sant'Ambrogio, G., & Del Portillo , H. (1960). Electromyography of the diaphragm in man and transdiaphragmatic pressure. *J Appl Physiol , 15*, 1093-1097.

Agur, A. M., & Dalley, A. F. (2013). In *Grant's atlas of anatomy thirteenth edition* (p. 75). Lippincott williams and wikins.

Agur, A. M., & Dalley, A. F. (2013). Anterior abdominal wall. In *Grant's atlas of anatomy thirteenth edition* (pp. 106-107). Lippincot williams and wilkins.

Agur, A. M., & Dalley, A. F. (2013). Muscles of respiration. In *Grant's atlas of anatomy* (p. 26). Lippincott Williams and Wikins.

Agur, A. M., & Dalley, A. F. (2013). Thorax . In *Grant's atlas of anatomy* (pp. 12-30). Lippincott Williams and Wikins.

Agur, A. M., & Dalley, A. F. (2013). Thorax. In *Grant's atlas of anatomy thirteenth edition* (p. 12). Lippincott Williams and Wilkins.

AJ Peacock, M. M. (1984). Optical mapping of the thoracoabdominal wall.

Ali Mohamed, S., Prosser, K., Weerasuriya , C., Iles, R., Cameron, J., & Lasenby, J. (2011). Validating structured light plethysmography (SLP) as a non-invasive method of measuring lung function when compared to Spirometry. *Thorax , 66* (Supp 4), A121-A121.

Aliverti, A. R. (2005). Effect of salbutamol on lung function and chest wall volumes at rest and during exercise in COPD. *Thorax , 60* (11), 916-924.

Aliverti, A. S. (2004). Regional chest wall volumes during exercise in chronic obstructive pulmonary disease. *Thorax , 59* (3), 210-216.

Aliverti, A., Bovio D., Fullin , I., Dellaca, R. L., Lo Mauro, A., Pedotti, A., et al. (2009). The abdominal circulatory pump. *PloS One , 4* (5), e5550.

Aliverti, A., Cala, S. J., Duranti, R., Ferrigno, G., Kenyon, C. M., Pedotti, A., et al. (1997). Human respiratory muscle actions and control during exercise. *J Appl Physiol , 83* (4), 1256-1269.

Aliverti, A., Dellaca, R., Pelosi, P., Chiumello, D., Gatihnoni, L., & Pedoti, A. (2001). Compartimental analysis of breathing in the supine and prone position by opto-electroninc plethysmography. *Ann Biomed Eng. , 29* (1), 60-70.

Aliverti, A., Dellaca, R., Pelosi, P., Chiumello, D., Pedotti, A., & Gattinoni, L. (2000). Optoelectronic plethysmography in intensive care patients. *Am J Respir Crit Care Med , 161* (5), 1546-1552.

Allison, R. D., Holmes, E. L., & Nyboer, J. (1964). Volumetric dynamics of respiration as measured by electrical impedance plethysmography. *J. Appl. Physiol. , 19*, 166-173.

Alvarez-Argote, S. e. (2016). The impact of midcervical contusion injury on diaphragm muscle function. *J Neurotrauma , 33* (5), 500-509.

American Thoracic Society . (1991). Lung function testing: selection of reference values and interpretative strategies. *Am Rev Respir Dis , 144*, 1202-1208.

Anderson, P. J., Wiste, H. J., Ostby, S. A., Miller, A. D., Ceridon, M. L., & Johnson, B. D. (2015). Sleep disordered breathing and acute mountain sickness in workers rapidly transported to the South Pole (2835 m). *Respir Physiol Neurobiol. , 210*, 38-43.

Aramendi, E., Ayala, U., Irusta, U., Alonso, E., Eftestol, T., & Kramer-Johansen, J. (2012). Suppression of the cardiopulmonary resuscitation artefacts using the instantaneous chest compression rate extracted from the thoracic impedance. *Resuscitation , 83* (6), 692-698.

Ashutosh, K., Gilbert, R., & Auchincloss, J H, et al. (1974). Impedance pneumograph and magnetometer methods for monitoring tidal volume. *J. Appl. Physiol. , 37*, 964-966.

Atkins, J. H., Mandel, J. E., Weinstein, G. S., & Mirza, N. (2010). A pilot study of respiratory inuctance plethysmography as a safe, noninvasive detector of jet ventilation under general aneshesia. *Anesth Analg , 111* (5), 1168-1175.

Babchenko, e. a. (1999). Fiber optic sensor for the measurement of the respiratory chest circumference changes.

Baidya, D. K., Khanna, P., & Maitra, S. (2014). Analgesic efficacy and safety of thoracic paravertebral and epidural analgesia for thoracic surgery: a systematic review and meta-analysis. *Interact Cardiovasc Thorac Surg. , 18* (5), 626-635.

Baird, T. M., & Neuman, M. R. (1991). Effect of infant position on breath amplitude measured by transthoracic impedance and strain gauges. *Pediatr Pulmonol , 10* (1), 52-56.

Barcelar Jde, M., Aliverti, A., Melo, T. L., Dornelas, C. S., Lim, C. S., Reinaux, C. M., et al. (2013). Chest wall regional volumes in obese women. *Respir Physiol Neurobiol , 189* (1), 167-173.

Benamore, R. E., Scott, K., Richards, C. J., & Entwisle, J. J. (2006). Image-guided pleural biopsy: diagnostic yield and complications. *Clinical radiology , 61* (8), 700.

Bernard, N. B. (2006). Evaluation of respiratory muscle strength by randomized controlled trial comparing thoracoscopy, transaxillary thoracotomy, and posterolateral thoracotomy for lung biopsy. *Eur J Cardiothoracic Surg. , 29* (4), 596-600.

Bernardi, E., Pomidori, L., Bassal, F., Contoli, M., & Cogo, A. (2015). Respiratory muscle training with normocapnic hyperpnea improves ventilatory pattern and thoracoabdominal coordination, and reduces oxygen desaturation during endurance exercise testing in COPD patients. *Int J Chron Obstruct Pulmon Dis. , 10*, 1899-1906.

Bianchi, C., & Bianchi, T. (2007). Malignant mesothelioma: global incidence and relationship with asbestos. *Ind Health , 45* (379-387).

Biederer, J., Bauman, G., Hintze, C., Fabel, M., & Both, M. (2011). Magnetresonanztomographie. *Der Pneumologe , 8*, 234-242.

Biederer, J., Beer, M., Hirsch, W., Wild, J., Fabel, M., Puderbach, M., et al. (2012). MRI of lung (2/3). Why ... when ... how? *insights imaging , 3* (4), 355-371.

Binazzi, B., Lanini, B., Gigliotti, F., & Scano, G. (2013). Breathing pattern and chest wall kinematic during phonation in chronic obstructive pulmonary disease patients. *Respiration , 86* (6), 462-471.

Biritish Thoracic Soceity . (2005). *Spirometry in practice .* Hants: BTS COPD Consortium.

Blanch, L., Bernabe, F., & Lucangelo , U. (2005). Measurement of air trapping, intrinsic positive end expiratory presure, and dynamic hyperinflation in mechanically ventilated patients. *Respir Care , 50* (1), 110-123.

Boudarham , J., Pradon, D., Prigent, H., Falazie , L., Durand, M. C., Meric, H., et al. (2013). Optoelectronic plethsmography as an alternative method for diagnosis of unilateral diaphragmatic weakness. *Chest , 144* (3), 887-895.

Boutin, C., & Rey, F. (1993). Thoracoscopy in pleural malignant mesothelioma: a prospective study of 188 consecutive patients. *I. Diagnosis. cANCER , 71*, 389-393.

Bradley, J. M., Kent, L., O'Neill, B., Nevill, a., Boyle, L., & Elborn, J. S. (2011). Cardiorespiratory measurments during fleild tests in CF: use of ambulatory monitoring system. *Pediatr Pulmonol , 46* (3), 253-260.

Brandao, D. C., Lage, S. M., Britto, R. R., Parreira, V. F., de Oliveira, W., Martins, S. M., et al. (2012). Chest wall regional volume in heart failure patients during inspiratory loaded breathing. *Respir Physiol Neurobiol , 180* (2-3), 269-274.

Braun, N. M., Arora, N. S., & Rochester , D. F. (1982). Force-length relationship of the normal human diaphragm. *J Appl Physiol , 53*, 405-412.

Brenner, D. J., & Hall, E. J. (2007). Computed Tomography — An Increasing Source of Radiation Exposure. *N Engl J Med , 357*, 2277-2284.

Brimacombe, J. (1993). Noninvasive monitoring of tidal volume with an extensometer: Laboratory and clinical studies. *Anesth. Intens. Care , 21*, 62-66.

Brimacombe, J. R., Macfie, A. G., & McCrirrick, A. (1991). The Extensometer – Potential applications in anaesthesia and intensive care. *Anaesthesia , 46*, 756-761.

Brims, F. A. (2012). Outcomes and complications following medical thoracoscopy. *Clin Respir J , 6* (3), 144-149.

British Thoracic Society and Society of Cardiothoracic Surgeons of Great Britain and Ireland Working Party. (2001). Guidlines on the slection of patients with lung cancer for surgery. *Thorax , 56*, 86-108.

Brouillette, e. a. (1987). Comparison of respiratory inductive plethysmography and thoracic impedance for apnea monitoring.

Brunelli, e. a. (2009). The European Respiratory Society and European Society of Thoracic Surgeons clinical guidelines for evaluating fitness for radical treatment (surgery and chemoradiotherapy) in patients with lung cancer. *Eur J Cardiothorac Surg , 36* (1), 181-184.

Brusasco, V. e. (2003). Mechanics of ventilation. In G. e. Gibson, *Respiratory Medicine* (pp. 299-315). Edinburgh: Saunders.

Cala, S. J., Kenyon, C. M., Ferrigno, G., Carnevali, P., Aliverti, A., Pedotti, A., et al. (1996). Chest wall and lung volume estimation by optical reflectance motion analysis. *J Appl Physiol , 81* (6), 2680-2689.

Carlo, W. e. (1982). The effect of respiratory distress syndrome on chest wall movements and respiratory pauses in preterm infants.

Casanova, C. e. (2005). Inspiratory-to-total lung capacity ratio predicts mortality in patients with chronic obstructive pulmo- nary disease. *Am J Respir Crit Care Med , 171*, 591-597.

Cassart, M., & et, a. (2001). Effects of lung volume reduction surgery for emphysema on diaphragm dimensions and configuration. *Am J Respir Crit Care Med , 163* (5), 1171-1175.

Celik, S., Celik, M., Aydemir, B., Tunckaya, C., Okay, T., & Doqusoy, I. (2010). Long-term results of diaphragmatic plication in adults with unilateral diaphragm paralysis. *5*, 1111.

Chadha, T. S., Watson , H., & Birch, S, et al. (1982). Validation of respiratory inductance plethysmography using different calibration procedures. *Am. Rev. Respir. Dis. , 125*, 644-649.

Chang, W. Y., Huang, C. C., Chen, C. C., Chang, C. C., & Yang, C. L. (2014). Design of a novel flexible capacitive sensing mattress for monitoring sleeping respiratory. *Sensors , 14* (11), 22021-22038.

Ciocchetti , M., Massaroni, C., Saccomandi, P., Caponero, M. A., Polimadei, A., Formica, D., et al. (2015). Smart Textile Based on Fiber Bragg Grating Sensors for Respiratory Monitoring: Design and Preliminary Trials. *Biosensors , 5* (3), 602-615.

Clarenbach, C. F., Senn, O., Brack, T., Kohler, M., & Bloch, K. E. (2005). Monitoring of Ventilation During Excercise by a Portable Respiratory Inductive Plethysmography. *Chest , 128* (3), 1282-1290.

Clark, S. J., Zoumot, Z., & Bamsey, O. (2014). Surgical Approches for lung volume reduction in emphysema. *Clin Med , 14* (2), 122-127.

Coates, A. e. (1997). Measurement of lung volumes by plethysmography. *Eur Respir J , 10*, 1415-27.

Cohen, K. P., Ladd, W. M., & Beams, D. M. (1997). Comparison of impedance and inductance ventilation sensors on adults during breathing, motion, and simulated airway obstruction. *IEEE Trans. Biomed. Eng. , 44*, 555-566.

Concha, M., Dagnino, J., Cariaga, M., Auilera, J., Aparicio, R., & Guerrero, M. (2004). Analgesia after thoracotomy: epidral fentanyl/bupivacaine compared with intercostal nerve block plus intravenous morphine. *J Cardiothoracc Vasc Anesth , 18* (3), 322-326.

Cooper, B. (2011). An update on contraindications for lung function testing. *Thorax , 66*, 714-723.

Corwin, M. j., Weese-Mayer, D. E., Neuman, M. R., Crowell, D., Ward, S., Brooks, L., et al. (1997). Apnea duration: Respiratory Inductance Plethysmography (RIP) and Transthoracic Impedance (TTI) Pneumography vs. Polysomnography (PSG). *Pediatric Reseach , 41*, 301-301.

Criee, C. e. (2006). Empfehlungen der Deutschen Atemwegsliga zur Spirometrie. *Pneumologie , 9*, 576-584.

Criee, C. P., Sorichter, S., Smith, H. J., Kardos, P., Merget, R., Heise, D., et al. (2011). Body plethysmogprahy - its principles and clinical use. *Respir Med , 105* (7), 959-971.

Crossebner, M. W., Arifi, A. A., Goddard, M., & Ritchie, A. J. (1999). Mesothelioma – VATS biopsy and lung mobilization improves diagnosis and palliation. *Eur J Cardiothorac Surg , 16* (6), 619-623.

Da Gama, A. E., de Andrade Carvalho, L., Feitosa, L. A., do Nascimento Junior, J. F., da Silva , M. G., Amorim, C. F., et al. (2013). Acute effects of incremental inspiratory loads on compartmental chest wall volume and predominant activity frequency of inspiratory muscle. *J Electromyogr Kinesiol , 23* (6), 1269-1277.

D'angelo, e. a. (2008). A system for respiratory motion detection using optical fibers embedded into textiles.

D'Angelo, M. G., Romei, M., Lo Mauro, A., Marchi, E., Gandossini, S., Bonato, S., et al. (2011). Respiratory pattern in an adult population of dystrophic patients. *J Neurol Sci , 306* (1-2), 54-61.

David, A. E., & Marshall, B. M. (2011). Review of Chest Wall Tumors: A Diagnostic, Therapeutic, and Reconstructive Challenge. *Semin Plast Surg. , 25* (1), 16-24.

Davies, A., & Moores, C. (2010). Struture of the respiratory system, related to function. In *The Respiratory system basic science and clinical conditions* (pp. 12-28). Elsevier limited .

Davis, C., Mazzolini, A., & Murphy, A. (1997). A new fibre optic sensor for respiratory monitoring. *Australas. Phys. Eng. Sci. Med. , 20*, 214-219.

De Boer, W. (2010). SLP: A Zero-Contact Non-Invasive Method for Pulmonary Function Testing. *Br Mach Vis Conf 2010. 85*, pp. 85.1-85.12. British Machine Vision Association.

De Groote, A., Van Muylem, A., Scillia, P., Cheron, G., Verleden, G., Paiva, M., et al. (2004). Ventilation asymmetry after transplantation for emphysema: role of chest wall and mediastinum. *Am J Respir Crit Care Med , 170* (11), 1233-1238.

De Jonckheere, J., Jeanne, M., Grillet, A., Weber, S., Chaud, P., Logier, R., et al. (2007). OFSETH: optical fibre embedded into technical textile for healthcare, an efficient way to monitor patient under magnetic resonance imaging. *Conf Proc IEEE Eng Med Biol Soc*, (pp. 3950-3953).

De Jonckheere, J., Narbonneau, F., Jeanne, M., Kinet, D., Witt, J., Krebber, K., et al. (2009). OFSETH: Smart Medical Textile for Continuous Monitoring of Respiratory Motions under Magnetic Resonance Imaging. *Conf Proc IEEE Eng Med Biol Soc* , 1473-1476.

Decramer, M., De Troyer, A., Kelly, S., Zocchi, L., & Macklem, P. T. (1984). Regional differences in abdominal pressure swings in dogs. *J Appl Physiol , 57* (6), 1682-1687.

Dellaca, R., Ventura, M., Zannin, E., Natile, M., Pedotti, A., & Tagliabue, P. (2010). Measurement of total and compartmental lung volume changes in newborn by optoelectronic plethysmography. *Pediatric Research , 67* (1), 11-16.

Dolgener, e. a. (1994). Validation of the Rockport Fitness Walking Test in College Males and Females. *Research Quarterly for Exercise and Sport , 65*, 152-158.

Downie, W. W., Leatham, P. A., Rhind, V. M., Wright, V., Branco, J. A., & Anderson, J. A. (1978). Studies with pain rating scare. *Ann Rheum Dis , 37*, 378-381.

Drakatos, P., Higgins, S., Duncan, I., Bridle, K., Briscoe, S., Leschziner, G. D., et al. (2016). The utility of respiratory inductance plethysmography in REM sleep scoring during multiple sleep latency testing. *Respir Physiol Neurobiol , 230*, 1-4.

DuBois, A. e. (1956). A new method for measuring airways resistance in man using a body plethysmograph: values in normal subjects and in patients with respiratory disease. *J Clin Invest , 35*, 327-335.

Dubols, A. e. (1956). A rapid plethysmographic method for measuring thoracic gas volume: a comparison with a nitrogen washout method for measuring functional residual capacity in normal subjects. *J Clin Invest , 35*, 322-326.

Duch, P., & Moller, M. H. (2015). Epidural analgesia in patients with traumatic rib fractures: a systematic review of randomised controlled trials. . *Acta Anaesthesiol Scand. , 59* (6), 698-709.

Dye , J. e. (2015). Whole body plethysmography reveals differential ventilatory responses to ozone in rat models of cardiovascular disease. *Inhal Toxicol , 27* (Suppl 1), 14-25.

Eibel, R., Herzog, P., Dietrich, O., Rieger, C., Ostermann, H., Reiser, M., et al. (2006). Pulmonary abdnormalities in immunocompromised patients: comparative detection with parallel acquisition MR imaging and thin-section helical CT. *Radiology , 241*, 880-891.

Estrada, L., Torres, A., Sarlabous, L., Fiz , J., Gea, J., Martinez-Llorens, J., et al. (2014). Estimation of bilateral asynchrony between diaphragm mechanomyographic signals in patients with chronic obstructive pulmonary disease. *Conf Proc IEEE Eng Med Biol Soc , 38*, 13-16.

McCool, F. D., Wang, J., & Ebi, K. L. (2002). Tidal volume and respiratory timing derived from a portable ventilator monitor. Chest, 122(2), 683-691.

Ferrigno , G., & Pedotti, A. (1985). ELITE: a digital dedicated hardware system for movement analysis via real-time TV signal processing. *IEEE Trans Biomed Eng , 32* (11), 943-950.

Ferrigno, G., Carnevali, P., Aliverti, A., Molteni, F., Beulcke, G., & Pedotti, A. (1994). Three-dimensional optical analysis of chest wall motion. *J Appl Physiol. , 77* (3), 1224-1231.

Fishman, A., Martinez, F., & Naunheim, K. (2003). National Emphysema Treatment Trial Research Group. A randomized trial comparing lung-volume-reduction surgery with medical therapy for severe emphysema. *N Engl J Med , 384* (21), 2059-2073.

Fokkema, D. S., Maarsingh, E. J., van Eykem, L. A., & van Aalderen, W. M. (2006). Different breathing patterns in healthy and asthmatic children: responses to an arithmetic task. *Respir. Med. , 100* (1), 148-156.

Freeman, R., Wozniak, T., & Fitzgerald, E. (2006). Functional and physiological results of video-assisted thoracoscopic diaphragm plication in adults patients with unilateral diaphram paralysis. *Ann Thoracic Surg , 81*, 1853-1857.

Fressler, H. S., Scharf, S. M., Ingenito, E. P., McKenna, R. J., & Sharafkhaneh, A. (2008). Physiologic basis for improved pulmonary function after lung volume reduction. *Proc Am Thorac Soc , 5* (4), 416-420.

Gaafar, R. M., & Eldin, N. H. (2005). Epidemic of mesothelioma in Egypt. *Lung Cancer , 49* (Suppl), S17-S20.

Garet, M. e. (2005). Estimating relative physical workload using heart rate monitoring: a validation by whole-body indirect calorimetry. *Eur J Appl Physiol. , 94* (1-2), 46-53.

Gastinger , S. e. (2011). A new method to estimate energy expenditure from abdominal and rib cage distances. *Eur J Appl Physiol , 111* (11), 2823-2835.

Gastinger, S., Sefati, H., Nicolas, G., Sorel, A., Gratas-Delamarche, A., & Prioux, J. (2011). A new method to estimate energy expenditure from abdominal and rib cage distances. *J Appl Physiol , 111* (11), 2823-2835.

Gastinger, S., Sefati, H., Nicolas, G., Sorel, A., Gratas-Delamarche, A., & Prioux, J. (2010). Estimates of ventilation from measurements of rib cage and abdominal distances: a portable device. *J Appl Physiol. , 109* (6), 1179-1189.

Geddes, D., Davies, M., & Koyama, H. (2000). Effect of lung-volume-reduction surgery in patients with severe emphysema. *N Engl J Med , 343* (4), 239-245.

Gilbert, R., Auchinocloss, J. H., Brodsky, J., & Boden, W. (1972). Changes in tidal volume, frequency, and ventilation induced by their measurement. *j Appl Physiol , 33* (2), 252-254.

Goldman, M. e. (2005). Whole body pletismography. *Eur Respir Mon , 31*, 15-43.

Goldman, M. e. (2001). Whole-body plethysmog- raphy. *Eur Respir Mon , 17*, 302-312.

González-Otero , D. M., Ruiz de Gauna , S., Ruiz , J., Daya, M. R., Wik, L., Russell, J. K., et al. (2015). Chest compression rate feedback based on transthoracic impedance. *Resuscitation , 93*, 82-88.

Gorman, R. B., McKenzie, D. K., Butler, J. E., Tolman, J. F., & Gandevia, S. C. (2005). Diaphragm length and neural drive after lung volume reduction surgery. *Am J Respir Crit Care Med , 172* (10), 1259-1266.

Gould, G., & Pearce, A. (2006). Assessment of suitablity for lung resction . *Contin Educ Anaesth Crit Care Pain , 6* (3), 97-100.

Gramse, V., De Groote, A., & Paiva, M. (2003). Novel Concept for noninvasive cardiopulmunary monitor for infants: A Pair of Pajamas with an Integrated Sensor Module. *Ann Biomed Eng , 31* (2), 152-158.

Grant, R. (1999). Con: every post thoracotomy patient does not deserve thoracic epidural analgesia. *J Cardiothoracic Vasc Anesth , 13*, 355-357.

Grenvik, S., Ballou, S., & McGinley, E, et al. (1972). Impedance pneumography – Comparison between chest impedance changes and respiratory volume in 11 healthy volunteers. *Chest , 62*, 439-443.

Gross, J. L., Younes, R. N., & Haddad, F. J. (2005). Soft-tissue sarcomas ot the chest wall: Prognostic factors. *127*, 902-908.

Guenard, H., Vieillefond, H., & Varene, P. (1977). Adaptation of body plethysmography to the study of respiratory mechanics during muscular exercise (author's transl). *Bull Eur Phsiopathol Respir , 13* (3), 399-407.

Gulbahar , G., Kocer, B., Muratli, S. N., Yildirim, E., Gulbahar, O., & Dural, K. (2010). A comparison of epidural and paravertebral catheterisation techniques in post-thoracotomy pain management. . *Eur J Cardiothoracic Surg , 37*, 467-472.

Hagaman, J. T., Rouan, G. W., Shipley, R. T., & Panos, R. J. (2009). Admission chest radiograph lacks sensitivity in the diagnosis of commmunity acquired pneumonia. *Am J Med Sci , 337* (4), 236-240.

Hamilton, L. H., Beard, J. D., Carmean, R. C., & Kory, R. C. (1967). An electrical impedance ventilometer to quantitate tidal volume and ventilation. *Med. Res. Eng. , 6*, 11-16.

Helm, E. M. (2010). Imaging of the pleura. *J Magn Reson Imaging , 32* (6), 1275-1286.

Helms, O., Mariano, J., Hentz, J. G., Santelmo, N., Falcoz, P. E., Massard, G., et al. (2011). Intra-operative paravertebral block for postoperative analgesia in thoracotomy patients: a randomized, double-blinded, placebo-controlled study. *Eur J Cardiothoracic Surg , 40* (4), 902-906.

Herbert, A., & Gallagher, P. J. (1982). Pleural biopsy in the diagnosis of malignant mesothelioma. *Thorax , 37* (11), 816-821.

Herth, F. J. (2012). Efficacy predictors of lung volume reduction with Zephyr valves in a European cohort. . *Eur Respir J , 39*, 1334-1342.

Hiilloskorpi, H. e. (2003). Use of heart rate to predict energy expenditure from lowto high ativity levels. *Int J Sports Med. , 24* (5), 332-336.

Hlilpertshauser, M. (2004, 1 1). *Iron lung CDC.jpg.* From https://en.wikipedia.org: https://en.wikipedia.org/wiki/Iron_lung#/media/File:Iron_lung_CDC.jpg

Hollier, C. A., Harmer, A. R., Maxwell , L., Menadue, C., Willson, G. N., Black, D. A., et al. (2014). Validation of respiratory inductive plethysmograpy (lifeshirt) in obesity and hypoventilation syndrome. *Respir Physiol Neurobiol , 194*, 15-22.

Hopkinson, N. S. (2011). Atelectasis and survival after bronchoscopic lung volume reduction for COPD. *Eur Respir J , 37* (6), 1346-1351.

Hubmayr, R. D., Litchy, W. J., Gay, P. C., & Nelson, S. B. (1989). Transdiaphragmatic twitch pressure. Effects of lung volume and chest wall shape. *Am Rev Respir Dis , 139* (3), 647-652.

Huijun Chen, e. a. (2010). Color structured light system of chest wall motion measurement for respiratory volume evaluation.

Illi, S. K., Hostettler, S., Aliverti, A., & Spengler, C. M. (2013). Compartmental chest wall volume changes during volitional hyperpnoea with constant tidal volume in healthy individuals. *Respir Physiol Neurobiol , 185* (2), 410-415.

Imperatori, A., Rotolo, N., Gatti, M., Nardecchia, E., De Monte, L., Conti, V., et al. (2008). Peri-operative complications of video-assisted thoracoscopic surgery (VATS). *Int J Surg. , 6* (Suppl 1), S78-81.

Impertori, A., Harrison, R. N., & Leitch, D. N. (2006). Lung cancer in Teesside (UK) and varese (Italy): a comparison of management and survival. *Thorax , 61* (3), 232-239.

Jack , R. H., Gulliford, M. C., & Ferguson, J. (2003). Geographical inequalities in lung cancer management and survival in South East England: evidence of variation in access to oncology services? *Br J Cancer , 88* (7), 1025-1031.

Jakobsen, e. a. (2012). High thoracic epidural analgesia in cardiac surgery. Part 1--high thoracic epidural analgesia improves cardiac performance in cardiac surgery patients. *J Cardiothorac Vasc Anesth , 26* (6), 1039-1047.

Jenkins, M., Vaughan, P., Place, D., & Kornaszewska, M. (2011). Endobroncial valve migration . *Eur J Cardiothorac Surg , 40* (5), 1258-1260.

Jett, J., & Aubry, M. (2008). Malignant Pleural Mesothelioma. In R. K. Albert, S. G. Spiro, & J. R. Jett, *Clinical Respiratory Medicine. Mosby 2nd edition* (pp. 735-741).

Joshi, T. K., Sahin, A. A., & Ozesmi, M. (2006). Asbestos ban in India: challenges ahead. *Ann NY Acad Sci , 1076*, 292-308.

Kartianou, E. A., Aliverti, A., Louvaris, Z., Vasilopoulou, M., Nasis, I., Asimakos, A., et al. (2015). Limitation in tidal volume expansion partially determines the intensity of physical activity in COPD. *J Appl Physiol , 118* (1), 107-114.

Kent, L., O'Neill, B., Davison, G., Nevill, A., Elborn, J. S., & Bradley, J. M. (2009). Validity and reliability of cardiorespiratory measurements recorded by the LifeShirt during exercise. *Respir Physiol Neurobiol , 167* (2), 162-167.

Kenyon, C. M., Cala, S. J., Yan, S., Aliverti, A., Scano, G., Duranti, R., et al. (1997). Rib cage mechanics during quiet breathing and exercise in humans. *J Appl Physiol , 83* (4), 1242-1255.

Kline , e. a. (1989). Estimation of VO from a one-mile track walk, gender, age, and body weight. *Medicine and Science in Sports and Exercise , 19*, 253-259.

Ko, M. A. (2009). Acquired Paralysis of the diaphragm . *Thorac Surg Clin* (19), 501-510.

Kogan, D., Jain, A., Kimbro, S., Gutierrez, G., & Jain, V. (2016). Respiratory Inductance Plethysmography improved Diagnositic Sensitivity and Specifity of Obstructive Sleep Apnea. *Respir Care , 61* (8), 1033-1037.

Komorniczak, M. (2009, 11 20). *Lung volumes and capacities*. From https://commons.wikimedia.org: https://commons.wikimedia.org/wiki/File:Lung_Volumes_And_Capacities_en.svg

Konno, K. M. (1967). Measurement of separate volume changes of rib cage and abdomen during breathing. *J Appl Physiol , 22* (3), 407-422.

Konno, K., & Mead, J. (1967). Measurement of the separate volume changes of rib cage and abdomen during breathing. *J Appl Physiol , 22* (3), 407-422.

Kotani, T., Akazawa, T., Sakuma, T., Nagaya, S., Sonoda, M., Tanaka, Y., et al. (2015). Effects of incentive Spirometry on Respiratory Motion in Healthy Subjects Using Cine Breathing Magnetic Resonance Imaging. *Ann Rehabil Med , 39* (3), 360-365.

Kotani, T., Minami, S., Takahashi, K., Isobe, K., Nakata, Y., Takaso, M., et al. (2004). An analysis of chest wall and diaphragm motions in patients with idiopathic scoliosis using dynamic breathing MRI. *Spine , 29* (3), 298-302.

Kouki, I. (2008). Pathology of mesothelioma. *Environ Health Prev Med. , 13* (2), 60-64.

Koulouris, N., Mulvey, D. A., Laroche, C. M., Goldstone, J., Moxham, J., & Green, M. (1989). The effect of posture and abdominal binding on respiratory pressures. *Eur Respir J , 2* (10), 961-965.

Koumbourlis, A. C. (2015). Pectus deformities and their imparct on pulmonary physiology. *Paediatr Respir Rev , 16* (1), 18-24.

Krayer, S., Rehder, K., Beck, K. C., Cameron, P. D., Didier, E. P., & Hoffman, E. A. (1987). Quantification of thoracic volumes by three-dimensional imaging. *J Appl Physiol , 62* (2), 591-598.

Kubiak, R., Habelt, S., Hammer, J., Hacker, F. M., Mayr J , & Bielek, J. (2007). Pulmonary function following completion of minimally invasive repair for pectus excavatum. *Eur J Pediatr Surg , 17*, 255-260.

Kumar, P., & Clark, M. (2009). Structure of the respiratory system . In *Clinical Medicine Seventh Edition* (pp. 811-814). Elsevier Limited.

Kumar, P., & Clark, M. (2009). The treachea, bronchi and bronchioles. In *Clinical medicine seventh edition* (p. 812). Elsevier Limited .

Kurbicek, E., Kinnen, E., & Edin, A. (1964). Calibration of an impedance pneumograph. *J. Appl. Physiol , 19*, 557-560.

Kuritzky, A. M., Ryder, B. A., & Ng, T. (2013). Long-Term Survival Outcomes of Video-assisted Thoracic Surgery (VATS) Lobectomy After Transitioning from Open Lobectomy. *Ann Surg Oncol , 20* (8), 2734-2740.

Kurpad, A. e. (2006). A simple method of measuring total energy expenditure and physical activity level from the heart rate in adult med. *Eur J Clin Nutr , 60* (1), 32-40.

La Mauro, A., D'Angelo, M. G., Romei, M., Motta, F., Colombo , D., Comi, G. P., et al. (2010). Abdominal volume contribution to tidal volume as an early indictor of respiratory impairment in Duchenne muscular dystrophy. *Eur Respir J , 35* (5), 1118-1125.

La Mauro, A., Pochintesta, S., Romei, M., D'Angelo, M. G., Pedotti, A., Turconi, A. C., et al. (2012). Rib Cage Deformities Alter Respiratory Muscle Action and Chest Wall Function in Patients with Severe Osteogenesis Imperfecta. *PLoS One , 7* (4).

Lanini, B., Masolini, M., Bianchi, R., Binazzi, B., Romagnoli, L., Gigliotti, F., et al. (2008). Chest wall kinematic during voluntary cough in neuromuscular patients. *Prspir Physiol Neurobiol , 161* (1), 62-68.

Lau, D., Chen, Z., Teo, J. T., Ng, S. H., Rumpel, H., Lian, Y., et al. (2013). Intensity-Modulated Microbend Fiber Optic Sensor for Respiratory Monitoring and Gating During MRI. *IEEE Trans. Biomed. Eng. , 60*, 2655-2662.

Layton, A. M., Garber, G. E., Thomashow, B. M., Gerardo, R. E., Emmert-Aronson, B. O., Armstrong , H. F., et al. (2011). Exercise ventilatory kinematics in endurance trained and untrained men and women. *Respir Physiol Neurobiol , 178* (2), 223-229.

Leung, A. N., Muller, N. L., & Miller, R. R. (1990). CT in differential diagnosis of diffuse pleural disease. *AJR Am J Roentgenol , 154*, 487-492.

Lima, C. A. (2014). Effects of noninvasive ventilation on treadmill 6-min walk distance and regional chest wall volumes in cystic fibrosis: randomized controlled trial. *Respir Med. , 108* (10), 1460-1468.

Lima, I. N., Fregonezi, G. A., Melo, R., Cabral, E. E., Aliverti, A., Campos, T. F., et al. (2014). Acute effects of volume-oriented incentive spirometry on chest wall volumes in patients after a stroke. *Respir Care , 59* (7), 1101-1107.

Livingstone, M. e. (2000). Energy expenditure by heart rate in children: an evaluation of calibration techniques. *Med Sci Sports Exerc. , 32* (8), 1513-1519.

Loddenkemper, R., & Schonfeld, N. (1998). Medical thoracoscopy. *Curr Opin Pulm Med. , 4* (4), 235-238.

Lotz, J., Kivelitz, D., FischbacH r, Beer, M., & Miller, S. (2009). Recommendations for utilizing computerized tomography and magnetic resonance tomography in heart diagnosis. 2-Magnetic resonance tomography. *Rofo , 181*, 800-814.

Lunardi, A. C., Paisani, D. M., Marques de Silva, C. C., Cano, D. P., Tanaka, C., & Carvalho, C. R. (2015). Comparison of lung expansion techniques on thoracoabdominal mechanics and incidence of pulmonary complications after upper abdominal surgery: a randomized and controlled trial. *Chest* , 148(4), 1003-1010.

Lunardi, A. C., Porras, D. C., Barbosa, R. C., Paisani, D. M., Marques da Silva, C. C., Tanaka, C., et al. (2014). Effect of volume-oriented versus flow-oriented incentive spirometry on chest wall volumes, inspiratory muscle activity, and thoracoabdominal synchrony in elderly. *Respir Care , 59* (3), 420-426.

Luo, S., Liu, X., & Mu, S. (2003). Asbestos related diseases from environmental exposure to crocidolite in Da-yao, China. I. Review of exposure and epidemiolgical data. *Occup Environ Med , 60*, 35-41.

MacIntre, N., Crapo, R., Viegi, G., Johnson, D., van der Grinten, C., Brusasco, V., et al. (2005). Standardisation of single-breath determination of carbon monoxide uptake in the lung. *Eur Respir J , 26* (4), 720-735.

Mador, M. J., Magalang, U. J., & Kufel, T. J. (1994). Twitch potentiation following voluntary diaphragmatic contraction. *Am J Respir Crit Care Med , 149* (3 Pt 1), 739-743.

Maeda, H. N. (1988). Diaphragm, function after pulmonary resection. *Am Rev Respir Dis , 137*, 678-681.

Mair, D. (2012, 1 31). *Male patient SLP.* From https://commons.wikimedia.org: https://commons.wikimedia.org/wiki/File:Male_Patient_SLP.jpg

Makarawo, T., Steyn, R., & Naidu, B. (2011). Prosthesis-free repair of pectus chest deformity. . *Br J Surg , 98* (11), 1660-1665.

Marin, J. M., Garrizo, S. J., Gascon, M., Sanchez, A., Gallego, B., & Celli, B. R. (2001). Inspiratory capacity, dynamic hyperinflation, breathlessness, and exercise performance during the 6-minute-walk test in chronic obstructive pulmonary disease. *Am J Respir Crit Care Med , 163* (6), 1395-1399.

Martinez, F. J., & et, a. (1997). Lung-volume reduction improves dyspnea, dynamic hyperinflation, and respiratory muscle function. *Am J Respir Crit Care Med , 155*, 1984-1990.

Martinez-Ferro, M., Fraire, C., & Bernard, S. (2008). Dynamic compression system for the correction of pectus carinatum. *Semin Pediatr Surg , 17*, 194-200.

Massaroni, C., Saccomandi, P., & Schena, E. (2015). Medical Smart Textiles Based on Fiber Optic Technology: An Overview. *J Funct Biomater , 6* (2), 204-221.

Morgan, M. D., Gourlay, A. R., & Denison D. M. (1984). An optical method of studyng the shape and the movement of the chest wall in recumbent patien*ts. Thorax ,* 39(2), 101-06.

Megahed, N. A. (2014, May-Aug). Comparison between analgesic effect of bupivacaine thoracic epidural and ketamine infusion plus wound infiltration with local anasthetics in open cholecystectomy. *Anesth Essays Res.* , 162-167.

Megahed, N. A., Ellakany , M., Elatter, A. M., & Moustafa, M. A. (2014). Comparison between analgesic effect of bupivacaine thoracic epidural and ketamine infusion plus wound infiltration with local anesthetics in open cholecystectomy. *Anesthe Essays Res , 8* (2), 162-167.

Meric, H., Calabrese, P., Pardon, D., Lejaille, M., Lofaso, F., & Terzi, N. (2014). Physiological comparison of breathing patterns with neurally adjusted ventilatory assist (NAVA) and pressure-support ventilation to improve NAVA settings. *Respir Physiol Neurobiol , 195*, 11-18.

Meyerhoff, R. R., Yang , C. F., Speicher, P. J., Gulack, B. C., Hartwig, M. G., D'Amico, T. A., et al. (2015). Impact of mesothelioma histologic subtype on outcomes in the Surveillance, Epidemiology, and End Results database. *J Surg Res , 196* (1), 23-32.

Microsoft, K. (n.d.). http://www.xbox.com/en-US/Kinect.

Mielke, C. H., & Winter, R. B. (1993). Pectus carinatum successfully treated with bracing. A case report. *Int Orthop. , 17* (6), 350-352.

Milic-Emili, J., Orzalesi, M. M., Cook, C. D., & Turner , J. M. (1964). Respiratory Thoraco-Abdominal Mechanics in Man. *J Appl Physiol , 19*, 217-223.

Miller, M. R., Hankinson, J., Brusasco, V., Burgos, F., Casaburi, R., Coates, A., et al. (2005). ATS/ERS Task Force Standardisation of spirometry. *Respir J , 26*, 319-338.

Miller, M., Crapo, R., Hankinson, J., Brusasco, V., Burgos, F., Casaburi, R., et al. (2005). General considerations for lung function testing. *Eur Respir J , 26* (1), 153-161.

Mogalle, K., Perez-Rovira, A., Ciet, P., Wens, S., van Doorn, P., Tiddens, H., et al. (2016). Quantification of diaphragm mechanics in Pompe disease using dynamc 3D MRI. *PLoS , 11* (7), e0158912.

Moore, A. J., Parker, R. J., & Wiggins, J. (2008). Malignant mesothelioma. *Orphanet Journal of Rare Diseases , 3*, 34.

NETT group . (2003). A Randomized Trial Comparing Lung-Volume–Reduction Surgery with Medical Therapy for Severe Emphysema. *N Eng J Med , 348*, 2059-2073.

Nomori, H., Horio, H., Fuyuno, G., Kobayashi, R., & Yashima, H. (1996). Respiratory muscle strength after lung resection with special reference to age and procedures of thoracotomy. . *Eur J Cardiothoracic Surg. , 10* (5), 352-358.

Nozoe, M., Mase, K., Takashima, S., Matsushita, K., Kouyama, Y., Hashizume, H., et al. (2014). Measurements of chest wall volume variation during tidal breathing in the supine and lateral positions in healthy subjects. *Respir Physiol Neurobiol , 193*, 38-42.

O'Donnell, C. e. (2010). Comparison of plethysmographic and helium dilution lung volumes: which is best for COPD? *Chest , 137*, 1108-1115.

Office for National Statistics. (2001). *Cancer Survival: England and Wales, 1991-2001, four major cancer*. Retrieved August 29, 2015 from Office for National Statistics: http://www.statistics.gov.uk/statbase/ssdataset.asp?vlnk=7091

Ohlmer , A., Leger, R., Scheiderer, U., Elfeldt, R., & Wulf, H. (1997). Pain therapy after thoracotomies- systemic patient-controlled analgesia (PCA) with opioid versus intercostal block and interpleural analgesia. *Anaesthesiol Reanim , 22* (6), 159-163.

Okten, F., Koksal, D., Onal, M., Ozcan, A., Simsek, C., & Erturk, H. (2006). Computed tomography findings in 66 patients with malignant pleural mesothelioma due to environmental exposure to asbestos. *Clin Imaging , 30* (3), 177-180.

Oncel, M., Tuscan, B., Akyol, K. G., Dereli, Y., & Sunam, G. S. (2013). Clinical experience of repair of pectus excavatum and carinatum deformities. *Cardiovasc J Afr , 24* (8), 318-321.

OpenStax College. (2013). *Inspiration and expiration.* From https://commons.wikimedia.org: https://commons.wikimedia.org/wiki/File:2316_Inspiration_and_Expiration.jpg

Otis, A. B., Fenn, W. O., & Rahn, H. (1950). Mechanics of breathing in man. *J Appl Physiol , 2* (11), 592-607.

Pail, O. (2003). Apparatus and Methods for indicating respiratory phase to improve speech/breathing synchronization.

Parker, J., Coleman, R., Grady, E., Royal, H., Siegel, B., Stabin, M., et al. (2012). SNM practice guideine for lung scintigraphy 4.0. *J Nucl Med Technol , 40* (1), 57-65.

Pattersen, V., & Bjorkov, K. (2009). Consequences from emotional stimulus on breathing for singing. *J Voice. , 23* (3), 295-303.

Perttunen, K., Nilsson, E., Heinonen, j., Hirvisalo, E. L., Salo, j. A., & Kalso, E. (1995). Extradural, paravertebral and intercostal nerve blocks for post-thoracotomy pain. . *Br J Anaesth , 75*, 541-547.

Pettersen, V. (2005). Muscular patterns and activation levels of auxiliary breathing muscles and thorax movement in classical singing. *Folia Phoniatr Logop , 57*, 255-277.

Pettersen, V., & Westgaard, R. H. (2004). The association between upper trapezius activity and thorax movement in classical singing. *J Voice , 18* (4), 500-512.

Plathow, C., Klopp, M., Schoebinger, M., Thieke, C., Fink, C., PuderbacH, M., et al. (2006). Monitoring oflung motion in patients with malignant pleural mesothelioma using two-dimensional and three-dimensional dynamic magnetic resonance imaging: comparison with spirometry. *Invest Radiol , 41* (5), 443-448.

Plathow, C., Ley, S., Fink, C., Puderbach, M., Heilmann, M., Zuna, I., et al. (2004). Evaluation of chest motion and volumetry during the breathing cycle by dynamic MRI in healthy subjects: comparison with pulmonary function tests. *Invest Radiol , 39* (4), 202-209.

Plathow, C., Schoelbinger, M., Fink, C., Ley, S., Puderback, M., Eichinger, M., et al. (2005). Evaluation of lung volumetry using dynamic three-dimensional magnetic resonance imaging. *Invest Radiol , 40* (3), 173-179.

Pride, N. e. (1986). Lung mechanics in disease. In M. e. Bethesda, *Mechanics of breathing* (Vol. 3, pp. 659-692). 1986: American Physiological Society .

Puderbach, M., Hintze, C., Ley, S., Eichinger, M., Kauczor, H., Biederer, J., et al. (2007). MR imaging of the chest: a practical approach at 1.5 T. *Eur J Radiol , 64*, 345-355.

Quanjer, P. e. (1993). Standardized lung function testing: lung volumes and forced ventilatory flows. *Eur Respir J , 6* (Suppl 16), 5-40.

Reeve, J. C., Nicol, K., Stiller, K. M., McPherson, P., Birch, I., & Gordon et al. (2010). Does physiotherapy reduce the incidence of postoperative plumonary complications following pulmonary resection via open thoracotomy? A preliminary randomised single-blind clinical tril. *Eur J Cardiothorac Surg , 37* (5), 1158-1166.

Richard Iles, R. W. (2010). SLP: A Zero-Contact Non-Invasive Method for Pulmonary Function Testing. *British Machine Vision Conference.* Aberystwyth.

Robertson, C. H., Eschenbocher, W. L., & Johnson, R. L. (1977). Respiratory muscle blood flow distribution during expiratory resistance. *J Clin Invest , 60* (2), 473-480.

Rochester, D. F. (1985). The diaphragm: contractile properties and fatigue. *J Clin Invest , 75* (5), 1397-1402.

Romagnoli, I., Gigliotti, F., Galarducci, A., Lanini , B., Bianchi, R., Cammelli, D., et al. (2004). Chest wall kinematics and respiratory muscle action in ankylosing spondylitis patients. *Eur Respir J , 24* (3), 453-460.

Romer , L. M., & Polkey, M. I. (2008). Exercise-induced respiratory muscle fatigue: implications for performance. *J Appl Physiol , 104* (3), 879-888.

Rusinkiewicz, S., Hall-Holt, O., & Levoy, M. (2002). Real-time 3d model acquisition. *ACM Transactions on Graphics , 21* (3), 438-446.

Russell, R. I., & Helms, P. J. (1994). Evaluation of three different techniques used to measure chest wall movements in children. *Eur. Respir. J. , 7* (11), 2073-2076.

Rygl, M. e. (2015). Abnormalities in pulmonary funcion in infacnt with high risk congenital diaphragmatic hernia. *Biomed Pap Med Fac Univ Palacky Olomouc Czech Repub , 159* (2), 497-502.

Sackner, M. A., Watson, H., Belsito, A. S., Feinerman, D., Suarez, M., Gonzalez, G., et al. (1989). Calibration of respiratory inductive plethysmograph during natural breathing. *J Appl Physiol , 66* (1), 410-420.

Sahakian, V., Tompkins, W. J., & Webster, J. G. (1985). Electrode motion artifacts in electrical impedance pneumography. *IEEE Trans. Biomed. Eng. , 32*, 448-451.

Sant, M., Aareleid, T., & Berrino, F. (2003). EUROCARE-3:survival of cancer patients diagnosed 1990-94-results and commentary. *Ann Oncal , 14* (Suppl 5), V61-V118.

Scarci, M., Joshi, A., & Attia, R. (2010). In patients undergoing thoracic surgery is paravertebral block as effective as epidural analgesia for pain management?. . *Interact Cardiovasc Thorac Surg , 10* (1), 92-96.

Scharstein, D., & Szeliski, R. (2003). High-accuracy stereo depth maps using structured light. *IEEE Comp. Soc. Conf. on Computer Vision and Pattern Recognition*, *1*, pp. 195-202.

Schneider , A. e. (2015). Whol-Body Plethysmography in suspected asthma: a prospective study of its added diagnostic value in 302 patients. *Dtsch Arztebl Int , 112* (24), 405-411.

Sciurba, F. C. (2010). A radomized study of endobronchial valves for advanced emphysema. *N Engl J Med , 363*, 1233-1244.

Scott, J., & Huskisson, E. C. (1979). Vertical or horizontal visual analogue scales. *Ann Rheum Dis , 38*, 560.

Silva, L., Barcelar Jde, M., Rattes, C. S., Sayao, L. B., Reinaux, C. A., Campos, S. L., et al. (2015). The influence of supine posture on chest wall volume changes is higher in obese than in normal weight children. *Appl Physiol Nutr Metab , 40* (2), 178-183.

Stagg, D., Goldman, M., & Davis, J. N. (1978). Computer-aided measurement of breath volume and time components using magnetometers. *J. Appl. Physiol. , 44*, 623-633.

Standring, S. (2008). Chest wall . In *Gray's anatomy the anatomical basis of clinical practice* (pp. 915-926). Elsevier limited.

Standring, S. (2008). Chest wall and breast, Muscles. In *Gray's anatomy, the anatomical basis of clinical practice* (pp. 924-926). Elsevier limited .

Standring, S. (2008). Diaphragm . In *Gray's anatomy, the anatomical basis of clinical practice* (pp. 1007-1012). Elsevier limited.

Stecher , F. S., Olsen, J. A., Stickney, R. E., & Wik, L. (2008). Transthoracic impedance used to evaluate performance of cardiopulmonary resuscitation during out of hospital cardiac arrest. *Resuscitation , 79* (3), 432-437.

Steinberg , M. T., Olsen, J. A., Brunborg, C., Persse, D., Sterz, F., Lozano, M. J., et al. (2015). Minimizing pre-shock chest compression pauses in a cardiopulmonary resuscitation cycle by performing an earlier rhythm analysis. *Resuscitation , 87*, 33-37.

Stephan, F., Boucheseiche, S., & Hollande, J. (2000). Pulmonary complications following lung resection: a comprehensive analysis of incidence and possible risk factors. *Chest , 118* (5), 1263-1270.

Stocks, J. e. (2001). ERS/ATS Task force on standards for infant respiratory function testing. Plethysmographic measurements of lung volume and airway resistance. *Eur Respir J , 17*, 302-312.

Stocks, J. (1996). *infant respiratory function testing.* New York : Wiley-Liss.

Stocks, J. (1996). Inspiratory and expiratory asynchrony. In J. Stocks, *Infant respiratory function testing* (pp. 155-156). John Wiley & Sons.

Stocks, J. (1995). Reference values for residual volume, functional residual capacity and total lung capacity.

Stocks, J., & Quanjer, P. H. (1995). Reference values for residual volume, functional residual capacity and total lung capacity. ATS Workshop on Lung Volume Measurements. Official Statement of The European Respiratory Society. *Eur Respir J , 8* (3), 492-506.

Strath, S. e. (2000). Evaluation of heart rate as a method for assessing moderate intensity physical activity. *Med Sci Sports Exerc. , 32* (9), S465-S470.

Stubbing, D. G., Pengelly, L. D., Morse, J. L., & Jones, N. L. (1980). Pulmonary mechanics during exercise in subjects with chronic airflow obstruction. *J Appl Physiol , 49*, 511-515.

Su, Z., Oto, J., Wang, J., Kimball, W. R., Chenelle, C. T., Kacmarek, R. M., et al. (2015). Validation of Respiratory Inductance Plethysmography for measuring tidal volume in swine. *Comp Med , 65* (3), 225-231.

Kundu, S. K., Kumagai, S., and Sasaki, M. (2013). A Wearable Capacitive Sensor for Monitoring Human Respiratory Rate. *Jpn J Appl Phys ,* 52 , 4S.

Suga, K., Tsukuda, T., Awaya, H., Takano, K., Koike, S., Matsunaga, N., et al. (1999). Impaired respiratory mechanics in pulmonary emphysema: evaluation with dynamic breahting MRI. *10* (4), 510-520.

Sutterlin, R. , LoMauro, A., Gandolfi, S., Priori, R., Aliverti, A., Frykolm, P., & Larsson, A. (2015). Influence of tracheal obstruction on the efficacy of superimposed high-frequency jet ventilation and single-freqquency jet ventilation. *Anesthesiology ,* 123(4), 799-809.

Hoffmann, T, Eilebrecht, B., & Leonhardt, S. (2011). Respiratory Monitoring System on the Basis of Capacitive Textile Force Sensors. *IEEE Sens J,* 11(5), 1112-119.

Takahashi, K., & Karjalainen, A. (2003). A cross-country comparative overview of the asbestos situation in ten Asian countries. *Int J Occup Environ Health , 9*, 244-248.

Takeda, S., Nakahara, K., Fujii, Y., Miyoshi , S., Mizuta, T., Minami, M., et al. (1991). Effects of diaphragm plication for phrenic nerve paralysis on respiratory mechanics and diaphragm function. *Nihon Gek Gakkai Zasshi , 9*, 1367-1370.

Tassavainen, A. (2004). Global use of asbestos and the incidence of mesothelioma. *Int J Occup Environ Health , 10*, 22-22.

Taylor, J. B., Allen, G. M., & Gandevia, S. C. (1996). Changes in motor cortical excitability during human muscle fatigue. *J Physiology , 490*, 519-528.

Teschler, H., & et, a. (1996). Effect of surgical lung volume reduction on respiratory muscle function in pulmonary emphysema. *Eur Respir J , 9*, 1779-1784.

Torres, A., Fiz, J. A., Galdiz, J. B., Gea, J., Morera, j., & Jane, R. (2006). Inspiratory pressure evaluation by means of the entropy of respiratory mechanomyographic signals. *Conf Proc IEEE Eng Med Biol Soc , 1*, 5735-5738.

Valairucha, S., Maboonvanon, P., Napachoti, T., Sirivanasandha, B., & Suraseranuvongse, S. (2005). Cost-effectiveness of thoracic patient-controlled epidural analgesia using bupivacaine with fentanyl vs bupivacaine with morphine after thoracotomy and upper abdominal surgery . *J Med Assoc Thai , 88* (7), 921-927.

Valentinuzzi, M. E., Geddes, L. A., & Baker, L. E. (1971). The law of impedance pneumography. *Med. Biol. Engng. , 9*, 157-163.

Vaughan, P., Oey, I., Nakas, A., Martin-Ucar, A., Edwards, J., & Waller, D. (2007). Is there a role for therapeutic lobectomy for emphysema? *Eur J Cardiothoracic Surg , 31* (3), 486-490.

Vercauteren, M. H. (2007). Anaethetic onsiderations for patients with a pre-existing neurological deficit: are neuraxial techniques safe? *Acta Anaesthesiol Scand. , 51* (7), 831-838.

Vercauteren, M., & Heytens, L. (2007). . Anaesthetic considerations for patients with a pre-existing neurological deficit: are neuraxial techniques safe? . *Acta Anaesthesiol Scand , 51* (7), 831-838.

Villarreal, M. (2007, December 13). *Respiratory system .* From https://en.wikipedia.org: https://en.wikipedia.org/wiki/File:Respiratory_system_complete_en.svg

Virta, R. L. (2013, January). *US Geological Survey: Mineral Commodity Summaries – Asbestos.* Retrieved August 25, 2015 from http://minerals.usgs.gov/minerals/pubs/commodity/asbestos/mcs-2013-asbes.pdf

Vogiatzis, I., Aliverti , A., Golemati, S., Georgiadou, O., Lo Mauro, A., & Kosmas, E. (2005). Respiratory kinematics by optoelectronic plethysmography during exercise in men and women. *Eur J Appl Physiol , 95* (5), 581-587.

Wanger, J. (2012). Lung volumes. In W. J, *Pulmonary function testing: a practical approach. 3rd ed.* (pp. 69-112). Burlington : Jones & Barlett Learning .

Wanger, J., Clausen, J. L., Coates, A., Pedersen, O. F., Brusasco, V., Burgos, F., et al. (2005). ATS/ERS Task force on standardisation of lung function testing. Standardisation of the measurement of lung volumes. *Eur Respir J , 26*, 511-522.

Warner, H. A. (2001). Status asthematicus in children: a review . *Chest , 119* (6), 1913-1929.

Wartzek, T., Wever, S., & Leonhardt, S. (2011). A differential capacitive electrical field sensor array for contactless measurement of respiratory rate. *Physiol Meas. , 32* (10), 1575-1590.

Wehrle, G., Nohama, P., Kalinowski, H. J., Torres, P. I., & Valente L. (2001). A fibre optic Bragg grating strain sensor for monitoring ventilatory movements. *Meas Sci Technol*, 12 , 7.

Welch, L., Dement, J., & West, G. (2015). Mortality among sheet metal workers participating in a respiratory screening program. *Am J Ind Med , 58* (4), 378-391.

West, J. (2004). The birth of clinical body plethysmography: it was a good week. *J Clin Invest , 114*, 1043-1045.

Wilkens, H., Weingard, B., Lo Mauro, A., Schena, E., Pedotti, A., Sybrecht , G. W., et al. (2010). Breathing pattern and chest wall volumes during exercise in patients with cystic fibrosis, pulmonary fibrosis and COPD before and after lung transplantation. *Thorax , 65* (9), 808-814.

Winston , W. T. (2014, April 23). *Mesothelioma Clinical Presentation*. Retrieved August 26, 2015 from Medscape: http://emedicine.medscape.com/article/280367-clinical

Wise, R. A., & Brown, C. D. (2005). Minimal clinically important differences in the six-minute walk test and the incermental shuttle walking test. *COPD , 2* (1), 125-129.

World Heatlh Organization (2006). *Elimination of Asbestos-Related Diseases.* Geneva: WHO.

Zaid, Z. (2015). Lung Volume Reduction in Emphysema Improves Chest Wal Asynchrony. *Chest , 148* (1), 185-195.

Zhang, H., Yang, Z., Huang, Z., Chen, B., Zhang, L., Li, H., et al. (2012). Transthoracic impedance for the monitoring of quality of manual chest compression during cardiopulmonary resuscitation. *Resuscitation , 83* (10), 1281-1286.

Zhang, L., Curelss, B., & Seitz, S. (2002). Rapid Shape Acquisition Using Color Structured Light and Multi-pass Dynamic Programming. *The 1st IEEE International Symposium on 3D Data Processing, Visualization, and Transmission*, (pp. 24-36). Padova-Italy.

Zhang, S., & Huang, P. S. (2006). High-resolution, real-time three-dimensional shape measurement. *In Optical Engineering , 45*.

Zimmerman, P. V., Connellan, S. J., Middleton, H. C., Tobona, M. V., Goldman, M. D., & Pride, N. (1983). Postural changes in rib cage and abdominal volume-motion coefficients and their effect on the calibration of a respiratory inductance plethysmograph. *Am Rev Respir Dis , 127* (2), 209-214.

Zoumot, Z., LoMauro, A., Aliverti, A., Nelson, C., Ward, S., Jordan, S., et al. (2015). Lung Volume Reduction in Emphysema Improves Chest Wall Asynchrony. *Chest , 148* (1), 185-195.